Metabolic Regulation of Human Vascular Endothelial Cell Function *in Vitro*

A Thesis Submitted to

The Faculty of Biomedical and Life Sciences

For the Degree of

DOCTOR OF PHILOSOPHY

By

Christine Frederike Kohlhaas, MBiol(Hons), MRes

Division of Biochemistry and Molecular Biology

University of Glasgow

May 2008

Author's Declaration

I declare that the work carried out in this thesis has been carried out by myself, unless otherwise stated. It is entirely of my own composition and has not, in whole or in part, been submitted for any other degree.

Christine F Kohlhaas

May 2008

Abstract

The vascular endothelium contributes to the maintenance of vascular health by regulating vascular tone and leukocyte adhesion, amongst others. The vasoregulatory actions of the endothelium are mediated through coordinated release of vasodilators such as nitric oxide (NO) and prostacyclin, and vasoconstrictors such as endothelin-1 and thromboxane A_2. Endothelial NO is the principal vasodilator in the vasculature and is produced by endothelial nitric oxide synthase (eNOS). Insulin is a vasoactive hormone that exerts its vasodilatory effects through eNOS-mediated NO production. Endothelial function is impaired in a number of disorders, including insulin resistance, diabetes and atherosclerosis, leading to dysregulated vasodilation as well as increased monocyte adhesion and plaque formation (atherosclerosis). The underlying molecular mechanisms leading to endothelial dysfunction are still in question.

The work presented in this thesis addressed this question by investigating how insulin signalling and eNOS-mediated NO and superoxide production in human vascular endothelial cells are affected under experimental hyperinsulinaemia (chapter 3) and experimental hyperglycaemia (chapter 4). Atherogenic processes in human aortic endothelial cells (HAEC) were investigated by assessing monocyte adhesion under experimental hyperinsulinaemia (chapter 3), and by determining the contribution of NO and AMP-dependent kinase (AMPK) activity to the regulation of endothelial chemokine production (chapter 6). The potential of insulin to modify the subcellular distribution of eNOS was investigated in chapter 5.

Clinical hyperinsulinaemia correlates with attenuated NO-mediated vasodilation, but it is not clear how hyperinsulinaemia impairs eNOS-mediated NO production. The present study modelled hyperinsulinaemia in HAEC and demonstrated a blunted response of hyperinsulinaemic cells to Ca^{2+}-stimulated, but not insulin-stimulated eNOS-mediated NO synthesis. To address the underlying mechanisms responsible, the protein expression levels of components of the metabolic and mitogenic insulin signalling pathways, and of the metabolic energy sensor, AMPK, were quantified. Experimental hyperinsulinaemia slightly and non-significantly increased basal and insulin-stimulated $eNOS^{S1177}$ phosphorylation in a time-dependent manner, and the levels of $eNOS^{T495}$ increased following acute insulin stimulation under these conditions. No marked dysregulation of individual insulin signalling pathway components was identified as a potential cause, but increased activating $AMPK^{T172}$ phosphorylation was found to be a potential cause of

increased unstimulated eNOS^{S1177} phosphorylation under experimental hyperinsulinaemia. Monocyte adhesion to hyperinsulinaemic HAEC did not differ from control HAEC, indicating that experimental hyperinsulinaemia did not act as a proatherogenic factor in the present study.

Overt diabetes was simulated by experimental hyperglycaemia in human umbilical vein endothelial cells (HUVEC) and its effect on insulin-stimulated eNOS phosphorylation and endothelial superoxide production assessed. Insulin tended to stimulate phosphorylation of eNOS^{S615} and eNOS^{S1177}, and decrease phosphorylation of eNOS^{S114}, eNOS^{T495} and eNOS^{S633} under control conditions. Experimental hyperglycaemia slightly reduced basal phosphorylation of Ser633 and significantly reduced insulin-stimulated phosphorylation of Ser114, but mildly increased basal Ser615 phosphorylation, indicating some dysregulation of eNOS phosphorylation. The upstream components of the metabolic insulin signalling pathway were not impaired in hyperglycaemic conditions.

The subcellular localisation of eNOS is thought to have implications for its function. This study showed that eNOS localises to the plasma membrane, the nucleus, the cytoplasm and, primarily, the perinuclear area of HAEC. Insulin stimulation did not affect this distribution. Phospho-eNOS species were found primarily at the plasma membrane, and insulin may modulate the abundance of an intracellular eNOS^{T495} species.

Previous work in our laboratory on AMPK-mediated reduction of adhesion molecule expression has lead to the investigation of AMPK- and NO-mediated regulation of chemokine production in the present study. Inhibition of NO synthesis increased the production of monocyte chemoattractant protein (MCP)-1 in HAEC. AMPK activity downregulated TNFa-stimulated MCP-1 expression, and this was NO-dependent in the short-term, but may be NO-independent during prolonged AMPK activation. These data implicate NO and AMPK as antiatherogenic mediators in vascular endothelial cells *in vitro*.

Taken together, the data in this thesis provide further insight into some of the molecular mechanisms involved in endothelial function and their response to hyperinsulinaemia, hyperglycaemia and proatherogenic stimulation.

Published Abstracts

Some of the work presented in this thesis has been previously published as

Kohlhaas, C.F. & Salt, I.P. (2007). Experimental hyperinsulinaemia does not alter insulin sensitivity of human endothelial cells or increase monocyte adhesion. *Diabetic Medicine* **24**, 40-40.

Acknowledgements

Firstly, I would like to thank my supervisor Dr Ian Salt for his enthusiasm, intellectual and technical input and continued support throughout my project. I want to express my thanks to him for allowing me to use his lab space and for giving me the opportunity to present at national and international conferences. I would also like to thank Prof Gwyn Gould for his helpful input into my project. Furthermore, I am indebted to the convenors of the Wellcome Trust 4-year PhD programme, especially Prof Bill Cushley, for their continued support that often went beyond the normal call of duty. I would like to thank the Wellcome Trust for funding this PhD, and for their generous granting of extra funds during the extension of my project.

A special mention goes to the members of Lab 241 for their collegial support and for making the time spent in the laboratory so enjoyable. I also acknowledge the members of my PhD-course as exceptional in their friendship and mutual support, which have helped to make my time at the University of Glasgow a very rewarding experience. In particular, I would like to thank Adrienne Edkins and Mridu Acharya for their technical assistance.

I would like to express my special thanks to my family, especially my parents, who have always believed in me and supported me throughout all these years. Without their continual encouragement, I would not be where I am today. Finally, I would like to thank my friends who have faithfully shown their loving support to me.

I have greatly enjoyed my time during this project, and have grown in my understanding and appreciation of research.

"How great are your works, O LORD, how profound your thoughts!"

Psalm 92, v 5

Contents

Figures

Tables

Abbreviations

AMPK	AMP-activated protein kinase
ATP	Adenosine triphosphate
BAEC	Bovine aortic endothelial cells
BH_4	Tetrahydrobiopterin
BSA	Bovine serum albumin
BZ	Benzamidine
CaM	Calmodulin
CaMKII	CaM-dependent kinase II
CaMKK	Ca^{2+}/CaM-dependent protein kinase kinase
cDNA	Copy (complementary) DNA
CT	C-terminal (domain)
DMEM	Dulbecco's modified Eagle medium
DTT	Dithiothreitol
EC	Endothelial cell(s)
ECL	Enhanced chemiluminescence
EDRF	Endothelium-derived relaxation factor
EGF	Epidermal growth factor

eNOS	Endothelial nitric oxide synthase
ERK	Externally-regulated kinase
FAD	Flavin adenine dinucleotide
FMN	Flavin mononucleotide
G6Pase	Glucose-6-phosphatase
HAEC	Human aortic endothelial cells
HCAEC	Human coronary artery endothelial cells
HES	HEPES-EDTA-Sucrose (buffer)
HUVEC	Human umbilical vein endothelial cells
HRP	Horseradish peroxidise
IGF	Insulin-like growth factor
IGF-1R	Insulin-like growth factor-1 receptor
iNOS	Inducible nitric oxide synthase
IR	Insulin receptor
IRR	Insulin receptor-related receptor
IRS	Insulin receptor substrate
JM	Juxtamembrane
KRH	Krebs-Ringer-HEPES
MAEC	Mouse aortic endothelial cells

MAPK	Mitogen-activated protein kinase
MCP-1	Monocyte chemoattractant protein-1
MLC	Myosin light chain
mRNA	Messenger RNA
NADPH	Nicotinamide adenine dinucleotide phosphate
NaPPi	Sodium pyrophosphate
nNOS	Neuronal nitric oxide synthase
PAEC	Porcine aortic endothelial cells
PCR	Polymerase chain reaction
PDE III	cAMP phosphodiesterase
PDGF	Platelet-derived growth factor
PDK-1, PDK-2	3-phosphoinositide-dependent protein kinase-1/-2
PH	Pleckstrin homology (domain)
PI3K	Phosphatidylinositide 3-kinase
PKA, PKB, PKC, PKG	Protein kinase A/B/C/G
PMSF	Phenylmethylsulphonyl fluoride
PTB	Phosphotyrosine-binding (domain)
PTEN	Phosphatase-and-tensin-homologue-deleted-

	on-chromosome-10
ROS	Reactive oxygen species
RTK	Receptor tyrosine kinase
SBTI	Soybean trypsin inhibitor
SDS	Sodium dodecyl sulphate
SERCA	Sarcoendoplasmic reticulum ATPase
SOD	Superoxide dismutase
TBS	Tris-buffered saline
TBST	Tris-buffered saline + Tween-20
TCA	Trichloracetic acid
TK	Tyrosine kinase
TZDs	Thiazoledinediones
VEGF	Vascular endothelial growth factor
wt	Wild type

1 Introduction

1.1 The vascular endothelium

The vascular endothelium is a single cell layer lining the lumen of blood vessels, providing a physical barrier between the blood vessel wall and the lumen. It is a key player in the maintenance of cardiovascular health. It regulates a number of processes, including the maintenance of vascular tone, passage of substances into and out of the bloodstream, platelet aggregation, coagulation, fibrinolysis and monocyte adhesion (Wheatcroft *et al.*, 2003).

Vascular tone is regulated by a number of endothelium-derived substances with vasodilator or vasoconstrictor function, which act on vascular smooth muscle cells in the underlying vascular wall. The principal vasodilators include nitric oxide (NO), prostacyclin and endothelium-derived hyperpolarising factor (EDHF), whereas the vasoconstrictors include endothelin-1 and thromboxane A_2. NO is the main endothelium-derived vasodilator in large blood vessels, while EDHF is more important in smaller vessels (Wheatcroft *et al.*, 2003). The maintenance of a correct balance between these vasoactive molecules is crucial, so that vascular tone can be adjusted appropriately to stimuli such as shear stress (passage of blood through the blood vessel), exercise, feeding, temperature changes and changes in blood volume.

Endothelial dysfunction can be defined as defective endothelium-dependent vasodilation and dysregulated expression of endothelial adhesion molecules and chemokines. Endothelial dysfunction is a component of metabolic disorders such as insulin resistance, Type II diabetes and the metabolic syndrome, as well as atherosclerosis. The relationship with each of these diseases is still under debate, and is discussed in sections 1.4 - 1.6.

1.2 Nitric oxide production in the vascular endothelium

1.2.1 Nitric oxide synthases

Nitric oxide synthases are enzymes that catalyse the conversion of L-arginine to NO and L-citrulline, and were first discovered in 1989 (see review by (Alderton *et al.*, 2001)). Mammalian nitric oxide synthases (NOS) exist in three isoforms: endothelial (eNOS, or NOS III), neuronal (nNOS, or NOS I) and inducible NOS (iNOS, or NOS II) (Andrew & Mayer, 1999, Stuehr, 1999). The NOS enzymes are homodimers consisting of an N-terminal oxygenase domain and a C-terminal reductase domain (see Figure 1-1). The latter shares at least 50% homology with the cytochrome P-450 reductase (Stuehr, 1999). These NOS dimers form heterotetramers with two molecules of calmodulin (CaM). NOS require the cofactors nicotinamide adenine dinucleotide phosphate (NADPH), flavin mononucleotide (FMN), flavin adenine dinucleotide (FAD), haem and tetrahydrobiopterin (BH_4) for enzymatic activity (Knowles & Moncada, 1994, Andrew & Mayer, 1999, Stuehr, 1999).

The haem group plays a crucial role in the dimerisation of all three NOS isoforms (Baek*et al.*, 1993, Klatt *et al.*, 1996, List *et al.*, 1997). BH_4 is postulated to modulate oxy-haem reactivity (Stuehr, 1999), and it stabilises the conformation and affects the activity of NOS (Mayer & Hemmens, 1997, Andrew & Mayer, 1999). Figure 1-2 illustrates the synthesis of NO by NOS. Some of the characteristics of each NOS isoform are outlined below.

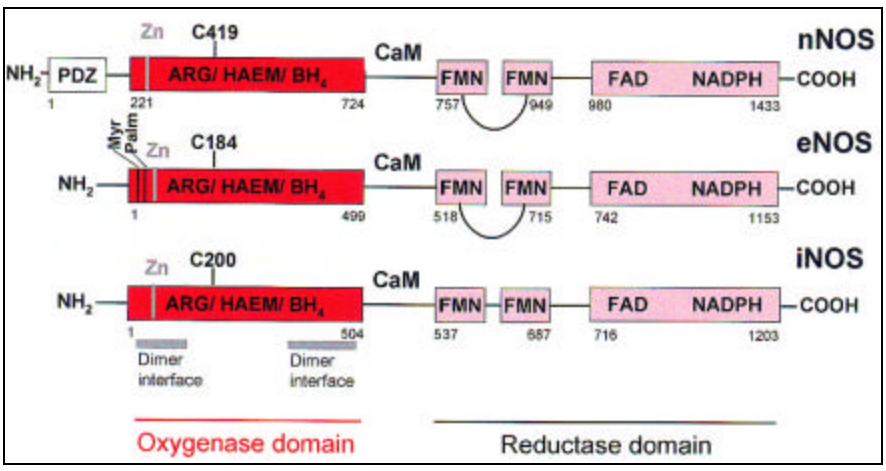

Figure 1-1 The domain structures of NOS

The myristoylation (Myr) and palmitoylation (Palm) sites on eNOS are shown. Diagram adapted from (Alderton *et al.*, 2001)

1.2.1.1 eNOS

As the principal source of endothelial NO, eNOS is of major importance to the normal functioning of the cardiovascular system. eNOS is activated by hormonalfactors, including insulin (Sobrevia *et al.*, 1996, Zeng & Quon, 1996) and vasopressin (Resta *et al.*, 1997), as well as by mechanical forces such as shear stress generated by blood flow through blood vessels (Corson *et al.*, 1996). Shear stress-mediated eNOS activation in vitro has been proposed to be dependent on the phosphatidylinositol-3 kinase (PI3K)-PKB pathway (Dimmeler *et al.*, 1999). Shear stress, exercise and hypoxia not only activate eNOS, but also upregulate eNOS transcription (reviewed in (Nathan & Xie, 1994)).

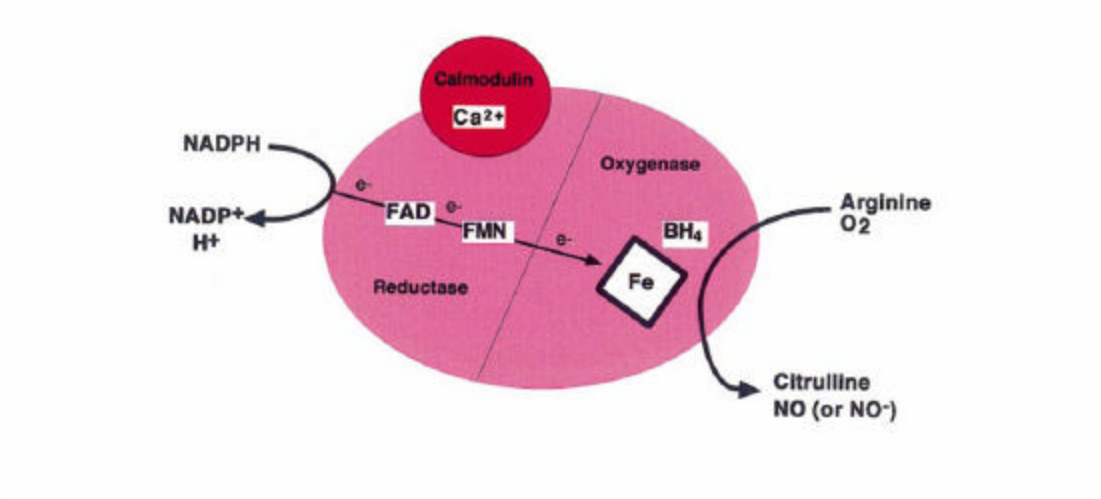

Figure 1-2 Nitric oxide synthesis by NOS

Electrons (e^-) are donated to the reductase domain of eNOS by NADPH and pass through the FAD and FMN domains to the haem iron in the oxygenase domain. Here, the electrons interact with BH_4 at the active site to catalyse the conversion of L-arginine and oxygen to L-citrulline and nitric oxide. This process depends on the binding of Ca^{2+}/CaM to eNOS. Diagram adapted from (Alderton *et al.*, 2001)

1.2.1.2 nNOS

Neuronal NOS (nNOS) (monomer size ~155 kDa) is widely expressed in central and peripheral neurones. Compared to eNOS, nNOS possesses an N-terminal extension of about 300 amino acid residues that encode a PDZ domain. The PDZ domain permits association of nNOS with cytoskeletal/structural proteins such as dystrophin and PSD-95 that serve to localise nNOS within the cell (reviewed in (Andrew & Mayer, 1999, Stuehr, 1999). Binding to caveolin-3 inhibits nNOS-mediated NO synthesis (Venema *et al.*, 1997).

At low concentrations of L-arginine, nNOS catalyses the production of $O_2^{\cdot -}$, H_2O_2 and peroxinitrite ($ONOO^{\cdot -}$) in a so-called uncoupled reaction (Mayer *et al.*, 1991, Heinzel *et al.*, 1992, Andrew & Mayer, 1999). These highly reactive oxygen species have damaging effects on cellular function that can lead to pathogenic outcomes.

1.2.1.3 iNOS

The inducible form of NOS, iNOS, is expressed at high levels in macrophages, endothelial cells, cardiac myocytes and smooth muscle cells in response to proinflammatory stimuli such as cytokines. A few other tissues, such as the lung epithelium, constitutively express iNOS (monomeric form: ~130 kDa). The enzyme is thought to play a role in host defence, but has also been implicated in inflammatory diseases and may have a negative effect on atherosclerotic lesions (Andrew & Mayer, 1999, Stuehr, 1999). By contrast, iNOS activity may also be beneficial in that it suppresses allograft atherosclerosis (Shears *et al.*, 1997, Andrew & Mayer, 1999).

1.2.2 Nitric oxide production

Early work showed that aortic rings explanted from rabbits and preconstricted with noradrenaline dilated in response to acetylcholine, but this response failed when the rings were denuded of the endothelial layer (Furchgott & Zawadzki, 1980). This was the first indication that an endothelium-derived factor was responsible for vasodilation (also termed vasodilatation or vasorelaxation). This factor was later termed endothelium-derived relaxation factor (EDRF). Griffith and co-workers then demonstrated that EDRF is a humoral agent whose production can be stimulated by acetylcholine (Griffith *et al.*, 1984), and this humoral agent was later proposed to be nitric oxide (NO) (Ignarro *et al.*, 1987, Palmer *et al.*, 1987). Some controversy remains to this day as to the true identity of EDRF. Other candidates for EDRF have been suggested, including the nitroxyl ion, which could then be oxidised to NO in a reaction with superoxide dismutase (SOD) (Murphy & Sies, 1991). It is, however, accepted that eNOS is the source of endothelial NO.

Ca^{2+}-stimulated activation of eNOS and nNOS occurs in response to an intracellular surge in calcium levels and involves binding of Ca^{2+} and CaM. iNOS, by contrast, is essentially

calcium-independent, as it binds CaM with high affinity (Andrew & Mayer, 1999, Stuehr, 1999). Shear-stress- and insulin-stimulated eNOS activation is independent of the intracellular Ca^{2+} concentration (Corson *et al.*, 1996, Fisslthaler *et al.*, 2000, Montagnani *et al.*, 2001, Boo *et al.*, 2002).

Upon binding of CaM to constitutive NOS, the co-factors FMN and FAD, which are bound to the NOS reductase domain, accept electrons from NADPH and transfer these to the haem iron in the oxygenase domain. This leads to O_2 binding, and activation of NOS (Stuehr, 1999, Alderton *et al.*, 2001). In the oxygenase domain, the electrons interact with the haem iron and BH_4 at the active site to catalyse the reaction of O_2 with L-arginine to produce NO and L-citrulline (see Figure 1-2). This reaction proceeds via the reaction intermediate N^G-hydroxy-L-arginine (Alderton *et al.*, 2001).

In the absence of Ca^{2+}/CaM, electron transfer between FAD and FMN is slow, indicating that Ca^{2+} ions are required for efficient eNOS activation (Matsuda & Iyanagi, 1999). In the catalytically active eNOS dimer, electrons pass from the flavin domain of one monomer to the haem residue of the other monomer (Siddhanta *et al.*, 1996). This explains the necessity for NOS dimerisation for catalytical activity.

1.2.3 Other possible products of eNOS

Under some conditions, eNOS can directly or indirectly catalyse the formation of other reactive oxygen species, including nitroxyl (NO^-) ions, peroxynitrite ($ONOO^-$), superoxide (O_2^-) and nitrosothiols. Superoxide is generated when eNOS is uncoupled from NADPH oxidation (Vasquez-Vivar *et al.*, 1998, Xia *et al.*, 1998). This process decreases NO synthesis. Superoxide can react with NO, leading to formation of both peroxynitrite and nitrate (Reiter *et al.*, 2000). Peroxynitrite, in turn, can reduce NO bioavailability further through oxidation and uncoupling of eNOS, leading to enhanced O_2^- production and decreased NO synthesis (Zou *et al.*, 2002). Nitrosothiol can be generated by stimulation of eNOS with bradykinin or Ca^{2+} ionophore in the presence of homocysteine (Upchurch *et al.*, 1997).

It has also been proposed that the nitroxyl ion is the initial reaction product of eNOS, which is then oxidised to NO in a reaction with superoxide dismutase (SOD) (Murphy &

Sies, 1991). It is, however, generally accepted that NO is the principal reaction product of eNOS.

1.2.4 Nitric oxide-mediated vasodilation

NO is a free radical (Mayer & Hemmens, 1997) and has an extremely short half-life of only 3-6 seconds (Griffith *et al.*, 1984, Ignarro *et al.*, 1987, Moncada & Higgs, 1991, Boger *et al.*, 1996). Once produced, NO has several targets, including the enzyme soluble guanylate cyclase (sGC), which catalyses the formation of cyclic guanosine monophosphate (cGMP), a secondary messenger that relays information to cGMP-responsive molecules. In the case of NO-mediated vasodilation, the cGMP-targeted molecules include two cGMP-dependent protein kinases, PKG I and PKG II (also known as cGK-I and -II) (Gewaltig & Kojda, 2002).

PKG I mediates vasodilation by phosphorylating various molecules involved in smooth muscle relaxation, including inositol 1,4,5-triphosphate receptor-associated G kinase (IRAG), myosin light chain (MLC) phosphatase, and phospholamban (Gewaltig & Kojda, 2002). In these cases, phosphorylation ultimately results in decreased intracellular Ca^{2+} levels: IRAG phosphorylation reduces the release of Ca^{2+} from the sarcoplasmic reticulum (Ammendola *et al.*, 2001), phosphorylation-activated MLC phosphatase prevents MLC phosphorylation and contraction (Surks *et al.*, 1999), and phospholamban phosphorylation mediates sarcoendoplasmic reticulum ATPase (SERCA) activation, resulting in the rapid sequestration of intracellular Ca^{2+} (Gewaltig & Kojda, 2002, Rivero-Vilches *et al.*, 2003).

A further NO-mediated vasodilatory mechanism is the activation of Ca^{2+}-activated K^+ (BK_{Ca}) channels by NO through the cGMP-PKG I pathway. Activation of the BK_{Ca} channels can occur either through direct activation of the BK_{Ca} channels by NO (Bolotina *et al.*, 1994) or by PKG I-dependent phosphorylation of the channel protein (Alioua *et al.*, 1998) or of a protein phosphatase (Hall & Armstrong, 2000, Sausbier *et al.*, 2000). BK_{Ca} channel activation increases the K^+ efflux, thus causing membrane hyperpolarisation and vasodilation (Gewaltig & Kojda, 2002).

eNOS-derived NO is vitally important as a vasodilator: Disruption of the eNOS gene in mice results in mild hypertension (Huang *et al.*, 1995, Gewaltig & Kojda, 2002); an increased blood pressure is also seen in humans when NO synthesis is inhibited

pharmacologically (Stamler *et al.*, 1994, Gewaltig & Kojda, 2002). Currently, it is thought that at physiological concentrations of NO, vasodilation is mediated via cGMP-PKG I-dependent mechanisms, while at high levels of NO (either pharmacologically induced or as encountered during endotoxic shock) (Thiemermann & Vane, 1990, Rosenberg *et al.*, 1994), this mechanism is bypassed and the alternative protein kinase A (PKA) pathway is activated by cGMP (Pfeifer *et al.*, 1998, Sausbier *et al.*, 2000).

1.2.5 Other roles of nitric oxide

Besides vasodilation, NO has antiatherogenic roles in the regulation of platelet function, monocyte adhesion (Kubes *et al.*, 1991) and smooth muscle cell proliferation (Mayer & Hemmens, 1997, Gewaltig & Kojda, 2002). Platelet aggregation is prevented by lowering intracellular Ca^{2+} concentration through activation of phospholamban and SERCA via the cGMP-PKG I pathway (reviewed in (Gewaltig & Kojda, 2002)).

Monocyte adhesion is dependent on the expression of chemokines and adhesion molecules, including vascular cell adhesion molecule (VCAM-1), monocyte chemoattractant protein-1 (MCP-1) and cytokines, on the surface of vascular endothelial cells. Unregulated monocyte adhesion contributes to atherogenesis. NO inhibits NF?B expression and activation. NF?B-dependent VCAM-1 expression is thus inhibited and monocyte adhesion decreased (reviewed in (Gewaltig & Kojda, 2002)).

Smooth muscle cell proliferation is inhibited *in vitro* by NO (Garg & Hassid, 1989) through inhibition of O_2^--producing enzymes (e.g. NADPH oxidase) (Clancy *et al.*, 1992). Proliferation may also be blocked by cGMP-dependent activation of PKA and cGMP-inhibition of cAMP phosphodiesterase (PDE III). Activated PKA is thought to inhibit the mitogenic molecule Raf-1, thus preventing smooth muscle cell proliferation (reviewed in (Gewaltig & Kojda, 2002)). Unregulated vascular smooth muscle cell proliferation is proatherogenic in that it can lead to artery thickening, thus increasing the risk of hypertension, stroke and infarction.

The immune system utilises macrophage-produced NO as a cytotoxic attack factor (Mayer & Hemmens, 1997) and tumour cytostatic agent (MacMicking *et al.*, 1997, Stuehr, 1999). In severe inflammatory conditions like septic shock, iNOS-catalysed NO synthesis can lead to potentially lethal hypotension (Mayer & Hemmens, 1997). NO has furthermore

been implicated in learning and memory (long-term potentiation, LTP), since LTP was markedly decreased in eNOS knockout mice (Son *et al.*, 1996, Mayer & Hemmens, 1997, Wilson *et al.*, 1997). The function of NO in long-term potentiation, together with other evidence for NO-controlled gene expression (Zeiher *et al.*, 1995), point to a role for NO in transcriptional regulation.

1.2.6 Regulation of eNOS activity

Given the vital role of nitric oxide in the vasculature, it is imperative that its production be tightly controlled. A number of distinct mechanisms regulate eNOS activity, including transcriptional control, acylation, phosphorylation, subcellular localisation and association with other cellular molecules.

1.2.6.1 Transcriptional control

The promoter of the eNOS gene contains two positive regulatory domains, PRD I and PRDII. The former contains a high-affinity Sp1 transcription factor recognition site, to which Sp1 and Sp3 transcription factors bind, while the latter binds Ets-1, Elf-1, YY1, Sp1, and MYC-associatedzinc finger protein (Karantzoulis-Fegaras *et al.*, 1999). Trans-acting factors have also been implicated in the regulation of eNOS transcription (Searles, 2006). An upstream enhancer sequence needs to interact with the promoter sequence for full promoter activity. Erg, AP-2 and Sp1-related factor have been shown to interact with the enhancer sequence (Laumonnier *et al.*, 2000, Searles, 2006). Shear stress, exercise and hypoxia not only activate eNOS, but also mediate upregulation of eNOS transcription (reviewed in (Nathan & Xie, 1994)).

1.2.6.2 Acylation and subcellular localisation

The eNOS monomer is post-translationally modified by myristoylation and palmitoylation. These modifications serve partly to target eNOS to various subcellular locations. eNOS is dually acylated by cysteine palmitoylation at cysteines 15 and/or 26, and by N-

myristoylation on glycine 2 of the bovine eNOS sequence. Myristoylation targets eNOS to the plasma membrane and the Golgi complex, while palmitoylation targets it to caveolae (Lamas *et al*., 1992, Busconi & Michel, 1993, Liu & Sessa, 1994, Garcia-Cardena *et al.*, 1996b, Liu *et al.*, 1996, Shaul *et al.*, 1996). Palmitoylation-deficient eNOS mutants were deficient in NO synthesis, suggesting that palmitoylation positively regulates NO release (Liu *et al.*, 1996).

Palmitoylation specifically targets eNOS to caveolae at the plasma membrane (Liu *et al.*, 1996). Caveolae are a form of so-called lipid rafts, microdomains devoid of phospholipids but rich in cholesterol and glycosphingolipids, as well as the coat protein caveolin-1 (Brown & London, 1998). It has been suggested that caveolae act as signal transducing domains because they are thought to bring transmembrane receptors such as the insulin receptor, in close proximity to their downstream targets by virtue of direct interaction of these signalling molecules with caveolin-1 (Kimura *et al.*, 2002, Saltiel & Pessin, 2003). Likewise, eNOS is known to bind caveolin-1 through its oxygenase and reductase domains, thereby being held at plasma membrane caveolae in an inactivating complex (Feron *et al.*, 1996, Garcia-Cardena *et al.*, 1996a, Garcia-Cardena *et al.*, 1997, Michel *et al.*, 1997, Feron *et al.*, 1998, Ghosh *et al.*, 1998). The presence of eNOS at the plasma membrane is thought to optimise eNOS activation and nitric oxide release to the extracellular environment (Garcia-Cardena *et al.*, 1996b, Shaul *et al.*, 1996).

Intracellularly, eNOS is found in the particulate subcellular fraction of bovine aortic endothelial cells (Forstermann *et al.*, 1991, Pollock *et al.*, 1991) and eNOS-transfecetd COS-7 cells (Busconi & Michel, 1993). Later studies showed that eNOS is targeted to the Golgi body of eNOS-transfected HEK cells (Sessa *et al.*, 1995). It has been suggested that the plasma membrane- and Golgi-pools of eNOS respond differently to agonist-mediated activation (Zhang *et al*., 2006). In the cell line ECV304, exogenous eNOS also localised to the plasma membrane and the perinuclear/Golgi area (Sowa *et al.*, 1999). However, the endothelial nature of ECV304 cells is controversial, as a recent genetic analysis found these cells to be identical to the bladder cancer-derived epithelial cell line T24/83 (Brown *et al.*, 2000). Therefore, their use as an endothelial cell model is questionable.

1.2.6.3 Phosphorylation

Human eNOS has several known phosphorylation sites: Ser114, Thr495, Ser615, Ser633 and Ser1177. Regulation of eNOS activity is thought to involve concerted phosphorylation and dephosphorylation of these sites (Michell *et al.*, 2001, Bauer *et al.*, 2003, Mount *et al.*, 2007). In addition, eNOS can be tyrosine-phosphorylated, which may regulate its interaction with caveolin-1 (Garcia-Cardena *et al.*, 1996a). Tyrosine phosphorylation is also postulated to decrease endothelium-dependent vasorelaxation in response to acetylcholine (Huang *et al.*, 2002), suggesting that it inhibits NO synthesis.

Ser1177 is the best-characterised eNOS phosphorylation site. It is located in the reductase domain and is phosphorylated by a number of kinases, including PKA (Michell *et al.*, 2001), PKB (Dimmeler *et al.*, 1999, Fulton *et al.*, 1999), AMPK (Fleming & Busse, 2003, Morrow *et al.*, 2003), PKG and CaM-dependent kinase II (CaMKII) (Fleming *et al.*, 2001) (reviewed in (Mount *et al.*, 2007)). Phosphorylation of $eNOS^{S1177}$ increases eNOS activity and is required for agonist-mediated NO synthesis (Dimmeler *et al.*, 1999, Fulton *et al.*, 1999, Michell *et al.*, 2001). Phosphorylation of $eNOS^{S1177}$ can be triggered by a number of factors, including shear stress, insulin, IGF-1, oestrogen, vascular endothelial growth factor (VEGF), bradykinin and ATP (Fleming *et al.*, 1998, Michell *et al.*, 2001, Bauer *et al.*, 2003, Mount *et al.*, 2007). Insulin-stimulation of eNOS increases NO production in HAEC ~4-fold (Salt *et al.*, 2003). Ser1177 is located in the CT domain of eNOS, which is situated between the two eNOS monomers, thereby blocking the transfer of electrons in an autoinhibitory fashion. Phosphorylation of $eNOS^{S1177}$ has been suggested to induce a conformational change that removes this CT domain block and increases eNOS activity (Lane & Gross, 2002).

Several lines of evidence suggest that $eNOS^{T495}$ phosphorylation negatively regulates nitric oxide synthesis, because its dephosphorylation enhances NO production (Chen *et al.*, 1999, Fleming *et al.*, 2001, Michell *et al.*, 2001, Greif *et al.*, 2002, Fleming & Busse, 2003, Matsubara *et al.*, 2003). $eNOS^{T495}$ was constitutively phosphorylated in porcine aortic endothelial cells (PAEC) in the basal state and was rapidly dephosphorylated upon bradykinin stimulation, leading to eNOS activation (Fleming *et al.*, 2001). In addition, PKA has been demonstrated to increase eNOS activation with associated Thr495 phosphorylation (Michell *et al.*, 2001). Furthermore, insulin stimulated a decrease in $eNOS^{T495}$ phosphorylation in HUVEC (Greif *et al.*, 2002, Federici *et al.*, 2004), and

mimicking Thr495 phosphorylation by site-directed mutagenesis decreased eNOS activity (Michell *et al.*, 2002).

The phosphorylation site Thr495 is situated in the CaM-binding domain of eNOS. PKC was identified as a candidate for $eNOS^{T495}$ phosphorylation, causing a decrease in eNOS activity through altering the binding of CaM (Fleming *et al.*, 2001, Matsubara *et al.*, 2003). Dephosphorylation of $eNOS^{S1177}$ and $eNOS^{T495}$ is proposed to be mediated by phosphatase PP2A and phosphatase PP1, respectively (Michell *et al.*, 2001, Greif *et al.*, 2002). PKC activation has been proposed to mediate dephosphorylation of eNOS at Ser1177 and simultaneous phosphorylation at Thr495, thus having an inhibitory effect (Fleming *et al.*, 2001). It has been suggested that the coordinated phosphorylation of Ser1177 and Thr495 is critical in determining agonist-stimulated eNOS activity (Fleming *et al.*, 2001, Fleming & Busse, 2003).

Although the other eNOS phosphorylation sites are less well-characterised, experimental evidence has demonstrated that the phosphorylation state of these sites also influences the stimulation and kinetics of eNOS activity, and may also modulate its interactions with other proteins. These findings highlight the complexity of eNOS regulation and the physiological importance of this enzyme.

Ser114 is located in the oxygenase domain of eNOS. The effect of $eNOS^{S114}$ phosphorylation on eNOS activity is controversial. Some groups demonstrated an upregulation of eNOS activity with increased $eNOS^{S114}$ phosphorylation. Shear stress and high density lipoprotein were both reported to increase $eNOS^{S114}$ phosphorylation and eNOS activity (Gallis *et al.*, 1999, Drew *et al.*, 2004). Site-directed mutagenesis of bovine eNOS and subsequent transfection into COS-7 cells suggested that mimicking phosphorylation at Ser114 increased eNOS activity. Controversially, in the same study, both the phosphorylation and dephosphorylation-mimetic $eNOS^{S114}$ mutants increased stimulated NO release (Bauer *et al.*, 2003). By contrast, another group found that mimicking dephosphorylation of $eNOS^{S114}$ by mutating the serine residue to alanine, increased eNOS activity, and that stimulation of eNOS with VEGF dephosphorylated Ser114 (Kou *et al.*, 2002). It has been proposed that $eNOS^{S114}$ phosphorylation modulates Ser1177 phosphorylation and increases the interaction of eNOS with hsp90 and PKB (Bauer *et al.*, 2003).

The role of the phosphorylation site Ser615 in the FMN binding domain of eNOS is not fully understood. $eNOS^{S615}$ phosphorylation has been reported to increase eNOS activity and in our own laboratory, $eNOS^{S615}$ phosphorylation is associated with insulin-stimulated NO release (Michell *et al.*, 2002, Ritchie *et al.*, 2007). The eNOS agonists VEGF, bradykinin and ATP have been shown to stimulate $eNOS^{S615}$ phosphorylation, suggesting that Ser615 is an activating site (Michell *et al.*, 2002). Ser615 phosphorylation increased the activity of eNOS at lower concentrations of CaM without affecting maximal activity (Michell *et al.*, 2002). PKB has been implicated in the phosphorylation of the bovine site equivalent to Ser615 in BAEC (Michell *et al.*, 2002). In agreement with this, insulin stimulated $eNOS^{S615}$ phosphorylation and NO release in HAEC (Ritchie *et al.*, 2007). By contrast, studies with eNOS phospho-mutants demonstrated that mimicked Ser615 phosphorylation slightly downregulated NO release (Bauer *et al.*, 2003). Phosphorylation of Ser615 was postulated to be an important modulator of phosphorylation at Ser1177 and increased the interaction of eNOS with hsp90 and PKB (Bauer *et al.*, 2003).

Phosphorylation of Ser633, which is also located in the FMN binding domain of eNOS, has been reported to increase eNOS activity. Similar to $eNOS^{S1177}$, $eNOS^{S633}$ is phosphorylated in response to shear stress, ATP, VEGF and bradykinin (Boo *et al.*, 2002, Michell *et al.*, 2002, Bauer *et al.*, 2003). Site-directed mutagenesis of eNOS phospho-sites demonstrated that the bovine site Ser635 (equivalent to human Ser633) is an important positive regulator of basal and ATP-stimulated NO release (Bauer *et al.*, 2003). Mimicking phosphorylation at Ser635 been shown to contribute to eNOS activity *in vitro* (Michell *et al.*, 2002).

In contrast to $eNOS^{S1177}$, $eNOS^{S633}$ appears to play a role in mediating prolonged, rather than acute, eNOS activity, as $eNOS^{S633}$ phosphorylation occurred more slowly than $eNOS^{S1177}$ phosphorylation (Boo *et al.*, 2002, Bauer *et al.*, 2003). Phosphorylation of bovine $eNOS^{S635}$ does not require a rise in intracellular Ca^{2+} to stimulate NO synthesis (Boo *et al.*, 2003). PKA has been identified as a likely candidate for $eNOS^{S633}$ phosphorylation, whereas PKB does not phosphorylate this site (Boo *et al.*, 2002, Michell *et al.*, 2002, Boo *et al.*, 2003).

1.2.6.4 Interaction of eNOS with other molecules

eNOS is known to form a complex with the molecular chaperone hsp90 and the activating kinase PKB. This complex has been proposed to permit rapid activation of eNOS (Garcia-Cardena *et al.*, 1998, Fontana *et al.*, 2002, Takahashi & Mendelsohn, 2003). It has been proposed that hsp90 acts as a molecular scaffold by binding to the N-termini of eNOS and PKB, bringing these two molecules into close proximity and promoting eNOS activation (Fontana *et al.*, 2002). This interaction is thought to be important for VEGF- and insulin-stimulated activation of eNOS *in vitro* (Fontana *et al.*, 2002, Takahashi & Mendelsohn, 2003).

An eNOS interaction partner called NOSTRIN (eNOS traffic inducer) has been identified by yeast-2-hybrid studies. This protein binds to eNOS *in vitro* and *in vivo*. In HUVEC, NOSTRIN colocalised with eNOS at the plasma membrane. NOSTRIN is postulated to influence the subcellular distribution and activity of eNOS (Zimmermann *et al.*, 2002).

NOSIP (eNOS interacting protein) is a further interaction partner of eNOS that has been identified by yeast-2-hybrid experiments. NOSIP is expressed in HUVEC and binds to the oxygenase domain of eNOS. It has been shown to mediate translocation of exogenously expressed eNOS from the plasma membrane to intracellular locations, thereby inhibiting NO synthesis (Dedio *et al.*, 2001).

1.3 Insulin signalling

Insulin is a polypeptide hormone that functions as an important mediator of metabolic and mitogenic cellular actions, including glucose, protein and lipid metabolism as well as cell growth and differentiation. It is produced from preproinsulin by proteolysis in pancreatic ß cells (see Figure 1-3), releasing C-peptide as a byproduct. Insulin secretion is stimulated by elevated blood glucose levels (Siddle, 2005).

In this section, the metabolic and mitogenic insulin signalling pathways and their components will be described, along with the downstream effects of insulin signalling.

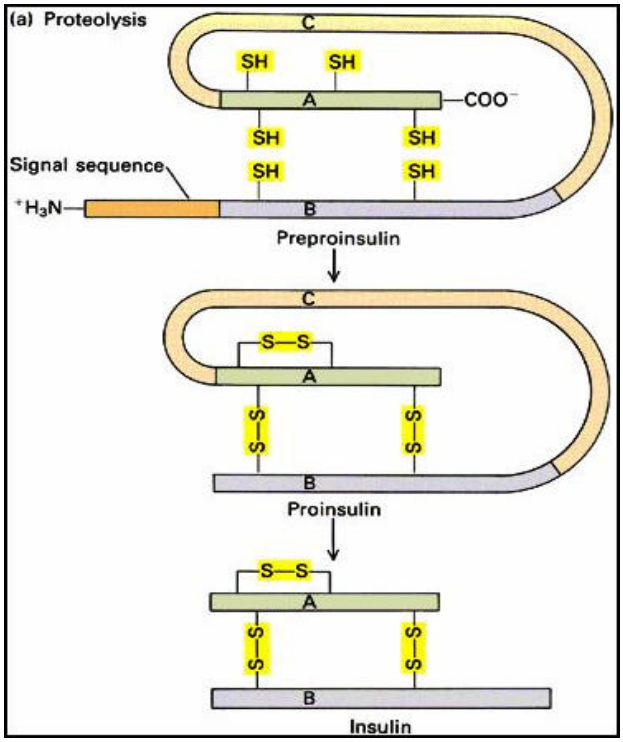

Figure 1-3 Production of insulin from preproinsulin

Insulin is produced from preproinsulin in the pancreatic ß cells after the N-terminal signal sequence and C-peptide have been cleaved by proteolysis. Diagram adapted from http://www.kensbiorefs.com/humphy.html

1.3.1 The insulin receptor

The existence of an insulin receptor was first proposed by House and Weidemann in 1970 (House & Weidemann, 1970). However, it was not until 1978 that direct evidence for the existence of the insulin receptor was obtained by Yip and co-workers (Yip *et al.*, 1978). The insulin receptor family belongs to the superfamily of receptor tyrosine kinases (RTKs) and contains three homologous, dimeric transmembrane receptors: the insulin receptor (IR), the insulin-like growth factor-1 receptor (IGF-1R) and the insulin receptor-related receptor (IRR). The RTK superfamily also comprises the monomeric RTKs epidermal growth factor (EGF) receptor (Ebina *et al.*, 1985), platelet-derived growth factor (PDGF) receptor and the vascular endothelial growth factor (VEGF) receptor (Fantl *et al.*, 1993, Deller & Yvonne Jones, 2000).

IR, IGF-1R and IRR share approximately 60% sequence identity (Ullrich *et al.*, 1986, Zhang & Roth, 1992). It is known that IR subunits can form hybrids with IGF-1R subunits (Moxham *et al.*, 1989, Soos & Siddle, 1989, Treadway *et al.*, 1989), and possibly with IRR subunits. No ligand has yet been identified for the IRR, though its tyrosine kinase domain is capable of phosphorylating the same spectrum of substrates as the IR (Zhang & Roth, 1992); therefore, the significance of these potentially occurring hybrids is unclear.

1.3.1.1 Insulin receptor structure

The functional insulin receptor is composed of two identical subunits, each being derived from a single, polypeptide pro-receptor (Siddle, 2005). Each subunit comprises an N-terminal extracellular α-subunit and a C-terminal, transmembrane domain-containing β-subunit that extends into the cytoplasm and contains the tyrosine kinase (TK) domain (Kasuga *et al.*, 1982, Ebina *et al.*, 1985).

One individual IR subunit is comprised of two β-helical domains (named L1 and L2) flanking a cysteine-rich (CR) domain, three fibronectin type III repeats (Fn0, Fn1 and Fn2; of which Fn1 contains the cleavage site between the α- and β-subunits), a juxtamembrane (JM) region, a tyrosine kinase (TK) domain and a CT domain, (see Figure 1-4). This domain structure is shared by the IGF-1R (Czech & Massague, 1982, Ullrich *et al.*, 1986). The individual IR subunits are disulphide-bonded in a β-α-α-β fashion (Czech & Massague, 1982).

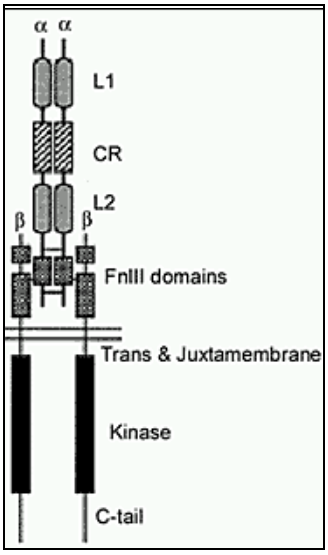

Figure 1-4 Insulin receptor domain structure

The dimeric insulin receptor is composed of extracellular a subunits and transmembrane ß subunits that contain the tyrosine kinase activity. Figure adapted from (Zhang)

1.3.1.2 Insulin binding to the insulin receptor

The insulin receptor has a high affinity and specificity for insulin (Siddle, 2005). Either one or two molecules of insulin can bind to the IR, in a negatively cooperative fashion, the affinity for insulin being determined by the IR dimerisation domain encoded by exon 10 (Surinya *et al.*, 2002, Siddle, 2005). One hydrophobic and one polar conformational surface in the IR have been identified as essential for insulin binding (Ottensmeyer *et al.*, 2000, De Meyts & Whittaker, 2002).

Binding of insulin to the IR induces conformational changes in the receptor, which activates the receptor TK domains to reciprocally autophosphorylate tyrosine residues in the ß-subunits. Several tyrosine residues in the JM, TK and CT regions can be autophosphorylated (Siddle, 2005), but the tyrosine residues 1158, 1162 and 1163 in the regulatory loop of each ß-subunit have been identified as important for the metabolic arm of insulin signalling (Ellis *et al.*, 1986, Frattali *et al.*, 1992, Cann & Kohanski, 1997). In the closed, inactive state, this regulatory loop blocks a cleft in the insulin receptor structure that contains the active site, but autophosphorylation is thought to cause repositioning of the loop to allow IR substrates access to the active site (Hubbard & Till, 2000).

Autophosphorylation of an $NPEY^{960}$ motif in the JM region of the IR is critical for creation of a binding site for the phosphotyrosine-binding (PTB) domains of insulin receptor substrate-1 and -2 (IRS-1 and -2) and Shc (Src-homology and collagen-like) proteins (Gustafson *et al.*, 1995, Wolf *et al.*, 1995); while the substrates APS (Hu *et al.*, 2003) and Grb10 (Stein *et al.*, 2003) bind to the phosphorylated tyrosine residues in the activation loop via their SH2 domains. Furthermore, autophosphorylation also plays a role in receptor internalisation.

The activated insulin-IR complex is internalised via clathrin-coated vesicles and targeted to endosomes, where the acidic pH causes dissociation of insulin from its receptor (Carpentier, 1994). Insulin is subsequently degraded by endosomal and/or lysosomal proteases (Bondy *et al.*, 1994, Carpentier, 1994, Di Guglielmo *et al.*, 1998). The IR is then dephosphorylated (and thus inactivated) by phosphotyrosine phosphatases such as PTP1B (Elchebly *et al.*, 1999, Klaman *et al.*, 2000) and the majority of insulin receptors are recycled to the plasma membrane (Carpentier, 1994).

1.3.1.3 Modulation of insulin receptor function

It has been suggested that insulin signalling may be transiently but significantly prolonged by IR-bound insulin in the endosome compartment, where the IR may have access to intracellular substrates (Di Guglielmo *et al.*, 1998). By contrast, serine/threonine phosphorylation of the IR by kinases, including several isoforms of protein kinase C (PKC), may downregulate receptor TK activity without affecting its insulin binding ability (Bollag *et al.*, 1986, Liu & Roth, 1994, Bossenmaier *et al.*, 1997, Strack *et al.*, 2000). Such downregulation of IR TK function has been suggested to be responsible for glucose-mediated inhibiton of insulin signalling (Berti *et al.*, 1994, Mosthaf *et al.*, 1995, Pillay *et al.*, 1996) and to contribute to obesity-associated insulin resistance (Zhou *et al.*, 1999).

1.3.2 Metabolic actions of insulin

Upon stimulation by insulin, the insulin receptor phosphorylates several cellular substrates via its tyrosine kinase domain and thus initiates a number of intracellular signalling pathways. The most well defined pathways are the metabolic phosphatidylinositide 3-kinase (PI3K)/protein kinase B (PKB) pathway, which stimulates glucose transporter translocation to the plasma membrane, as well as production of NO by eNOS in endothelial cells and stimulation of the mitogenic MAPK/ERK pathway.

As discussed above, activation of the IR by autophosphorylation results in creation of substrate binding sites and the subsequent phosphorylation of these substrates by the IR. The insulin receptor substrates-1 and -2 (IRS-1 and -2) are major components of both metabolic and mitogenic insulin signalling (White, 1998, 2002). They are 180-190 kDa proteins (White *et al.*, 1985) that contain tandem pleckstrin homology (PH) (Shaw, 1993, Sun *et al.*, 1995) and phosphotyrosine binding (PTB) domains (Sun *et al.*, 1995) and act as highly efficient scaffolding proteins in the recruitment of the lipid kinase PI3K (Sun *et al.*, 1991). With its tandem SH2 domains, PI3K then binds preferentially to the phosphotyrosine residues that are arranged in YxxM motifs of IRS-1 and -2 (White, 1998). Although there is some functional redundancy between IRS-1 and IRS-2, they also have specific roles (Bruning *et al.*, 1997, White, 2002) and differ in their tissue-specific expression: IRS-1 is more prominent in skeletal muscle and IRS-2 more abundant in the liver (Kido *et al.*, 2000).

PI3K is composed of a p85/55 adaptor subunit and a p110 catalytic subunit, both of which exist in multiple isoforms (Shepherd *et al.*, 1998). Phosphorylated IRSs recruit PI3K to the plasma membrane, where PI3K catalyses the conversion of its preferred substrate, the membrane phospholipid phosphatidyl inositol (4,5)bis-phosphate ($PI(4,5)P_2$), to phosphatidyl inositol (3,4,5)tris-phosphate ($PI(3,4,5)P_3$) (Siddle, 2005). $PI(3,4,5)P_3$ serves to anchor PI3K and the 3-phosphoinositide dependent protein kinase-1 (PDK-1) to the plasma membrane (Shepherd *et al.*, 1998). $PI(3,4,5)P_3$ also has a high affinity for the 57 kDa protein kinase B (PKB, also known as Akt), which colocalises with $PI(3,4,5)P_3$ at the plasma membrane.

The phosphatase PTEN (Phosphatase-and-tensin-homologue-deleted-on-chromosome-10) counteracts PI3K activity by dephosphorylating $PI(3,4,5)P_3$ to $PI(4,5)P_2$, thereby negatively regulating PI3K activity (Oudit *et al.*, 2004). PTEN is also involved in the inhibition of eNOS activation via insulin signalling pathway components in response to

various pathological conditions, including the metabolic syndrome (Shen *et al.*, 2006a, Shen *et al.*, 2006b, Wang *et al.*, 2006).

PDK-1 and PDK-2 activate PKB in a PI3K-dependent manner (Burgering & Coffer, 1995, Kroner *et al.*, 2000). PKB is phosphorylated by PDK-1 at threonine 308 (Wick *et al.*, 2000), and by PDK-2 at serine 473 (Kroner *et al.*, 2000). Activated PKB then phosphorylates a variety of substrates, including glycogen synthase kinase-3 (GSK-3), phosphofructokinase-2 (PFK-2), the proapoptotic BAD proteins and caspase 9 (Vanhaesebroeck & Alessi, 2000, Lawlor & Alessi, 2001, Vivanco & Sawyers, 2002, Whiteman *et al.*, 2002). This triggers further signalling cascades that, in the case of glucose transport, result in the translocation of glucose transporter 4 (GLUT4)-containing vesicles to the plasma membrane of adipocytes and striated muscle, thus enabling glucose transport into the cell (Wang *et al.*, 1999, Whiteman *et al.*, 2002).

Importantly, insulin can dose-dependently stimulate eNOS activity in endothelial cells (Aljada & Dandona, 2000) via calcium-independent, PI3K- and PKB-dependent phosphorylation at serine 1177 (Zeng & Quon, 1996, Dimmeler *et al.*, 1999, Fulton *et al.*, 1999, Zeng *et al.*, 2000). This phosphorylation activates eNOS-mediated production of NO (see Figure 1-5). Insulin also stimulates the uptake by endothelial cells of the NOS substrate L-arginine via the L-arginine transporter y+ (Sobrevia *et al.*, 1996), thus ensuring the substrate supply for increased eNOS-mediated NO production and vasodilation.

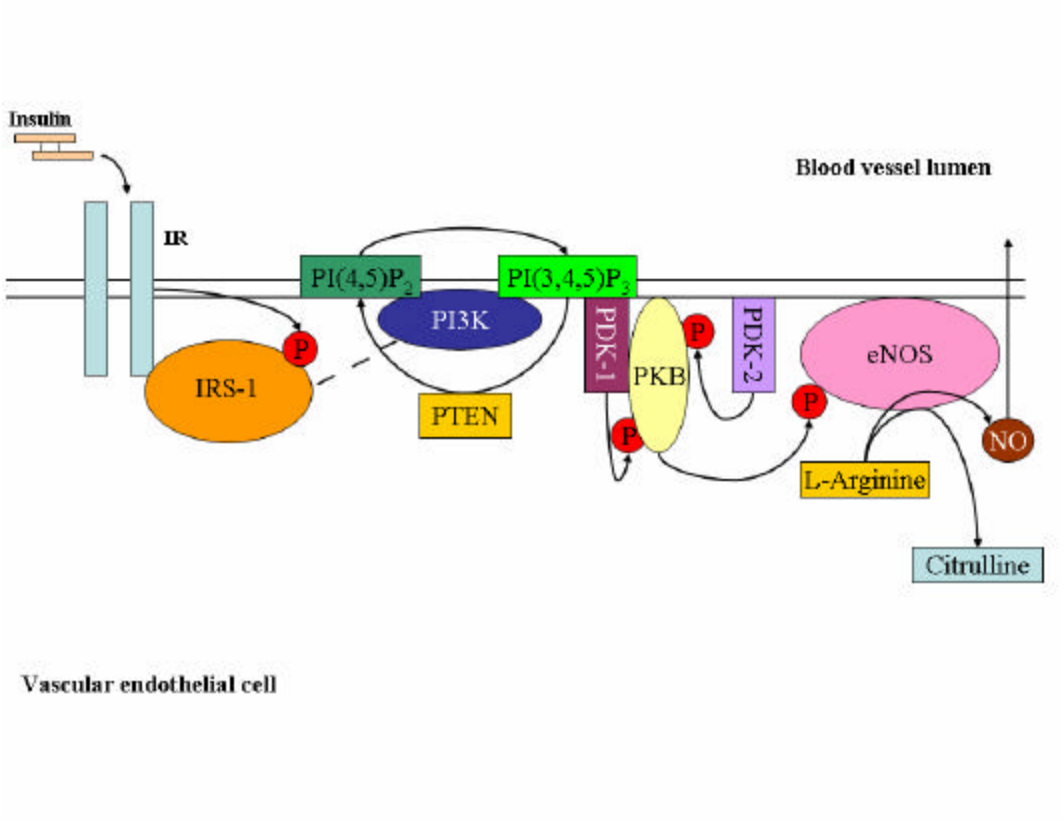

Figure 1-5 The metabolic insulin signalling pathway and NO production

Insulin binds to its receptor (IR) and triggers IR autophosphorylation. The IR then phosphorylates the IR substrate (IRS), which in turn binds to PI3K and recruits it to the plasma membrane. PKB is dually phosphorylated by PDK-1 and PDK-2 in a PI3K-dependent manner. Activated PKB then activates eNOS by direct phosphorylation at Ser1177, stimulating NO synthesis.

1.3.3 Mitogenic actions of insulin

Another major signalling pathway triggered by insulin is the extracellular-regulated kinase (ERK)/mitogen-activated protein kinase (MAPK) pathway, which regulates the transcription of genes required for cell growth and division (Denton & Tavare, 1995, Lazar *et al.*, 1995, Azpiazu *et al.*, 1996), as well as the genes for insulin-like-growth-factor-binding protein 1 (IGFBP-1) and the glucose-6-phosphatase (G6Pase) catalytic subunit (O'Brien & Granner, 1996, O'Brien *et al.*, 2001). The insulin receptor phosphorylates IRSs and Shc (Src-homology and collagen-like) proteins (Kovacina & Roth, 1993, Pronk *et al.*, 1993), both of which are capable of binding the adaptor protein Grb2 (Skolnik *et al.*, 1993), which then activates the ERK/MAPK pathway through binding of SOS and activation of Ras and Raf (Avruch *et al.*, 1994, Okada *et al.*, 1998, Siddle, 2005).

The mitogenic pathway also contributes to regulation of glucose metabolism, as insulin-mediated inhibition of the expression of phosphoenolpyruvate carboxykinase (PEPCK) and G6Pase in the liver leads to suppression of hepatic gluconeogenesis (O'Brien & Granner, 1996, Patel *et al.*, 2003). Patients with type I and type II diabetes show lack of insulin-mediated suppression of gluconeogenesis (Basu *et al.*, 2004), as has also been demonstrated in experimental animal models (Barzilai & Rossetti, 1993, Hofmann *et al.*, 1995). Overexpression of PEPCK in animals causes impaired glucose tolerance and insulin resistance (Valera *et al.*, 1994), while elevated G6Pase expression in mice gives rise to a state resembling type II diabetes (Trinh *et al.*, 1998).

1.3.4 Other aspects of insulin signalling

Additional pathways that are modulated by insulin action include the CAP/Cbl/TC10 pathway, which plays a role in glucose transport (Baumann & Saltiel, 2001, Saltiel & Pessin, 2003), and the JAK-STAT pathway, which exerts effects on gene expression (Gual *et al.*, 1998, Sawka-Verhelle *et al.*, 2000, Le *et al.*, 2002). Furthermore, an additional insulin receptor substrate, IRS-4, is postulated in humans to bind PI3K and Grb2 (Lavan *et al.*, 1997a). IRS-3 is found only in rodents and has no functional human orthologue (Lavan *et al.*, 1997b, Bjornholm *et al.*, 2002).

1.4 Insulin resistance and hyperinsulinaemia

Insulin resistance can be defined as dysregulated glucose-insulin homeostasis, in which peripheral tissues (such as skeletal muscle and adipose tissue) show decreased glucose uptake in response to insulin. Obesity and physical inactivity are the environmental factors most strongly associated with insulin resistance, but genetic factors also add to susceptibility (Chisholm *et al.*, 1997, Wheatcroft *et al.*, 2003).

Hyperinsulinaemia is commonly described as a compensatory mechanism triggered by insulin resistance, rather than the cause of resistance (Ginsberg, 2000). Nevertheless, hyperinsulinaemia may also contribute to the maintenance of insulin resistance, since experimental hyperinsulinaemia causes insulin resistance in rats (Juan *et al.*, 1999) and mice (Marban *et al.*, 1989), and because insulin sensitivity in obese subjects generally improves following weight loss (Reaven, 2005).

Insulin resistance and hyperinsulinaemia are both independent risk factors for a number of pathological disorders, such as cardiovascular disease (Despres *et al.*, 1996, Bokemark *et al.*, 2001), hypertension (Welborn *et al.*, 1966, Ginsberg, 2000), atherosclerosis (Howard *et al.*, 1996, Stolar & Chilton, 2003, Wheatcroft *et al.*, 2003), dyslipidaemia (Ginsberg, 2000), and type II diabetes (Stolar & Chilton, 2003). However, insulin resistance/hyperinsulinaemia likely acts in concert with other risk factors in the pathogenesis of all of these diseases, as patients with insulin-secreting tumours (insulinomas) do not tend to have hypertension (Haffner *et al.*, 1992) or atherosclerosis (Leonetti *et al.*, 1993).

The involvement of hyperinsulinaemia/insulin resistance in the context of endothelial dysfunction is discussed below, and some of the mechanisms that have been postulated to contribute to the causes and effects of insulin resistance and hyperinsulinaemia are described.

1.4.1 Insulin resistance and endothelial dysfunction

Insulin resistance is strongly linked to endothelial dysfunction, but it is still debated whether insulin resistance is a cause or a result of endothelial dysfunction (Wheatcroft *et al.*, 2003). The course of pathological events in animal models of insulin resistance suggests that insulin resistance may promote endothelial dysfunction (Katakam *et al.*,

2001, Mather *et al.*, 2001, Wheatcroft *et al.*, 2003). However, it has also been postulated that peripheral endothelial dysfunction, at the arteriolar and capillary level, is the main cause for the development of insulin resistance and its associated metabolic disturbances, while central, large vessel endothelial dysfunction promotes atherogenesis without significantly affecting metabolism. Thus, insulin resistance may be a marker, rather than a causative agent, of peripheral endothelial dysfunction (Pinkney *et al.*, 1997). In keeping with this hypothesis, eNOS-knockout mice develop insulin resistance (Shankar *et al.*, 2000). In humans, pathological and experimental hyperinsulinaemia are linked to impaired vasodilation, suggesting that hyperinsulinaemia may be not only a contributor to, but also a cause of endothelial dysfunction (Steinberg *et al.*, 1996, Balletshofer *et al.*, 2000, Cleland *et al.*, 2000).

Insulin sensitivity and basal NO production in humans are closely and positively correlated (Petrie *et al.*, 1996). Insulin-resistant patients show defective endothelium-dependent vasodilation (Steinberg *et al.*, 1996, Laine *et al.*, 1998, Cleland *et al.*, 2000). Furthermore, endothelial dysfunction is also evident in first-degree relatives of patients with type II diabetes (Balletshofer *et al.*, 2000).

Many insulin-resistant patients have elevated endothelin-1 levels proportional to the degree of hyperinsulinaemia (Mather *et al.*, 2001). A possible cause for this observation is the ability of insulin to directly stimulate the production of endothelin-1 *in vitro* (Yanagisawa *et al.*, 1988). At the vascular level, increased endothelin-1 production could further aggravate the imbalance between vasodilators and vasoconstrictors, as NO and endothelin-1 can reciprocally regulate one another at several levels, including the transcriptional level (Mather *et al.*, 2001). Endothelin-1 has been shown to inhibit the PI3K pathway in vascular smooth muscle cells (Jiang *et al.*, 1999b). If endothelin-1 also inhibits the endothelial PI3K pathway, imbalanced production of NO and endothelin-1 could potentially exacerbate impaired vasodilation and endothelial dysfunction.

1.4.2 Insulin resistance and proinflammatory mediators

Inflammation has been implicated in the pathogenesis of insulin resistance and is also strongly linked to endothelial dysfunction (Kubes *et al.*, 1991, Yudkin *et al.*, 1999, Aljada *et al.*, 2000, Ziccardi *et al.*, 2002, Wheatcroft *et al.*, 2003, Dandona *et al.*, 2004). Elevated levels of C-reactive protein (CRP), and the proinflammatory adipocytokines tumour

necrosis factor a (TNFa) and IL-6 have all been postulated as inflammatory mediators of endothelial dysfunction and insulin resistance (Feinstein *et al.*, 1993, Valverde *et al.*, 1998, Winkler *et al.*, 1999, Yudkin *et al.*, 1999, Halse *et al.*, 2001, Bastard *et al.*, 2002, Ritchie *et al.*, 2004). It is known that these proinflammatory cytokines trigger a positive feedback loop: via phosphorylation of I?B and activation of NF?B, they mediate their own transcription, as well as that of cell adhesion molecules (ICAM-1 and VCAM-1), monocyte chemoattractant protein-1 (MCP-1) and CRP (Dandona *et al.*, 2002).

Obese individuals present with elevated adipose-derived TNFa concentrations, and this correlates with hyperinsulinaemia and insulin resistance (Winkler *et al.*, 1999, Yudkin *et al.*, 1999, Ritchie *et al.*, 2004). Pharmacological administration of TNFa in humans gives rise to insulin resistance, and TNFa knockout mice do not develop obesity-induced insulin resistance (reviewed in (Wheatcroft *et al.*, 2003)). TNFa is known to impair the phosphorylation of the insulin receptor by triggering serine phosphorylation of IRS-1, which blocks insulin receptor kinase activity (Hotamisligil *et al.*, 1994a, Hotamisligil *et al.*, 1994b, Hotamisligil *et al.*, 1996), thus likely blunting the insulin-stimulated response. Furthermore, TNFa enhances PKB dephosphorylation and inactivation in endothelial cells, thus potentially triggering pro-apoptotic signalling cascades in these cells (Ritchie *et al.*, 2004). TNFa also promotes monocyte adhesion through increased expression of adhesion molecules (Ritchie *et al.*, 2004).

Insulin can counter inflammatory stimuli in human aortic endothelial cells *in vitro* and in human mononuclear cells *in vivo* via the inhibition of NF?B and the stimulation of I?B (Dandona *et al.*, 2001). Physiological levels of insulin were thus able to suppress expression of ICAM-1 and MCP-1 *in vitro* (Aljada *et al.*, 2000, Aljada *et al.*, 2001). Consistent with this observation, the insulin-sensitising thiazoledinedione drugs inhibit NF?B and thus block TNFa-mediated insulin resistance (Peraldi *et al.*, 1997, Dandona *et al.*, 2002). Furthermore, administration of the anti-inflammatory drug aspirin improves insulin sensitivity by inhibiting hepatic gluconeogenesis (Dandona *et al.*, 2002, Hundal *et al.*, 2002). These data provide evidence for an anti-inflammatory effect of insulin at physiological concentrations (Dandona *et al.*, 2002).

1.4.3 Endothelial dysfunction and leukocyte adhesion

Increased leukocyte adhesion to endothelial cells is a feature of endothelial dysfunction. This process is proatherogenic, forming a key early event in the formation of atherosclerotic plaques. Likewise, transendothelial migration of leukocytes contributes to the initiation of atherosclerosis (Okouchi *et al.*, 2002a) and possibly to the rupture of atherosclerotic plaques (van der Wal *et al.*, 1994). Transendothelial migration (also known as transmigration or diapedesis) is regulated through the expression of endothelial adhesion molecules and chemotactic molecules including monocyte chemotactic protein-1 (MCP-1). *In vitro* studies routinely use leukocyte subtypes such as neutrophils and monocytic cell lines to study leukocyte migration behaviour.

A number of studies have demonstrated that elevated insulin concentrations alter the expression of cellular adhesion molecules in endothelial cells. *In vitro*, insulin was reported to upregulate the expression of PECAM-1 and to promote neutrophil transendothelial migration in a dose-dependent manner via the MAPK pathway (Okouchi *et al.*, 2002a). Likewise, the MAPK pathway was also implicated in promoting *in vitro* neutrophil transendothelial migration and elevated expression of intercellular adhesion molecule-1 (ICAM-1) in human umbilical vein endothelial cells (HUVEC) exposed to pathophysiological concentrations of insulin (Okouchi *et al.*, 2002b, Okouchi *et al.*, 2003). Conversely, Aljada and co-workers (Aljada *et al.*, 2000) found that experimental hyperinsulinaemia decreased the expression of ICAM-1 mRNA and protein in cultured human aortic endothelial cells (HAEC) through increased eNOS expression and endothelial NO production, thereby acting as an antiatherogenic stimulus. A potential explanation for these conflicting findings may be the use of different endothelial cell types in these studies.

Expression levels of vascular cell adhesion molecule-1 (VCAM-1) were reported to be upregulated through the MAPK pathway, when HUVEC were treated with pathophysiological concentrations of insulin for up to 24 hours (Madonna *et al.*, 2004). However, *in vivo* data from a study using the euglycaemic hyperinsulinaemic clamp demonstrated that short-term hyperinsulinaemia has no adverse effect on the levels of circulating soluble ICAM-1, VCAM-1 or E-selectin in healthy males (Jilma *et al.*, 2000). In support of this, although plasma concentrations of soluble VCAM-1 are elevated in diabetic patients, hyperinsulinaemia did not upregulate VCAM-1 expression *in vitro* or secretion *in vivo* (De Mattia *et al.*, 1999).

It is possible that membrane-bound and secreted (soluble) adhesion molecules serve different purposes. Adhesion molecules on the surface of endothelial cells anchor leukocytes to the endothelium, thus promoting plaque formation. By contrast, secreted adhesion molecules may bind to the integrins expressed on the surface of leukocytes, thus preventing them from binding to the vascular endothelium and counteracting atherogenesis. The precise role of secreted adhesion molecules requires further clarification. Therefore, the overall effect of hyperinsulinaemia on endothelial expression and secretion of adhesion molecules and the resulting impact on atherogenesis remain unclear.

Chemokines play a crucial role in the attraction of monocytes to the vascular endothelium. Vascular endothelial cells have been shown to secrete a number of chemokines, including MCP-1, -2 and -3, MIP-1a and -1ß, MIG, Eotaxin, RANTES, GRO and IP-10 (Pellegrino *et al.*, 2005, Simionescu, 2007). MCP-1 has been implicated in monocyte recruitment to the vascular endothelium (Charo & Taubman, 2004, Simionescu, 2007), but the precise roles of endothelial chemokines in atherogenesis are still under investigation.

1.5 Hyperglycaemia

All tissues in the body use glucose as an energy source, though only the brain and erythrocytes have an absolute requirement for glucose. The main target tissues for glucose disposal after a meal are muscle, liver and adipose tissue, which store excess glucose as glycogen (in liver and muscle) and triglycerides (in adipose). Muscles store about 90% of ingested glucose. Stored glucose is used to meet energy demands of the tissue. The liver is the only organ able to release glucose into the circulation in response to decreasing blood glucose levels. The liver produces glucose through glycogenolysis and gluconeogenesis.

Hyperglycaemia is a consequence of dysregulated glucose homeostasis. It is characterised by pathologically elevated blood glucose concentrations (fasting >7 mmol/L; post-prandial >11.1 mmol/L), and is a defining feature of overt diabetes. In Type I diabetes, insulin-secreting pancreatic ß cells are destroyed by an autoimmune response that eventually leads to a complete loss of insulin secretion. Hyperglycaemia becomes diagnostic of Type II diabetes when secretion of insulin by pancreatic ß cells can no longer meet the demand of insulin-resistance for insulin, and undergo cell death as a result. In Type II diabetes, residual insulin secretion may remain, but this is insufficient to overcome the tissue's

resistance to insulin. As a consequence of inappropriate or absent insulin secretion, glucose is no longer appropriately taken up into target tissues and hepatic gluconeogenesis is not inhibited, causing a rise in blood sugar levels (see Figure 1-6).

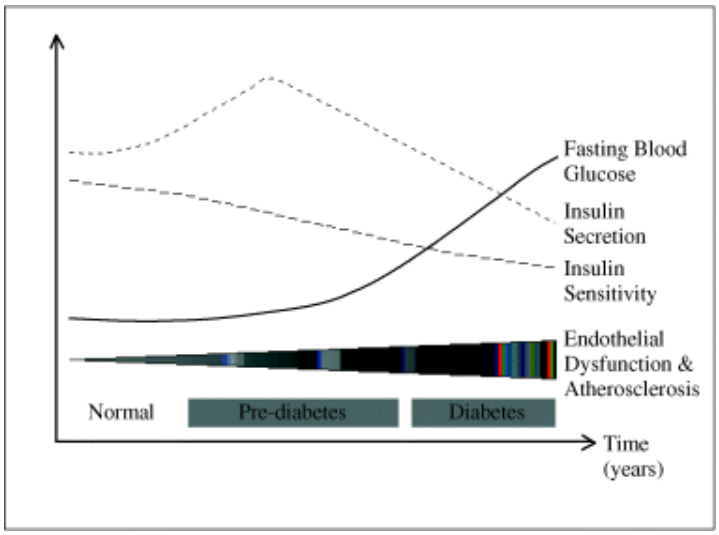

Figure 1-6 Correlation between insulin sensitivity and the development of Type II diabetes

With progressive loss of insulin sensitivity, endothelial function and the control of blood sugar levels worsen and type II diabetes develops. Figure adapted from (Wheatcroft *et al.*, 2003)

1.6 Insulin resistance, hyperglycaemia and associated disorders

Insulin resistance/hyperinsulinaemia and hyperglycaemia are strongly associatedwith several disorders, including obesity, Type II diabetes, atherosclerosis, hypertension and cardiovascular disease (for reviews, see (Ginsberg, 2000, Stolar & Chilton, 2003, Wheatcroft *et al.*, 2003). It is estimated that about 25% of the adult population in the UK and the United States have some degree of insulin resistance, many of whom will go on to develop Type II diabetes (Ritchie *et al.*, 2004).

The metabolic syndrome (also known as insulin-resistance syndrome or syndrome X) is a term used for a specific cluster of metabolic disorders that frequently manifest together, especially in the obese. These disorders comprise insulin resistance, hyperinsulinaemia, hyperglycaemia, central (visceral) obesity, hypertension, dyslipidaemia (especially elevated triglyceride and decreased high-density lipoprotein (HDL) cholesterol

concentrations), endothelial dysfunction and impaired fibrinolysis (Stolar & Chilton, 2003).

1.6.1 Obesity

There is a clear correlation between obesity and the degree of insulin resistance (Steinberg *et al.*, 1996, Yudkin *et al*., 1999, Ritchie *et al.*, 2004). Most obese individuals present with some degree of insulin resistance (Ritchie *et al.*, 2004). According to the World Health Organisation's report 2002, a high body mass index accounts for 75% (males) to 83% (females) of the total risk for type II diabetes (World Health Organisation, 2002), which is itself a common consequence of insulin resistance. Weight loss, even as little as 5-10% of the body weight, has significant beneficial effects on insulin sensitivity, vascular endothelial function and NO bioavailability (Ziccardi *et al.*, 2002, Ritchie *et al.*, 2004, Reaven, 2005). Since obesity is characterised by increased adiposity, it is reasonable to speculate that the bioactive adipocytokines secreted by adipose tissue are involved in the regulation of endothelial function and insulin sensitivity (Ritchie *et al.*, 2004). In fact, adiposity has been postulated to cause a state of chronic, low level inflammation due to its secretion of proinflammatory molecules, which in turn may induce endothelial dysfunction and insulin resistance (Yudkin *et al.*, 1999).

1.6.2 Diabetes mellitus

Diabetes mellitus has traditionally been classified as either early-onset, hereditary "Type I diabetes" or maturity-onset "Type II diabetes". However, it is becoming increasingly clear that not all diagnosed cases of diabetes fit into these broad categories, and the boundaries between these two classes are often blurred. Type II diabetes is now increasingly found in the young. Conversely, Type I diabetes, which can occur as early as the neonatal stadium and traditionally has most commonly been diagnosed before the age of 20, is now sometimes diagnosed significantly later in life.

Type II diabetes (previously called "non-insulin-dependent diabetes mellitus" (NIDDM)) is a complex, multisystem disorder characterised by hyperglycaemia and insulin resistance (Stolar & Chilton, 2003). It is primarily associated with obesity and physical inactivity, but the disproportionately high incidence in Blacks, Hispanic/Latin Americans and American

Indians (Stolar & Chilton, 2003) suggests that genetic factors predispose to type II diabetes. Type II diabetes accounts for 90-95% of all diabetes cases (Stolar & Chilton, 2003, Schulze & Hu, 2005). The remaining 5-10% are attributable to insulin-dependent (type I) diabetes, an autoimmune disease to which sufferers are genetically predisposed (Friday *et al*., 1999). Type II diabetes develops secondary to insulin resistance and hyperinsulinaemia, and, like obesity, has been postulated to be a proinflammatory state (Pickup *et al.*, 1997, Dandona *et al.*, 2002, Wellen & Hotamisligil, 2005).

Subjects in the prediabetic state present with endothelial dysfunction and insulin resistance, but not with hyperglycaemia. The current aetiologic theory is that the pancreatic beta-cells secrete more insulin in response to peripheral insulin resistance (thus causing hyperinsulinaemia), but the increasing secretory burden accelerates apoptosis of the ß cells; insulin secretion declines progressively and is eventually lost. This process brings with it dysregulated glucose homeostasis, since glucose is no longer appropriately taken up into muscle and adipose tissue. In addition, hepatic gluconeogenesis is no longer suppressed (Basu *et al.*, 2004); therefore, hyperglycaemia ensues, which requires therapeutic intervention (Stolar & Chilton, 2003). Furthermore, because insulin suppresses lipolysis and thereby regulates the plasma concentrations of free fatty acids (FFA) under normal physiological conditions, loss of insulin secretion will also affect the levels of plasma free fatty acids. Once insulin resistance ensues, plasma FFA concentrations rise. In addition, low/absent insulin concentrations are no longer sufficient to suppress hepatic gluconeogenesis. This, together with dysregulated postprandial glucose uptake, contributes to hyperglycaemia (Reaven, 1988).

Type II diabetes is frequently associated with the components of the metabolic syndrome, and bears a two-fold increased risk of premature death (Centers for Disease Control and Prevention, 2003). Patients with type II diabetes suffer microvascular and macrovascular complications. Diabetic microvascular complications are the main cause of nephropathy (kidney failure), retinopathy (blindness) and non-traumatic amputations (Schulze & Hu, 2005). Macrovascular disorders, such as infarction and stroke, are the major cause of death in diabetic patients (Centers for Disease Control and Prevention, 2003), accounting for 75% of all deaths amongst adult type II diabetics (Laakso, 1995, Stolar & Chilton, 2003). Overall, Type II diabetes was the sixth most common cause of death in the United States in 1999 (Stolar & Chilton, 2003).

Type II diabetes is highly prevalent, in particular in so-called "westernised" countries, where the population tends to eat energy-dense, high-fat, high-sugar diets (Schulze & Hu, 2005). The global incidence of Types I and II diabetes in adults over 20 years of age was estimated to be 171 million cases in the year 2000, and is expected to rise to 366 million cases by 2030 (Wild *et al.*, 2004). The World Health Organisation reports that diabetes mellitus caused 987,816 deaths worldwide in 2002, which made up approximately 1.7% of all deaths in that year (World Health Organisation, 2002). In 2001, there were an estimated 1.8 million people affected by Type II diabetes in the UK, plus another one million thought to have not yet been diagnosed (Diabetes UK, 2001). The public health and economic burden of type II diabetes and its associated morbidity and mortality is enormous (Wild *et al.*, 2004), and annually accounts for many years of life spent either with disability or lost (World Health Organisation, 2002, Hedner *et al.*, 2005).

In the context of hyperglycaemia and diabetes, it has frequently been shown that endothelial function and NO bioavailability are impaired ((Calver *et al.*, 1992, McVeigh *et al.*, 1992, Hogikyan *et al.*, 1998); reviewed in (De Vriese *et al.*, 2000, Rask-Madsen & King, 2007)), and that this association is independent of the presence of the complicating risk factors, obesity and hypertension (Hogikyan *et al.*, 1998). Consequently, patients with diabetes have an increased propensity to cardiovascular and microvascular disease and associated morbidity and mortality (Stratton *et al.*, 2000, Rahman *et al.*, 2007).

The degree of insulin resistance predicts the extent of impairment of endothelium-dependent vasodilation (Ardigo *et al.*, 2006), and the risk for vascular complications strongly correlates with the level of hyperglycaemia in patients (Stratton *et al.*, 2000). However, this association is not definite, since two studies suggested that insulin-induced vasodilation was similar in the coronary vasculature of healthy and Type I diabetic subjects and was not impaired by short-term hyperglycaemia (Smits *et al.*, 1993, Sundell *et al.*, 2002). It may be that the extent and/or nature of endothelial dysfunction differs in Type I and Type II diabetes.

1.6.3 Atherosclerosis

Hyperinsulinaemia and hyperglycaemia are often associated with oxidative stress and endothelial dysfunction, marked by adhesion of inflammatory cells to vascular endothelial cells and transendothelial migration of leukocytes. In the subendothelial space, monocytes

transform into foam cells by ingestion of oxidised low-density lipoprotein (LDL) cholesterol, and eventually undergo apoptosis, thus forming so-called fatty streaks, while T lymphocytes contribute to inflammation through the release of cytokines (Stolar & Chilton, 2003). All of these factors contribute to the formation of atherosclerotic plaques, which, once formed, can turn into unstable plaques that rupture, resulting in unstable angina or myocardial infarction. This process is called atherogenesis.

Because insulin resistance-mediated endothelial dysfunction is also characterised by increased platelet activation/decreased platelet inhibition, elevated procoagulant expression, and impaired fibrinolysis, patients with Type II diabetes are also at increased risk of thrombus formation (Carr, 2001, Stolar & Chilton, 2003), which in turn affects the risk for cardiovascular events such as stroke. Figure 1-7 illustrates the parallel progression between insulin resistance and atherogenesis.

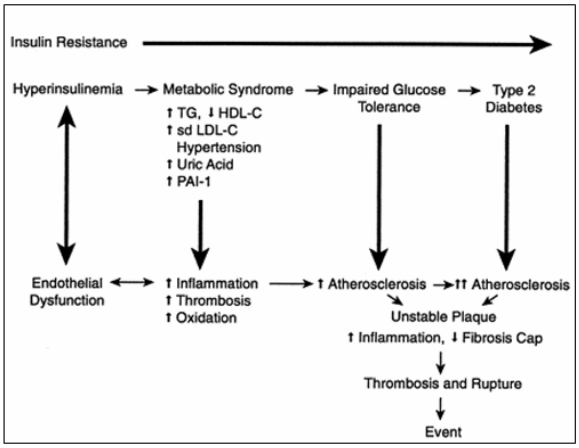

Figure 1-7 The parallel progression between insulin resistance and atherogenesis
Hyperinsulinaemia promotes endothelial dysfunction, which greatly increases the risk for both type II diabetes and atherosclerosis. Figure adapted from (Hsueh & Law, 2003)

1.6.4 Animal models

A number of animal models have been developed to study various aspects of insulin resistance, hyperglycaemia/diabetes, obesity, and endothelial dysfunction. Briefly, these animal models include the "Zucker" (fa/fa) rat model for insulin resistance (Kasiske *et al.*, 1992), the "non-obese diabetic" (NOD) mouse and BioBreeding (BB) rat models for hyperglycaemia/Type I diabetes (Yang & Santamaria, 2006), the diabetic (db/db) mouse

model for Type II diabetes and associated disorders (Kobayashi *et al.*, 2000), the obese (ob/ob) mouse model of obesity (Tschöp & Heiman, 2001), the "insulin receptor knockout" (IRKO) mouse (Wheatcroft *et al.*, 2004) and the "vascular endothelial insulin receptor knockout" (VENIRKO) mouse (Vicent *et al.*, 2003) for the study of IR function and insulin signalling, and "eNOS knockout" ($eNOS^{-/-}$) mouse (Huang *et al.*, 1995) for the assessment of eNOS function *in vivo*.

In addition, non-genetic models such as streptozotocin-induced diabetes in rats and mice (Cameron & Cotter, 1992, Hink *et al.*, 2001, Ho *et al.*, 2001, Kurlawalla-Martinez *et al.*, 2005, Song *et al.*, 2007, Fukuda *et al.*, 2008), and short-term hyperglycaemia induced by intraperitoneal glucose injection (Stalker *et al.*, 2003) have been used in research.

1.6.5 Oxidative stress in endothelial dysfunction

Reactive oxygen species (ROS) such as hydrogen peroxide and O_2^- are generated by enzymes such as NADPH oxidase and uncoupled eNOS. ROS are detrimental to endothelial function because they reduce NO bioavailability and thus interfere with vasodilation. Superoxide, for example, can react with NO, leading to formation of both peroxynitrite and nitrate (Reiter *et al.*, 2000). Peroxynitrite in turn can reduce NO bioavailability through oxidation and uncoupling of eNOS, leading to enhanced superoxide production and decreased NO synthesis (Zou *et al.*, 2002).

It has been demonstrated that experimental hyperinsulinaemia equivalent to concentrations typically encountered in insulin-resistant states, impairs endothelium-dependent vasodilation in the large conduit arteries in healthy humans (Arcaro *et al.*, 2002). In the study of Arcaro and co-workers (Arcaro *et al.*, 2002), oxidant stress was postulated to be the underlying reason for hyperinsulinaemia-induced endothelial dysfunction, since the antioxidant vitamin C completely reversed the adverse effects of experimental hyperinsulinaemia. It should be noted, though, that this was a study of short-term hyperinsulinaemia, and may not be representative of the *in vivo* state in patients.

In small coronary arteries from obese Zucker rats, a model of insulin resistance, insulin caused the production of superoxide anions that resulted in diminished NO bioavailability and increased vasoconstriction (Katakam *et al.*, 2005). Furthermore, when NADPH oxidase was inhibited pharmacologically, or when ROS were neutralised by the enzyme

superoxide dismutase, insulin's vasodilatory function was restored in these arteries. Interestingly, the coronary arteries of these obese Zucker rats expressed higher levels of eNOS, which was speculated to be a compensatory mechanism for the decreased NO bioavailability (Katakam *et al.*, 2005).

Previous work has shown that exposure to high glucose concentrations impaired vasodilation in rabbit aorta (Tesfamariam *et al.*, 1990) and increased superoxide anion generation in HAEC (Cosentino *et al.*, 1997) and rat aorta (Hink *et al.*, 2001). Oxidative stress has been proposed as a physiological mediator of endothelial dysfunction (De Vriese *et al.*, 2000, Hink *et al.*, 2001, Srinivasan *et al.*, 2004), although this link is subject to ongoing investigation and debate.

1.7 AMPK

The AMP-activated protein kinase (AMPK) is an enzyme involved in the regulation of energy homeostasis at the cellular and whole body level. AMPK was first discovered in 1973 on account of two of its enzymatic activities, which were later attributed to the same kinase (Beg *et al.*, 1973, Carlson & Kim, 1973, Carling *et al.*, 1987, Sim & Hardie, 1988).

AMPK is a heterotrimeric complex composed of a catalytic a-subunit, a glycogen-binding domain-containing ß-subunit and a ?-subunit, which binds AMP and/or ATP. The N-terminal domain of the a-subunit contains the kinase domain (see Figure 1-8). AMPK is expressed ubiquitously. For each AMPK subunit, several isoforms exist, which exhibit different tissue expression patterns (Towler & Hardie, 2007).

AMPK is phosphorylated on Thr172 by the upstream kinase LKB1, a tumour suppressor protein. Phosphorylation and activation of AMPK is triggered by increases in the cellular AMP:ATP ratio. Binding of AMP makes AMPK a worse substrate for AMPK phosphatases (Towler & Hardie, 2007), thereby increasing the proportion of phosphorylated AMPK. In a limited number of cell types, such as neurones and T cells, AMPK can be phosphorylated at Thr172 and activated in a calcium-dependent manner by the Ca^{2+}/CaM-dependent protein kinase kinase (CaMKK) (Hawley *et al.*, 2005, Woods *et al.*, 2005).

1.7.1 Roles of AMPK

As a regulator of energy homeostasis, AMPK is activated in response to metabolic stress, switching off energy-consuming pathways and activating ATP-producing pathways. Its main roles include stimulating glycolysis, glucose uptake and fatty acid oxidation, and inhibiting the synthesis of glycogen, fatty acids and cholesterol. AMPK also negatively regulates transcription and translation, as well as cell growth and proliferation (Towler & Hardie, 2007).

Importantly, AMPK has been shown to directly activate eNOS in human aortic endothelial cells by phosphorylation at Ser1177 *in vitro*, and increases endothelial NO synthesis in cultured HAEC in response to AICAR and VEGF (Morrow *et al.*, 2003, Reihill *et al.*, 2007). Therefore, AMPK is an attractive target for antidiabetic drugs, as it promotes an antiatherogenic phenotype and is involved in the regulation of glucose homeostasis.

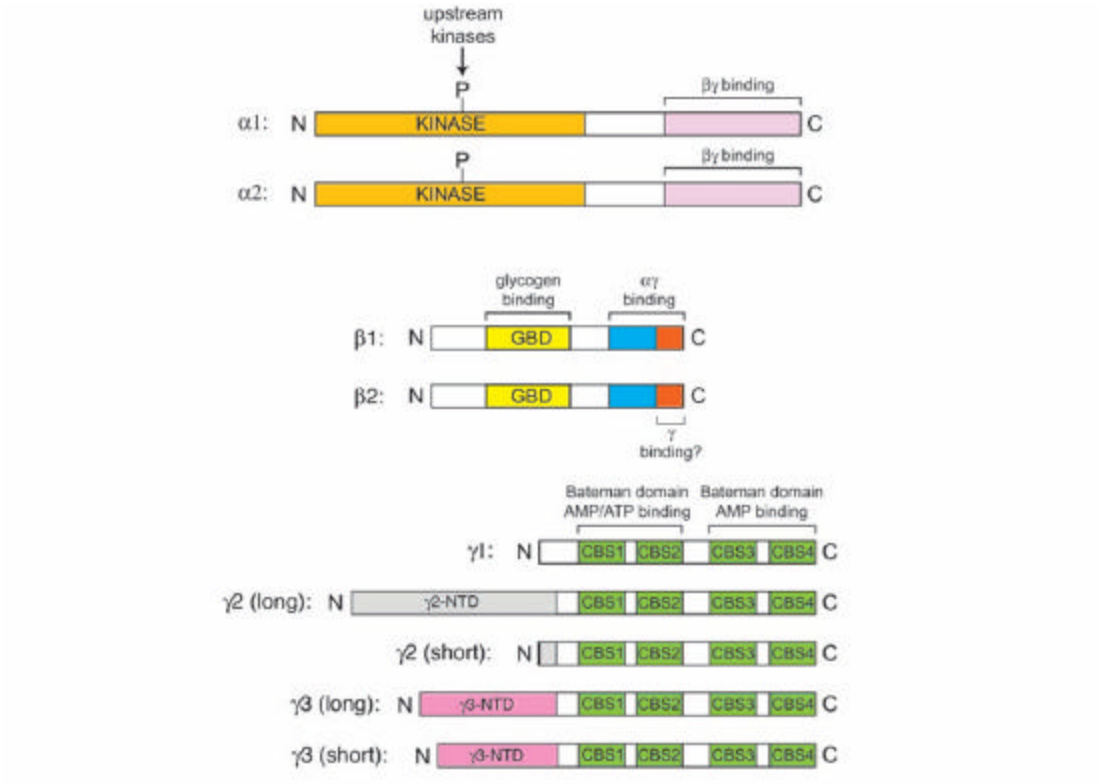

Figure 1-8 AMPK subunit structure

AMPK consists of one kinase domain-containing a-subunit, a glycogen binding domain-containing ß-subunit and a ?-subunit containing the AMP/ATP binding domains. Splice variants of subunits are shown. Figure adapted from (Towler & Hardie, 2007)

1.7.2 Regulation of AMPK activation

AMPK can be regulated by a number of factors, including blood glucose levels, hypoxia, adipocytokines, insulin and pharmacological agents (Towler & Hardie, 2007). Activation of AMPK in pancreatic ß cells and the liver by low blood glucose levels is dependent on the expression of glucokinase in these cells (Salt *et al.*, 1998, da Silva Xavier *et al.*, 2000). Glucokinase has a low affinity for glucose, thereby acting as a glucose sensor, so that cellular ATP levels fall with decreasing blood glucose levels as a result of decreased glycolysis. This in turn raises the AMP:ATP ratio, thus activating AMPK.

In some cell types, ligands acting on G_q-coupled receptors can activate AMPK, presumably through CaMKK-mediated AMPK phosphorylation. Bradykinin has been reported to activate recombinant AMPK expressed in Chinese hamster ovary (CHO) cells by a G-protein coupled mechanism (Kishi *et al.*, 2000), while thrombin dose- and time-dependently activates AMPK in HUVEC via a G_q-protein-mediated pathway that is independent of the cellular ATP:AMP ratio (Stahmann *et al.*, 2006).

The so-called adipocytokines (also known as adipokines) leptin and adiponectin are able to regulate AMPK activity. Adipocytokines are secreted from adipose cells and have been implicated in the regulation of whole body energy homeostasis and inflammation. Leptin has been shown to activate AMPK in the muscle of rats, leading to stimulation of fatty acid oxidation (Minokoshi *et al.*, 2002). Conversely, leptin inhibited AMPK activity in the paraventricular region in the hypothalamus of fasted mice, lowering food intake (Minokoshi *et al.*, 2004). Adiponectin has a blood glucose-lowering effect, as it stimulates glucose uptake and fatty acid oxidation in muscle, and inhibits gluconeogenesis in the liver by activating AMPK (Tomas *et al.*, 2002, Yamauchi *et al.*, 2002).

Insulin inhibited AMPK activity in all hypothalamic areas of fasted mice, thus reducing food intake. Furthermore, expression of dominant-negative AMPK in mice led to weight loss, whereas constitutively active AMPK expression resulted in increased food intake (Minokoshi *et al.*, 2004). These data suggest that modulation of AMPK activity alone can affect food intake and weight gain.

1.7.3 AMPK and insulin signalling

In general, the insulin signalling and AMPK pathways have opposite effects. In cardiac myocytes, insulin has been reported to inhibit AMPK, yet the two pathways also have similar effects on glucose homeostasis, since both pathways promote glucose uptake in skeletal muscle and suppress the transcription of enzymes involved in gluconeogenesis in the liver (Towler & Hardie, 2007). Like insulin, AMPK stimulates $eNOS^{S1177}$ phosphorylation, promoting NO synthesis (Morrow *et al.*, 2003, Reihill *et al.*, 2007).

1.7.4 AMPK as a target for antidiabetic drugs

The widely prescribed hypoglycaemic drug metformin has been shown to activate AMPK in a LKB1-dependent fashion (Zhou *et al.*, 2001, Shaw *et al.*, 2005), thereby presumably inhibiting gluconeogenesis. Similarly, the related drug phenformin, which is no longer prescribed, also stimulates AMPK activity *in vitro* (Hawley *et al.*, 2003).

Insulin-sensitising drugs such as the thiazoledinediones (TZDs) troglitazone, rosiglitazone and pioglitazone, have been widely used in the treatment of Type II diabetes (Chisholm *et al.*, 1997, Peraldi *et al.*, 1997, Fujiwara & Horikoshi, 2000, Ritchie *et al.*, 2004). TZDs bind with high affinity to PPAR?, a transcription factor that regulates the expression and release of adipocytokines and free fatty acids. TZDs stimulate the release of adiponectin, which inhibits gluconeogenesis in the liver by activating AMPK (Tomas *et al.*, 2002, Yamauchi *et al.*, 2002).

1.8 Summary

The vascular endothelium is a key player in the maintenance of vascular health and is involved in the regulation of vascular tone and leukocyte adhesion. Dysregulated endothelial function is associated with insulin resistance, diabetes and atherosclerosis. At normal physiological concentrations, insulin is an important regulator of endothelial function, as it promotes NO-mediated vasodilation and potentially inhibits atherogenic processes, but these effects are attenuated or abrogated in hyperinsulinaemic and hyperglycaemic states.

The metabolic energy sensor AMPK is involved in the regulation of energy homeostasis at the cellular and whole body level. AMPK is important as a drug target for insulin-sensitising drugs, as AMPK activity improves glucose homeostasis. Activation of AMPK stimulates endothelial NO release, thereby promoting an antiatherogenic phenotype.

The precise molecular mechanisms underlying endothelial dysfunction are unclear, and their clarification may aid our understanding of vascular endothelial cell function and lead to novel therapeutic approaches.

2 Materials and Methods

2.1 Materials

2.1.1 List of materials and suppliers

Supplier	Materials
Acros Organics (Geel, Belgium)	Glacial acetic acid (nitrogen-flushed)
	$NaNO_2$
	Tetrasodium pyrophosphate (NaPPi)
Becton Dickinson Biosciences (Oxford, UK)	Corning cell culture flasks, 10 cm-diameter cell culture dishes and multiwell plates, transwell plates for migration assays
Beckman Coulter™ (High Wycombe, UK)	Ultra-Clear™ ultracentrifuge tubes
BioSource Europe S.A. (Nivelles, Belgium)	Human Chemokine Multiplex Bead Immunoassay
BOC Gases (Manchester, UK)	N_2, O_2
Finnzymes (Espoo, Finland)	DyNAmo™ SYBR® Green 2-step RT-PCR kit

Fisher Scientific UK Ltd (Loughborough, UK)	Acetone
	D-glucose
	Ethanol
	Glycine
	Microscope slides
	Coverslips (22 mm-diameter and 22 x 22 mm)
	NaOH
	Tris base
	Tricarboxylic acid (TCA)
GE Healthcare UK Ltd (Little Chalfont, Buckinghamshire, UK)	ECL™ HRP-linked secondary antibodies
Hopkin & Williams (Chadwell Heath,UK)	NaN_3
Hycor Biomedical Ltd (Edinburgh, UK)	Glasstic® slides
Inverclyde Biologicals (Bellshill, Lanarkshire, UK)	Nitrocellulose membrane, 0.45 µm pore size

Invitrogen Ltd (Paisley, UK)	AlexaFluor488- and AlexaFluor 568-linked secondary antibodies
	Dulbecco's Modified Eagle Medium (DMEM) and Roswell Park Memorial Institute (RPMI) 1640 cell culture media
	Foetal calf serum (EU origin)
	L-glutamine
	Moloney Murine Leukaemia Virus (M-MuLV) reverse transcriptase + first strand buffer + DTT for RT-PCR
	Penicillin and streptomycin
	Trypsin (0.05% (v/v) in 0.53 mM EDTA•4Na)
Kodak Industrie (Chalon-sur-Saône, France)	Kodak MXB film
Lonza Walkersville Inc. (formerly Cambrex Bio Science Walkersville Inc.) (Walkersville, MD, USA)	Human aortic endothelial cells (HAEC)
	Endothelial cell basal medium (EBM®-2) + supplements
Melford Laboratories Ltd (Ipswich, UK)	DTT

Neuro Probe, Inc., Gaithersburgh, MD, USA; via Receptor Technologies Ltd., Adderbury, UK	Polyvinylpyrrolidone (PVP)-free polycarbonate track-etch (PCTE) membranes for migration assays (2 µm pore size)
New England Biolabs (Hitchin, UK)	Prestained protein marker
Novo Nordisk (Crawley, UK)	Actrapid® human insulin (for acute stimulation) Porcine insulin (for long-term stimulation)
Premier International Foods Ltd (Spalding, UK)	Dried skimmed milk
Promega (Southampton, UK)	Taq DNA polymerase + buffer + molecular grade $MgCl_2$ dATP, dCTP, dGTP, dTTP
PromoCell GmbH (Heidelberg, Germany)	Human aortic endothelial cells
Qiagen (Crawley, UK)	RNA extraction kit

Sartorius Biotech GmbH (Göttingen, Germany)	Sterile syringe filters (0.2 µm)
Severn Biotech Ltd (Kidderminster, Worcester, UK)	Acrylamide:Bisacrylamide (37.5:1; 30% (w/v) Acrylamide)
Sigma-Aldrich (Steinheim, Germany; Seelze, Germany; St Louis, MO, USA), including all Riedel-de-Haën chemicals	Ammonium peroxydisulphate (APS)
	Bromophenol blue
	Bovine serum albumin (BSA)
	Benzamidine
	D-mannitol
	DAPI (4',6-Diamidino-2-phenyindole)
	Deoxycholic acid
	Dimethyl sulphoxide (DMSO)
	EDTA (ethylenediamine tetraacetic acid)
	EGTA (ethylene glycol-bis (ß-amino-ethylether)-N,N,N',N'-tetraacetic acid)
	37% (w/v) formaldehyde solution
	Glycerol
	Hexanucleotide primers

Isopropanol

L-NAME (NG-nitro-L-arginine methyl ester)

Luminol (5-Amino-2,3-dihydro-1,4-phthalazinedione)

Methanol

NADPH (?-Nicotinamide adenine dinucleotide 2'-phosphate reduced tetrasodium salt hydrate)

NaF

$NaHCO_3$

Na_2HPO_4

NaH_2PO_4

NaI (nitrogen-flushed)

Na_4VO_3

Nonidet™ P-40 substitute (mixture of 15 homologues)

OptiPrep® Density Gradient Medium, 60% (w/v) iodixanol (5,5'-[(2-hydroxy-1,3-propanediyl)-bis(acetylimino)]bis-[N,N'-bis(2,3-dihydroxypropyl)-2,4,6-triiodo-1,3-benzenedicarboxamide]) in water

p-Coumaric acid

RT-PCR primers

	Soy bean trypsin inhibitor (SBTI)
	Sodium dodecyl sulphate (SDS)
	N,N,N',N'-Tetramethylethylenediamine (TEMED)
	Triton X-100 (4-(1,1,3,3-Tetramethylbutyl)phenyl-polyethylene glycol)
	Trypan blue
	Tween-20 (Polyethylene glycol sorbitan monolaurate)
	Type IV collagen
TCS CellWorks (Botolph Claydon, UK)	Human aortic endothelial cells
	Large vessel endothelial cell basal medium + supplements
Thermo Fisher Scientific Inc. (Pittsburgh, PA, USA)	Immu-Mount mounting medium for coverslips
Toronto Research Chemicals (Toronto, ON, Canada)	AICAR (5-aminoimidazole-4-carboxamide-1-beta-4-ribofuranoside)
VWR International (Lutterworth, Leicestershire, UK), including all BDH chemicals	Borosilicate coverslips (22 mm diameter)
	$CaCl_2$ solution
	Falcon^{TM} 10 cm-diameter cell culture dishes

and multiwell plates

30% (v/v) H_2O_2

HEPES

KCl

KH_2PO_4

$MgCl_2$

NaCl

Na_2HPO_4

NaH_2PO_4

2.1.2 List of specialist equipment and suppliers

Supplier	Equipment
Analytix Ltd (Durham, UK)	Sievers® Nitric Oxide Analyzer 280
	Exmire microsyringe and needles for NO analysis
Beckman Coulter™ (High Wycombe, UK)	J2-21 centrifuge, Optima™ MAX ultracentrifuge, JA-20 rotor
	TLS-55 rotor
	TLA-110 and TLA 110.4 rotors
Becton Dickinson (Franklin Lakes, NJ, USA)	FACScan Flow Cytometer
Biometra biomedizinische Analytik GmbH (Göttingen, Germany)	TGradient Thermocycler
Bio-Rad Laboratories (Hemel Hempstead, UK)	Agarose gel (Mini-Sub/Wide Mini-Sub Cell GT)
	Protein gel casting and Western blotting equipment (Mini Protean III)
	Luminex 100™ detection system for Human

	Chemokine Multiplex Bead Immunoassay analysis
Carl Zeiss Ltd (Welwyn Garden City, Hertfordshire, UK)	Axiovert 135 microscope LSM Exciter laser scanning microscope
Fisher Scientific UK Ltd (Loughborough, UK)	Polycarbonate freezing container
Herolab (Wiesloch, Germany)	UVT-28 MP UV transilluminator
Neuro Probe, Inc., Gaithersburgh, MD, USA; via Receptor Technologies Ltd., Adderbury, UK	AP48 Boyden chamber
Optika Microscopes (Ponteranica, Italy)	XDS-1B light microscope
Shimadzu Europa GmbH (Duisburg, Germany)	UV-1201 spectrophotometer
WPA (Cambridge, UK)	S2000 spectrophotometer

2.1.3 List of antibodies and conditions of use

2.1.3.1 Primary antibodies for Western blotting

Table 2-1 List of primary Western blotting antibodies and their conditions of use

All rodent antibodies, as well as the rabbit anti-JNK, the rabbit anti-P-I?Ba Ser32 and anti-phospho-p44/42 MAPK, are monoclonal; TBST: Tris-buffered saline; Discntd: discontinued; n/a: not applicable.

Epitope	Host species	Dilution	Diluent (w/v in TBST)	Source	Catalogue number
a-AMPKa1	Sheep	1:1000	1% milk	In-house from University of Dundee (Woods *et al.*, 1996)	n/a
a-AMPK T172	Rabbit	1:200	5% BSA	Cell Signaling	2531
a-Caveolin-1	Mouse	1:1000	TBST	Transduction Laboratories	610058
a-CAP	Rabbit	1:1000	3% milk	Upstate	06-994
a-Cbl	Mouse	1:1000	3% milk	Upstate	05-440
a-eNOS	Rabbit	1:5000	1% BSA	Sigma	N-2643
a-eNOS S116 (Ser114)	Rabbit	1:1000	5% milk	Upstate	07-357
a-eNOS T495	Rabbit	1:1000	5% milk	Upstate	Discntd

a-eNOS T495	Rabbit	1:1000	5% BSA	Cell Signaling	9574
a-eNOS S617 (Ser615)	Rabbit	1:1000	5% milk	Upstate	07-561
a-eNOS S635 (Ser633)	Rabbit	1:1000	5% milk	Upstate	07-562
a-eNOS S1177	Rabbit	1:1000	5% BSA	Cell Signaling	9571
a-GAPDH (clone 6C5)	Mouse	1:1500	5% milk	Ambion	4300
a-I?Ba	Rabbit	1:1000	3% milk	Upstate	06-494
a-IKBa Ser32 (clone 14D4)	Rabbit	1:1000	5% milk	Cell Signaling	2859
a-IKKß	Mouse	1:500	3% milk	Upstate	05-535
a-JNK (56G8)	Rabbit	1:1000	5% BSA	Cell Signaling	9258
a-JNK T183/Y185	Rabbit	1:1000	5% BSA	Cell Signaling	9251
a- p44/42 MAPK	Rabbit	1:1000	5% BSA	Cell Signaling	9102
a-Na+/K+-ATPase a	Mouse	1:4000	3% milk	Upstate	05-369

a-NF?B p65	Rabbit	1:1000	3% milk	Kind gift of Dr T. Palmer	n/a
a-p38 MAPK	Rabbit	1:1000	5% BSA	Cell Signaling	9212
a-p38 MAPK T180/Y182	Rabbit	1:1000	5% BSA	Cell Signaling	9211
a-PDK-1	Sheep	1:1000	5% milk	Upstate	07-047
a-PI3K-p85	Rabbit	1:1000	3% milk	Upstate	06-497
a-PI3K-p110ß	Rabbit	1:1000	3% milk	Santa Cruz	sc-602
a-PKBa	Sheep	1:1000	3% milk	Upstate	07-416
a-PKB	Rabbit	1:1000	5% milk	Cell Signaling	9272
a-PKB T308	Rabbit	1:1000	3% milk	Upstate	05-802
a-PKB S473	Rabbit	1:1000	5% BSA	Cell Signaling	9271
a-PTEN	Rabbit	1:1000-1:2000	3% milk	Upstate	07-016
a-Rab 4	Rabbit	1:1000	5% milk	Abcam	ab13252
a-Rab 11a	Rabbit	1:1000	5% milk	Zymed Laboratories	71-5300

a-Syntaxin 6	Mouse	1:1000	1% BSA	Transduction Laboratories	610635

2.1.3.2 Secondary detection agents for Western blotting

Table 2-2 List of secondary Western blotting detection agents and their conditions of use

n/a: not applicable

Linked molecule	Epitope	Host species	Dilution	Diluent (w/v in TBST)	Source	Catalogue number
HRP	Mouse IgG	Sheep	1:1000-1:2000	1% milk	GE Healthcare	NA931
HRP	Rabbit IgG	Donkey	1:1000-1:2000	1% milk	GE Healthcare	NA934
HRP	Rat IgG	Goat	1:1000-1:2000	1% milk	GE Healthcare	NA935
HRP	Streptococcus sp. Protein G	n/a	1:1000-1:2000	1% milk	Sigma	P8170

2.1.3.3 Primary antibodies for immunocytochemistry

Table 2-3 List of primary immunocytochemistry antibodies and their conditions of use

PB: permeabilisation buffer

Epitope	Host species	Dilution	Diluent (w/v in PB)	Source	Catalogue number
a-Caveolin-1	Mouse	1:100	3% BSA	Transduction Laboratories	610058
a-eNOS	Rabbit	1:100	3% BSA	Sigma	N-2643

2.1.3.4 Secondary antibodies for immunocytochemistry

Table 2-4 Secondary antibodies for immunocytochemistry and their conditions of use

Linked molecule	Epitope	Host species	Dilution	Diluent (w/v in PB)	Source	Catalogue number
AlexaFluor488	Rabbit IgG	Goat	1:100	3% BSA	Invitrogen	A11008
AlexaFluor568	Mouse IgG	Goat	1:100	3% BSA	Invitrogen	A21043

2.1.4 Standard solutions

Unless stated otherwise, all buffers and reagents were made up with distilled water.

Bradford's Reagent

35.0 mg/L Coomassie brilliant blue
5.0% (v/v) Ethanol
5.1% (v/v) Orthophosphoric acid
Bradford's Reagent was filtered and stored in the dark.

6X DNA loading buffer

0.5% (w/v) Bromophenol blue
15% (w/v) Ficoll

Endothelial cell lysis buffer

50 mM Tris-HCl pH 7.4 (at 4°C)
50 mM NaF
1 mM Tetrasodium pyrophosphate (NaPPi)
1 mM EDTA
1 mM EGTA
1% (v/v) Triton X-100
250 mM Mannitol
1 mM DTT
1 mM Na_3VO_4
0.1 mM Benzamidine
0.1 mM PMSF
5 µg/ml SBTI

} added on day of use

Enhanced chemiluminescence (ECL) detection reagents

Solution 1

0.1 mM Tris-HCl pH 8.5
450 mg/L Luminol in 2% (v/v) DMSO
130 mg/L Coumaric acid in 1% (v/v) DMSO

Solution 2

0.1 mM Tris-HCl pH 8.5
1.83 x 10^{-4} % (v/v) H_2O_2

HEPES-EDTA-Sucrose (HES) buffer

20 mM Hepes-NaOH pH 7.4
1 mM EDTA
250 mM sucrose
1 mM DTT
1 mM Na_3VO_4
0.1 mM Benzamidine
0.1 mM PMSF
5 µg/ml SBTI
50 mM NaF
1 mM NaPPi
} added on day of use

Krebs-Ringer-HEPES (KRH) buffer

119.0 mM NaCl
20.0 mM HEPES-NaOH pH 7.4
5.0 mM $NaHCO_3$
5.0 mM Glucose
4.8 mM KCl
2.5 mM $CaCl_2$
1.2 mM $MgSO_4$
1.2 mM NaH_2PO_4

0.1 mM L-Arginine

Phosphate-buffered saline (PBS) (pH 7.2)

85 mM NaCl
1.7 mM KCl
5 mM Na_2HPO_4
0.9 mM KH_2PO_4

Ponceau S Stain

0.2% (w/v) Ponceau S
1% (v/v) Acetic acid

SDS-PAGE running buffer

190 mM Glycine
62 mM Tris
0.1% (w/v) SDS

SDS sample buffer

200 mM Tris-HCl pH 6.8
40% (v/v) Glycerol
8% (w/v) SDS
0.4% (w/v) Bromophenol blue

The above recipe for 4X SDS sample buffer was used neat, or diluted with distilled water to 2X or 1X working concentration as required. DTT was added to a final concentration of 200 mM before use (i.e. 20% (v/v) from 1 M stock).

Tris-buffered saline + Tween-20 (TBST)

20 mM Tris-HCl pH 7.5
137.5 mM NaCl
0.1% (v/v) Tween-20

Transfer buffer

25 mM Tris base
192 mM Glycine
20% (v/v) Ethanol

2.2 Methods

2.2.1 Cell culture

2.2.1.1 Revival and culture of cryopreserved HAEC and HUVEC

Aliquots of cryopreserved (passage 2 or 3, depending on supplier) endothelial cells (EC) were rapidly thawed in a 37°C water bath. Cells were then added to complete endothelial cell medium pre-equilibrated in a humidified incubator containing 5% (v/v) CO_2, 95% (v/v) air, at 37°C. The cell suspension was then divided equally between six to ten 25 cm^2 cell culture flasks and incubated at 37°C in a humidified incubator supplemented with 5% (v/v) CO_2. Cell medium was replaced every 2-3 days with fresh complete medium. For experiments, EC were cultured on non-coated Falcon dishes and multiwell plates as required. No coating agent was used as Falcon™ cell-cultureware, in conjunction with the extracellular matrix produced by EC, provided sufficient support for EC adhesion and growth.

2.2.1.2 Determination of endothelial cell phenotype of cultured HAEC

In order to prevent differentiation from the endothelial phenotype of HAEC and HUVEC, only EC in passages 4-6 were used for experiments. To assess the maintenance of the endothelial phenotype, the presence of the endothelial cell marker CD31 in cultured HAEC was ascertained by immunocytochemistry. Dr Ian Montgomery (University of Glasgow) carried out these studies.

For immunocytochemistry, HAEC were grown on coverslips and fixed with methanol for 10 minutes. After washing, the coverslips were attached to glass slides using vaseline and were circled using a Dako PAP pen to form a watertight seal. The cells were rinsed in PBS and blocked with 1:30 goat serum in PBS. Anti-CD31 primary antibody (1:40 dilution in PBS + 1% (w/v) BSA) was incubated in a humidified chamber on an orbital shaker for 1h. After washing in PBS, the coverslips were incubated with biotinylated goat anti-mouse IgG (1:20 dilution in PBS + 1% (w/v) BSA) for 30 minutes. After thorough washing in PBS, cells were incubated for a further 30 minutes in ExtrAvidin Peroxidase (1:20 dilution in PBS + 1% (w/v) BSA). Following washing in PBS, the AEC substrate reagent was

prepared and incubated for 5-10 minutes. Coverslips were then rinsed with distilled water, stained with haematoxylin for 1 minute and rinsed gently. The coverslips were carefully removed from the glass slides and mounted on clean slides using Aquamount mounting medium and left to dry overnight. Stained cells were examined using a Zeiss Axiophot microscope and images were captured using a JVC video camera and AverCAP video card in a Viglen computer.

The plasma membrane of CD31-positive cells was rose-red to brownish-red, with weaker cytoplasmic staining, and the nucleus was stained pale blue/purple. Cytoplasmic staining is a feature of the antibody used. As a negative control, HAEC were stained in the absence of primary antibody (see Figure 2-1).

2.2.1.3 Experimental hyperinsulinaemia treatment of HAEC

For experimental hyperinsulinaemic conditions, HAEC complete medium was supplemented with 100 nM of purified porcine insulin (Novo Nordisk), dissolved in 10 mM HCl and sterilised, for the indicated period of time (24-48h). Insulin was replaced as required when the cell culture medium was replaced.

2.2.1.4 Experimental hyperglycaemia treatment of HUVEC

For experimental hyperglycaemic conditions, complete EC medium, containing 4 mM glucose, was supplemented with 21 mM glucose to give a final concentration of 25 mM glucose. As an osmotic control, cells were cultured in complete EC medium supplemented with 20 mM mannitol and 1 mM glucose, to give a final concentration of 5 mM glucose and 25 mM total monosaccharide. EC were cultured under these conditions for 48h.

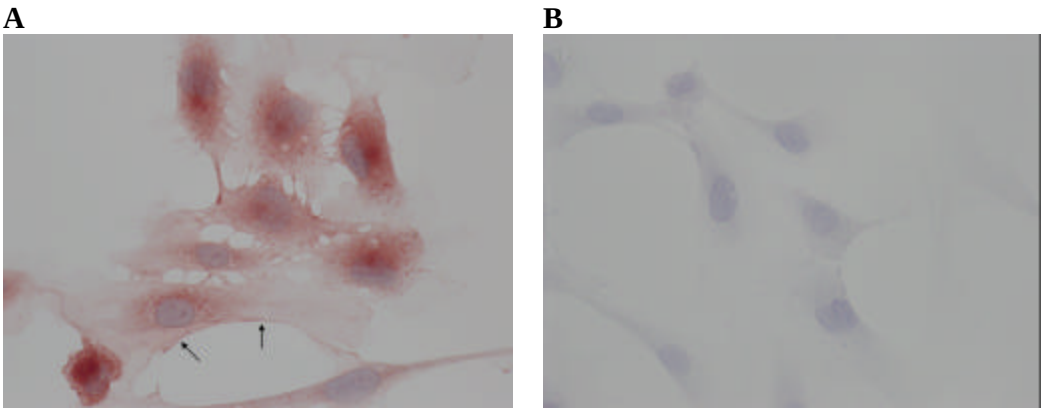

Figure 2-1 HAEC stained with anti-CD31 antibody and haematoxylin

In order to confirm the endothelial phenotype of HAEC, immunocytochemistry was carried out by Dr Ian Montgomery as described in section 2.2.1.2. HAEC positive for the endothelial cell marker CD31 show red-stained plasma membrane (see arrows) and weaker cytoplasmic staining (panel A), while unlabelled control cells do not stain (panel B). Cell nuclei appear blue after staining with haematoxylin (both panels).

2.2.1.5 Passaging of HAEC and HUVEC

For experiments, only EC in passages 4 to 6 were used. Cells were routinely subdivided 1/3-1/7 in 75 cm^2 tissue culture flasks. For passaging, EC (~80% confluence) were washed once in 2-4 ml of basal EC medium and detached with 1-2 ml trypsin (0.05% (v/v) in EDTA). Cells were briefly incubated at 37°C until the cells fully detached upon tapping of the cell culture flask. Trypsin was neutralised by addition of 1-3 ml of complete EC medium. Cells were pooled in a 50 ml centrifuge tube and centrifuged at 146 x g for 5 minutes. The supernatant was aspirated and the cell pellet resuspended in 5 ml complete EC medium prior to dilution into an appropriate volume of complete EC medium. The cell suspension was divided between 75 cm^2 tissue culture flasks (Corning) and 10 cm-diameter cell culture dishes and/or multiwell plates (both Falcon), as required.

2.2.1.6 Culturing of U937 and THP-1 pre-monocytic cells

U937 cells and THP-1 cells were cultured in complete RPMI 1640 medium (supplemented with 10% (v/v) foetal calf serum (FCS), 100 U/ml penicillin, 100 µg/ml streptomycin and 2 mM L-glutamine) and subdivided every 2-3 days by 1/2 to 1/3 dilution with complete medium. Cells were incubated at 37°C in a humidified incubator, in an atmosphere of 5% (v/v) CO_2:95% (v/v) air. U937 and THP-1 cells were generous gifts from Dr W. A. Sands/Dr T. Palmer and A. Edkins/Prof W. Cushley, respectively (all University of Glasgow).

2.2.1.7 Cryopreservation and revival of U937 pre-monocytic cells

U937 cells were cryopreserved after centrifugation at 146 x g and resuspension in 90% (v/v) FCS, 10% (v/v) DMSO, by overnight incubation in a polycarbonate freezing container at -80°C. The following day, cells were transferred to liquid nitrogen storage. To revive U937 pre-monocytic cells, cells were removed from liquid nitrogen and rapidly thawed in a 37°C water bath. Cells were then added to complete U937 cell medium pre-equilibrated in a humidified incubator containing 5% (v/v) CO_2, 95% (v/v) air, at 37°C. The cell suspension was then added to a 75 cm^2 cell culture flask and incubated at 37°C in

a humidified incubator supplemented with 5% (v/v) CO_2. Revived pre-monocytes were subdivided a few times before use in experiments.

2.2.2 HAEC and HUVEC lysate preparation

Unless otherwise stated, all treatments were carried out in duplicate for each experiment. EC, stimulated as indicated, were serum-starved by aspirating the cell culture medium, washing the cells once with 10 ml of fresh, pre-warmed Krebs-Ringer-HEPES (KRH) buffer and replacing it with 5 ml/100 mm-petri dish of fresh KRH buffer. Cells were incubated for 2-4h at 37°C. Subsets of cells were then acutely stimulated with 1 µM insulin for 10 minutes. Thereafter, the buffer was aspirated and dishes were placed on ice. To each petri dish, 0.4 ml fresh, ice-cold lysis buffer was added and cells were scraped off using a cell lifter. Resulting cell lysates were transferred to pre-cooled 1.5 ml-microcentrifuge tubes, vortexed for 10 seconds and centrifuged at maximum speed (17,530 x g) for 3 minutes in a 4°C bench-top centrifuge. Lysate supernatants were transferred to fresh, pre-cooled 1.5 ml-microcentrifuge tubes. The protein concentration of each sample was determined by spectrophotometric analysis at 595 nm according to the method of Bradford (see section 2.2.3) (Bradford, 1976). Samples were stored at -20°C short-term or at -80°C long-term.

2.2.3 Protein concentration determination

Spectrophotometric analysis of EC lysates according to the Bradford method (Bradford, 1976) was carried out at 595 nm in a spectrophotometer using disposable plastic cuvettes. Duplicates of 2 µg, 4 µg and 6 µg BSA were made up to 100 µl with H_2O and utilised as reference standards. Duplicates of 5 µl from each sample were added to 95 µl distilled H_2O. To all samples and reference standards, 1 ml Bradford's reagent was added and spectrophotometric analysis performed in a WPA 2000 spectrophotometer (WPA) within 10 minutes of reagent addition. The mean absorbance for each sample duplicate was calculated and the protein concentration determined by comparison to the calculated mean A595/µg BSA derived from the linear portion of the BSA reference standard curve.

2.2.4 Iodixanol gradient centrifugation

Iodixanol (5,5'-[(2-hydroxy-1,3-propanediyl)-bis(acetylimino)]bis -[N,N'-bis(2,3-dihydroxypropyl)-2,4,6-triiodo-1,3-benzenedicarboxamide]) is a density gradient compound that forms a continuous gradient upon centrifugation, making it possible to collect high yields of cellular organelles at high purity (Graham *et al.*, 1994). For subcellular fractionation by iodixanol gradient centrifugation, HAEC were grown in 10 cm-dishes and serum-starved for 2h in KRH buffer before treatment with 1 µM human insulin for 10 minutes or no treatment. Cells were then scraped off the dishes in 0.3-0.4 ml of HES buffer and pooled according to treatment group (typically 4 dishes were used per treatment). The cells were homogenised with ten passes through a ball-bearing homogeniser with a 16 µm-ball. Nuclei were pelleted by spinning the homogenates for 3 minutes at 5000 rpm (4088 x g). The resulting supernatants were diluted with 60% (w/v) iodixanol in HES buffer to a density of 40% (v/v), and 0.5 ml thereof placed at the bottom of separate centrifuge tubes and overlaid sequentially with 0.5 ml each of 37.5%, 35%, 32.5%, 30%, 25%, 20% and 10% (w/v) iodixanol in HES buffer. Samples were then centrifuged for 3h at 72,000 rpm (216,276 x g), 4°C, in a TLA-100.4 rotor. The resulting fractions were collected as eight separate 500 µl aliquots, starting with the least dense fraction from the top of the tube. Fractions were precipitated on ice for 30 minutes using 0.015% (w/v) deoxycholic acid and 11 % (w/v) TCA. Precipitated proteins were pelleted by centrifugation at 17,530 x g, 4°C, for 3 minutes. The supernatants were aspirated and pellets were resuspended in 50 µl 2X SDS-sample buffer and 20 µl of 2 M Tris base prior to Western blot analysis (samples were not heated before loading onto SDS-gels).

2.2.5 SDS-polyacrylamide gel electrophoresis (SDS-PAGE)

SDS-polyacrylamide gel electrophoresis was carried out according to the method of Laemmli (Laemmli, 1970). Cell lysate samples (see section 2.2.2) were mixed 3:1 with 4X SDS-containing sample buffer (SDS-SB) and heated to 95°C in a heating block for 2-5 minutes. Subcellular fractionation samples (see section 2.2.4) were prepared in 4X SDS-SB (supernatants) or 1X SDS-SB (pellets) and heated to 95°C as above, or heated to 37°C for 5 minutes if high temperature was not required.

Unless otherwise indicated, SDS-gels for cell lysates routinely consisted of 8% (w/v) acrylamide resolving gels overlaid with 5% (w/v) stacking gels; for subcellular

fractionations, 10% (w/v) resolving gels with 5% (w/v) stacking gels were used. All gels were cast in Mini-Protean III gel casting equipment (Bio-Rad). Gel lanes were loaded with equal amounts of protein (3-10 µg). Samples were resolved at 80 V until the samples had reached the resolving gel, then the voltage was increased to 180 V and the samples were resolved until the dye front had migrated the entire length of the gel. Subcellular fractionation (iodixanol gradient) samples were usually resolved at 80-100 V.

2.2.6 Western blotting and immunodetection of proteins

Protein-containing samples were transferred from SDS-gels onto nitrocellulose membranes at 60V for 2h, or at 40 mA overnight, using Mini-Protean II/III equipment (Bio-Rad). Membranes were briefly stained with Ponceau to check for equal loading of the gels, and blocked for 1h in Tris-buffered saline (TBST) containing 5% (w/v) non-fat dried milk. Following brief washing in TBST, the membranes were incubated overnight with primary antibody, diluted as shown in Table 2-1. All washes and incubation steps were carried out under agitation. After primary antibody probing, membranes were washed three times in TBST and incubated for 1h in HRP-linked species-specific secondary antibodies, diluted 1:1000-1:2000 in TBST containing 1% (w/v) milk (for primary antibodies raised in sheep, an HRP-conjugated protein G secondary detection agent was used; see Table 2-2). Following three washes with TBST, 2 ml of each of the ECL reagents (produced in-house) was added to each nitrocellulose membrane and incubated for 1 minute. Chemiluminescence was detected with a Kodak X-Omat using Kodak MXB blue-sensitive X-Ray film. In order to assess the genuine phosphorylation levels of a protein, the Western blot band intensity of a phosphorylated protein, detected with a site-specific phospho-antibody, was measured and expressed as a ratio to the corresponding total protein within the same sample.

2.2.7 Densitometric quantification of protein bands

The antibody-detected bands on the developed film were scanned on a Mercury 1200c scanner, using Adobe Photoshop software. The intensity of the immunodetected protein bands on the film was measured using Scion Image or ImageJ software. Densitometric analysis was performed on different exposures of the same band to ensure that quantifications were within the linear range.

2.2.8 Nitric oxide measurement

Nitric oxide (NO) released from cells reacts with dissolved oxygen in the cell culture medium or buffer to form nitrate and, predominantly, nitrite. NO production by HAEC was hence analysed by a nitrite reduction method (described below) using a Sievers Nitric Oxide Analyzer 280 (see Figure 2-2). The NO analyser calculates the amount of NO produced by the cells from the amount of nitrite present in the cell culture supernatant sample.

To set up the NO analyser for nitrite reduction, a reducing agent (composed of 5 ml nitrogen-flushed glacial acetic acid and 50 mg nitrogen-flushed NaI dissolved in 1.5 ml of de-ionised water) was added to the purge vessel and flushed with N_2 gas to purge any traces of NO_2^- from the vessel. After 30 minutes of purging, the purge vessel was sealed with a septum and the reducing agent was refluxed under N_2 gas.

Prior to each experiment, a nitrite standard curve was prepared: From a standard solution of 100 mM $NaNO_2$, serial dilutions of 50 µM, 10 µM, 1 µM and 100 nM were prepared and injected into the purge vessel using an Exmire microsyringe. Under the nitrite-reducing conditions used, nitrite present in the standards was reduced to NO as shown in Equation 1. The NO produced was then detected by the NO analyser, where it reacted with O_2 to produce O_3, which was detected by chemiluminescence. The chemiluminescence signal was converted to an electrical potential and displayed as mV by the NO analyser. The amount of NO produced by duplicates of each nitrite standard was recorded by the analyser and used to produce a calibration curve.

After calculation of the standard curve, cell culture supernatant samples (prepared as described in 2.2.8.1) were injected into the purge vessel using an Exmire microsyringe. Samples were injected at 1 minute intervals to allow the output curve to return to baseline. The output in mV was then related to the amount of nitrite present in the sample using the nitrite standard curve prepared on that day.

$$I^- + NO_2^- + 2H^+ \longrightarrow NO + \tfrac{1}{2}I_2 + H_2O$$

Equation 1 Production of nitric oxide from nitrite

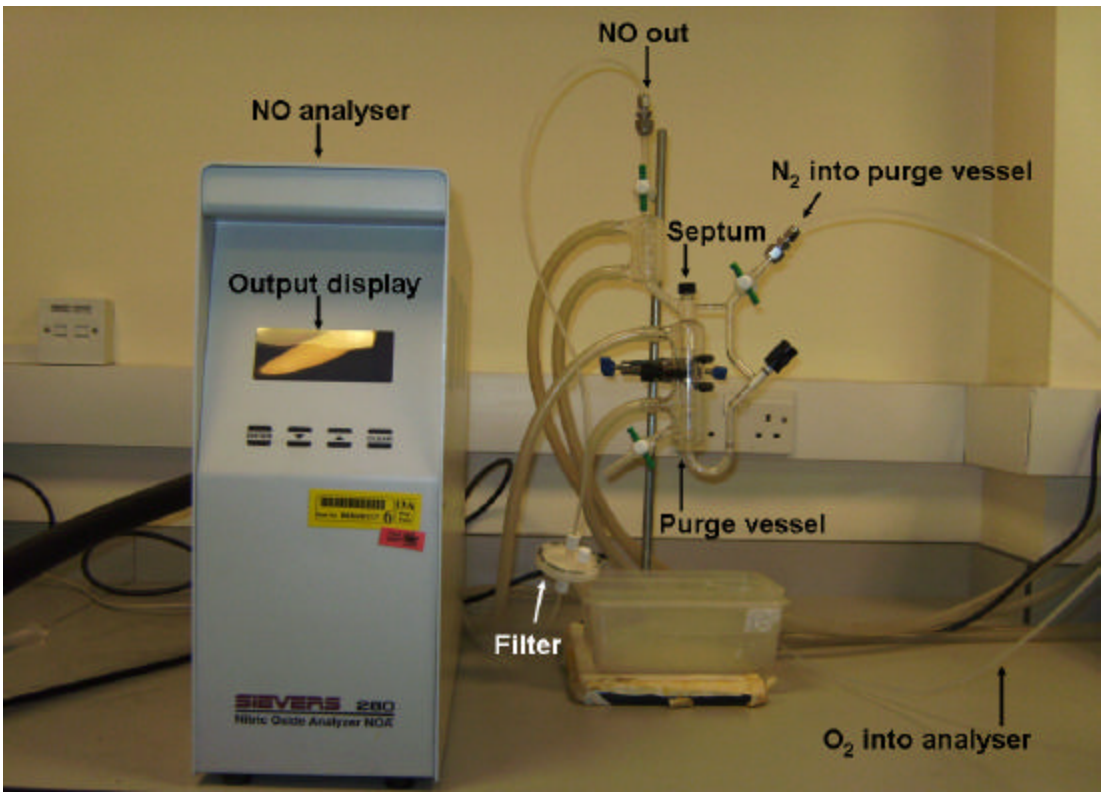

Figure 2-2 The Sievers Nitric Oxide Analyzer 28

2.2.8.1 Preparation of cell culture supernatants for NO analysis

HAEC were grown to near-confluency in 6-well plates and subsequently treated with 100 nM porcine insulin for 48h or left untreated. The distribution of treatment conditions on the culture plates was randomised to avoid artefacts. After 48h, cells were washed once and serum-starved in serum-free medium for 2h at 37°C in a humidified incubator containing 5% (v/v) CO_2. Thereafter, cells were washed once in KRH, transferred to a 37°C water bath and acclimatised for 20-40 min. Samples (80 µl) of cell culture supernatant were taken prior (t = 0) to and 12 min (t = 12) after addition of 1 µM insulin, 3 µM ionomycin (positive control) or no treatment, and analysed immediately with a Sievers Nitric Oxide Analyzer 280, as described above.

The calcium ionophore ionomycin is an antibiotic produced by *Streptomyces conglobatus* ATCC 31005, which binds extracellular Ca^{2+} ions and transports them across the cell membrane (Liu & Hermann, 1978). This raises intracellular Ca^{2+} levels and thus activates eNOS in a calcium-dependent manner, leading to NO production.

The calculated amount of NO obtained for each (t = 12) sample was then corrected for the amount of NO lost in the initial (t = 0) sample. The amount of NO produced/min (in nM) was calculated from the linear part of a sodium nitrite standard curve prepared prior to each assay. Per experiment, all treatments except the ionomycin controls were carried out at least in duplicate.

2.2.9 Measurement of superoxide production

Superoxide production in HUVEC was measured using the lucigenin method. Lucigenin is a chemiluminescence-based technique, with lucigenin-amplified chemiluminescence (LC) based on the following reactions:

Reaction 1: $O_2^{\cdot-} + LC^{2+} \rightarrow LC^{\cdot+} + O_2$

Reaction 2: $LC^{\cdot+} + O_2 \rightarrow LCO_2$

Reaction 3: $LCO_2 \rightarrow 2$N-methylacridone + h?

The luminometer measures the photon of light emitted from the energy rich dioxetan molecule (LCO_2).

HUVEC were treated as described in section 2.2.1.4 and lysates were prepared as described in section 2.2.2. Lysate (500µL) was added to 1.5 ml of KRH buffer and preincubated with 5 µM lucigenin (a kind gift from Dr C.M. Hamilton, BHF/GCRC, University of Glasgow) and 100 µM NADPH for six minutes. Single photon counts were measured over 3 minutes and the average value calculated over that time period. Counts per lysate were calculated by subtracting background ROS values (scintillation tubes containing 2 ml of KRH preincubated with lucigenin and NADPH as above), and were corrected to 1 µg/µl lysate.

2.2.10 Monocyte adhesion assays

HAEC were seeded into 24-well cell culture plates. At near-confluency, 10 wells of cells per treatment group were stimulated with 10-100 nM insulin for 24-48h as appropriate, or left untreated. As a positive control, 4 wells per plate were treated with 10 ng/ml TNFa for 6h. Thereafter, the cell culture medium was aspirated and HAEC were overlaid with $1x10^5$/well U937 pre-monocytic cells in basal RPMI medium. The monocytes were allowed to attach at 37°C, 5% (v/v) CO_2, for 1h. The cell suspension was then aspirated and all non-adherent monocytes were washed off by three washing steps with 1 ml/well basal DMEM. The cells were fixed with 0.5 ml/well 4% (w/v) paraformaldehyde (PFA), 5% (w/v) sucrose in PBS, pH 7.2 overnight at 4°C.

Adherent U937 monocytes were counted at X100 magnification by brightfield microscopy. Three separate fields per well of confluent HAEC were counted and the number of total U937 cells attached per field of confluent HAEC was expressed as an average of all replicates within a treatment group. If HAEC were not confluent, the number of HAEC in 7 individual fields from seven separate wells was determined. The total number of attached monocytes/100 HAEC was then calculated and expressed as an average of all the wells within a treatment group.

2.2.11 Stimulation of HAEC chemokine production

Per experiment, all treatments were carried out in duplicate and pooled according to treatment. Samples were stored at -80°C after preparation.

HAEC were grown to ~80% confluency in 6-well plates (Falcon) and stimulated with 2 mM AICAR for 45 min or 4h with or without co-incubation with 10 ng/ml TNFa for 4h and/or 200 µM L-NAME (all diluted in complete endothelial cell medium). All treatments were started so that the experiment was concluded at the same time. After this incubation period, HAEC were washed three times in serum-free (SF)-RPMI 1640 medium and incubated with 0.5 ml/well SF-RPMI for 1h at 37°C, 5% (v/v) CO_2. After 1h, the conditioned SF-RPMI medium was collected. Controls included i) SF-RPMI medium (with and without L-NAME) incubated with untreated HAEC for 1h (basal HAEC control) and ii) conditioned medium from HAEC treated with 10 ng/ml TNFa (with and without L-NAME) (positive control for stimulation of HAEC chemokine production).

2.2.12 Analysis of HAEC chemokine production

Conditioned medium from stimulated HAEC (see section 2.2.11) was used for chemokine analysis with a Multiplex Bead Immunoassay (BioSource™ 10-Plex system), testing for the presence of human chemokines MCP-1, -2, -3, MIP-1a, MIP-1ß, Eotaxin, GRO, RANTES, IP-1- and MIG. This assay allows the simultaneous detection of several molecules bound specifically to beads coated with relevant antibodies. These beads have distinct spectral properties and are linked to fluorophores, which permit the Luminex 100™ detection system to distinguish between different beads, and thus, different antibody-bound molecules, while simultaneously measuring the quantity of associated fluorophore.

The assay was carried out as per manufacturer's instructions, but antibodies and enzyme substrates were used at half the recommended concentration. All steps were carried out at room temperature and in the dark. Briefly, 50 µl per sample of conditioned medium was added to 50 µl assay diluent and 50 µl incubation buffer, and incubated under shaking with primary antibody-coated beads for 2h. After two washes with wash solution, biotinylated detector antibody was added for 1h under agitation. Two further washes preceded incubation with streptavidin-RPE for 30 minutes. Prior to detection in a Bio-Plex system (Bio-Rad), the assay was washed three times with wash solution. Serial dilutions of

chemokine standards were included in duplicate in each experiment as a reference, from which the chemokine concentrations in each sample were then calculated.

2.2.13 Immunocytochemistry

HAEC were grown to near-confluency on 22mm glass coverslips in 6-well cell culture plates and treated as indicated. Cells were serum-starved in KRH at 37°C for 2-3h and treated with 1 µM human insulin as indicated. Cells were washed once in PBS and coverslips were placed into fresh 6-well plates. Cells were fixed in 4% (w/v) formaldehyde in PBS for 10 minutes, followed (on most occasions) by a 10 minute blocking step in 20 mM NH_4Cl in PBS. Thereafter, all incubations were carried out at room temperature in a dark, humidified chamber. Following a brief wash in PBS, cells were permeabilised in PBS containing 0.5% - 1% (v/v) Triton X-100 for 5-10 minutes, washed in permeabilisation buffer (PB, PBS + 0.1% Triton X-100) and blocked for 30 min in 10% (v/v) goat serum in PB. Cells were washed once in PB before incubation with the primary antibody (anti-eNOS and/or anti-caveolin-1 antibody, each diluted 1:100 in PB + 3% (w/v) BSA) for 2h. Cells were washed three times in PB and incubated with the secondary antibody (AlexaFluor 488-linked goat anti-rabbit antibody and/or AlexaFluor 568-linked goat anti-mouse antibody, each diluted 1:100 in PB + 3% (w/v) BSA) for 1h. Following three washes in PBS, cells were stained with DAPI (1:10,000 in PBS) for 5 minutes. After three further washes in PBS, the coverslips were mounted onto microscope slides with mounting medium and allowed to dry overnight at room temperature in the dark before storage at 4°C. Negative controls included i) no treatment with primary antibody and ii) treatment with primary antibody and irrelevant secondary antibody.

2.2.13.1 Image acquisition and quantification of fluorescence intensity

Immunolabelled samples were analysed using a Zeiss LSM Exciter laser scanning microscope and LSM imaging software. Cells were visualised with a Plan-Apochromat X63/1.4 Oil DIC objective and the relevant filter. The pinhole was set to 1 Airy unit, and the scan speed was maximal. The detector gain in the fluorescence channel was set such that the corresponding negative control sample appeared completely black to eliminate any false signals resulting from cell autofluorescence. Images from one visual field were

acquired in all relevant channels and subsequently overlaid using LSM imaging software. DAPI-staining was visualised with a pseudo-DAPI setting (mercury light source, FSet49 beam splitter and NT 80/20 emission filter) at maximal pinhole opening. One to four images were taken per sample.

The fluorescence intensity of individual antibody-labelled cells was quantified with ImageJ software. Square or rectangular boxes were drawn neatly around the areas of interest and the fluorescence intensity measured. The box size and shape were identical within individual cells, but varied between cells. Three measurements from different areas of the cytoplasm were taken per cell to obtain an average measurement for cytoplasmic fluorescence intensity. Three cells per image, and ten images per treatment group were analysed (n = 30 per treatment group). Data for each cell were expressed as fluorescence intensity relative to nuclear fluorescence intensity.

2.2.14 Statistical analysis

The "two-sample Student's t-test assuming unequal variance" ("Student's t-test") or the "paired two-sample t-test for means" ("paired t-test") were used for the statistical analysis of data as indicated in the results sections. Statistical significance was defined by a two-tailed p-value of less than 0.05.

3 The Effect of Experimental Hyperinsulinaemia on NO Production and Insulin Signalling in Human Vascular Endothelial Cells

3.1 Introduction

3.1.1 Background

Insulin is a vasoactive hormone that stimulates increased blood flow through vasodilation (Scherrer *et al.*, 1993); an effect that has subsequently been attributed to insulin-stimulated nitric oxide (NO) release (Scherrer *et al.*, 1994). Insulin has been demonstrated to stimulate endothelial nitric oxide synthase (eNOS)-mediated NO production in human umbilical vein endothelial cells (HUVEC) by signalling through the insulin receptor (Zeng & Quon, 1996, Zeng *et al.*, 2000). This process depends on phosphatidylinositol 3-kinase (PI3K) and protein kinase B (PKB) (Zeng *et al.*, 2000) to activate eNOS at the activating residue Ser1177 (Dimmeler *et al.*, 1999, Fulton *et al.*, 1999), but is independent of the intracellular Ca^{2+} concentration (Montagnani *et al.*, 2001). In several metabolic disease states, including the metabolic syndrome, insulin resistance and Type II diabetes, decreased nitric oxide bioavailability is a hallmark of endothelial dysfunction (Rask-Madsen & King, 2007).

Nitric oxide is known to have vasoprotective properties (Gewaltig & Kojda, 2002, Hsueh & Quinones, 2003, Wheatcroft *et al.*, 2003), and there is evidence that links decreased NO bioavailability to endothelial dysfunction and proatherogenic processes (Li *et al.*, 2002, Dickhout *et al.*, 2005, Rask-Madsen & King, 2005, Tesauro *et al.*, 2005). Short exposures to physiological concentrations of insulin, as experienced under normal physiological conditions, are thought to be vasoprotective, maintaining appropriate vasodilation through stimulation of NO production, and preventing atherogenesis. By contrast, prolonged exposure to pathophysiological insulin concentrations, as encountered during hyperinsulinaemia/insulin resistance, are postulated to promote atherogenesis by selectively inhibiting NO release and increasing vasoconstrictive responses (Pandolfi *et al.*, 2005).

Clinical studies, as well as animal and *in vitro* experiments, suggest that prolonged hyperinsulinaemia leads to dysregulation of vascular endothelial nitric oxide production. Patients with insulin resistance and Type II diabetes exhibit a smaller NO-mediated vasodilatory response to insulin than healthy subjects, and this decrease is proportional to the level of insulin resistance (Steinberg *et al.*, 1996, Balletshofer *et al.*, 2000, Cleland *et al.*, 2000, Ardigo *et al.*, 2006). While many groups reported this decreased vasodilatory effect as specific to endothelium-dependent (insulin- or acetylcholine-mediated) vasodilation (including (Hogikyan *et al.*, 1998, O'Driscoll *et al.*, 1999, Cheetham *et al.*, 2000, Cleland *et al.*, 2000, Arcaro *et al.*, 2002)), others have found that endothelium-

independent vasodilation mediated by an NO donor such as glyceryl trinitrate (GTN), is also impaired (McVeigh *et al.*, 1992).

Impaired insulin-induced vasodilation can also be demonstrated in experimental animals: small coronary arteries from insulin-resistant obese Zucker rats were less responsive to insulin than vessels from Zucker lean rats (Fulton *et al.*, 2004b, Katakam *et al.*, 2005), but this effect was obliterated by pretreatment with the reactive oxygen species (ROS) scavenger, superoxide dismutase (SOD) (Katakam *et al.*, 2005). By contrast, *in vitro* studies mimicking hyperinsulinaemia showed that unstimulated human coronary artery endothelial cells produced ~50% more NO than controls when cultured with 10-100 nM insulin for 24h (Ding *et al.*, 2000). Thus, the effect of hyperinsulinaemia in cultured human endothelial cells appears to contradict observations in man and obese Zucker rats.

Together, these data suggest that NO bioavailability is altered in insulin resistance and associated hyperinsulinaemia. However, the underlying molecular mechanisms responsible for the reduced vasodilation that is characteristic of clinical hyperinsulinaemia have not been fully addressed. Several studies have investigated the effect of insulin resistance or experimental hyperinsulinaemia on vasodilation, and a few studies have addressed the effect of experimental hyperinsulinaemia on cellular/vascular NO-production (Ding *et al.*, 2000, Pandolfi *et al.*, 2005, Potenza *et al.*, 2005). To date, however, no studies have looked at the effect of experimental hyperinsulinaemia on insulin-stimulated NO production and insulin signalling at the cellular level. A logical speculation would be that the insulin signalling pathway that leads to NO production is impaired by hyperinsulinaemia, thus resulting in lower NO bioavailability. This hypothesis has not been thoroughly investigated, and previous studies in human vascular endothelial cells have yielded contradicting results (Ding *et al.*, 2000).

3.1.2 Aims of the chapter

The work presented in this chapter was designed to determine whether experimental hyperinsulinaemia blunted NO production by human vascular endothelial cells in response to acute stimulation with insulin (section 3.2.2). In addition, the expression and insulin-responsive phosphorylation levels of the insulin signalling pathway components (PI3K, PTEN, PDK-1, PKB, eNOS and p44/42 MAPK) and the cellular energy sensor molecule AMPK, which might be involved in any such potential dysregulation were investigated (section 3.2.3).

3.2 Results

3.2.1 Selection of experimental conditions

Given that culture of human coronary artery endothelial cells with 10-100 nM insulin for 24h was sufficient to observe an effect on NO production (Ding *et al.*, 2000), it was reasoned that 48h of culture in 100 nM insulin would be sufficient to see an effect on NO production in HAEC. These conditions are referred to as experimental hyperinsulinaemia in this text. For reasons of simplification, cells cultured under conditions of experimental hyperinsulinaemia are frequently referred to as "hyperinsulinaemic" in this thesis, despite not originating from donors who were known to have hyperinsulinaemia.

Previous experiments in this laboratory have established that the short-term addition of insulin at concentrations as low as 5 nM results in eNOS-mediated nitric oxide production in human aortic endothelial cells (Salt *et al.*, 2003). Pilot experiments showed that maximal stimulation was achieved with an insulin concentration of 1 µM, which caused an approximately 50% increase in NO production in HAEC, with concommitant stimulation of PKB^{S473} and $eNOS^{S1177}$ phosphorylation at the molecular level (Ritchie *et al.*, 2007). At the molecular level, acute stimulation of human umbilical vein endothelial cells with a range of insulin concentrations demonstrated that 1 µM insulin resulted in maximal stimulation of PKB^{S473} phosphorylation within 10 minutes (see Figure 3-1). Therefore, in all subsequent experiments, recombinant human insulin was used at a final concentration of 1 µM for acute (10 min) stimulation.

A

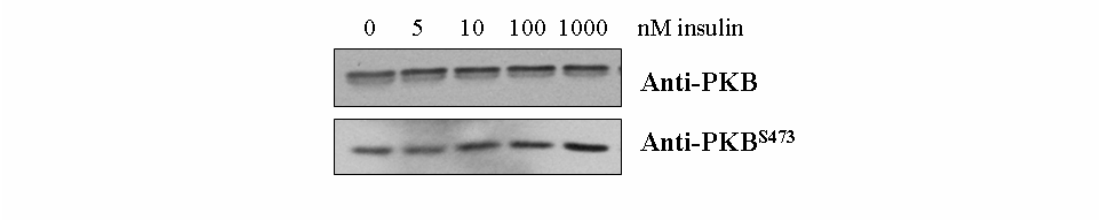

B

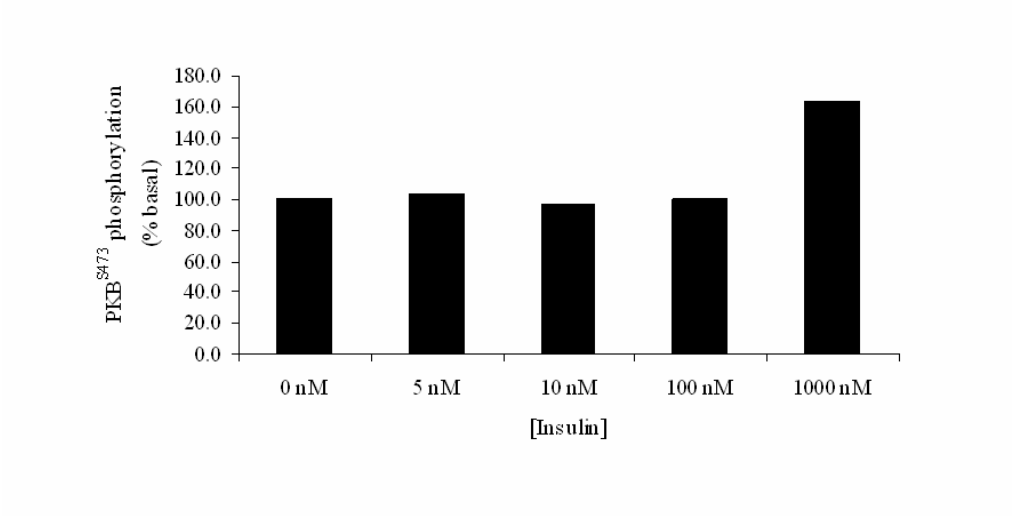

Figure 3-1 Acute stimulation of HUVEC with 1 µM insulin stimulates PKB^{S473} phosphorylation.

HUVEC were serum-starved in Krebs-Ringer-Hepes (KRH) buffer for 2h and stimulated acutely with 0 nM – 1 µM insulin. Cell lysates were prepared, and 10 µg of protein/sample were resolved by SDS-PAGE and Western blotted. A: Membranes were probed with antibodies as indicated. B: The intensity of the resulting immunolabelled protein bands was determined by densitometry. Data shown are the results of one experiment.

3.2.2 NO production in endothelial cells in response to experimental hyperinsulinaemia

Based on the hypothesis that experimental hyperinsulinaemia would likely disrupt insulin-stimulated, eNOS-mediated NO production, the production of NO by HAEC grown under experimental hyperinsulinaemic conditions was examined in response to an acute insulin stimulus.

To this end, human aortic endothelial cells were cultured under normal or experimental hyperinsulinaemic conditions, serum-starved and stimulated acutely with 1 µM insulin to mimic a postprandial rise in insulin levels. As a positive control, the calcium ionophore ionomycin was used. Cell culture supernatants were analysed on a Sievers Nitric Oxide Analyzer 280 as described in section 2.2.8. The results of nine independent experiments are summarised in Figure 3-2.

These experiments showed that acute treatment of HAEC with insulin causes a small but significant increase in NO production under control, but not hyperinsulinaemic conditions (11±3% ($p<0.05$) and 17±6% over unstimulated control for normal and hyperinsulinaemic cells, respectively). Basal and acutely insulin-stimulated hyperinsulinaemic cells produced similar levels of total NO compared to the respective control levels.

As expected, NO production in control cells was markedly sensitive to stimulation with the calcium ionophore ionomycin (49±12% increase, $p<0.005$ compared to basal control). Interestingly, hyperinsulinaemic cells showed a less pronounced increase in NO production upon ionomycin treatment (26±13% increase compared to basal control). Furthermore, the difference between insulin-stimulated and ionomycin-stimulated NO production was smaller in hyperinsulinaemic than control HAEC (9% and 38%, respectively). However, only two experiments (with cells from one donor) included ionomycin-treated hyperinsulinaemic cells, therefore, statistical analysis of these samples was not possible.

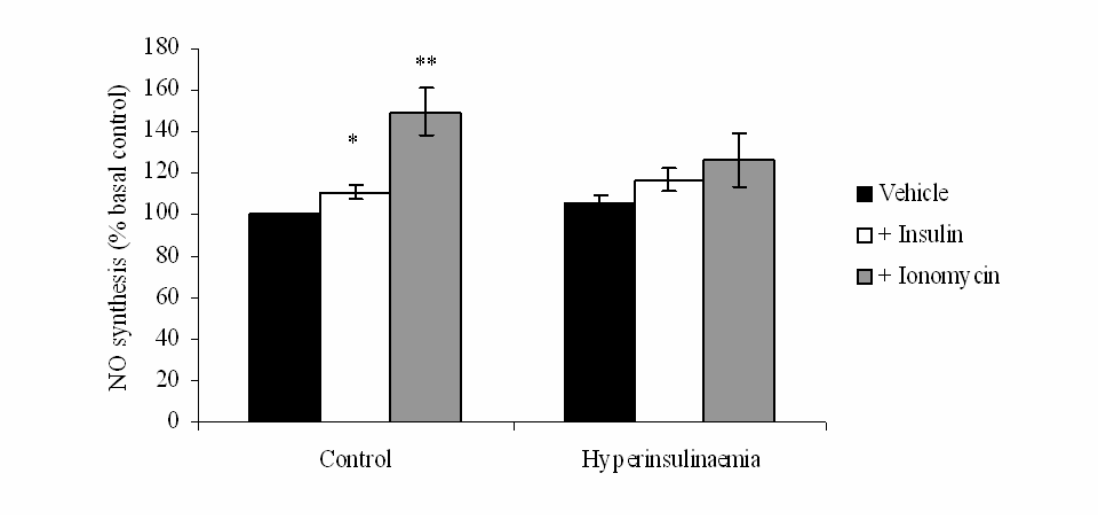

Figure 3-2 Experimental hyperinsulinaemia impairs nitric oxide production in HAEC.

HAEC were cultured with 100 nM insulin for 48h (Hyperinsulinaemia) or left untreated. Insulin (1 µM)- and ionomycin (3 µM)-stimulated NO synthesis over 12 minutes was measured as described in section 2.2.8. The data are derived from 9 independent experiments (from 5 different HAEC donors), and are presented as the mean percentage of amount of NO produced/min ± SEM, relative to the mean of the unstimulated control samples for each experiment. *$p<0.05$ for insulin-stimulated compared to basal control, **$p<0.005$ for ionomycin-stimulated control compared to basal control (Student's t-test).

3.2.3 Protein expression and phosphorylation under experimental hyperinsulinaemia

Current evidence points to a role for NO in vasoprotection and a proatherogenic propensity in states of reduced NO bioavailability. There is strong evidence to suggest that disruption of the insulin signalling pathway contributes to endothelial dysfunction, as *in vitro* data from HUVEC carrying a mutant version of IRS-1 (G972R) (Federici *et al.*, 2004) and clinical studies with G972R heterozygote carriers (Perticone *et al.*, 2004) show (discussed in section 3.3.2).

While no impairment of insulin-responsive, eNOS-mediated NO synthesis was observed in the present study (Figure 3-2), it was investigated whether experimental hyperinsulinaemia affected individual components of the metabolic insulin signalling pathway at the molecular level. In addition, pilot studies evaluated whether experimental hyperinsulinaemia affected the expression and phosphorylation of the mitogen-activated protein kinase, p44/42 MAPK (also known as externally-regulated kinase, ERK1/2), a component of the mitogenic insulin signalling pathway. This was done in order to determine whether hyperinsulinaemia differentially affects the metabolic and mitogenic branches of the insulin signalling pathway, as has been suggested by other studies (Jiang *et al.*, 1999a, Cusi *et al.*, 2000, Montagnani *et al.*, 2002, He *et al.*, 2006, Rask-Madsen & King, 2007).

For these studies, HAEC were cultured under experimental hyperinsulinaemic conditions, following which protein expression and phosphorylation levels of key components of the metabolic insulin signalling pathway (PI3K, PTEN, PDK-1, PKB and eNOS), the mitogenic insulin signalling pathway molecule p44/42 MAPK and cellular energy charge (AMPK) were quantified by SDS-PAGE and Western blotting of HAEC lysates. All phosphoprotein levels were normalised to the amount of total protein of the same species, or to the protein levels of a molecule whose expression was unchanged by experimental hyperinsulinaemia. The results of these studies are summarised toward the end of this chapter in Table 3-1.

3.2.3.1 eNOS and PKB

The protein levels of total eNOS (Figure 3-3, panel A) showed a small and insignificant trend to increase during prolonged experimental hyperinsulinaemia (+14±6% and +25±12% in HAEC stimulated with 100 nM insulin for 24h and 48h, respectively, compared to untreated control HAEC). PKB protein expression (Figure 3-3, panel B) did not change with ongoing experimental hyperinsulinaemia.

To demonstrate that stimulation with 1 µM insulin did not affect total protein expression levels, acute (10 min) stimulation with insulin is indicated on the Western blots in Figure 3-3. From this figure, it is evident that there is no change in total protein expression levels between acutely insulin-treated cells and controls at all three time points tested. Hence, the protein expression data from acutely stimulated and untreated cells were collated separately for each time point. Consequently, in all subsequent figures, acute insulin stimulation is only indicated where protein phosphorylation levels were investigated.

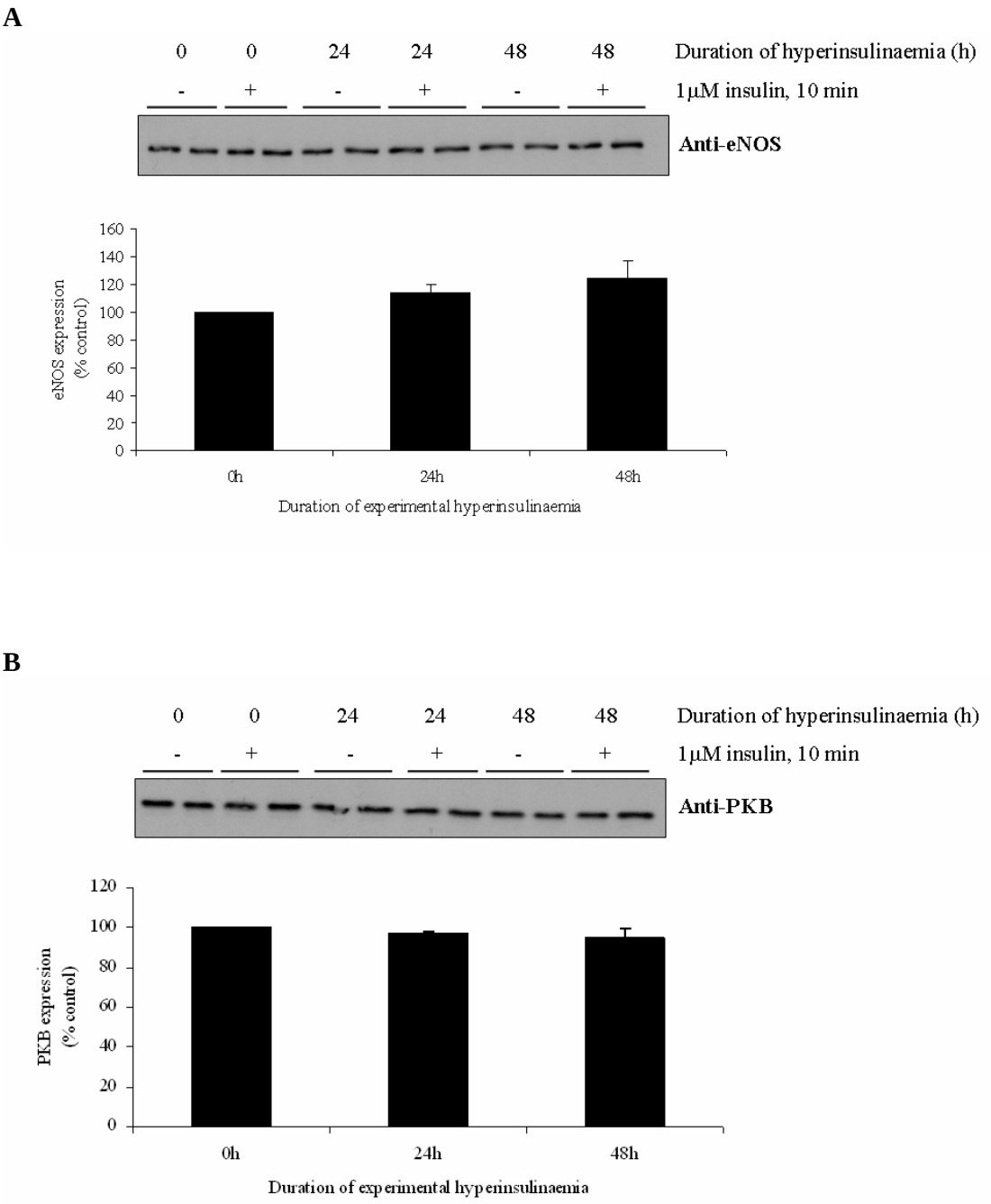

Figure 3-3 Experimental hyperinsulinaemia does not alter eNOS or PKB expression.

HAEC were treated with 100 nM insulin for 24-48h or left untreated. Cells were then serum-starved for 2h, and subsets of cells were stimulated acutely with insulin for 10 minutes. Cell lysates were prepared as described in section 2.2.2, and equal amounts of protein (3-10 µg) were resolved on SDS-polyacrylamide gels. After Western transfer, membranes were probed with antigen-specific antibodies as indicated. Representative Western blots are shown. Protein expression of eNOS (panel A) and PKB (panel B) is unchanged by experimental hyperinsulinaemia. Data represent the mean + SEM expression of 5 independent experiments. HAEC were derived from 3 different individual donors.

In order to determine whether eNOS was phosphorylated as expected for functional eNOS activity under experimental hyperinsulinaemia, the phosphorylation levels of the two best-characterised phosphorylation sites of eNOS, Ser1177 ($eNOS^{S1177}$) and Thr495 ($eNOS^{T495}$) were quantified. NO production is proposed to require the coordinated regulation of these two phosphosites: Phosphorylation of the activating site Ser1177 is necessary for eNOS activity in response to growth factors (Dimmeler *et al.*, 1999, Fulton *et al.*, 1999, Michell *et al.*, 2001), while experimental evidence suggests that the inhibitory site Thr495 is dephosphorylated for effective NO production (Chen *et al.*, 1999, Fleming *et al.*, 2001, Greif *et al.*, 2002, Fleming & Busse, 2003, Matsubara *et al.*, 2003). Insulin can cause rapid phosphorylation of $eNOS^{S1177}$ (Kim *et al.*, 2001) and simultaneous dephosphorylation of $eNOS^{T495}$ (Federici *et al.*, 2004).

As expected, acute stimulation of HAEC with insulin caused an increase over basal in $eNOS^{S1177}$ phosphorylation under all conditions (fold increases over basal control were 2.3±0.6 for insulin-stimulated control, 2.4±0.7 for 24h and 3.1±1.6 for 48h of experimental hyperinsulinaemia), although this was not statistically significant due to large interexperimental variation (Figure 3-4, panel A). There was a small and non-significant trend toward increased basal $eNOS^{S1177}$ phosphorylation with ongoing hyperinsulinaemia (fold increases over basal control were 1.2±0.2 for 24h and 1.5±0.4 for 48h).

The basal phosphorylation level of $eNOS^{T495}$ did not change during prolonged hyperinsulinaemia, as is evident from comparison to total eNOS levels (Figure 3-4, panel B). Acute insulin did not cause a significant change in $eNOS^{T495}$ phosphorylation at any time point tested. However, there was a tendency toward an increased $eNOS^{T495}$/eNOS ratio during experimental hyperinsulinaemia (fold-changes compared to corresponding unstimulated control were -1.3±0.5 for control and +1.2±0.7 for 48h). Again, large interexperimental variation was observed, and due to the low repeat number, no statistical analysis could be performed.

A

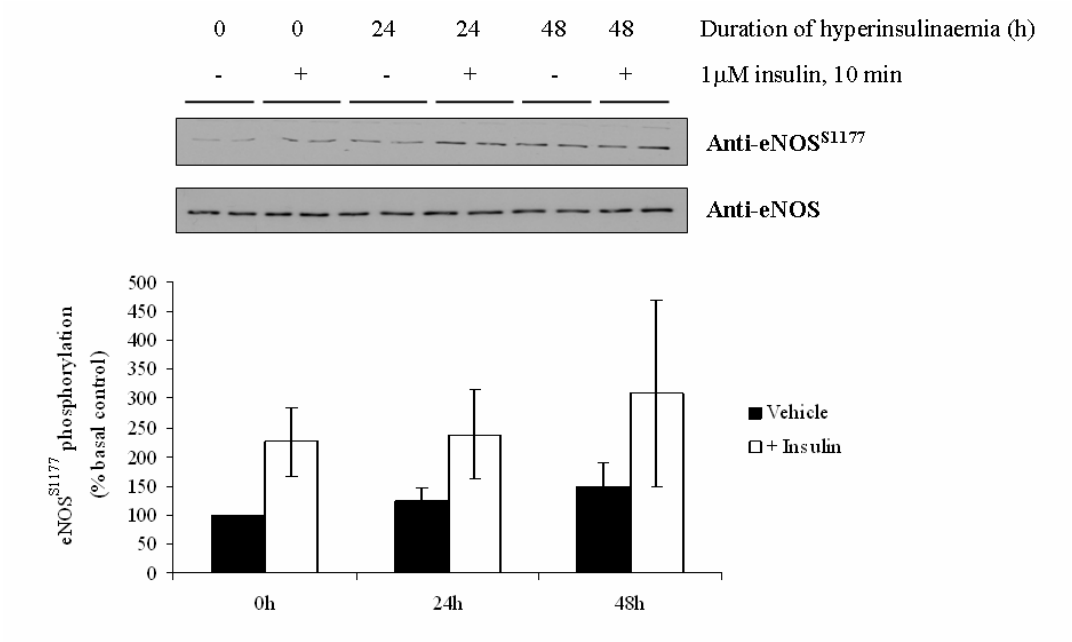

B

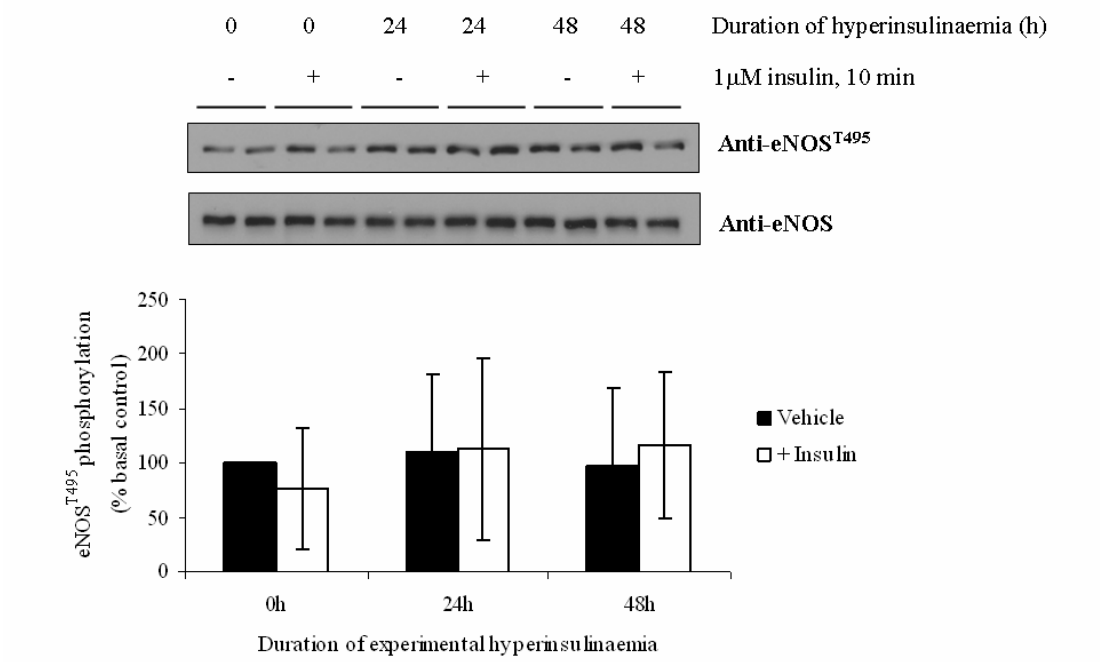

Figure 3-4 Experimental hyperinsulinaemia does not significantly alter phosphorylation of eNOS at Ser1177 or Thr495.

HAEC lysates were subjected to immunoblotting analysis as described (section 2.2.6) to quantify the levels of eNOS^{S1177} (panel A) and eNOS^{T495} (panel B). Representative Western blots are shown. A: Data shown are the mean ± SEM expression from 5 independent experiments (3 different donors). B: Data are shown as mean ± range expression from 2 independent experiments (2 donors).

In order to determine whether PKB phosphorylation was affected by experimental hyperinsulinaemia, the phosphorylation levels of the PKB activating site Ser473 (PKB^{S473}) were quantified from the same HAEC lysates that had been used for eNOS quantification. PKB^{S473} phosphorylation was used as an indicator of PKB activity. As illustrated in Figure 3-5, phosphorylation of PKB^{S473} was responsive to acute insulin stimulation under all conditions tested. However, there was a trend toward decreased insulin-mediated PKB^{S473} phosphorylation with ongoing hyperinsulinaemia, although this was not statistically significant. This trend was caused by increased basal and decreased insulin-responsive phosphorylation of Ser473. The fold increases of stimulated compared to corresponding basal phosphorylation were 6.8±4.7 for control, 4.2±2.6 for 24h and 3.4±1.8 for 48h. Due to large interexperimental variation, these fold stimulations were not statistically significant.

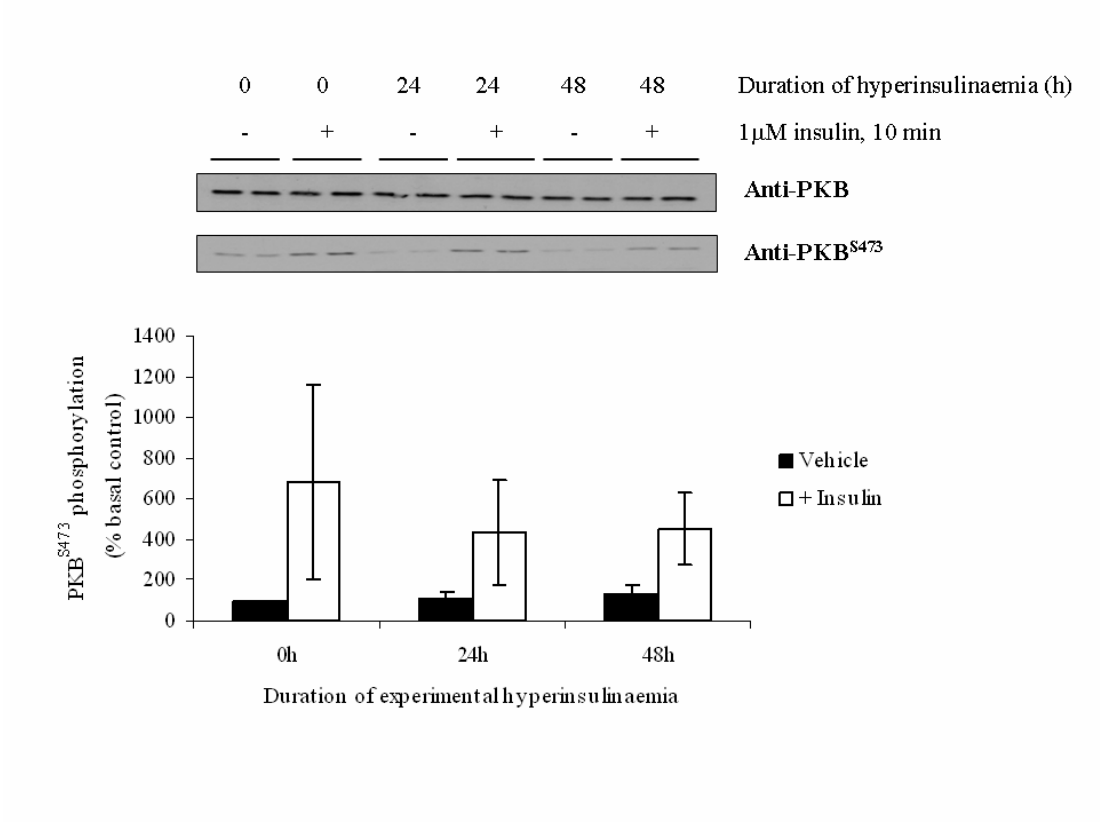

Figure 3-5 The insulin-sensitivity of PKB^{S473} phosphorylation decreases under experimental hyperinsulinaemia.

HAEC lysates from 3 different donors were prepared and analysed as described (sections 2.2.2 and 2.2.6). Data from 5 independent experiments are shown as mean ± SEM expression relative to basal control. Representative Western blots are shown along with densitometric quantification of the levels of PKB^{S473}/PKB (no statistically significant differences).

3.2.3.2 AMPK

Given that insulin-responsive PKB^{S473} phosphorylation was not greatly impaired by experimental hyperinsulinaemia (Figure 3-5), PKB activity was likely to be normal and thus unlikely to negatively affect eNOS^{S1177} phosphorylation (Figure 3-4). The AMP-activated kinase AMPK is known to phosphorylate eNOS at Ser1177 (Chen *et al.*, 1999, Fleming & Busse, 2003, Morrow *et al.*, 2003). Therefore, the expression levels of AMPK and the phosphorylation status of its activating site Thr172 were investigated, to determine whether AMPK could be an effector of the slightly increased basal eNOS^{S1177} phosphorylation at 24h and 48h of experimental hyperinsulinaemia. The majority of the samples used in these experiments were identical to those used for the quantification of eNOS and PKB expression.

Total AMPK expression levels showed a slight and non-significant trend to decline during experimental hyperinsulinaemia (fold changes with respect to control were 0.88±0.1 and 0.90±0.07 for 24h and 48h, respectively; see Figure 3-6, panels A and B). Basal phosphorylation of AMPK^{T172} was increased ~2.2±1.2-fold after 48h of experimental hyperinsulinaemia. Acute stimulation with insulin increased AMPK^{T172} phosphorylation under control conditions and after 24h of experimental hyperinsulinaemia (fold increase for stimulated compared to corresponding basal control were 2.7±1.2 for control and 2.8±1.1 for 24h). However, after 48h of experimental hyperinsulinaemia, basal AMPK^{T172} phosphorylation was 2.2±1.2-fold higher than basal control, while insulin-stimulated phosphorylation was 3.0-fold lower than insulin-stimulated control, and comparable to basal control levels (see Figure 3-6, panels A and C). There was a 2.5-fold reduction in insulin-stimulated compared to basal phosphorylation at 48h. Due to variation within treatment groups, none of these changes were statistically significant.

A

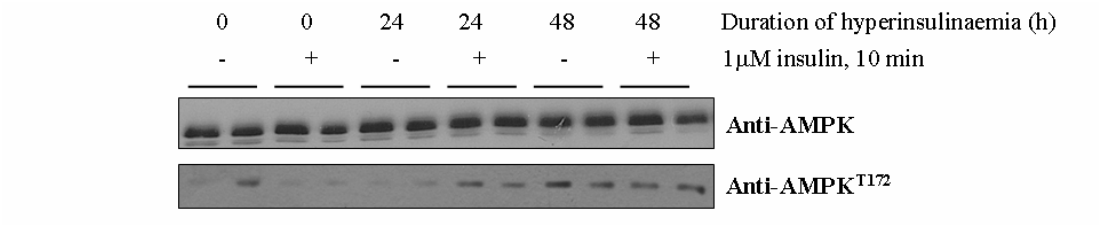

B

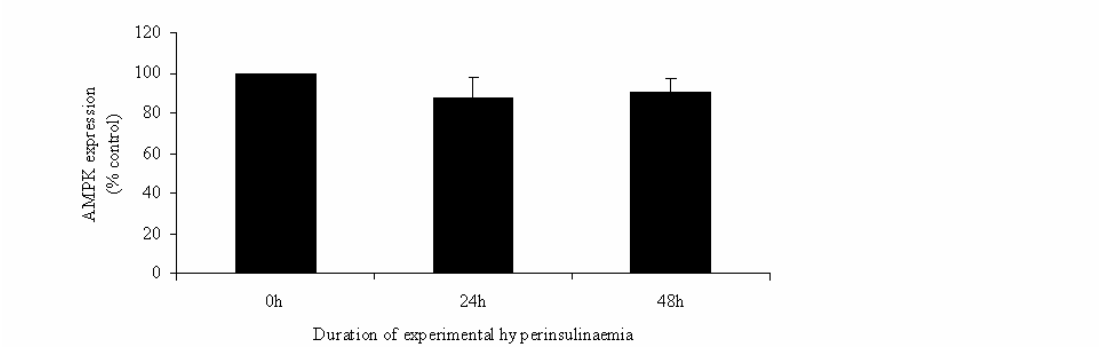

C

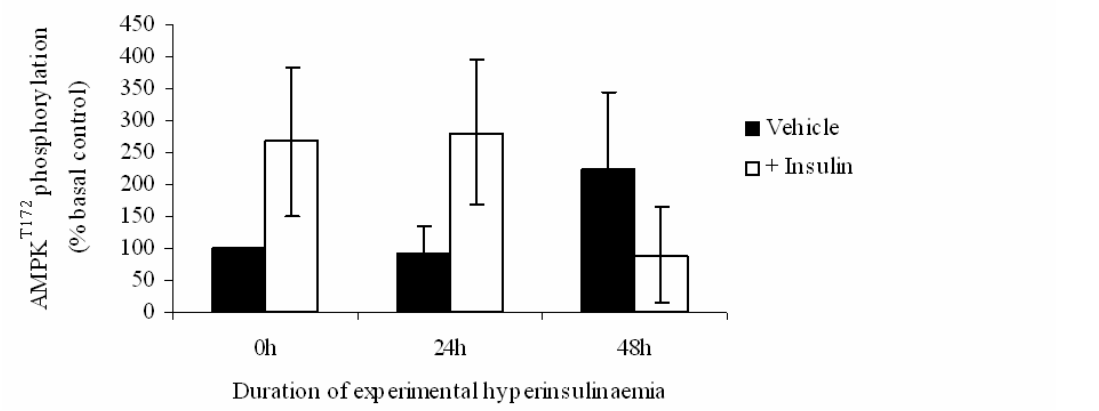

Figure 3-6 AMPK expression is unchanged, while insulin-stimulated AMPK^{T172} phosphorylation is decreased after 48h of experimental hyperinsulinaemia.

HAEC lysates were prepared, resolved by SDS-PAGE and subjected to Western blotting as described in sections 2.2.2 and 2.2.6. Representative Western blots are shown (panel A). While AMPK expression levels were unchanged (panel B), the basal and insulin-stimulated AMPK^{T172}/AMPK ratios after 48h of experimental hyperinsulinaemia are inversed with respect to control (panel C) (no statistically significant differences). Data shown are the mean ± SEM expression of 3 independent experiments with HAEC derived from 2 individual donors.

3.2.3.3 PDK-1, PI3K and PTEN

To further characterise the effect of experimental hyperinsulinaemia on the metabolic insulin signalling pathway, the expression levels of the 3-phosphoinositide-dependent protein kinase-1 (PDK-1), which phosphorylates PKB, and the regulatory (p85) and catalytic (p110ß) subunits of the upstream phosphatidylinositol 3-kinase, PI3K, which is required for PDK-1 activity, were quantified. For these experiments, the same HAEC lysates that had been used to quantify eNOS and PKB levels were used The results are shown in Figure 3-7, panels A (PDK-1) and B (PI3K-p85 and -p110ß).

It was also investigated whether the protein levels of the phosphatase PTEN were affected by experimental hyperinsulinaemia. PTEN dephosphorylates $PI(3,4,5)P_3$ to $PI(4,5)P_2$, thereby negatively regulating PI3K activity (Oudit *et al.*, 2004). PTEN is also involved in the inhibition of eNOS activation via insulin signalling pathway components in response to various pathological conditions, including the metabolic syndrome (Shen *et al.*, 2006a, Shen *et al.*, 2006b, Wang *et al.*, 2006), and therefore represents a potential – albeit indirect – regulator of eNOS phosphorylation in the present system. The majority of the samples used for PTEN analysis were identical to those used for the quantification of eNOS and PKB expression levels (see Figure 3-8).

While PDK-1 expression appeared to be slightly upregulated after 48h of experimental hyperinsulinaemia (1.2±0.09-fold; Figure 3-7, panel A), this increase was not statistically significant. Quantification of the expression of the PI3K p85 regulatory subunit and the p110ß catalytic subunit revealed that neither of these expression levels changed under hyperinsulinaemic conditions (Figure 3-7, panel B). The expression of the phosphatase PTEN declined over the time course of experimental hyperinsulinaemia, resulting in decreased protein levels by 48h (fold changes compared to control were 0.95±0.01 and 0.82±0.03 for 24h and 48h, respectively) (see Figure 3-8).

In addition to the above molecules, the expression levels of the insulin receptor substrates (IRS)-1 and -2 were investigated. However, these experiments yielded insufficient results due to poor antibody recognition of these proteins (data not shown).

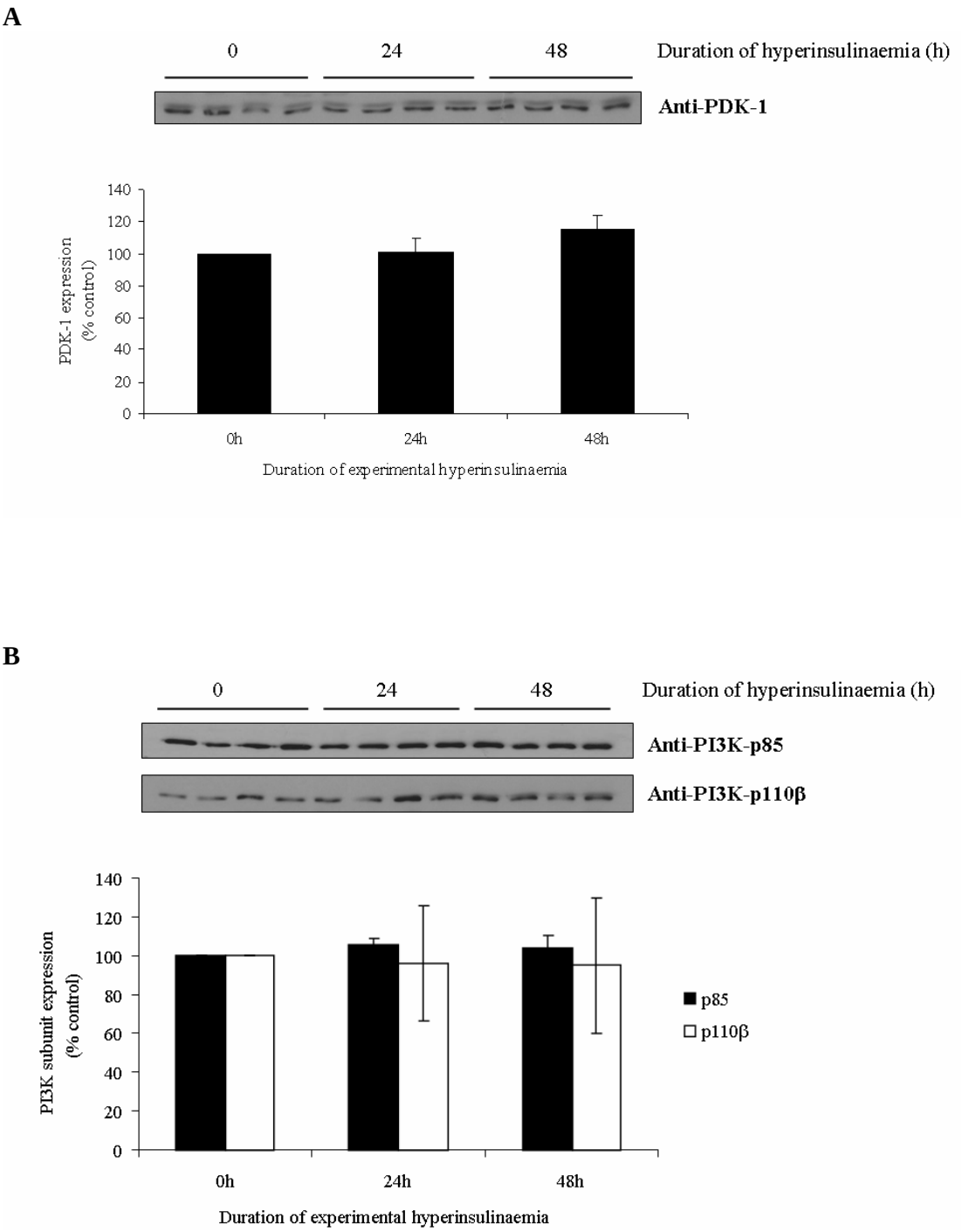

Figure 3-7 Experimental hyperinsulinaemia does not alter PDK-1 and PI3K levels.

HAEC lysates were prepared and equal amounts of protein used for SDS-PAGE and Western transfer (see sections 2.2.5 and 2.2.6). Representative Western blots are shown. A: PDK-1 expression levels are not altered by experimental hyperinsulinaemia. Data (mean ± SEM expression) are derived from 3 independent experiments with HAEC from 2 individual donors. B: PI3K-p85 and –p110ß expression remain unchanged during experimental hyperinsulinaemia. Data shown are the mean ± SEM expression of 4 independent experiments (3 individual donors) for the PI3K-p85 subunit, or 3 independent experiments (2 individual donors) for the p110ß subunit.

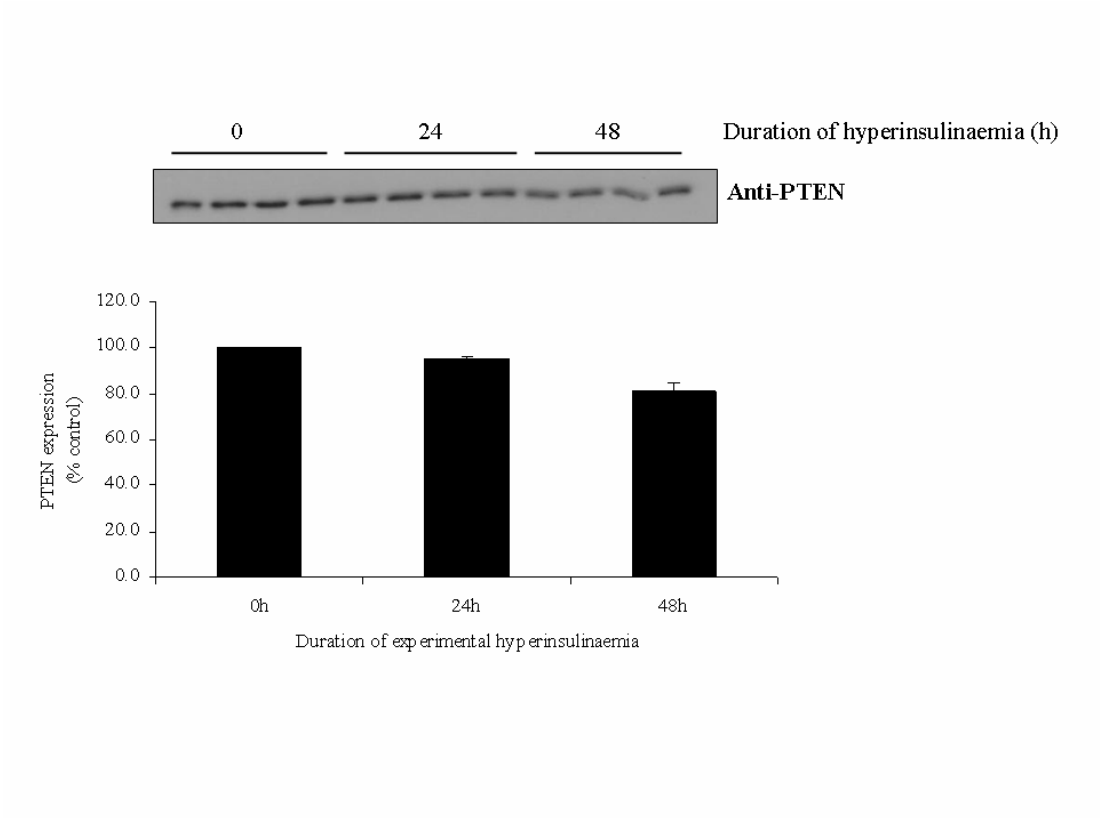

Figure 3-8 Expression of PTEN shows a trend to decreases during experimental hyperinsulinaemia.

HAEC were treated as above and equal amounts of protein (3-10 µg) subjected to SDS-PAGE and Western transfer. Densitometric analysis demonstrated that the amount of PTEN protein declined with ongoing experimental hyperinsulinaemia. Data (mean + range expression; no statistical analysis possible) from 2 independent experiments with HAEC from one donor are shown along with a representative Western blot.

3.2.3.4 p44/42 MAPK

In order to investigate whether experimental hyperinsulinaemia had an effect on the mitogenic insulin signalling pathway, the expression and phosphorylation levels of the mitogen-activated protein kinase, p44/42 MAPK, were quantified in the same HAEC lysates that had been used to quantify the expression levels of the metabolic insulin signalling pathway components.

Panel B in Figure 3-9 shows that the expression of p44/42 MAPK is upregulated 1.2±0.13-fold compared to control by 24h of experimental hyperinsulinaemia, but declines to control levels by 48h. These changes were not statistically significant.

The results of these studies are summarised below in Table 3-1.

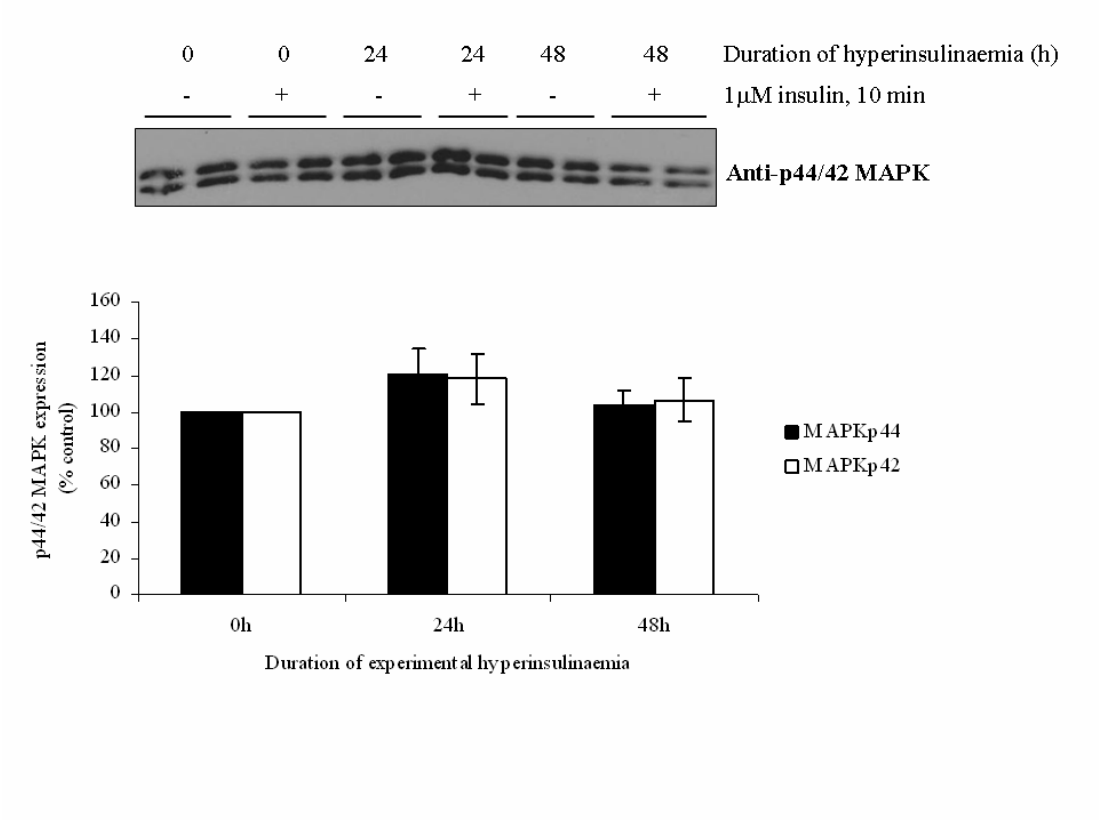

Figure 3-9 Experimental hyperinsulinaemia does not change p44/42 MAPK expression.

HAEC lysates were prepared as above and subjected to immunoblot analysis. A representative Western blot is shown. Expression levels of p44/42 MAPK are unchanged during experimental hyperinsulinaemia. Data shown are the mean ± SEM expression of 3 independent experiments with HAEC from 3 individual donors.

Table 3-1 Experimental hyperinsulinaemia has no marked effect on the expression levels of several signalling proteins.

This table summarises the findings of the present expression and phosphorylation level quantification studies carried out in HAEC.

Molecule	Effect of experimental hyperinsulinaemia
eNOS	Time-dependent increase of protein expression (1.25-fold at 48h); not statistically significant
eNOS^{S1177}/eNOS	Insulin-responsive under all conditions; increase in basal phosphorylation (1.5-fold) at 48h; not statistically significant
eNOS^{T495}/eNOS	Tendency toward inversed insulin-responsive phosphorylation (-1.3-fold under control conditions, +1.2-fold at 48h); not statistically significant
PKB	No change in expression levels
PKB ^{S473}/PKB	Insulin-responsive under all conditions tested; trend toward decreased insulin-stimulated phosphorylation (6.8-fold under control conditions, 3.4-fold after 48h); not statistically significant
AMPK	Unchanged expression levels
AMPK^{T172}/AMPK	2.2-fold increased basal and 3-fold reduced insulin-stimulated phosphorylation at 48h compared to respective controls; no statistically significant differences
PDK-1	Tendency toward increased expression over time (1.2-fold at 48h); not statistically significant
PI3K-p85 and -p110ß	No change in expression
PTEN	Time-dependent decline (0.8-fold of control at 48h); not statistically significant
p44/42 MAPK	1.2-fold increased expression at 24h (not statistically significant), expression back to control levels after 48h

3.2.4 Assessment of monocyte adhesion to hyperinsulinaemic HAEC

The effect of experimental hyperinsulinaemia on monocyte attachment to HAEC was investigated. HAEC were incubated in the presence or absence of 10-100 nM insulin for 24-48h, and subsets were stimulated with 10 ng/ml TNFa for 6h. Thereafter, HAEC were washed thoroughly and overlaid with U937 pre-monocytic cells. Monocytes were allowed to attach for 1h before unbound U937 cells were washed off and attached U937 cells were fixed with paraformaldehyde (see section 2.2.10 for a detailed description).

Under control and hyperinsulinaemic conditions, few U937 cells attached to HAEC but, as expected, TNFa-treatment resulted in marked stimulation of monocyte adhesion, although this was not significant due to interexperimental variation. Experimental hyperinsulinaemia did not exacerbate TNFa-stimulated monocyte adhesion (see Figure 3-10).

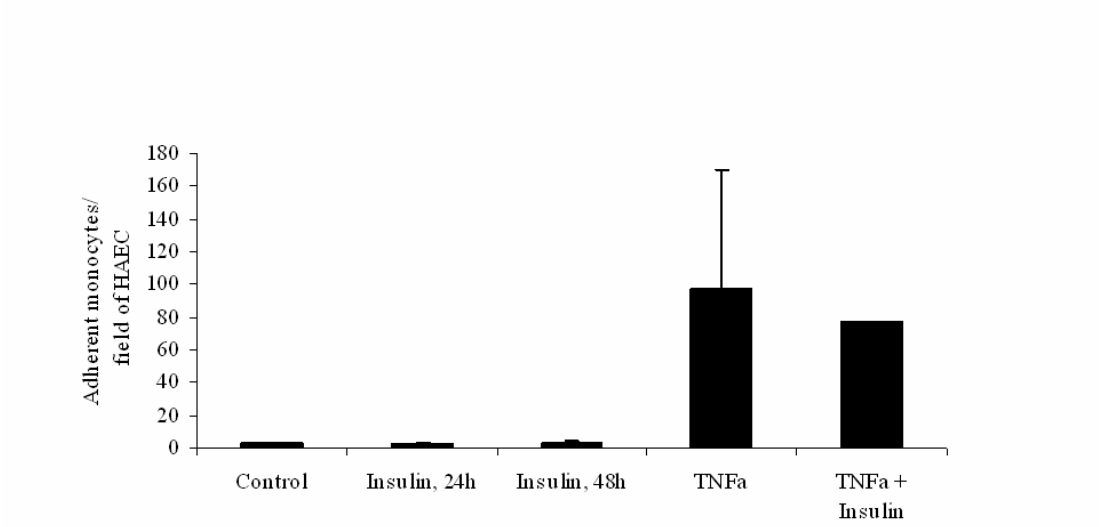

Figure 3-10 Experimental hyperinsulinaemia does not increase monocyte adhesion.

HAEC were stimulated with 0-100 nM insulin for the times indicated in the presence or absence of TNFa. Monocytes were allowed to attach to HAEC for 1h after which time unbound monocytes were washed off. Attached monocytes were counted microscopically at X100 magnification. Data shown are mean + SEM attached monocytes per field of HAEC from 3 independent experiments (1 experiment for TNFa + insulin-treated cells). The means were calculated for each experiment. The total number of separate fields counted per treatment group was 540 (control), 270 (insulin, 24h), 270 (insulin, 48h), 188 (TNFa) and 24 (TNFa + insulin). TNFa-treatment caused a non-significant increase in monocyte adhesion.

3.3 Discussion

3.3.1 Nitric oxide production

The present study shows that insulin stimulated a small but significant increase in nitric oxide production in HAEC under control conditions, as has been demonstrated previously in HUVEC (Zeng & Quon, 1996, Zeng *et al.*, 2000). In addition, this study demonstrates that insulin stimulated NO production in HAEC under hyperinsulinaemic conditions, but this increase was not statistically significant (see Figure 3-2). Under control conditions, HAEC were more responsive to the calcium ionophore ionomycin than to insulin. In hyperinsulinaemic cells, this response to ionomycin was attenuated, but the small number of experiments performed under these conditions limits the significance of these findings.

The stimulation of NO synthesis by insulin was less than expected in these experiments, reaching only ~11% under control conditions. This indicates that the HAEC model employed in this study is not particularly insulin-sensitive, and is therefore of limited use as a model for experimental hyperinsulinaemia. However, because this small increase was consistent, it was statistically significant. In a previous study, a ~35% increase in NO release from mouse aorta *ex vivo* elicited by 1 µM insulin was reported (Hartell *et al.*, 2005). It is noteworthy though, that Hartell and co-workers used the fluorescent dye DAF-2, which reacts with intracellular NO but is strongly affected by divalent cation concentration in the system and by incident light (Broillet *et al.*, 2001). This experimental approach is therefore difficult to control and standardise, and as such is of limited use.

In the present study, the overall NO levels produced by HAEC were not decreased by experimental hyperinsulinaemia. However, the difference between basal and insulin-stimulated NO production was no longer significant. In the light of the limited insulin-sensitivity of the HAEC used here, this finding will have to be verified in a more sensitive model. The current findings stand in contrast to other studies: In skin fibroblasts from insulin-resistant individuals, insulin failed to augment eNOS activity (as measured by the conversion of [^{3}H]-L-Arginine to [^{3}H]-L-Citrulline, an indirect marker of NO production), whereas activity was increased ~1.7-fold in fibroblasts from insulin-sensitive individuals (Pandolfi *et al.*, 2005). Potenza and co-workers reported that experimental rats with hyperinsulinaemia (spontaneously hypertensive rats, SHR) showed a 20% smaller vasodilation response to insulin than control rats (Potenza *et al.*, 2005). Likewise, gracilis arteries of hyperinsulinaemic obese Zucker rats showed only half the control dilation response to acetylcholine *in vivo* (Fulton *et al.*, 2004b). Arcaro and co-workers showed that

short-term hyperinsulinaemia abrogated endothelium-dependent vasodilation in femoral and brachial conduit arteries of healthy subjects (Arcaro *et al.*, 2002). All of these previous reports point to a negative effect of hyperinsulinaemia on nitric oxide synthesis and bioavailability, which is not mirrored in the present study. This discrepancy may reflect the mixture of tissues used and the length of hyperinsulinaemia studied.

While limited stimulation of NO production was observed in the experiments presented here, it is, of course, possible that NO synthesis was stimulated to a greater extent than evident from the measurement of nitrite in these experiments. For example, the levels of reactive oxygen species may have been high in the cells used. If this was the case, ROS would have reacted with NO. Superoxide, for example, can react with NO, leading to formation of both peroxynitrite and nitrate (Reiter *et al.*, 2000). Peroxynitrite in turn can reduce NO bioavailability through oxidation and uncoupling of eNOS, leading to enhanced superoxide production and decreased NO synthesis (Zou *et al.*, 2002). It is therefore possible that a proportion of the NO produced by the HAEC in this experimental system was not detected due to rapid reaction with ROS.

Duncan and co-workers postulated that endothelial cell superoxide production during mild hyperinsulinaemia in older insulin receptor knockout (IRKO) mice may be a mechanism underlying early reduction in NO bioavailability (Duncan *et al.*, 2007). Indeed, an earlier study by Shinozaki and co-workers had also demonstrated decreased eNOS activity and vasorelaxation in the aortae of hyperinsulinaemic, insulin-resistant fructose-fed rats (Shinozaki *et al.*, 1999). Interestingly, not only was endothelium-dependent vasorelaxation impaired in these rats, but NO production was decreased in response to the calcium ionophore A23187, while superoxide generation was increased. Reduced ionophore-stimulated NO production in hyperinsulinaemic cells was also seen in the present study (Figure 3-2), pointing to a potential mild dysregulation of NO bioavailability in this system. It remains to be determined whether this may be due to increased superoxide/ROS production.

With the set-up used in these experiments, the nitric oxide analyser measures nitric oxide and its reaction product nitrite, but not nitrate or peroxynitrite. Because any potential reaction between ROS/superoxide and NO diminishes the amount of nitrite formed, the levels of nitrite formed under these conditions may not be representative of the total amount of NO produced. It is therefore conceivable that enhanced NO production is masked by elevated nitrate and/or peroxynitrite formation in these cells, if the cells were

suffering from oxidative stress. Suitable means for detecting oxidant stress under these experimental conditions include the use of lucigenin-based chemiluminescence assays for the detection of superoxide (Liochev & Fridovich, 1997) and the use of fluorescein-phenol-coupling-based assays for the detection of ROS (Heyne *et al.*, 2006). In future experiments, oxidative stress of the cells could be controlled by the addition of antioxidants such as ascorbic acid to the cell culture medium/buffer (Dr Carol Colton, Duke University Medical Centre, personal communication).

3.3.2 Protein expression and phosphorylation

Quantitative analysis of molecular components of the metabolic (eNOS, PKB, PI3K, PDK-1 and PTEN) and mitotic (p44/42 MAPK) insulin signalling pathways, as well as the cellular energy sensor molecule AMPK, revealed that experimental hyperinsulinaemia does not markedly alter the expression levels of these molecules within 48h. Similarly, the phosphorylation levels of $eNOS^{S1177}$, $eNOS^{T495}$, PKB^{S473} and $AMPK^{T172}$ were not significantly changed during experimental hyperinsulinaemia, although some trends toward a less NO-productive environment were observed (see Table 3-1). For instance, the degree of insulin-stimulated PKB^{S473} phosphorylation decreased by ~50% over time with ongoing hyperinsulinaemia, and insulin-responsive $AMPK^{T172}$ phosphorylation was decreased 3-fold after 48h of experimental hyperinsulinaemia. In their phosphorylated state, both of these molecules promote $eNOS^{S1177}$ phosphorylation, and can lead to NO production. Under the same conditions, acute insulin failed to promote $eNOS^{T495}$ dephosphorylation, which is thought to enhance NO production. Overall, these findings indicate that 48h of experimental hyperinsulinaemia may begin to promote a less insulin-sensitive phenotype at the molecular level in HAEC. Below, these observations are discussed in the light of the current literature.

The finding of ~1.25-fold increased eNOS protein expression during experimental hyperinsulinaemia (Figure 3-3), while not statistically significant in the present study, is in line with previous reports of increased eNOS expression (~1.4-fold) in human coronary artery endothelial cells cultured with 10 or 100 nM insulin for 24h (Ding *et al.*, 2000). Furthermore, Aljada & Dandona reported an insulin dose-dependent increase in eNOS expression in HAEC during experimental hyperinsulinaemia (Aljada & Dandona, 2000). Two studies with obese Zucker rats, an animal model of hyperinsulinaemia and insulin resistance (Chua *et al.*, 1996), suggested that eNOS protein expression was increased in small coronary arteries (~7.2-fold) (Katakam *et al.*, 2005) and in aorta lysates (Toba *et al.*, 2006). Others, however, found that eNOS expression was unaltered in whole aorta lysates of obese Zucker rats (Fulton *et al.*, 2004b, Naruse *et al.*, 2006), and in the hearts of two further animal models of insulin resistance, the fructose-fed rat and the ob/ob mouse (Fulton *et al.*, 2004b).

In an animal model of mild hyperinsulinaemia, the heterozygous insulin receptor knockout (IRKO) mouse, eNOS protein levels were increased ~5-fold in the aortae of 6 month-old mice, while eNOS mRNA levels were comparable to wild-type controls (Duncan *et al.*, 2007). However, in vascular endothelial cell insulin receptor knockout (VENIRKO) mice,

eNOS mRNA levels were reduced by 30-60% in endothelial cells, aorta and heart compared to controls. By six months of age, VENIRKO mice had developed mild insulin resistance, but remained glucose-tolerant (Vicent *et al.*, 2003). The differences between these various models described above emphasise the complexity of physiological systems and the ensuing difficulty in defining the mechanisms underlying a model's responses to stimuli such as insulin.

In the context of vasorelaxation, a decrease in eNOS expression would be predicted to be associated with elevated blood pressure due to decreased production of the vasodilator NO. Indeed, heterozygous and homozygous eNOS knockout mice show increased blood pressure that is attributable to the decrease/loss of eNOS protein expression (Shesely *et al.*, 1996). By contrast, elevated eNOS protein levels during hyperinsulinaemia do not necessarily have to correlate with increased NO levels, but may equally represent a greater proportion of uncoupled eNOS. This, in turn, could diminish NO synthesis and enhance superoxide generation (Zou *et al.*, 2002), leading to impaired vasodilation. This has been demonstrated in IRKO mice, which show increased aortic eNOS protein levels with increased endothelial ROS and blunted endothelium-dependent vasodilation (Duncan *et al.*, 2007). While vasodilation cannot be assessed in the present system, superoxide levels in HAEC can be measured, which would represent an interesting extension to the present body of work.

In the present study, experimental hyperinsulinaemia mildly increased the basal and insulin-stimulated phosphorylation of eNOS at Ser1177 (~1.5-fold increase of basal, and 1.4-fold increase of insulin-stimulated phosphorylation at 48h compared to the corresponding controls; see Figure 3-4, panel A). These findings are corroborated by the observation that basal eNOS^{S1177} phosphorylation (as normalised to total eNOS expression) was elevated in hyperinsulinaemic obese Zucker rats compared to control rats. However, two other animal models of hyperinsulinaemia , the fructose-fed rat and the ob/ob mouse showed no difference in the eNOS^{S1177}/eNOS ratio compared to controls. None of these models demonstrated a statistically significant change in the basal eNOS^{T495}/eNOS ratio (Fulton *et al.*, 2004b). This agrees with the present results, which demonstrate that experimental hyperinsulinaemia does not change basal eNOS^{T495} phosphorylation in HAEC.

Studies with IRS-1 G972R polymorphic HUVEC, which have a known insulin signalling defect, showed decreased basal and up to 51% reduced insulin-stimulated eNOS^{S1177}

phosphorylation compared to wild type HUVEC (Federici *et al.*, 2004). At the same time, basal eNOS^{T495} phosphorylation in these variant HUVEC was upregulated compared to control HUVEC. Acute insulin stimulation caused an increase in eNOS^{T495} phosphorylation above basal, and a 40% increase compared to insulin-stimulated wild type cells (Federici *et al.*, 2004). Assuming that experimental hyperinsulinaemia impairs insulin signalling, the present eNOS^{T495} findings (see Figure 3-4, panel B) agree with the mutant HUVEC data reported by Federici and co-workers, in that eNOS^{T495} phosphorylation in acutely stimulated hyperinsulinaemic HAEC was greater than in control cells in the present study. The present data on eNOS^{S1177} do not agree with the study by Federici and co-workers.

PKB expression (Figure 3-3) and PKB Ser473 phosphorylation (Figure 3-5) were largely unchanged in the present experiments, although a trend toward decreased insulin-responsive Ser473 phosphorylation was observed. These changes in PKB phosphorylation are not reflected by decreased insulin-stimulated eNOS^{S1177} phosphorylation; therefore, further studies with PI3K inhibitors such as wortmannin, which prevent PKB phosphorylation, are required to verify that PKB is indeed the kinase that phosphorylates eNOS^{S1177} under the present experimental conditions. Toba and co-workers reported that PKB and PKB^{S473} levels were upregulated in the aortae of hyperinsulinaemic rats (Toba *et al.*, 2006), while another group found that insulin failed to stimulate PKB^{S473} phosphorylation *in vivo* (as measured in whole aorta preparations from hyperinsulinaemic obese Zucker rats), but caused a 3 ±1-fold rise in control rats (Naruse *et al.*, 2006). G972R variant HUVEC showed a smaller PKB^{S473}/PKB ratio under basal and insulin-stimulated (40% reduction) conditions than control HUVEC (Federici *et al.*, 2004).

Phosphorylation of the kinase AMPK at Thr172 was quantified as an indirect marker of AMPK activity. Insulin stimulated AMPK^{T172} phosphorylation under control conditions and after 24h of experimental hyperinsulinaemia, but had no stimulating effect after 48h (Figure 3-6). Instead, basal phosphorylation of AMPK^{T172} was increased to insulin-stimulated control levels after 48h of experimental hyperinsulinaemia, whereas Thr172 phosphorylation was decreased after acute insulin treatment. While activated AMPK is a mediator of eNOS^{S1177} phosphorylation (Chen *et al.*, 1999, Morrow *et al.*, 2003), it has not previously been shown to phosphorylate eNOS in response to insulin. However, increased basal AMPK^{T172} phosphorylation may be responsible for the significantly higher basal eNOS^{S1177} phosphorylation observed in the present study, but this will have to be verified by the use of inhibitors to AMPK and/or its upstream kinases.

This hypothesis is indirectly supported by studies in fibroblasts that stably express human insulin receptors, which showed that co-transfection with eNOS and a dominant-negative AMPK mutant did not prevent $eNOS^{S1179}$ (homologous to human $eNOS^{S1177}$) phosphorylation in response to insulin (Chen *et al.*, 2003). Similarly, the findings of Morrow and co-workers demonstrated that knockdown of AMPK does not affect insulin-stimulated $eNOS^{S1177}$ phosphorylation. This suggests that AMPK does not play a crucial role in eNOS phosphorylation in response to insulin in the fibroblast model system, but it cannot be excluded that AMPK contributes to the elevated basal $eNOS^{S1177}$ phosphorylation levels in HAEC subjected to experimental hyperinsulinaemia.

PI3K is a critical mediator of cellular insulin signalling and lies upstream of PKB (Franke *et al.*, 1995, Zeng *et al.*, 2000). The PI3K p85a subunit has been shown to be a critical regulator of insulin sensitivity, using p85a knockout mice (Taniguchi *et al.*, 2006). The data presented here illustrate that experimental hyperinsulinaemia did not affect the expression levels of the PI3K p85 regulatory and p110ß catalytic subunits (Figure 3-7, panel B). By contrast, PI3K mRNA expression was increased in aortae of hyperinsulinaemic rats (Toba *et al.*, 2006). However, mRNA levels do not necessarily reflect the amount of protein present in a cell, and changes in mRNA expression may be translated into altered protein levels at a later time point. In another study, insulin-stimulated PI3K activity in IRS-1 variant HUVEC was reduced compared to controls (Federici *et al.*, 2004). Since PI3K levels were unaffected by experimental hyperinsulinaemia in the present study, this demonstrates that dysregulation of insulin signalling in HAEC does not occur at the level of PI3K expression within the time scale tested, although any potential effect on PI3K activity remains to be investigated.

PDK-1 is a downstream effector of PI3K that phosphorylates PKB at the primary activating site Thr308 (Alessi *et al.*, 1996, Vanhaesebroeck & Alessi, 2000). PDK-1 expression levels were modestly increased after 48h of experimental hyperinsulinaemia (not statistically significant, see Figure 3-7, panel A). It is therefore possible that elevated PDK-1 levels caused greater phosphorylation of PKB at Thr308, thus resulting in greater PKB activity despite normal PKB^{S473} phosphorylation. Phosphorylation of both Thr308 and Ser473 is necessary for PKB activity, but the sites are independent of one another (Alessi *et al.*, 1996). If disparate phosphorylation of PKB were the case here, it could account for the rise in $eNOS^{S1177}$ phosphorylation induced by long-term hyperinsulinaemia in these experiments. This speculation calls for further experimental investigation, for

example by direct measurement of PKB enzyme activity and quantification of the PKB^{T308}/PKB protein ratio under these conditions.

PTEN expression levels were mildly reduced after 48h of experimental hyperinsulinaemia (not statistically significant, see Figure 3-8). To date, no data concerning vascular endothelium-specific expression of PTEN under hyperinsulinaemic conditions have been reported, but several studies looking at the role of PTEN in muscle and adipose tissue have been published. Mice with an adipose tissue-specific deletion of PTEN displayed heightened insulin sensitivity and 1.8-fold greater PKB^{S473} phosphorylation (Kurlawalla-Martinez *et al.*, 2005). Further, a muscle-specific PTEN deletion protected mice from diet-induced hyperinsulinaemia, insulin resistance and diabetes (Wijesekara *et al.*, 2005). When fed a high-fat diet, these mice had twice the control level of insulin-induced PKB^{T308} phosphorylation in soleus, but not extensor digitorum longus muscles. By contrast, on a normal diet, these mice showed a reduced insulin-responsive PKB^{T308}/PKB ratio (Wijesekara *et al.*, 2005). In line with these findings, hyperinsulinaemic obese Zucker rats had raised PTEN mRNA and protein levels in soleus muscle (Lo *et al.*, 2004).

These and other data document that PTEN is a negative regulator of insulin signalling and insulin sensitivity in fat and muscle. If this is the case in vascular endothelial cells, decreased PTEN expression would imply increased insulin sensitivity, providing a possible explanation for increased basal $eNOS^{S1177}$ phosphorylation. However, given the time scale of the present study, the modest changes in $eNOS^{S1177}$ phosphorylation and PTEN expression and the lack of effect of experimental hyperinsulinaemia on PKB^{S473}, further studies are necessary to determine the effect of reduced PTEN expression in this system.

The expression and phosphorylation of p44/42 MAPK, a component of the mitogenic insulin signalling pathway, was studied. It is well-documented that the metabolic and the mitogenic branch of the insulin signalling pathway can be differentially affected in hyperinsulinaemia and Type II diabetes (Jiang *et al.*, 1999a, Cusi *et al.*, 2000, Montagnani *et al.*, 2002, He *et al.*, 2006, Rask-Madsen & King, 2007). A modest (not statistically significant) increase of p44/42 MAPK expression was seen after 24h, but not after 48h of experimental hyperinsulinaemia (Figure 3-9, panel B). Further studies of the mitogenic pathway, including the activity levels of its pathway components, during experimental hyperinsulinaemia are required.

While the molecular mechanism(s) underlying the changes observed in the present study are not clear, alternative mechanisms that have not been investigated may play a role. For example, increased basal phosphorylation of $eNOS^{S1177}$ and upregulated insulin-stimulated $eNOS^{T495}$ phosphorylation could be due to reduced dephosphorylation of these sites, rather than increased phosphorylation. PKC activation has been proposed to mediate dephosphorylation of eNOS at Ser1177 and phosphorylation at Thr495. The phosphatases PP1 dephosphorylates Thr495, while PP2A can dephosphorylate both Thr495 and Ser1177 (Michell *et al.*, 2001, Greif *et al.*, 2002). Moreover, other kinases could be responsible for altered eNOS phosphorylation, including PKA (Michell *et al.*, 2001), PKG and CAMKII (Fleming *et al.*, 2001) (reviewed in (Mount *et al.*, 2007)).

Given that eNOS activity is thought to be determined by a concerted regulation of several phosphosites (Michell *et al.*, 2001, Bauer *et al.*, 2003, Mount *et al.*, 2007), including negative regulation by tyrosine phosphorylation (Garcia-Cardena *et al.*, 1996a, Huang *et al.*, 2002), it is unclear whether an altered eNOS phosphorylation profile necessarily creates a (measurable) change in eNOS activity. Experimental hyperinsulinaemia might also affect transcription, myristoylation (Busconi & Michel, 1993, Liu & Sessa, 1994, Shaul *et al.*, 1996), palmitoylation (Lamas *et al.*, 1992) and association of eNOS with other cellular components, thus potentially further affecting eNOS regulation. As these potential modes of regulation were not investigated in the current study and eNOS activity was not measured directly, it cannot be concluded that eNOS is dysregulated by experimental hyperinsulinaemia.

The differences between the effects of experimental hyperinsulinaemia observed in the present system and published studies highlight the discrepancy between different experimental models and the ensuing difficulty in drawing a consensus conclusion. Since the *in vitro* and *in vivo* models used in these studies varied, and the conditions of hyperinsulinaemia differed, the results document that hyperinsulinaemia has different effects in heterologous systems. Overall, the effects of hyperinsulinaemia seem to be exacerbated in certain *in vivo* models compared to *in vitro* models. Therefore, for example, it cannot be said with certainty that eNOS protein levels are increased in hyperinsulinaemic states, although there is strong *in vitro* evidence in favour of this thought.

Taking into account the present NO synthesis data and the fact that $eNOS^{S1177}$ and $eNOS^{T495}$ phosphorylation levels were only modestly affected, it is likely that in the current experimental setting, hyperinsulinaemia influences the phosphorylation status of

eNOS at Ser1177 and Thr495 without significantly affecting eNOS activity and NO production. Whether ionomycin-stimulated, calcium-dependent NO production is affected by experimental hyperinsulinaemia, requires further investigation that is beyond the scope of this work. The changes observed here may suggest that hyperinsulinaemic HAEC have a subtle insulin signalling impairment, which differs in some aspects to other experimental and clinical systems discussed above.

Overall, the HAEC used in the present study were a weak model for insulin resistance, since their response to acute insulin treatment was often small and varied greatly between different experiments. This may, in part, reflect the insulin-sensitivity of individual HAEC donors, but experimental error may have contributed to this variation. There is little evidence that the HAEC used here became insulin resistant after 48h of experimental hyperinsulinaemia. The present studies were carried on because initial results indicated robust insulin-responsiveness under control conditions along with more substantial changes induced by experimental hyperinsulinaemia.

It is likely that the short time scale of experimental hyperinsulinaemia employed in the present study is insufficient to cause substantial alterations in endothelial insulin signalling. Potentially, exposure of vascular endothelial cells to longer periods of experimental hyperinsulinaemia might exacerbate these changes. Ideally, healthy human vascular endothelial cells should therefore be cultured under hyperinsulinaemic conditions for several days or even weeks. However, since insulin's action as a growth factor and the growth characteristics of these cells *in vitro* present a challenge to such future studies, explanted vascular endothelial cells from patients with established hyperinsulinaemia might provide a suitable alternative model system. However, the potential presence of other confounding disease factors that might affect insulin signalling makes this model impractical. Refined experimental systems and further studies are required to define how hyperinsulinaemia affects endothelial function at the molecular level.

3.3.3 Monocyte adhesion to HAEC

This study investigated whether experimental hyperinsulinaemia affected monocyte attachment to hyperinsulinaemic HAEC. Experimental hyperinsulinaemia in the present study was found not to affect the adhesion of monocytic cells to HAEC cultured with 10 nM, 50 nM or 100 nM insulin for up to 48h (Figure 3-10). This stands in contrast to the hypothesis that hyperinsulinaemia promotes proinflammatory activation of HAEC, thus increasing monocyte attachment. Given that patients with clinical hyperinsulinaemia are thought to experience a state of persistent, low-level inflammation, along with endothelial activation (Fernandez-Real & Ricart, 2003), an extension of the present study is necessary to investigate the effects of experimental hyperinsulinaemia on vascular endothelial adhesion molecule expression and chemokine production.

Previously, several studies have reported that experimental hyperinsulinaemia can affect the expression of chemokine and adhesion molecule mRNA and protein (Aljada *et al.*, 2000) (Aljada *et al.*, 2001). This correlated with enhanced leukocyte adhesion and was postulated to enhance neutrophil transendothelial migration (Okouchi *et al.*, 2002a). Furthermore, incubation of mouse lung endothelial cells with insulin alone (10 nM, 24h) did not significantly increase rolling adhesion and arrest of monocytes, but simultaneous inhibition of PI3K resulted in significantly enhanced monocyte-endothelial cell interactions (Montagnani *et al.*, 2002). By contrast, circulating levels of the soluble adhesion molecules ICAM-1, VCAM-1 and E-selectin in the plasma of healthy individuals were found not to be elevated after 6 hours of euglycaemic hyperinsulinaemic (3 mU/kg/min) clamp, suggesting that short-term hyperinsulinaemia does not induce endothelial cell adhesion molecule protein expression (Jilma *et al.*, 2000).

4 The Effect of Experimental Hyperglycaemia on eNOS and Insulin-Responsive Pathways

4.1 Introduction

4.1.1 Background

Functional endothelial nitric oxide synthase (eNOS) activity is vital to vascular health, as eNOS is involved in vasorelaxation through the production of nitric oxide. As discussed in chapter 3, NO can be produced in response to insulin (Zeng & Quon, 1996) and is thought to have vasoprotective properties (Gewaltig & Kojda, 2002, Wheatcroft *et al.*, 2003). Phosphorylation of eNOS at Ser1177 plays an important part in insulin-stimulated NO production, which may involve the concerted regulation of several other phosphorylation sites (Michell *et al.*, 2001, Bauer *et al.*, 2003, Mount *et al.*, 2007).

In the context of hyperglycaemia and diabetes, it has frequently been reported that endothelial function and NO bioavailability are impaired ((Calver *et al.*, 1992, McVeigh *et al.*, 1992, Hogikyan *et al.*, 1998); reviewed in (De Vriese *et al.*, 2000, Rask-Madsen & King, 2007)), and that this association is independent of the presence of the complicating risk factors, obesity and hypertension (Hogikyan *et al.*, 1998). Consequently, patients with diabetes have an increased propensity to cardiovascular and microvascular disease and associated morbidity and mortality (Stratton *et al.*, 2000, Rahman *et al.*, 2007). The risk for vascular complications strongly correlates with the level of hyperglycaemia in patients (Stratton *et al.*, 2000).

Despite the proposed association between hyperglycaemia and endothelial dysfunction, two small studies suggested that insulin-induced vasorelaxation was similar in the coronary vasculature of healthy and Type I diabetic subjects and was not impaired by short-term hyperglycaemia (Smits *et al.*, 1993, Sundell *et al.*, 2002). Taking into account the small study populations (11 and 9 patients with diabetes, respectively), and the fact that the vasodilation response varies even within the healthy population (Ardigo *et al.*, 2006), it is possible that these studies are not representative. Furthermore, patients with diabetes are likely to suffer recurrent and/or prolonged, rather than short-term, periods of hyperglycaemia prior to diagnosis. This will increase their risk of suffering vascular complications due to endothelial dysfunction (Stratton *et al.*, 2000). Therefore, it is important to assess the impact of hyperglycaemia on vascular endothelial cell function to inform our understanding of the events that contribute to vascular disease risk.

Previous work has shown that exposure to high glucose concentrations impaired vasodilation in rabbit aorta (Tesfamariam *et al.*, 1990) and increased superoxide anion

generation in HAEC (Cosentino *et al.*, 1997) and rat aorta (Hink *et al.*, 2001). Oxidative stress has been proposed as a mediator of endothelial dysfunction (De Vriese *et al.*, 2000, Hink *et al.*, 2001, Srinivasan *et al.*, 2004), although this is subject to ongoing debate.

Experimental hyperglycaemia has been reported to impair the metabolic insulin signalling pathway and its individual components (Sobrevia *et al.*, 1998, Federici *et al.*, 2002, Salt *et al.*, 2003). Human umbilical vein endothelial cells (HUVEC) isolated from women with gestational diabetes were less sensitive to insulin and showed reduced insulin-responsive nitric oxide synthesis after culture with 25 mM glucose (Sobrevia *et al.*, 1998). Likewise, insulin-stimulated NO production was impaired in human aortic endothelial cells (HAEC) following culture in 25 mM glucose for 48h (Salt *et al.*, 2003), although these conditions did not affect the phosphorylation of eNOS at the activating site Ser1177. By contrast, insulin-stimulated $eNOS^{S1177}$ phosphorylation was reduced in human coronary artery endothelial cells (HCAEC) cultured with 20 mM glucose, while eNOS glycosylation was increased, leading to reduced insulin-responsive eNOS activity (Federici *et al.*, 2002).

Since the precise causes leading to endothelial dysfunction in hyperglycaemia/diabetes are uncertain, the underlying molecular mechanisms need to be further investigated.

4.1.2 Aims of the chapter

Previous studies in this laboratory have indicated that experimental hyperglycaemia differentially affects certain aspects of insulin signalling in HAEC. Experimental hyperglycaemia was shown to specifically inhibit insulin-stimulated NO synthesis without changing eNOS Ser1177 or Thr495 phosphorylation or PKB activity, but it did reduce insulin receptor substrate (IRS)-2 expression and PI3K recruitment to IRS-1 and -2 (Salt *et al.*, 2003). Furthermore, the insulin-regulated CAP-Cbl pathway was also deregulated by experimental hyperglycaemia (Salt *et al.*, 2003), indicating a negative effect of hyperglycaemia on vascular endothelial cell signalling.

The effect of experimental hyperglycaemia on the eNOS phosphorylation status at sites other than Ser1177 and on other insulin-responsive pathways has yet to be fully investigated in vascular endothelial cells. Therefore, the work presented in this chapter was designed to assess whether the metabolic insulin signalling pathway, and eNOS phosphorylation in particular, may be involved in mediating endothelial dysfunction during experimental hyperglycaemia (section 4.2.2). Furthermore, the contribution of several other insulin-responsive pathways, some of which regulate eNOS function, was investigated (section 4.2.3). Superoxide production under hyperglycaemic and normoglycaemic conditions was quantified as an indicator of endothelial dysfunction (section 4.2.4).

4.2 Results

4.2.1 Selection of experimental conditions

Previous work in this laboratory has been carried out in HAEC, which are large conduit vessel endothelial cells. For the present study, human umbilical vein endothelial cells (HUVEC) were chosen as a model system. These are peripheral vein endothelial cells, which may respond differently to stimuli such as glucose and insulin in the blood. Furthermore, work carried out during this study demonstrated that HUVEC are more robust with respect to insulin responsiveness than HAEC (data not shown). Commercially obtained HUVEC possess the advantage that each lot is pooled from 20 individual donors; therefore, the variation between different lots of cells is greatly reduced compared to single-donor HAEC. This may be part of the reason for the more robust insulin-responsiveness of HUVEC.

Experimental hyperglycaemia is a model for overt clinical hyperglycaemia as seen in both Type I and Type II diabetes. The glucose concentration (25 mM) chosen for experimental hyperglycaemia in these studies corresponds to high pathophysiological plasma glucose concentrations seen in the clinic (Ohmura *et al.*, 2005).

HUVEC were cultured in the presence of 25 mM glucose ("glucose", G) or 20 mM mannitol plus 5 mM glucose ("mannitol", M), to obtain a total concentration of 25 mM monosaccharide as an osmotic control, for 48h. In addition, "standard control" cells (C) were cultured in normal vascular endothelial cell medium containing 4 mM glucose alone to detect any osmotic effects caused by either glucose or mannitol. As described for hyperinsulinaemic HAEC (chapter 3), HUVEC were serum-starved after 48h and subsets of cells were stimulated with 1 µM insulin for 10 minutes prior to preparation of whole cell lysates.

In order to assess the effect of experimental hyperglycaemia on the expression of eNOS and the phosphorylation levels of its phosphorylation sites Ser114 ($eNOS^{S114}$), Thr495 ($eNOS^{T495}$), Ser615 ($eNOS^{S615}$), Ser633 ($eNOS^{S633}$) and Ser1177 ($eNOS^{S1177}$), vascular endothelial cell lysates were prepared and protein levels quantified by Western blotting and densitometric analysis. The levels of phospho-protein were expressed as a ratio to total protein in all cases.

All data for these studies have been derived from a pool of four independent experiments using one lot of HUVEC; hence, the expression and phosphorylation levels of the molecules investigated can be related to one another, as they have been measured in the same pool of samples.

For reasons of simplification, cells cultured under conditions of experimental hyperglycaemia are frequently referred to as “hyperglycaemic” in the text, despite not originating from donors who were known to have hyperglycaemia or diabetes. Likewise, cells cultured with mannitol are referred to as “normoglycaemic”.

4.2.2 eNOS expression and phosphorylation under experimental hyperglycaemia

4.2.2.1 eNOS

Previous work in this laboratory has demonstrated that, in HAEC, insulin-responsive eNOS phosphorylation at the main insulin-responsive site Ser1177 and at Thr495 is not altered by experimental hyperglycaemia (Salt *et al.*, 2003). Little is known about the effect of hyperglycaemia on the three other eNOS phosphorylation sites (Ser114, Ser633 and Ser615), or indeed their roles in insulin-responsive signalling. Therefore, in order to characterise more fully the effects of acute insulin and experimental hyperglycaemia on eNOS expression and phosphorylation at these five main phosphorylation sites, their phosphorylation status in HUVEC under normoglycaemic, hyperglycaemic and standard control (4 mM glucose, no mannitol) conditions, in presence or absence of acute stimulation with insulin, was measured by Western blotting (see sections 2.2.1.4 and 4.2.1).

The data in Figure 4-1 show that total eNOS expression in hyperglycaemic cells is unchanged compared to normoglycaemic cells (94±16% of normoglycaemic samples). Culturing cells in mannitol for 48h also caused no significant change in eNOS expression levels with respect to cells cultured under standard conditions (110±14% of standard control (4 mM glucose, no mannitol)). As expected, acute stimulation with insulin had no effect on total eNOS expression under any condition tested and is therefore not indicated on the Western blot. All subsequent phospho-eNOS levels were expressed as a ratio to the unaltered levels of total eNOS.

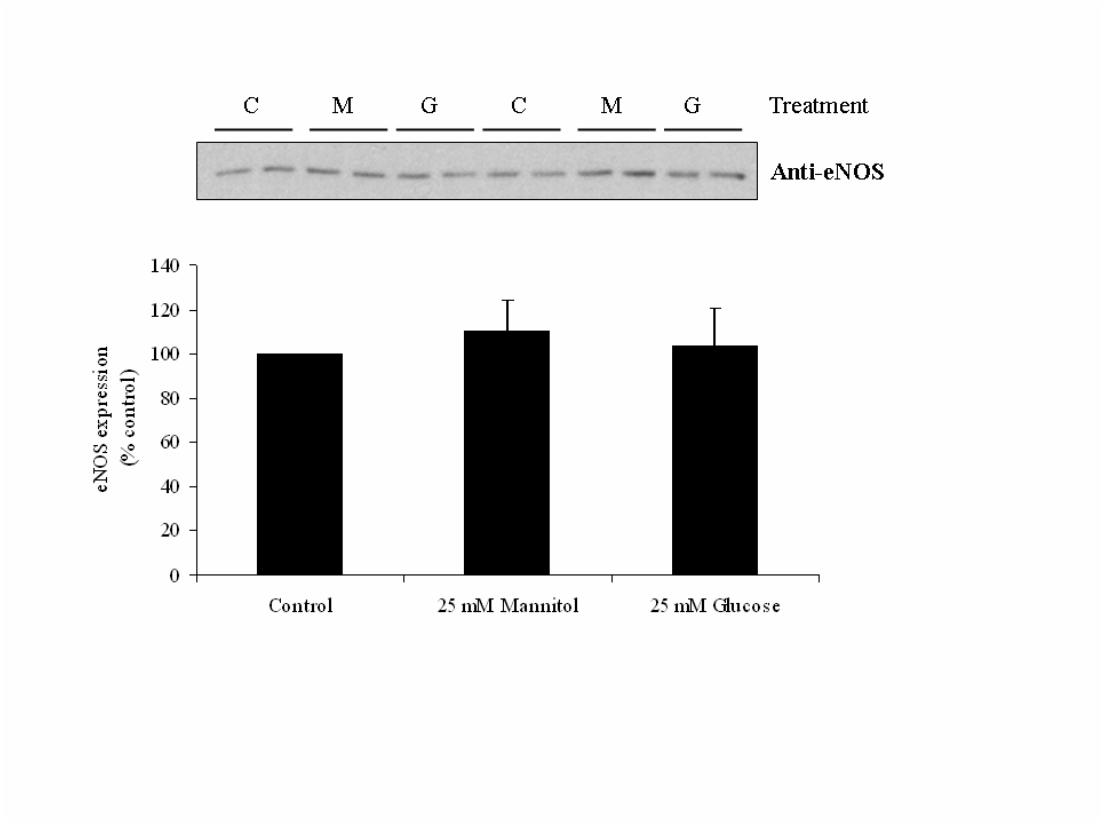

Figure 4-1 eNOS expression is unaffected by experimental hyperglycaemia.

HUVEC were cultured with 25 mM glucose (G) or 20 mM mannitol plus 5 mM glucose (M) for 48h. Control (C) cells were cultured with 4 mM glucose. Prior to lysis preparation, cells were serum-starved for 2-4h in KRH buffer. Equal amounts of protein (3-10 µg) were resolved by SDS-PAGE and Western blotted onto nitrocellulose membranes. An eNOS-specific antibody was used to detect immunoreactive bands, which were then quantified by densitometric analysis. Data shown are the mean + SEM expression of 3 independent experiments (treatments in quadruplicates) with a single lot of HUVEC. A representative Western blot is shown.

4.2.2.2 eNOS^{S615} and eNOS^{S1177}

Phosphorylation of the eNOS sites Ser615 and Ser1177 has been shown to be responsive to insulin (Dimmeler *et al.*, 1999, Fulton *et al.*, 1999, Ritchie *et al.*, 2007). Therefore, the effect of experimental hyperglycaemia on the insulin-stimulated phosphorylation status of these sites was investigated.

Data from the present study confirm that, under standard control conditions, eNOS^{S615} and eNOS^{S1177} are phosphorylated after acute (10 min) stimulation with insulin to 1.4±0.3-fold and 2.4±0.7-fold of basal levels, respectively (Figure 4-2). While these changes were clear, they were not statistically significant due to interexperimental variation. Insulin elicited smaller increases in Ser615 and Ser1177 phosphorylation under normoglycaemic conditions (1.2±0.4-fold and 1.4±0.3-fold increases compared to unstimulated normoglycaemic cells, respectively; no statistically significant differences). However, 48h of experimental hyperglycaemia abrogated insulin-stimulation of eNOS^{S615} phosphorylation with respect to normoglycaemic and standard control cells (0.76-fold and 0.79-fold of stimulated normoglycaemic and standard control levels, respectively). This was partly due to increased basal phosphorylation of eNOS^{S615} under hyperglycaemic conditions (see Figure 4-2, panel B).

There was no difference in basal phosphorylation of eNOS^{S1177} under experimental hyperglycaemia, but insulin-stimulated phosphorylation of eNOS^{S1177} was reduced to 0.84-fold of stimulated normoglycaemic phosphorylation and 0.6-fold of stimulated phosphorylation in standard control. The insulin-stimulated increase over unstimulated eNOS^{S1177} phosphorylation was 1.5±0.3-fold in hyperglycaemic cells.

In addition to the above results, culturing of HAEC under the same experimental conditions as used for HUVEC resulted in loss of insulin-stimulated eNOS^{S1177} phosphorylation in normoglycaemic (mannitol-treated) HAEC, while hyperglycaemic HAEC showed a 2.5-fold increase over basal in insulin-responsive eNOS^{S1177} phosphorylation (data not shown; compare with Figure 4-2, panel C).

A

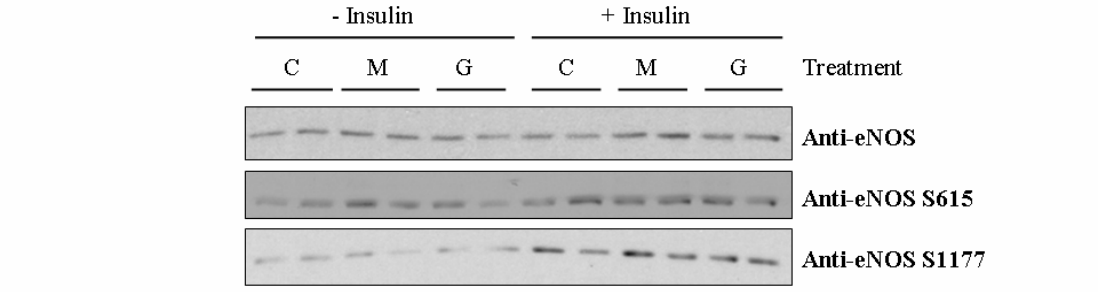

B

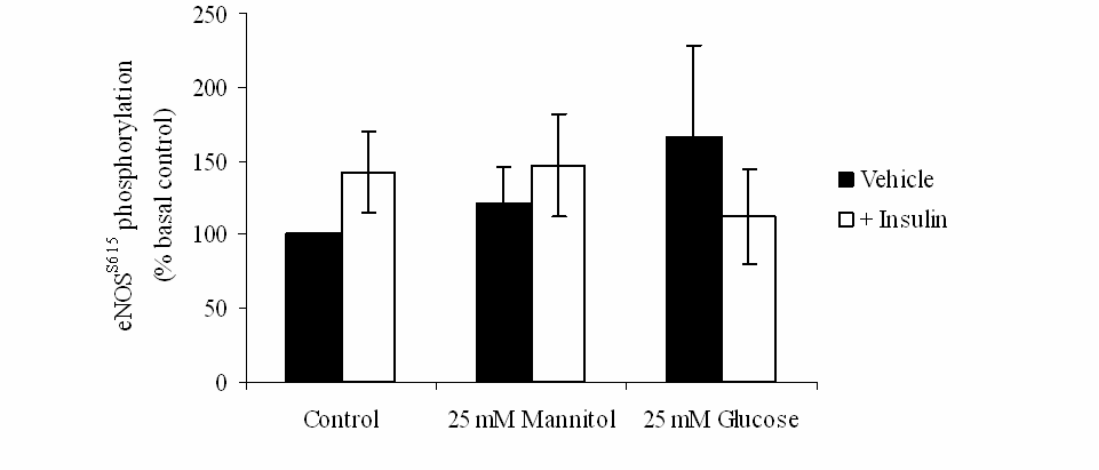

C

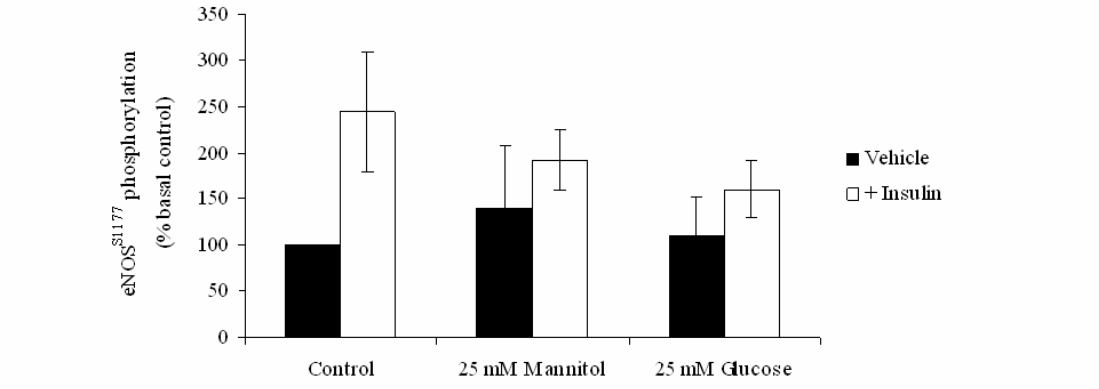

Figure 4-2 Insulin increases phosphorylation of eNOS^{S615} and eNOS^{S1177}.

HUVEC were cultured as described (see section 2.2.1.4) and subsets of cells were stimulated with 1 µM insulin for 10 min prior to preparation of cell lysates. After SDS-PAGE and Western blotting, antibodies were used as indicated and immunoreactive bands quantified with respect to total eNOS. Panel A shows representative Western blots. B: eNOS^{S615}/eNOS; C: eNOS^{S1177}/eNOS (*$p<0.05$ for basal compared to insulin-stimulated standard control; paired t-test). Data shown are the mean ± SEM expression from 3 independent experiments.

4.2.2.3 eNOS^{S633}

Ser633 is postulated to be another eNOS activating phosphorylation site (Michell *et al.*, 2002). In this study, acute stimulation with insulin resulted in a reduction of eNOS^{S633} phosphorylation levels under standard control conditions to 0.7±0.1-fold of basal levels (not statistically significant; see Figure 4-3).

Basal phosphorylation of eNOS^{S633} was decreased under experimental hyperglycaemia to 0.67±0.05-fold of basal normoglycaemic phosphorylation (not statistically significant). Basal phosphorylation in mannitol-treated cells was also reduced to 0.7±0.2-fold with respect to standard control, but this change was not statistically significant. The reduction in basal hyperglycaemic phosphorylation was therefore more pronounced with respect to standard control (0.5±0.2-fold of basal standard control levels), although this was not statistically significant due to interexperimental variation.

Insulin treatment did not change eNOS^{S633} phosphorylation levels under normoglycaemic or hyperglycaemic conditions with respect to standard control, although slightly lower eNOS^{S633} levels were measured in insulin-stimulated hyperglycaemic cells than normoglycaemic cells.

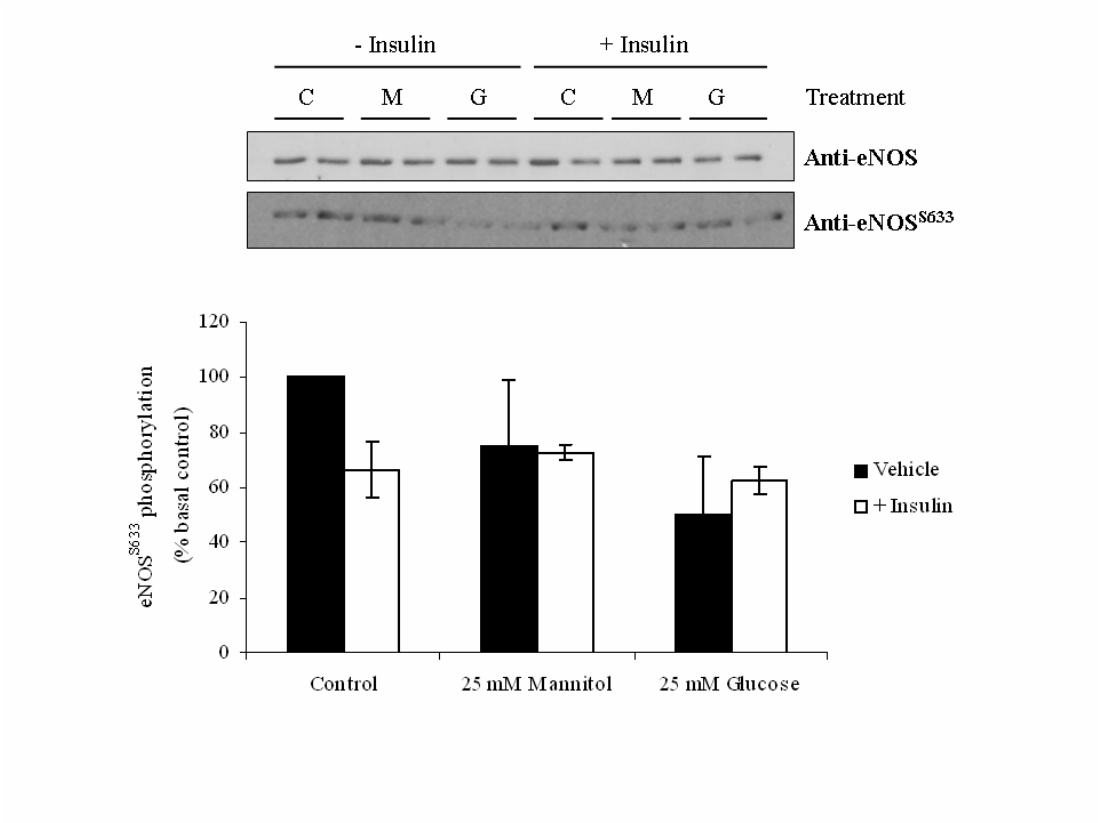

Figure 4-3 Experimental hyperglycaemia does not affect eNOS^{S633} phosphorylation.

HUVEC were treated as described before (section 2.2.1.4) and lysates were produced for Western blotting. Representative Western blots are shown. Data are the mean ± SEM eNOS^{S633}/eNOS expression of 3 independent experiments. Neither Mannitol (M) nor glucose treatment for 48h had any statistically significant effect upon eNOS^{S633} phosphorylation.

4.2.2.4 eNOS^{S114} and eNOS^{T495}

The phosphorylation status of the sites Ser114 and Thr495 was investigated under control, normoglycaemic and hyperglycaemic conditions.

Basal eNOS^{S114} phosphorylation levels were comparable under all conditions (Figure 4-4, panels A and B). Acute treatment with insulin resulted in a small and not statistically significant reduction in eNOS^{S114} phosphorylation under normoglycaemic and control conditions (to 0.6±1-fold and 0.8±0.2-3old of basal control, respectively). There was no statistically significant difference between insulin-responsive phosphorylation in normoglycaemic and standard control cells. Under hyperglycaemic conditions, insulin caused a marked but not statistically significant reduction in Ser114 phosphorylation levels (0.3±0.1-fold of unstimulated hyperglycaemic cells). This was almost twice the reduction seen with normoglycaemic cells and 2.6-fold that of standard control.

Unstimulated phosphorylation of eNOS^{T495} was unchanged under all three conditions (Figure 4-4, panels A and C). As expected, acute insulin significantly reduced eNOS^{T495} phosphorylation levels under normoglycaemic conditions (to 0.7±0.04-fold of basal normoglycaemic phosphorylation ($p<0.05$, paired t-test). The reduction under standard control conditions was less pronounced and not statistically significant (0.8±0.07 compared to basal control). There was no significant difference between insulin-responsive phosphorylation in normoglycaemic and control cells. Hyperglycaemic cells also showed strongly decreased phosphorylation of Thr495 after insulin treatment (to 0.6±0.2-fold of basal hyperglycaemic phosphorylation), but due to the spread of data points this was not statistically significant.

A

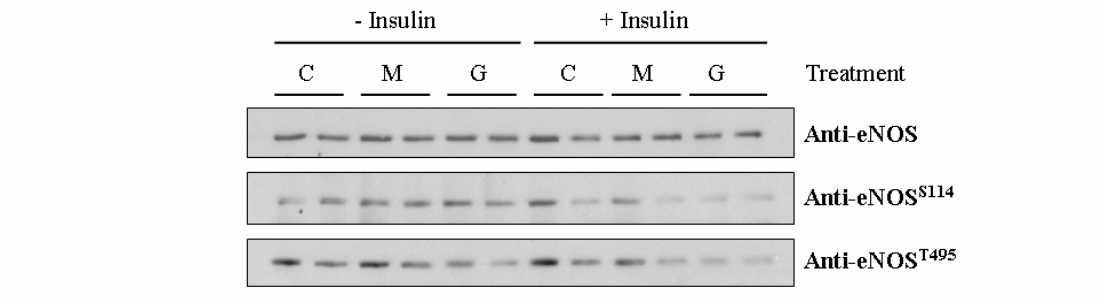

B

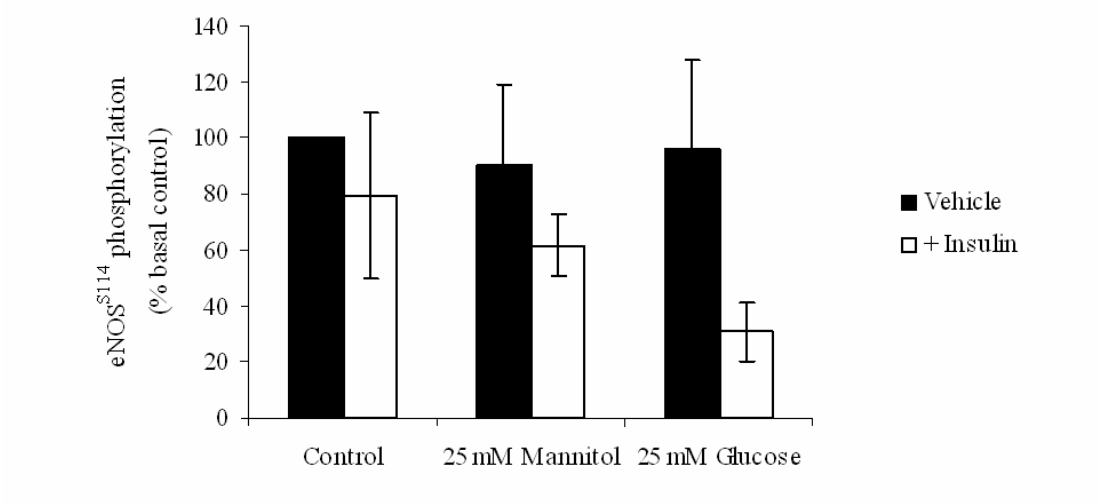

C

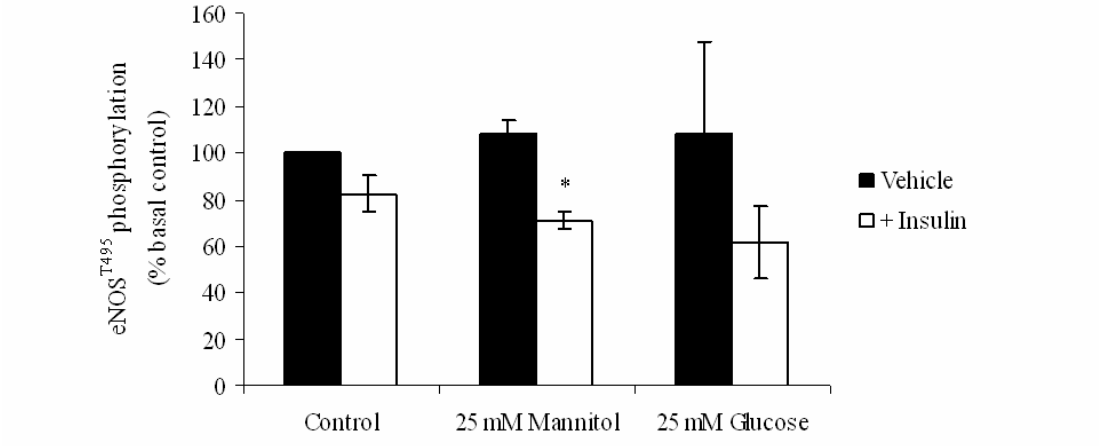

Figure 4-4 Acute insulin tends to reduce Ser114 and Thr495 phosphorylation.

HUVEC lysates were prepared as described (see section 2.2.2) and equal amounts of protein were Western blotted. Representative Western blots are shown in panel A. Data from 3 independent experiments are given as mean ± SEM expression for eNOS^{S114}/eNOS in panel B and for eNOS^{T495}/eNOS in panel C (*$p<0.05$ for normoglycaemic cells in presence and absence of insulin; paired t-test).

The phosphorylation status of the five investigated eNOS phospho-sites is summarised in Figure 4-5. Since mannitol reduced the basal phosphorylation of eNOS^{S633} and diminished the insulin-responsive phosphorylation of eNOS^{S1177} with respect to standard control, this suggests that high mannitol levels in the cell culture medium may exert an osmotic effect on cellular signalling pathways. Therefore, eNOS expression and phosphorylation levels are compared to standard control levels, here, to better model the difference between hyperglycaemic and normoglycaemic individuals with normal blood osmolarity.

Panel A of Figure 4-5 shows the effect of experimental hyperglycaemia on basal phosphorylation of these sites as compared to unstimulated standard control. Panel B illustrates the insulin-stimulated phosphorylation status compared to stimulated control. Since the expression levels of total eNOS protein did not change upon acute stimulation with insulin, total eNOS levels in hyperglycaemic cells are expressed as the percentage of combined (basal + stimulated) control. There was no difference in eNOS expression between control and hyperglycaemic cells.

Basal eNOS phosphorylation at Ser633 was reduced to 50% of control levels in hyperglycaemic samples (not statistically significant due to spread of data points), while basal eNOS^{S615} levels were increased 1.9±0.6-fold (no statistically significant difference). No changes in basal phosphorylation were seen at the other phosphorylation sites investigated. Significantly, insulin-responsive dephosphorylation of eNOS^{S114}/eNOS in hyperglycaemic HUVEC was 2.3-fold greater than in control cells ($p<0.05$; paired t-test). The ratio of insulin-stimulated eNOS^{S1177}/eNOS was also reduced to 72% of control levels under experimental hyperglycaemia (not statistically significant). No other statistically significant changes were seen in insulin-responsive phosphorylation.

A

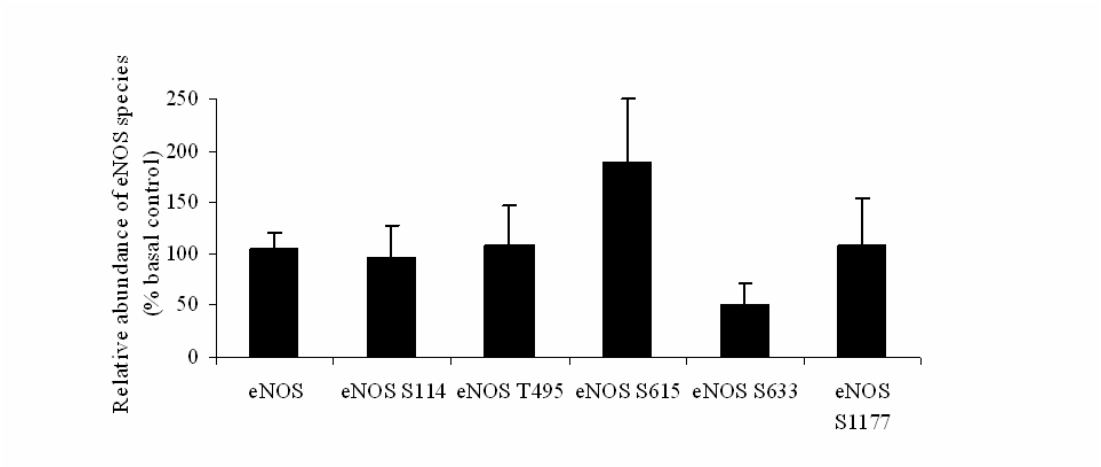

B

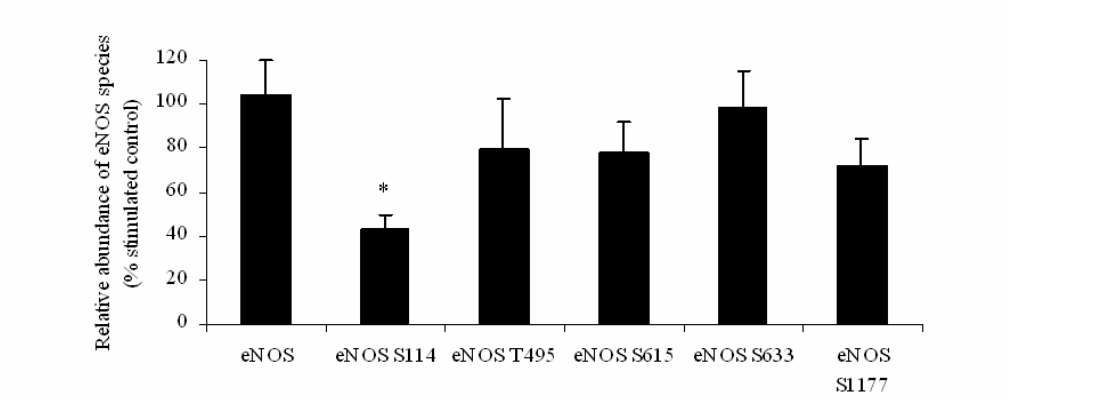

Figure 4-5 Experimental hyperglycaemia modifies the eNOS phosphorylation profile.

Lysates were prepared from hyperglycaemic and control HUVEC and subjected to Western blotting as described (sections 2.2.2 and 2.2.6). Data are shown as mean + SEM abundance and are derived from the same 3 independent experiments for all eNOS species. Given that total eNOS expression levels did not change during acute stimulation with insulin, the expression levels of total eNOS for both basal and stimulated cells are expressed as % control rather than % basal or % stimulated control. Phospho-eNOS species are expressed as a ratio to total eNOS in hyperglycaemic cells. A: Basal eNOS phosphorylation in hyperglycaemic compared to control cells B: insulin-stimulated eNOS phosphorylation in hyperglycaemic cells compared to stimulated controls; *$p<0.05$ compared to $eNOS^{S114}$ phosphorylation in insulin-stimulated control cells (paired t-test)

4.2.3 The effect of experimental hyperglycaemia on insulin-regulated pathways

Insulin triggers a number of signalling cascades in endothelial cells, which may also contribute to the transcriptional and post-translational regulation of eNOS in endothelial cells. Previously, work in this laboratory has shown that experimental hyperglycaemia disrupts metabolic insulin signalling at the level of IRS-2 expression and PI3K association with IRS-1 and -2, and decreases insulin-regulated CAP-Cbl signalling in HAEC (Salt *et al.*, 2003). Therefore, it was decided to investigate more fully the effect of experimental hyperglycaemia on the expression and phosphorylation of components of these and other insulin-responsive signalling pathways in HUVEC. Pathways studied include the metabolic insulin signalling pathway (PI3K-p85, PDK-1, PTEN and PKB), the transcription-regulating NFκB pathway (NF?B, I?Ba, IKKß and JNK) and the CAP-Cbl pathway.

4.2.3.1 The metabolic insulin signalling pathway

The metabolic insulin signalling pathway is known to play a role in the regulation of eNOS phosphorylation in response to insulin (Zeng & Quon, 1996). Hence, the expression of its components PKB, PDK-1, PTEN and the regulatory p85 subunit of PI3K (PI3K-p85) were quantified, along with PKB phosphorylation, to determine whether there was any dysregulation of this pathway that could account for the altered eNOS phosphorylation status described above (section 4.2.2).

As observed for eNOS, there was no effect of acute insulin stimulation on PKB expression under any condition tested; hence, insulin-stimulated samples are not indicated on the Western blot in Figure 4-6. PKB expression was unaffected by experimental hyperglycaemia (97±10% and 96±10% of normoglycaemic and standard control samples, respectively).

Phosphorylation levels of the insulin-responsive PKB activating sites Thr308 and Ser473 were quantified with respect to total PKB expression (Figure 4-7). Basal and insulin-responsive phosphorylation levels of PKB^{T308} were comparable for all three conditions, with insulin consistently stimulating Thr308 phosphorylation to 3.3±1.1-fold (control), 3.7±0.7-fold (mannitol) and 3.5±0.5-fold (glucose) over basal control phosphorylation (no statistical analysis possible due to small repeat number; see Figure 4-7, panels A and B).

By contrast, basal PKB^{S473} phosphorylation in HUVEC was reduced after 48h of glucose treatment (to 0.60±0.08-fold of basal normoglycaemic cells and 0.36±0.08-fold of basal standard control cells). Insulin-responsive Ser473 phosphorylation remained comparable under all conditions: Insulin stimulated Ser473 phosphorylation 1.4±0.3-fold (control), 1.8±0.4-fold (mannitol) and 1.7±0.3-fold (glucose) above unstimulated standard control. Basal PKB^{S473} phosphorylation was also reduced under normoglycaemic (0.6±0.06-fold compared to standard control conditions) (see Figure 4-7, panels A and C). No statistical analysis of these data was possible due to the small repeat number.

Further to the study in HUVEC, insulin-stimulated phosphorylation of PKB^{T308} was absent and was less pronounced for PKB^{S473} in normoglycaemic and hyperglycaemic HAEC (~1.2-fold and ~1.3-fold over basal, respectively) compared to HUVEC (data not shown; compare with Figure 4-7).

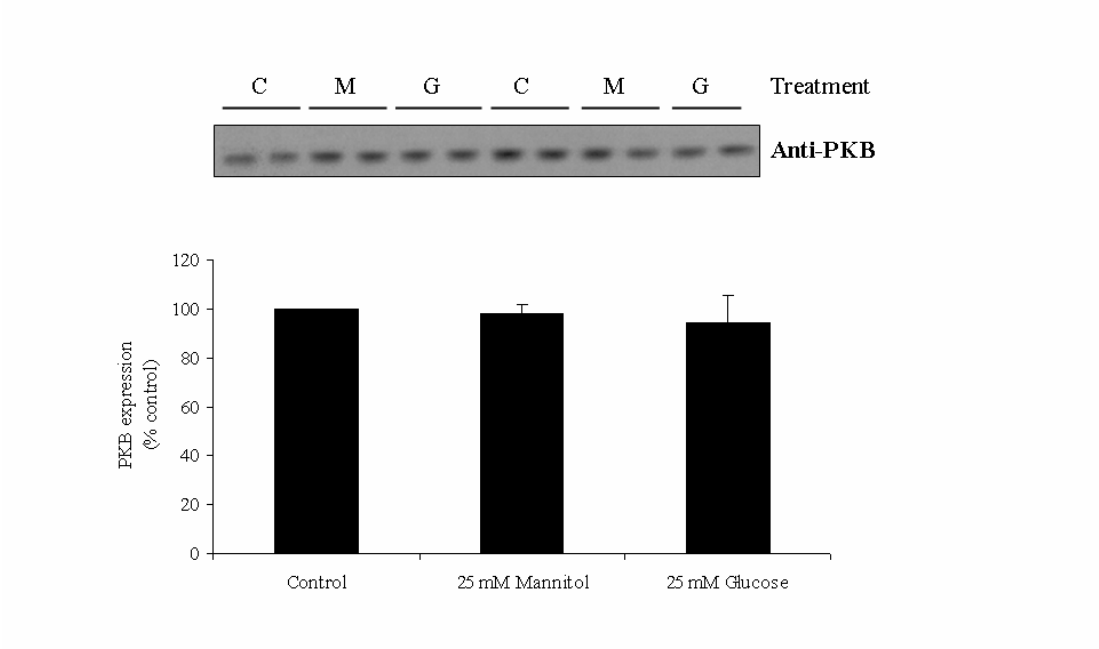

Figure 4-6 PKB expression is unaffected by experimental hyperglycaemia.

HUVEC were treated and lysed as described (sections 2.2.1.4 and 2.2.2) and subjected to Western blotting. Densitometric analysis of immunoreactive bands demonstrated that PKB expression does not change during experimental hyperglycaemia (G) or mannitol treatment (M) compared to control (C). Data shown are the mean + SEM expression of 3 independent experiments. A representative Western blot is shown.

A

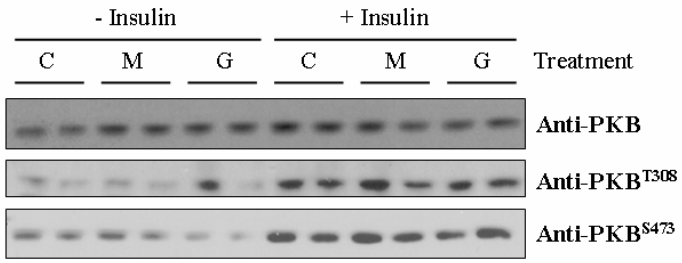

B

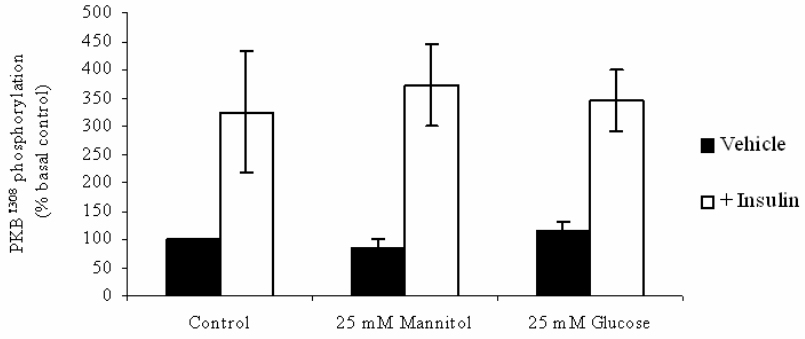

C

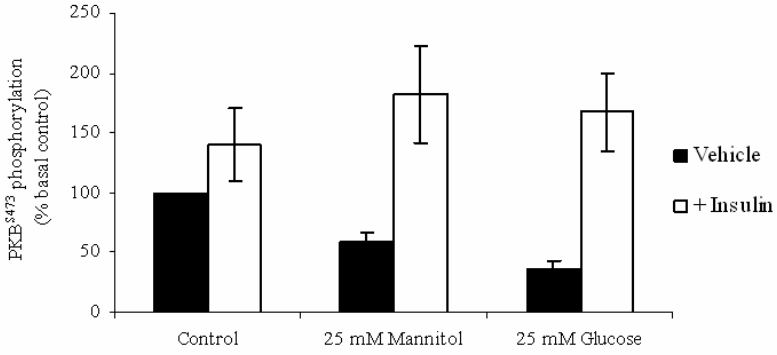

Figure 4-7 PKB phosphorylation remains insulin-responsive under experimental hyperglycaemia.

HUVEC lysates were prepared as described (section 2.2.2) and subjected to Western blotting. Phospho-specific antibodies were used as indicated on the representative blots in panel A. Data shown are the mean ± range abundance of phospho-PKB/PKB derived from 2 independent experiments. Panel B: PKB^{T308}/PKB; Panel C: PKB^{S473}/PKB. C = control, M = mannitol, G = glucose

The expression levels of the upstream insulin signalling pathway components PI3K-p85, PTEN and PDK-1 were quantified and found to be unchanged by experimental hyperglycaemia with respect to mannitol treatment and standard control conditions. Percentage expression in hyperglycaemic compared to normoglycaemic (mannitol-treated) cells was 98±4% for PI3K-p85 (Figure 4-8, panel A), 95±4% for PTEN (Figure 4-8, panel B) and 89±12% for PDK-1 (Figure 4-9). All three molecules had comparable expression levels in mannitol-treated and standard control cells.

In addition to the above data, the present study briefly investigated whether experimental hyperglycaemia affected the stress-activated p38 MAPK signalling pathway in HUVEC by quantifying the expression and insulin-stimulated phosphorylation levels of p38 MAPK. Data from one experiment indicated that expression of p38 MAPK in hyperglycaemic cells was unchanged compared to normoglycaemic cells. Under normoglycaemic and standard control and conditions, insulin treatment caused 1.5-fold and 1.3-fold increases in p38 MAPK phosphorylation, respectively, but this stimulation was reduced to 1.2-fold in hyperglycaemic cells (data not shown).

A

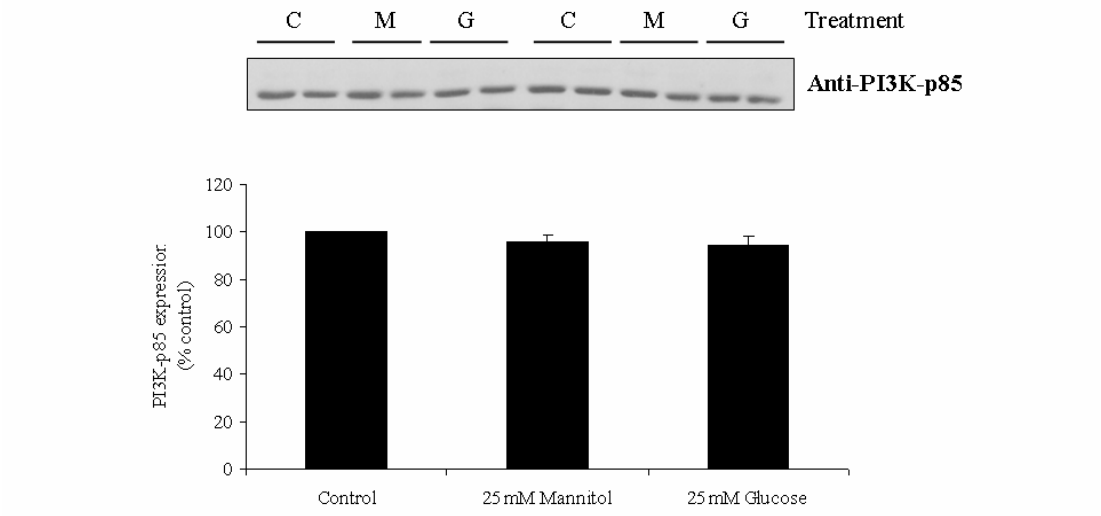

B

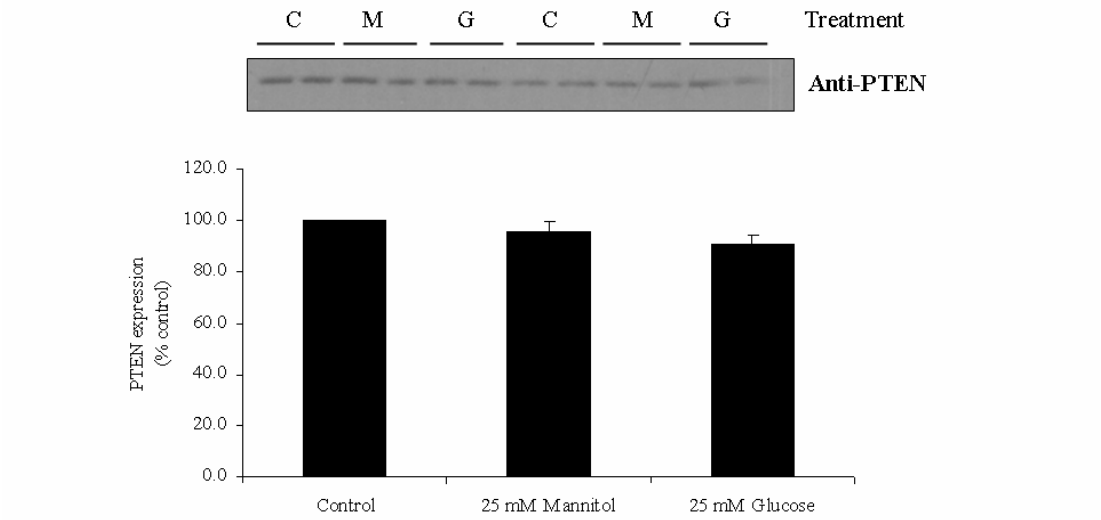

Figure 4-8 PI3K-p85 and PTEN expression are unchanged after experimental hyperglycaemia

Cell lysates from HUVEC, treated as described (section 2.2.1.4), were subjected to Western blotting with the antibodies indicated above. Representative blots are shown. Data represent the mean + range expression of 2 independent experiments (all samples in quadruplicates). A: PI3K-p85; B: PTEN. No statistical analysis could be performed due to the small repeat number. C = control, M = mannitol, G = glucose

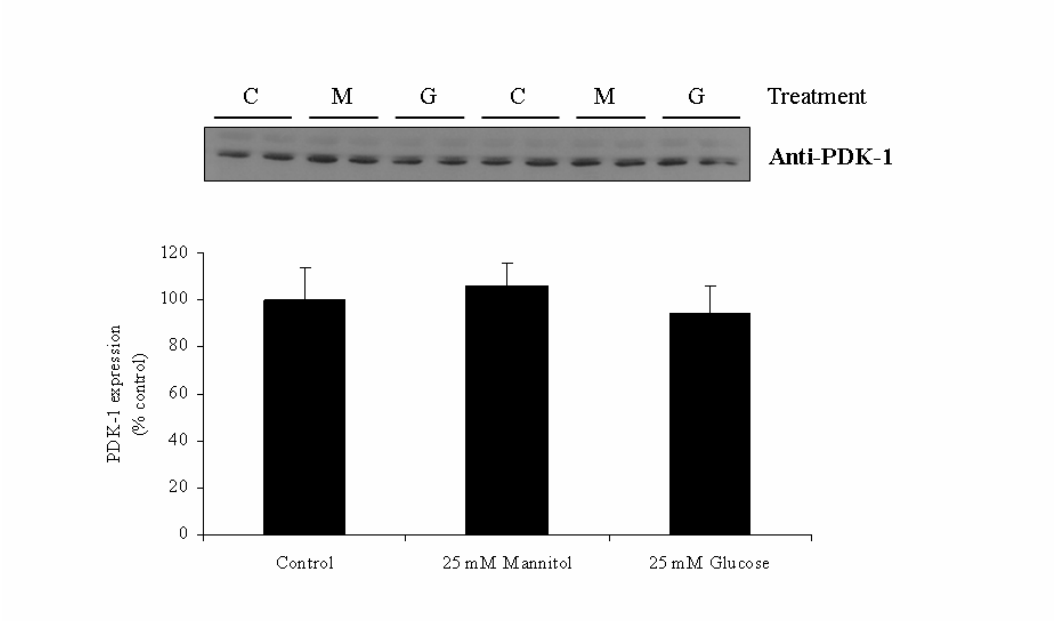

Figure 4-9 PDK-1 expression is unaffected by experimental hyperglycaemia.

HUVEC lysates were produced as described (section 2.2.2) and Western blotted. Data from one experiment (samples in quadruplicates) are shown as mean + range expression along with the Western blot. C = control, M = mannitol, G = glucose

4.2.3.2 The NF?B pathway

NF?B is a transcription factor that regulates the expression of genes involved in the innate and adaptive immune response, including cell adhesion molecules and inducible nitric oxide synthase (iNOS). In its inactive state, NF?B is bound to I?B, which undergoes proteosomal degradation upon phosphorylation by the upstream kinase IKK, thus releasing NF?B to enter the nucleus and bind to the promoters of target genes (reviewed in (Gilmore, 2006)). The c-jun N-terminal kinase (JNK) is a member of the mitogen-activated protein kinase (MAPK) family and forms part of a stress-activated pathway, which can promote the ubiquitination (and thus the degradation) of I?Ba (Ki *et al.*, 2007). Given the proposed proinflammatory and proatherogenic status during endothelial dysfunction, it was decided to investigate whether the NF?B and JNK pathways were dysregulated by experimental hyperglycaemia. Therefore, the expression levels of the molecules NF?B and IKKß, along with the expression and phosphorylation levels of JNK and I?Ba, were quantified.

NF?B levels were comparable between hyperglycaemic and mannitol-treated, normoglycaemic cells in presence (90±19%) and absence (99±20%) of insulin (see Figure 4-10). Under standard control conditions, the abundance of NF?B was slightly reduced to 0.8±0.06-fold of basal levels by treatment with acute insulin (not statistically significant).

Quantification of I?Ba levels showed that they remained stable under all conditions tested, with neither acute insulin nor experimental hyperglycaemia having a statistically significant effect (% abundance in hyperglycaemic cells was 71±3% compared to unstimulated and 106±34% compared to stimulated normoglycaemic cells; see Figure 4-11, panels A and B). There was no significant difference in I?Ba expression between normoglycaemic and standard control cells.

Basal I?Ba Ser32 phosphorylation levels were similar under all conditions tested, although mannitol-treatment reduced basal phosphorylation to 0.6±0.3-fold of unstimulated standard control levels (no statistical analysis possible due to low repeat number). Acute insulin treatment reduced the ratio of Ser32-phosphorylated I?Ba to 0.4±0.06-fold (mannitol), 0.7±0.003-fold (glucose) and 0.3±0.08-fold (standard control) of unstimulated standard control phosphorylation (see Figure 4-11, panels A and C).

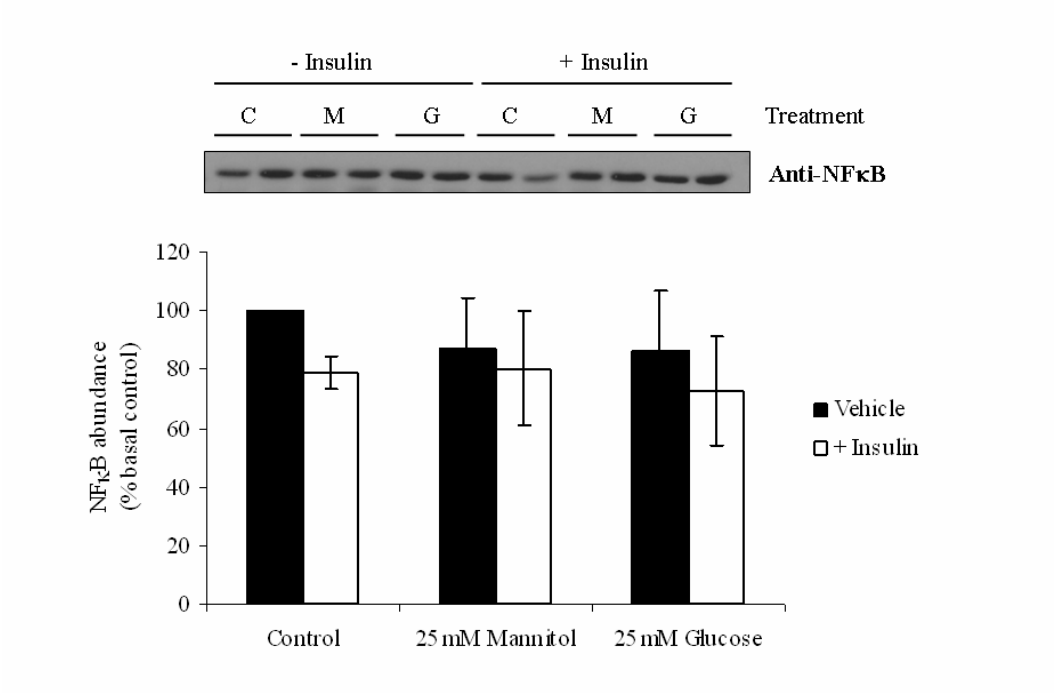

Figure 4-10 NF?B levels are not affected by experimental hyperglycaemia.

HUVEC lysates were prepared as described (section 2.2.2) and subjected to Western blotting. A representative blot is shown along with data from 3 independent experiments expressed as mean ± SEM expression. Levels of NF?B were comparable under all conditions tested. C = control, M = mannitol, G = glucose

A

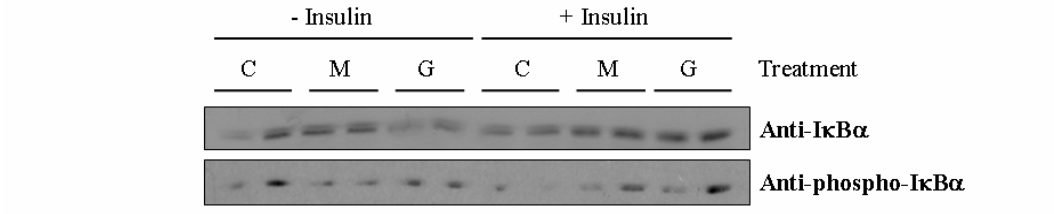

B

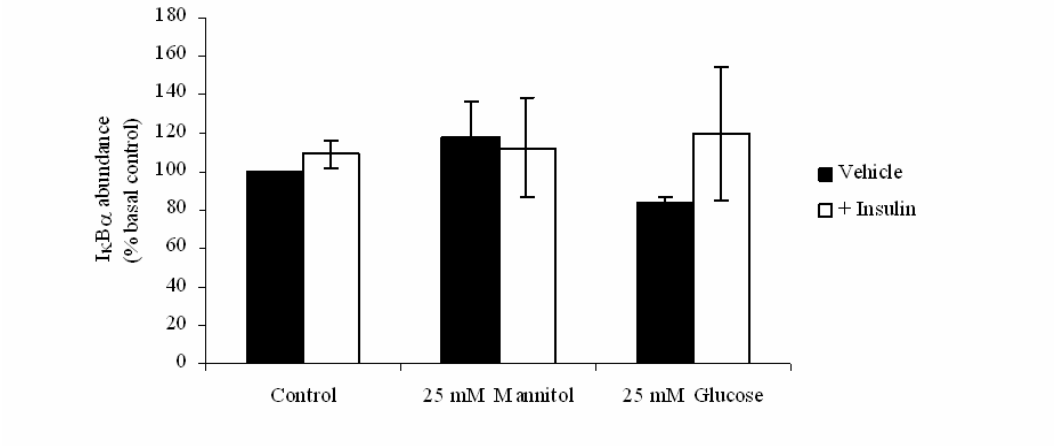

C

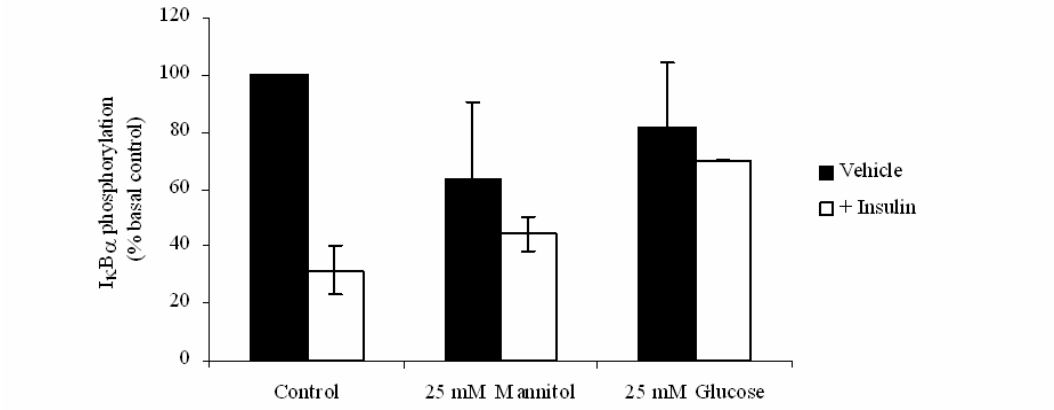

Figure 4-11 Hyperglycaemia tends to impair insulin-triggered I?Ba dephosphorylation.

HUVEC lysates were prepared as described (section 2.2.2) and subjected to Western blotting. Representative blots are shown in panel A. B: Data are shown as mean ± SEM abundance of 3 independent experiments. C: Levels of I?Ba^{Ser32}/I?Ba were reduced by acute insulin treatment under control but not experimental hyperglycaemic conditions in 2 independent experiments (mean ± range abundance). C = control, M = mannitol, G = glucose

The expression levels of the upstream kinases IKKß and JNK were investigated for their potential dysregulation during experimental hyperglycaemia. There was no difference between normoglycaemic and hyperglycaemic expression of IKKß in the presence or absence of insulin. Hyperglycaemic and normoglycaemic IKKß levels in the presence and absence of insulin were also comparable to standard control levels in the presence of insulin; however, basal levels were significantly lower in standard control cells than hyperglycaemic and normoglycaemic (mannitol-treated) cells (0.6-fold lower for standard control compared to hyperglycaemic cells). Hence, insulin stimulated a rise in IKKß levels only under standard control conditions. This increase was abrogated in the presence of glucose or mannitol (Figure 4-12). No statistical analysis was performed due to the low repeat number of experiments.

The expression of the 54 kDa isoform of JNK and phospho-JNK were quantified. Levels of the 46 kDa isoform of JNK and phosphorylated JNK mirrored that of the 54 kDa isoform under all conditions tested (data not shown). Basal expression of the 54 kDa JNK isoform in HUVEC was comparable under all conditions tested. Insulin treatment resulted in small and comparable decreases in JNK abundance in all cases, which were not statistically significant (0.9±0.08 for control, 0.8±0.1 for normoglycaemic and 0.8±0.08 for hyperglycaemic cells compared to levels in absence of insulin; see Figure 4-13, panel B).

In order to determine whether JNK phosphorylation might be affected during experimental hyperglycaemia, the phosphorylation levels of JNK at Thr183 and Tyr185 were quantified, serving as an indirect indicator of JNK activity. Acute stimulation with insulin had no marked effect on JNK phosphorylation. The ratio of phospho-JNK to total JNK indicated that experimental hyperglycaemia may cause an increase in basal phosphorylation (2.7±0.6-fold of basal normoglycaemic levels and 1.8±0.6-fold compared to basal control; Figure 4-13, panel C). No statistical analysis was performed due to the low repeat number of experiments.

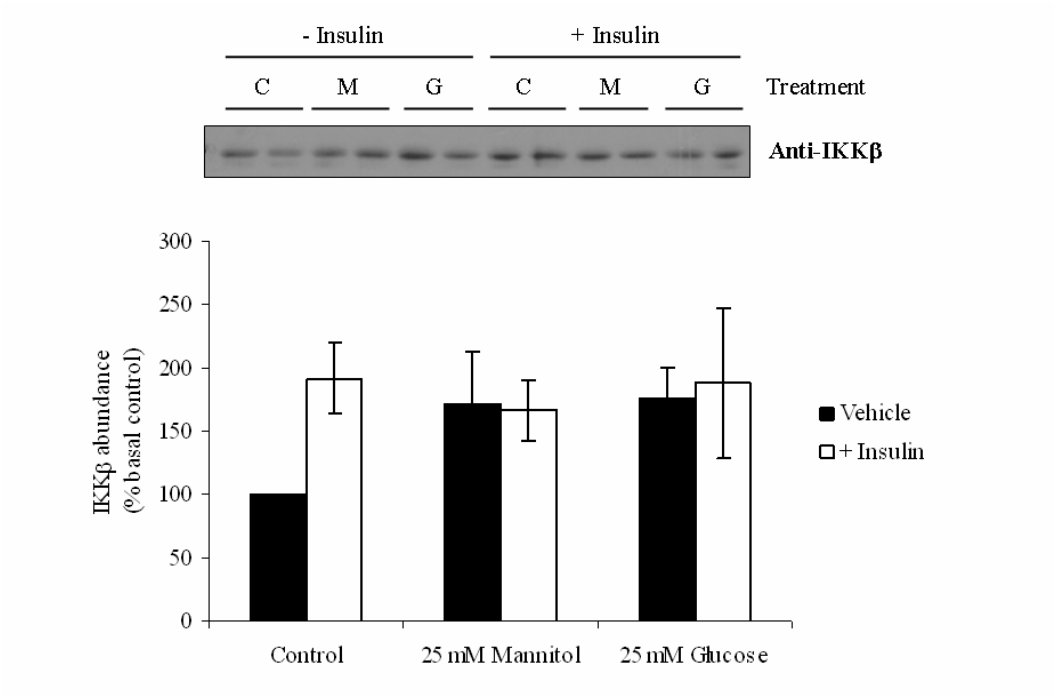

Figure 4-12 IKKß levels are increased after acute insulin treatment under control conditions.

HUVEC lysates were prepared as described (section 2.2.2) and subjected to Western blotting. Representative blots are shown. Data are shown as mean ± range abundance of 2 independent experiments. Control IKKß levels are increased after insulin stimulation.
C = control, M = mannitol, G = glucose

A

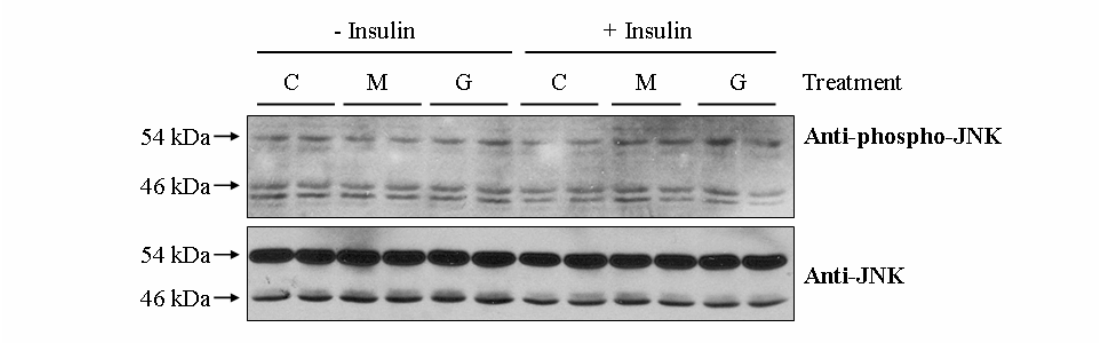

B

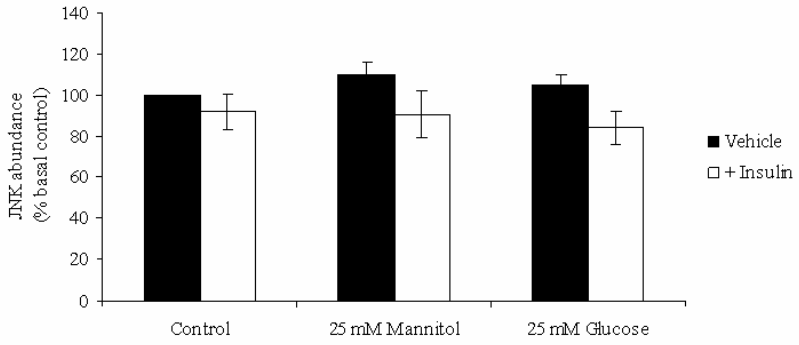

C

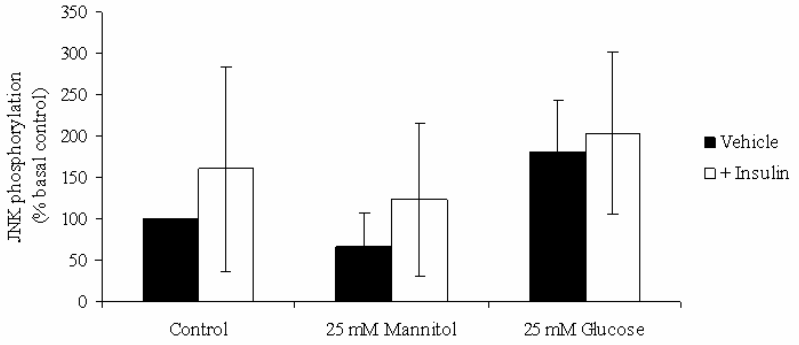

Figure 4-13 Basal JNK phosphorylation tends to increase under experimental hyperglycaemia.

Representative Western blots of hyperglycaemic and control HUVEC lysates are shown in panel A. B: JNK expression was unchanged by experimental hyperglycaemia (data shown are the mean ± SEM abundance of 3 independent experiments). C: Levels of phosphorylated JNK (54 kDa) are expressed as a ratio to total JNK from 2 experiments (mean ± range).
C = control, M = mannitol, G = glucose

4.2.3.3 The CAP-Cbl pathway

The CAP-Cbl pathway is an insulin-stimulated pathway that plays a role in whole-body fuel homeostasis by regulating glucose transport (Baumann *et al.*, 2000, Chiang *et al.*, 2001). Cbl is a proto-oncogene product that interacts with the insulin receptor via the adaptor protein CAP, and is phosphorylated by the tyrosine kinase action of the insulin receptor. Thereafter, the CAP-Cbl complex dissociates from the insulin receptor and binds to flotillin in caveolin-enriched lipid rafts, where it is thought to modulate glucose transport in adipocytes (Baumann *et al.*, 2000).

Previous work in this laboratory (Salt *et al.*, 2003) has demonstrated that the expression of CAP and Cbl in HAEC was decreased under experimental hyperglycaemia, and that the phosphorylation of Cbl was also decreased in response to insulin. Hence, in order to investigate whether other insulin-responsive pathways were also dysregulated by experimental hyperglycaemia in HUVEC, CAP and Cbl expression was quantified.

Expression levels of CAP demonstrated large inter-sample variation, and no statistically significant differences were found under any condition tested. However, basal levels in hyperglycaemic cells were 2.1±1.8-fold higher than in normoglycaemic cells, while no difference in abundance was found between these two treatment groups in the presence of insulin. Under standard control conditions, insulin treatment caused an apparent rise in CAP abundance to 3±2-fold above basal. This insulin-mediated increase in CAP levels was abrogated in normoglycaemic and hyperglycaemic cells, in which the abundance of CAP was 0.5±0.6-fold and 0.6±0.07-fold of insulin-treated standard control (Figure 4-14, panel A).

Basal expression of Cbl was comparable under all conditions, and acute insulin had no effect on Cbl levels in control or normoglycaemic HUVEC. However, following experimental hyperglycaemia, acute insulin treatment resulted in a reduction in Cbl abundance to 0.5±0.04-fold of basal levels in normoglycaemic and standard control cells (Figure 4-14, panel B). No statistical analysis was performed due to the low repeat number of experiments.

A

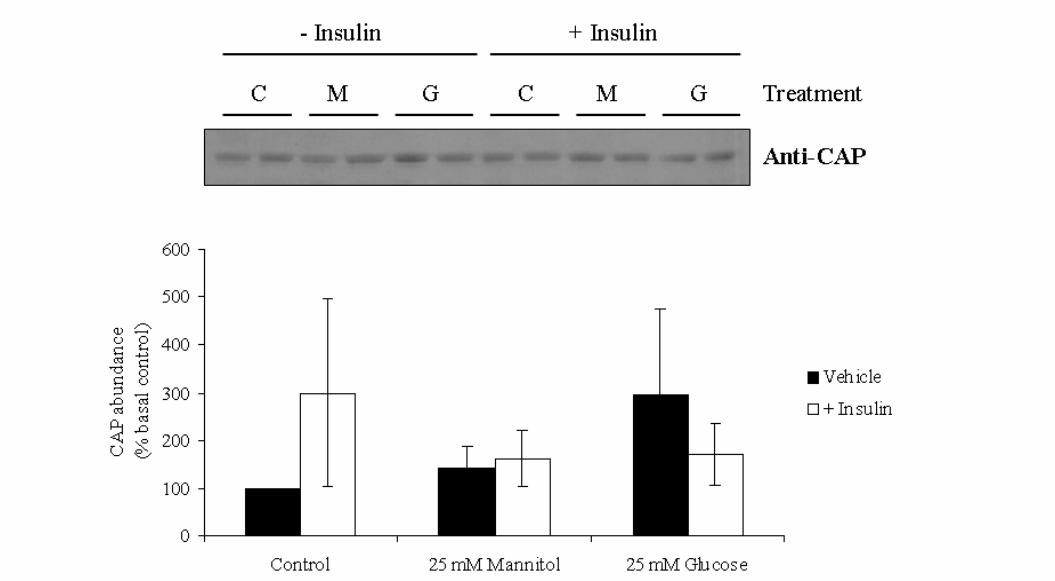

B

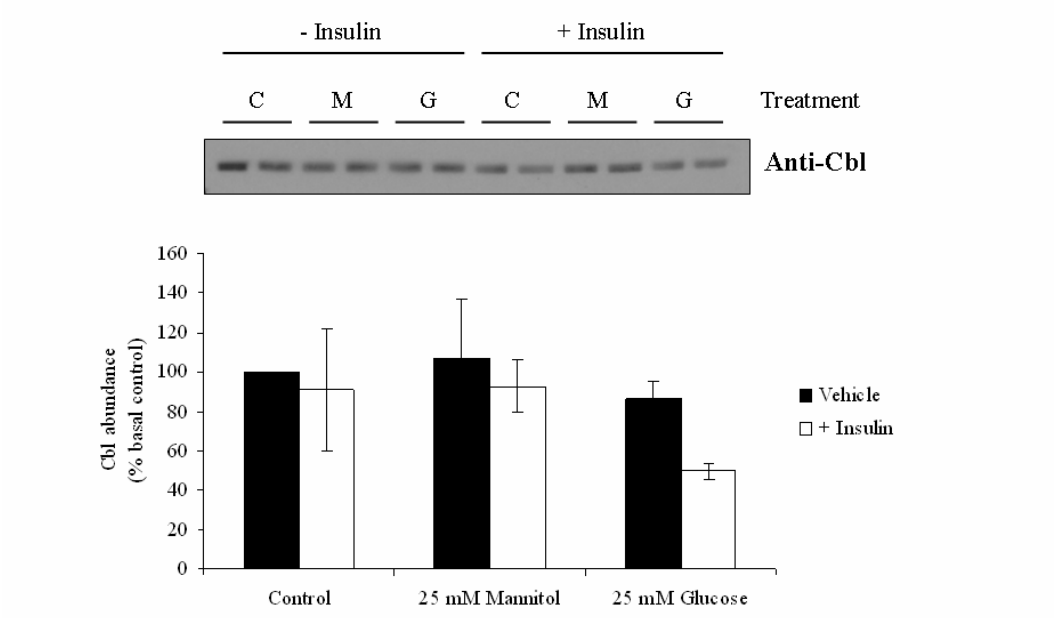

Figure 4-14 Cbl, but not CAP expression is modified by experimental hyperglycaemia.

HUVEC lysates were prepared as described (section 2.2.2) and subjected to Western blotting with the relevant antibodies as indicated. A: Data shown are the mean ± SEM abundance of CAP from 3 independent experiments. B: Data shown are the mean ± range abundance of Cbl from 2 independent experiments. Sample Western blots are shown.
C = control, M = mannitol, G = glucose

4.2.4 Superoxide production under experimental hyperglycaemia

To investigate whether experimental hyperglycaemia affected superoxide (O_2^-) production in HUVEC, superoxide levels were quantified in cells cultured under experimental hyperglycaemic or normoglycaemic conditions for 48h. In addition, the compound N G-nitro-L-arginine methyl ester (L-NAME), which inhibits eNOS-mediated nitric oxide production, was used to determine the effect of NO bioavailability on superoxide levels. Superoxide levels in hyperglycaemic and normoglycaemic HUVEC lysates were measured by means of a lucigenin-based chemiluminescence assay (see section 2.2.9 for a full description).

Basal superoxide production in hyperglycaemic and normoglycaemic cells was comparable. Inhibition of NO production with L-NAME resulted in a ~2.5-fold (normoglycaemic cells) and a ~2.2-fold (hyperglycaemic cells) increase in O_2^- generation compared to the respective basal levels. As expected, TNFa treatment caused increased O_2^- synthesis compared to basal levels in both normoglycaemic and hyperglycaemic cells (~1.6-fold and ~2.6-fold, respectively). Due to the low sample number, statistical analysis could not be performed.

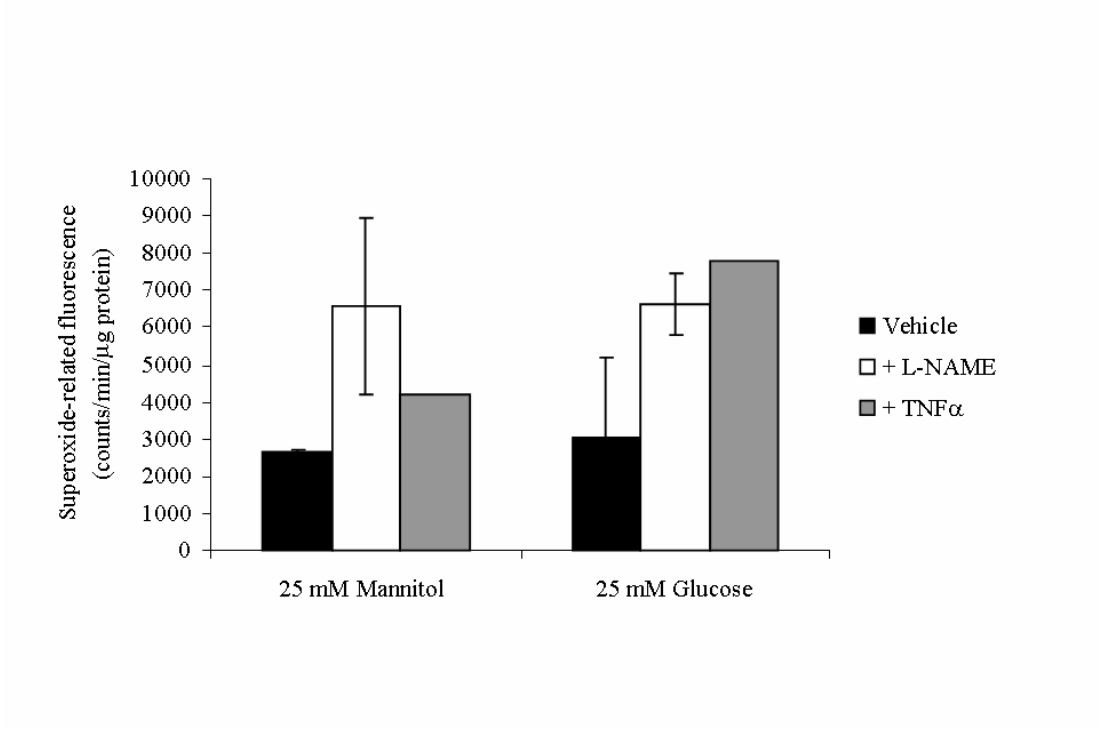

Figure 4-15 Superoxide levels in HUVEC are increased by eNOS inhibition.

HUVEC were cultured under experimental hyperglycaemic or normoglycaemic conditions in presence or absence of 100 µM L-NAME for 2h. Cells were serum-starved and subsets of cells treated with 10 ng/ml TNFa for 2h. Superoxide levels were measured in HUVEC lysates using a lucigenin-based chemiluminescence assay (described in section 2.2.9). Data are derived from one experiment (duplicates of vehicle and L-NAME samples; singlicates of TNFa samples) and are shown as mean ± range superoxide-related fluorescence.

4.3 Discussion

4.3.1 eNOS expression

The present study shows that experimental hyperglycaemia mildly modulates some aspects of insulin signalling in HUVEC. Several previous studies have investigated the effects of hyperglycaemia on various aspects of insulin signalling, and here, the present findings will be discussed in the light of these studies.

Exposure to high levels of glucose has been shown to have different effects on eNOS expression and phosphorylation, depending on the length of exposure and the model system studied. In agreement with this study, no change in eNOS protein expression was observed in BAEC and rat aorta exposed to 30 mM glucose for 48h (Du *et al.*, 2001), in HAEC after 48h of culture with 25 mM glucose (Salt *et al.*, 2003), and in HUVEC after 30 min of exposure to 25 mM glucose (Rojas *et al.*, 2003). Other groups reported a ~25 % decrease in eNOS levels in human coronary artery endothelial cells (HCAEC) exposed to 25 mM glucose for 7 days (Ding *et al.*, 2000), and bovine aortic endothelial cells (BAEC) exposed to 22 mM glucose for 2 weeks were shown to express 20-30% less eNOS protein (Noyman *et al.*, 2002). Expression of eNOS mRNA in HAEC cultured with 25 mM glucose was decreased by 25% and 46% after 3 and 7 days, respectively, while eNOS protein expression initially increased by 8% after 4h and then decreased by 64% after 7 days (Srinivasan *et al.*, 2004). Likewise, mRNA levels were decreased by 60% in diabetic (db/db) mouse aortic endothelial cells (MAEC) (Srinivasan *et al.*, 2004).

Conversely, several other studies demonstrated upregulated eNOS expression levels: Cosentino and co-workers reported a 2-fold increase in mRNA and protein levels in HAEC cultured with 22.2 mM glucose (Cosentino *et al.*, 1997). In HUVEC, Lin and co-workers showed that eNOS protein expression was elevated after exposure to 33 mM glucose for up to 24h, and was maximal after 6h (~2-fold over control) (Lin *et al.*, 2005), while another group reported that eNOS protein levels in HUVEC were elevated after 2-6h of exposure to 33 mM glucose (maximal at ~2.5-fold over control), but gradually returned to control levels by 48h (Ho *et al.*, 1999). Quagliaro and co-workers demonstrated a ~2.7-fold increase over control in eNOS protein levels in HUVEC cultured with 20 mM glucose for 14 days (Quagliaro *et al.*, 2007).

The discrepancies between these individual results highlight the differences between the various tissues used, and suggest that glucose concentration and length of exposure

differentially affect the outcome. This is corroborated by findings from the present study, in which data obtained with HAEC subjected to the same conditions as described above for HUVEC, differed in some aspects from those observed in HUVEC: As previously shown in this laboratory (Salt *et al.*, 2003), experimental hyperglycaemia did not affect insulin-stimulated eNOS^{S1177} phosphorylation in HAEC, which, in the present study, was 2.5-fold higher than basal (data not shown, compare to the 1.5-fold increase in hyperglycaemic HUVEC, Figure 4-2, panel C) and thus comparable to the insulin-stimulated increase observed in HUVEC under standard control conditions. Mannitol-treatment abrogated insulin-stimulated eNOS^{S1177} phosphorylation in HAEC (data not shown). Furthermore, insulin-stimulated phosphorylation of PKB^{T308} was absent and was less pronounced for PKB^{S473} in normoglycaemic and hyperglycaemic HAEC (~1.2-fold and ~1.3-fold over basal, respectively; data not shown) compared to HUVEC (Figure 4-7), indicating that HAEC were less insulin-sensitive than HUVEC under these conditions. These findings highlight discrepancies between different cell types used.

Based on these findings, both high glucose and high mannitol affect different vascular endothelial cell types differently, accounting in part for the diversity of published results. It is tempting to speculate that the origin of these endothelial cells might affect their response to various treatments, such as insulin, glucose and mannitol, in this case. The glucose concentrations encountered by different vascular beds in man are likely to vary, as might their insulin-sensitivity. In general, efferent blood vessels, and conduit arteries in particular, ought to be more responsive to vasodilatory stimuli than afferent blood vessels (veins) and arterioles, where vasodilation may not play such an important role. Also, the blood glucose concentration in peripheral veins is likely to be lower than in arteries, given that glucose is taken up from the blood into insulin-responsive tissues such as muscle, fat and liver. An important exception here is the hepatic portal vein, which drains the small intestine and would thus encounter higher blood glucose concentrations.

However, even with the same experimental model, different groups report varying results, as in the case of HUVEC cultured with 33 mM glucose: eNOS protein levels were reported to be upregulated only for up to 6h, and downregulated to near-control levels by 24h by one group (Ho *et al.*, 1999), while another found increased protein levels for up to 24h (Lin *et al.*, 2005). Similarly, comparable concentrations of glucose (22.2 mM and 25 mM) had different effects on HAEC with respect to eNOS mRNA and protein expression: in one study, the levels were increased 2-fold (Cosentino *et al.*, 1997), whereas they were decreased ~2-fold in another study (Srinivasan *et al.*, 2004). Such findings point out that

experimental systems often respond dissimilarly in different hands, owing in part to small variations of experimental conduct.

While no consensus conclusion regarding eNOS expression can be drawn from the studies described above, it is tentative to speculate that experimental hyperglycaemia has disparate short-term and long-term effects on eNOS expression: In the short-term (2-6h), hyperglycaemia appears to upregulate eNOS mRNA and protein expression, while longer-term hyperglycaemia (24h+) has most frequently been reported to normalise or decrease eNOS levels.

4.3.2 eNOS phosphorylation

In order to determine the effect of acute insulin treatment on the eNOS phosphorylation sites Ser114, Thr495, Ser615, Ser633 and Ser1177, cells cultured under standard control conditions (4 mM glucose, no mannitol) were included in the experimental design. In addition, an osmotic control ("normoglycaemic" cells cultured with 5 mM glucose and 20 mM mannitol) was used to determine the effects of high (25 mM) glucose *per se*, independent of high osmolarity. Therefore, the present experimental design contains an inherent quality control by comparing the effects of high mannitol concentrations to standard control conditions. The effect of high mannitol on HUVEC is discussed at the end of this section.

As has previously been demonstrated for $eNOS^{S615}$ (Ritchie *et al.*, 2007) and $eNOS^{S1177}$ in HAEC (Salt *et al.*, 2003), acute insulin stimulated the phosphorylation of $eNOS^{S615}$ and $eNOS^{S1177}$ in HUVEC under standard control conditions in the present study (see Figure 4-2). Similarly, the insulin-stimulated decrease in $eNOS^{T495}$ phosphorylation previously observed in HUVEC (Federici *et al.*, 2004) was also observed in the present study (see Figure 4-4, panel C). In addition, this study reports the novel findings that acute insulin treatment decreased the phosphorylation of $eNOS^{S114}$ and $eNOS^{S633}$ in HUVEC under standard control conditions (see Figure 4-3 and Figure 4-4, panel B). Most of the insulin-induced changes were small, and none were statistically significant.

Based on these results, it is tentative to speculate on the roles of these eNOS phosphorylation sites in relation to eNOS activity in HUVEC. Phosphorylation of Ser114, Thr495 and Ser633 may inhibit basal eNOS activity, while their dephosphorylation in response to insulin may increase eNOS activity. Conversely, low basal phosphorylation levels of $eNOS^{S615}$ and $eNOS^{S1177}$ may translate into low basal eNOS activity, which is increased upon insulin-stimulated phosphorylation of these sites. These findings corroborate the activating roles of insulin-stimulated Ser615 and Ser1177 phosphorylation that have been reported *in vitro* (Michell *et al.*, 2002), in HAEC (Salt *et al.*, 2003, Ritchie *et al.*, 2007) and BAEC (Montagnani *et al.*, 2001). Several other groups have demonstrated the activating properties of Ser615 and Ser1177 in response to other stimuli (Fleming *et al.*, 1998, Michell *et al.*, 2001, Michell *et al.*, 2002, Bauer *et al.*, 2003).

The negative regulatory role of Thr495 phosphorylation on eNOS activity is well documented. Dephosphorylation of Thr495 increases eNOS activity and NO production *in*

vitro as well as in HUVEC and PAEC (Chen *et al.*, 1999, Fleming *et al.*, 2001, Michell *et al.*, 2001, Greif *et al.*, 2002, Fleming & Busse, 2003, Matsubara *et al.*, 2003). This is in agreement with the present finding that insulin, a stimulator of eNOS activity, decreased $eNOS^{T495}$ phosphorylation.

Current experimental evidence suggests that the role of $eNOS^{S114}$ phosphorylation may vary according to the nature of the stimulus. Shear stress and high density lipoprotein have been shown to increase Ser114 phosphorylation and eNOS activity (Gallis *et al.*, 1999), whereas VEGF stimulation of eNOS activity lead to dephosphorylation of Ser114 and mimicry of Ser114 dephosphorylation increased eNOS activity (Kou *et al.*, 2002). Site-directed mutagenesis of bovine eNOS and subsequent transfection into COS-7 cells suggested that mimicking phosphorylation at Ser114 increased eNOS activity. Controversially, in the same study, both the phosphorylation and dephosphorylation $eNOS^{S114}$ mutants increased stimulated NO release (Bauer *et al.*, 2003). The present study suggests that insulin dephosphorylates $eNOS^{S114}$, but the impact on eNOS activity remains to be investigated.

Several lines of evidence suggest that phosphorylation of Ser633 maintains eNOS activity after initial eNOS phosphorylation at Ser1177. Similar to $eNOS^{S1177}$, $eNOS^{S633}$ is phosphorylated by shear stress, ATP, VEGF and bradykinin (Boo *et al.*, 2002, Michell *et al.*, 2002, Bauer *et al.*, 2003). Ser633 phosphorylation has been demonstrated to increase NO production in a Ca^{2+}-independent manner (Boo *et al.*, 2003). This stands in contrast to the present result, in which insulin stimulated a decrease in $eNOS^{S633}$ phosphorylation.

Studies of eNOS phospho-mutants, in which the amino acid residues of these phosphorylation sites have been mutated to mimic constitutive phosphorylation (aspartate mutants) or dephosphorylation (alanine mutants), have already provided important evidence about the role of each of the eNOS phosphorylation sites. A previous study with bovine eNOS phospho-mutants transfected into COS-7 cells has suggested that the sites equivalent to Ser633 and Ser1177 are important positive regulators of eNOS-mediated NO release in response to ATP (Bauer *et al.*, 2003). In the same study, Ser615 phosphorylation slightly downregulated NO release, but was suggested to be important as a modulator of phosphorylation at the other eNOS phosphorylation sites and of protein-protein interactions (Bauer *et al.*, 2003).

Ser114 and Ser615 were postulated to be important positive modulators of phosphorylation at Ser1177 and increased the interaction of eNOS with hsp90 and PKB (Bauer *et al.*, 2003). Another report suggested that mimicking phosphorylation at the sites equivalent to Ser633 and Ser1177 contributed to eNOS activity *in vitro*, whereas Thr495 phosphorylation decreased eNOS activity and Ser615 increased the activity of eNOS at lower concentrations of calmodulin without affecting maximal activity (Michell *et al.*, 2002).

In order to define the clinical relevance of these findings, the proposed roles of individual eNOS phosphorylation sites will have to be verified in human vascular endothelial cells, and vascular explants, where possible. Their impact on eNOS activity in presence and absence of insulin and other stimuli will have to be measured, for example by using L-arginine conversion assays and NO synthesis assays. Furthermore, it would be of great value to extend the present study to determine the effect of hyperglycaemia on eNOS activity.

The effect of experimental hyperglycaemia on the phosphorylation state of eNOS phosphorylation sites Ser114, Thr495, Ser615, Ser633 and Ser1177 was investigated in the present study. Previous data from this laboratory demonstrated that experimental hyperglycaemia in HAEC did not affect $eNOS^{T495}$ or $eNOS^{S1177}$ phosphorylation (Salt *et al.*, 2003). The aim behind the present study was to investigate in HUVEC the phosphorylation status of eNOS at all five main phosphorylation sites. Other groups have previously studied the phosphorylation and activity levels of eNOS in the context of hyperglycaemia. Most available data concern the phosphorylation of the Ser1177 site, though a few studies have also investigated other eNOS phosphorylation sites. No published studies of prolonged (48h) hyperglycaemia have been carried out in HUVEC, though other cell types have been used for modelling 48h+ hyperglycaemia.

In hyperglycaemic BAEC (48h) and diabetic rat aorta, basal $eNOS^{S1177}$ phosphorylation was decreased by 45% and 50%, respectively, while glycosylation at this site was increased 1.85-fold (BAEC) and 2.1-fold (rat aorta), resulting in 32% (BAEC) and 57% (rat aorta) decreases in eNOS activity (Du *et al.*, 2001). In a study by Federici and co-workers, ^{32}P-incorporation by constitutively active PKB into $eNOS^{S1177}$ immunoprecipitated from hyperglycaemic HCAEC was also impaired (46% lower than control), while glycosylation of eNOS around the Ser1177 site was 2.9-fold higher than in controls (Federici *et al.*, 2002), suggesting that hyperglycaemia induced glycosylation

around the Ser1177 site and thus prevented its effective phosphorylation. Similarly, insulin-stimulated eNOS^{S1177} phosphorylation after 72h of experimental hyperglycaemia was reduced by 37%, while insulin-stimulated eNOS activity was decreased 27% compared to control (Federici *et al.*, 2002). By contrast, Salt and co-workers reported no change in basal or insulin-stimulated eNOS^{S1177} phosphorylation after 48h of experimental hyperglycaemia in HAEC (Salt *et al.*, 2003).

Studies of short-term experimental hyperglycaemia demonstrated that exposure to 25 mM glucose for 30 minutes induced a ~ 2.8-fold increase over control in eNOS^{S1177} phosphorylation and increased L-citrulline production by hyperglycaemic HUVEC ~2.2-fold, indicating greater eNOS activity than in control cells (Rojas *et al.*, 2003). Also in HUVEC, Lin and co-workers observed increased phosphorylation levels of eNOS after 2-6h of high glucose (maximal at 4h with ~4.5-fold elevation), which returned to basal after 24h (Lin *et al.*, 2005). However, longer-term hyperglycaemia was demonstrated to have the opposite effect: Two weeks of experimental hyperglycaemia decreased eNOS activity by 25% in BAEC and abrogated insulin-stimulated eNOS activity (Noyman *et al.*, 2002). Similarly, unstimulated eNOS^{S1177} phosphorylation 5 weeks post-induction of diabetes was decreased by 25% (without a change in total eNOS expression) in partially purified rat penile tissue (including vascular endothelium), while glycosylation was increased by 90% (Musicki *et al.*, 2005). In their study, shear stress also failed to increase Ser1177 phosphorylation (Musicki *et al.*, 2005).

In the present study, basal eNOS^{S1177} phosphorylation was unchanged in hyperglycaemic HUVEC compared to control cells (Figure 4-5, panel A). However, insulin-stimulated Ser1177 phosphorylation was slightly and non-significantly reduced after 48h of experimental hyperglycaemia compared to control cells (Figure 4-2, panel B). The observed trend of decreased insulin-responsive eNOS^{S1177} phosphorylation agrees with findings in HCAEC (Federici *et al.*, 2002) and contrasts other reports (Rojas *et al.*, 2003, Salt *et al.*, 2003), but given the variation in duration of experimental hyperglycaemia and the different cell types used, this only emphasises the discrepancies between different experimental models.

Two groups have reported no changes to basal eNOS^{T495} phosphorylation in hyperglycaemic HAEC (Salt *et al.*, 2003) and diabetic rat penis (Musicki *et al.*, 2005), which is in line with the present finding that neither basal nor insulin-stimulated eNOS^{T495} phosphorylation is altered by experimental hyperglycaemia (Figure 4-4, panel C). The

study by Musicki and co-workers showed that basal eNOS^{S615} and eNOS^{S633} phosphorylation was not affected by hyperglycaemia in diabetic rats (Musicki *et al.*, 2005). This contrasts with the current results, where basal eNOS^{S615} phosphorylation was increased by experimental hyperglycaemia, albeit not to statistical significance (Figure 4-2, panel B), and basal eNOS^{S633} phosphorylation was reduced to 50% of control levels (not statistically significant; see Figure 4-3 and Figure 4-5, panel A). Site-directed mutagenesis studies have suggested that basal phosphorylation of eNOS^{S633} is important for eNOS activity (Bauer *et al.*, 2003), which would imply that the trend toward reduced eNOS^{S633} phosphorylation observed under experimental hyperglycaemia in the present study might reduce eNOS activity.

No literature has been published regarding the effect of hyperglycaemia on eNOS^{S114} phosphorylation. In this study, insulin-stimulated Ser114 phosphorylation was significantly reduced compared to stimulated control samples (Figure 4-5, panel B).

The effect of insulin on eNOS activity has been assumed to be stimulatory, based on the observation that insulin treatment increases eNOS-mediated NO production (Scherrer *et al.*, 1994, Zeng & Quon, 1996). While phosphorylation of eNOS^{S1177} is required for agonist-mediated NO synthesis (Dimmeler *et al.*, 1999, Fulton *et al.*, 1999, Michell *et al.*, 2001), and eNOS^{T495} dephosphorylation is thought to enhance NO generation (Chen *et al.*, 1999, Fleming *et al.*, 2001, Michell *et al.*, 2001, Greif *et al.*, 2002, Fleming & Busse, 2003, Matsubara *et al.*, 2003), less is known about the roles of the other eNOS phosphorylation sites in insulin signalling.

Based on the insulin-stimulated effect on eNOS phosphorylation sites under standard control conditions in the present study, phosphorylation of Ser114, Thr495 and Ser633 may inhibit eNOS activity in HUVEC, while phosphorylation of Ser615 and Ser1177 most likely activates eNOS. During experimental hyperglycaemia, basal eNOS^{S615} phosphorylation showed a trend toward upregulated phosphorylation, whereas basal eNOS^{S633} phosphorylation tended to be downregulated with respect to standard control (see Figure 4-5, panel A). This suggests experimental hyperglycaemia may promote basal eNOS activity. Insulin-stimulated eNOS phosphorylation at Ser114 was significantly decreased with respect to standard control, whereas none of the other sites was significantly affected (see Figure 4-5, panel B). If Ser114 phosphorylation is indeed a negative regulator of eNOS activity in HUVEC, its decreased phosphorylation would imply increased eNOS activity during experimental hyperglycaemia.

It is important to bear in mind that the phosphorylation status of each of these sites may influence that of others. Furthermore, some phosphorylation sites may not be important for insulin-stimulated eNOS activity, but rather serve to modulate eNOS interactions with other proteins, as has been suggested for Ser615 (Bauer *et al.*, 2003). In order to determine the role of each of these phosphorylation sites in insulin-stimulated eNOS activity under normal and hyperglycaemic conditions, further investigations are therefore required.

It is interesting to note that eNOS phosphorylation levels at $eNOS^{S633}$ and $eNOS^{S1177}$ differed in mannitol-cultured (normoglycaemic) HUVEC compared to control cells cultured with 4 mM glucose alone. Although culture with 20 mM mannitol and 5 mM glucose had been designed as an osmotic control and was expected to have no effect on protein expression and phosphorylation, an osmotic effect seems to be precipitated by the addition of high levels of mannitol to the cell culture medium. Insulin-responsive phosphorylation levels of $eNOS^{S1177}$ were altered in mannitol-treated cells, the stimulated increase being less pronounced than in control cells (see Figure 4-2). Furthermore, basal $eNOS^{S633}$ phosphorylation was also lower in normoglycaemic compared to control cells, and insulin-stimulated dephosphorylation was abrogated (Figure 4-3).

Although neither of these changes was statistically significant with respect to the standard control, these findings suggest that mannitol, despite being cell-impermeable and thus not metabolised by cells, can interfere with normal insulin signalling. A recent report suggests that hyperosmotic mannitol (550 mM) can induce large structural changes in rat brain endothelial cells (Bálint *et al.*, 2007), while previous findings demonstrated that 100 mM mannitol can cause apoptosis of endothelial cells (Malek *et al.*, 1998). Although these mannitol concentrations are much higher than the concentration used here, it remains to be investigated whether high concentrations of mannitol have a biologically significant impact on cellular signalling processes.

Investigating the effect of high mannitol concentrations on cellular function would be a relevant study, considering that several groups (Cosentino *et al.*, 1997, Ho *et al.*, 1999, Du *et al.*, 2001, Federici *et al.*, 2002, Rojas *et al.*, 2003, Salt *et al.*, 2003, Srinivasan *et al.*, 2004, Quagliaro *et al.*, 2007) used mannitol as a negative control when studying the effects of experimental hyperglycaemia. None of these groups reported any osmotic effects with mannitol. Two groups compared cells cultured in normal versus mannitol-supplemented medium (Federici *et al.*, 2002, Srinivasan *et al.*, 2004), but neither of these groups reported

any changes with mannitol compared to control medium regarding the parameters measured.

Inclusion of an osmotic control is important for the study of experimental hyperglycaemia in cultured endothelial cells, though some groups (Ding *et al.*, 2000, Noyman *et al.*, 2002, Lin *et al.*, 2005) have failed to include osmotic controls, instead comparing cells cultured in high glucose to cells cultured in normal medium with low glucose concentrations alone. Such an experimental design makes it impossible to determine whether the effects observed with high glucose are genuine or due to osmotic stress. An alternative control for experimental hyperglycaemia is the use of equimolar concentrations of non-metabolisable L-glucose, although the cost of this compound prevents its routine use for experiments such as those presented here. One group (Rojas *et al.*, 2003) used equimolar L-glucose as an additional control, and reported no effect.

The present study also puts into question whether the effects observed under experimental hyperglycaemia are actually glucose-specific, or whether they are, at least in part, due to osmotic effects. While it is vital to include an osmotic control in experiments investigating the effects of experimental hyperglycaemia, mannitol does not seem to be a suitable choice, since the present study showed that culture of HUVEC with 20 mM mannitol mildly affects the phosphorylation of eNOS^{S633}, eNOS^{S1177}, PKB^{S473} and I?Ba^{S32} and the expression of IKKß (see also section 4.3.3), when compared to cells cultured with 4 mM glucose alone. While these osmotic effects may be specific to HUVEC, it is likely that other vascular endothelial cells are also affected by this phenomenon. Therefore, the results of studies which have used mannitol as an osmotic control without comparing the findings to cells cultured under normal osmolarity, must be questioned with respect to their validity.

4.3.3 Insulin-regulated pathways

In order to determine whether some other insulin-responsive pathways were affected by experimental hyperglycaemia and are therefore potential candidates for dysregulated eNOS function under hyperglycaemic conditions, components of the metabolic insulin signalling pathway, the NF?B transcription pathway and the stress-activated JNK and CAP-Cbl pathways were assessed for expression and phosphorylation levels.

PKB, which phosphorylates eNOS at Ser1177, showed no change in expression under any condition tested (Figure 4-6), and phosphorylation of its principal activating site Thr308 was consistently stimulated >3-fold by acute insulin (Figure 4-7, panel B). Likewise, insulin-stimulated phosphorylation of the second activating site, Ser473, increased >1.4-fold over basal under control, normoglycaemic and hyperglycaemic conditions (Figure 4-7, panel C). Despite reduced unstimulated PKB^{S473} phosphorylation under normoglycaemic and hyperglycaemic conditions, these results indicate that PKB phosphorylation, and thus most likely PKB activity, are unaffected by hyperglycaemia in this experimental system and that PKB remains insulin-sensitive. Expression levels of the upstream components PI3K-p85, PTEN and PDK-1 were unaltered with respect to control, again suggesting that the upstream components of the metabolic insulin signalling pathway in HUVEC are not impaired by 48h of experimental hyperglycaemia.

Previous studies have demonstrated that protein expression of PKBa, PI3K-p85 and -p110ß, PTEN, PDK-1 and IRS-1 was unchanged in HAEC after 48h of experimental hyperglycaemia, while IRS-2 levels were reduced by 30% compared to control (Salt *et al.*, 2003). Insulin-stimulated PKBa activity was unaffected, which supports the present findings, although basal PKB activity was increased 2.4-fold with respect to control (Salt *et al.*, 2003). Unstimulated PKB serine phosphorylation in BAEC was unchanged after 2 weeks of experimental hyperglycaemia compared to control, but eNOS activity was reduced by 25% (Noyman *et al.*, 2002).

Unlike the present study, one group reported that insulin-dependent PKB^{S473} phosphorylation in HCAEC after 72h of experimental hyperglycaemia was 30% lower than in control cells (Federici *et al.*, 2002). In the same study, PI3K activity was decreased by 55%, and PI3K association with IRS-1 and IRS-2 was reduced by 20% and 40%, respectively, compared to control cells (Federici *et al.*, 2002). This is mirrored by findings that PI3K recruitment to IRS-1 was reduced by 24%, whereas PI3K recruitment to IRS-2, which showed a 71% decrease in expression, was abolished under experimental

hyperglycaemia (Salt *et al.*, 2003), indicating a defect in PI3K and/or IRS function. Federici and co-workers also reported decreased phosphorylation of the insulin receptor (by 50%) and IRS-1 (by 55%), and simultaneous increases in the glycosylation of IRS-1 (600%), IRS-2 (210%) and PI3K-p85 (200%) (Federici*et al.*, 2002), again suggesting that experimental hyperglycaemia may exert a damaging impact on insulin signalling through increased glycosylation of proteins.

The reduction in basal PKB^{S473} phosphorylation of ~67%, seen in hyperglycaemic HUVEC in the present study, was also reported for penile tissue of diabetic rats, where basal PKB^{S473} phosphorylation levels were decreased by 60% (Musicki *et al.*, 2005). Shear stress induced phosphorylation of PKB^{S473} to levels comparable to control, indicating normal PKB function, but not phosphorylation of $eNOS^{S1177}$ (Musicki*et al.*, 2005). Varma and co-workers reported that 40 mM glucose decreased basal PKB^{T308} phosphorylation by ~50% and PKB activity by ~75%, as well as reducing basal tyrosine phosphorylation of PI3K by ~40%, in HUVEC exposed to experimental hyperglycaemia for 8 days (Varma *et al.*, 2005). This contrasts the present finding that basal PKB^{T308} phosphorylation was unaltered by experimental hyperglycaemia.

Overall, these findings suggest that, depending on the tissue used, defective eNOS phosphorylation under hyperglycaemic conditions is unlikely to be caused by impaired PKB activity alone. There is some evidence that hyperglycaemia induces changes in PI3K activity, which may likely affect eNOS regulation via PKB. Other factors, such as defects in other insulin signalling pathway components, or hyperglycaemia-induced glycosylation, may also contribute to the alterations in eNOS phosphorylation observed in this and other studies.

Given the unchanged insulin-sensitivity of the metabolic insulin signalling pathway components investigated here, other insulin-responsive pathways were assessed for their potential dysregulation by experimental hyperglycaemia. Investigation of the NF?B pathway revealed that there were no changes in the expression levels of NF?B (Figure 4-10) and I?Ba (Figure 4-11, panel B) under any condition tested. Phosphorylation of I?Ba at Ser32, however, was basally decreased under normoglycaemic and hyperglycaemic conditions compared to control, while insulin-induced dephosphorylation of Ser32 seen in control samples was mildly impaired under these conditions. The insulin-responsiveness of I?Ba dephosphorylation would point to lower NF?B bioavailability, thus potentially resulting in a reduction of NF?B-regulated transcription after insulin stimulation. By

contrast, a slight decrease in NF?B levels following insulin treatment was observed in the present study. However, there was a slight basal increase in NF?B levels after mannitol and glucose treatment, possibly as a result of increased basal phosphorylation (and thus degradation) of I?Ba under these conditions.

Conversely, basal levels of the I?Ba-phosphorylating kinase IKKß were slightly and not statistically significantly increased under normoglycaemic and hyperglycaemic conditions (Figure 4-12), predicting increased phosphorylation of I?Ba, which was not observed in the present study. Acute treatment with insulin increased the abundance of IKKß in standard control samples, which contradicts the present finding of decreased IκBa^{S32} levels in insulin-stimulated control samples. However, these insulin-induced changes in IKKß and I?Ba^{S32} levels were abolished in normoglycaemic and hyperglycaemic samples and were not statistically significant. Since IKKß activity was not measured in this study, no conclusion about the effect of raised IKKß levels on I?Ba phosphorylation can be drawn.

Previously, dose-dependent activation of NF?B nuclear translocation by high (25-35 mM), but not lower (15 mM) concentrations of glucose has been observed in BAEC (Pieper & Riaz ul, 1997). NF?B activity was increased in nuclear fractions within 1h and was maximal at 2-4h, suggesting that alteration of NF?B bioavailability is an early hyperglycaemia-induced event that may contribute to endothelial dysfunction and atherosclerosis (Pieper & Riaz ul, 1997). Similarly, incubation of BAEC with 30 mM glucose increased NF?B activation 1.8-fold (Nishikawa *et al.*, 2000). These findings would have to be validated in HAEC, as the present study did not address NF?B activity, but only its expression levels.

In the present study, acute insulin treatment induced very small decreases in JNK expression levels (not statistically significant), but did not change JNK phosphorylation levels (Figure 4-13). However, basal JNK phosphorylation was slightly elevated in hyperglycaemic cells compared to mannitol-cultured cells (not statistically significant), suggesting that high glucose levels may promote JNK phosphorylation in HUVEC. Previously, 25 mM glucose was shown to transiently increase JNK1 activity in bovine pulmonary artery endothelial cells (BPAEC) (activity being maximally increased (2-fold) with respect to control at 24h) (Liu *et al.*, 2000).

The JNK pathway can be activated by oxidative stress and has been implicated in the development of diabetes and atherosclerosis (reviewed in (Kaneto *et al.*, 2007)). Mice

lacking JNK are protected from macrophage-mediated pancreatic beta-cell apoptosis and subsequent hyperglycaemia, which is likely due to reduced TNFa secretion from macrophages (Fukuda *et al.*, 2008). This suggests that active JNK plays a crucial role in promoting cytokine-induced beta-cell destruction and aggravates the prodiabetic profile. The present study indicates that in HUVEC, increased hyperglycaemia-mediated JNK activation through phosphorylation is a potential prodiabetic candidate mechanism, although these results are preliminary and require further confirmation.

The expression of CAP was largely unchanged under all conditions tested, although large inter-sample variation in expression levels prevented the drawing of any definitive conclusions. Cbl expression levels were comparable under all conditions, except for insulin-treated hyperglycaemic cells, in which there was a 50% decrease with respect to unstimulated control and normoglycaemic cells (not statistically significant; see Figure 4-14). Previous work in hyperglycaemic HAEC showed that CAP and Cbl expression was reduced to 54% and 60% of control levels, respectively, and that insulin-induced Cbl phosphorylation in control cells was abrogated in hyperglycaemic HAEC (Salt *et al.*, 2003). In mice, knockout of Cbl lead to macrophage activation and contributed to peripheral insulin resistance and glucose intolerance (Hirasaka *et al.*, 2007). If Cbl is also downregulated by hyperglycaemia in humans, this would exacerbate glucose intolerance.

It is interesting to note that acute treatment with insulin for 10 minutes seemed to have a modulatory, though not statistically significant, effect on the quantities of the molecules IKKß, JNK and Cbl, compared to their basal levels. Acute insulin treatment is unlikely to affect the actual protein expression levels of molecules within the 10-minute time scale tested. More likely, the small changes observed here are due to other factors, such as inter-sample variation. It is, however, conceivable that insulin may trigger degradation of these molecules, or regulatory events other than those investigated here, such as phosphorylation, ubiquitination and myristoylation, which may render the molecules in question undetectable to the antibodies used here.

The present study has shown that acute insulin treatment can lead to the rapid dephosphorylation of I?Ba, thus potentially decreasing levels of free NF?B and acting as an antiatherogenic mediator. However, in the present study, insulin-induced I?Ba dephosphorylation in control samples were not mirrored by equally reduced NF?B levels in the same samples. Insulin has not previously been reported to cause dephosphorylation of $I?Ba^{S32}$, but rather its phosphorylation (Pandey *et al.*, 2002). While the results shown

here may be representative of the actual abundance levels of these molecules, a number of other factors, including inter-sample variation and the effectiveness of the protease inhibitors used during sample preparation, could have influenced these measurements. Quantification of further samples, preferably using other pools of HUVEC, would reduce inter-sample variation and provide more accurate results for the abundance levels of all molecules investigated here.

Data from one experiment indicated that expression of the stress-activated p38 MAPK in hyperglycaemic cells was unchanged compared to normoglycaemic cells, whereas insulin-stimulated p38 MAPK phosphorylation was reduced by ~24% in hyperglycaemic HUVEC (data not shown). Noyman and co-workers showed that experimental hyperglycaemia reduced basal p38 MAPK activation in BAEC to 43% of control levels (Noyman *et al.*, 2002). In a previous report, the basal phosphorylation and activity of p44/42 MAPK, and the activity of p38 MAPK were not affected by culture of BPAEC in 25 mM glucose (Liu *et al.*, 2000), indicating that hyperglycaemia does not interfere with the basal activity of these mitogenic insulin signalling pathway components. It would be interesting, however, to address the effect of experimental hyperglycaemia on insulin-stimulated phosphorylation and activity of these and other components more thoroughly.

As observed for the phosphorylation levels of eNOS^{S633} and eNOS^{S1177}, culture of HUVEC with 20 mM mannitol and 5 mM glucose also affected the basal expression level of IKKß and the unstimulated phosphorylation levels of PKB^{S473} and I?Ba^{S32}. While only the decrease in basal PKB^{S473} phosphorylation in normoglycaemic cells was statistically significant with respect to unstimulated control, these findings suggest that high concentrations of mannitol in the culture medium exert an osmotic effect on HUVEC. Further investigations are needed to determine whether this is a robust effect or merely an artefact of the experimental procedures. These findings put into question the use of equimolar mannitol concentrations as a suitable control for experimental hyperglycaemia, and will reduce the potency of any conclusions drawn from such experiments.

Overall, the effects observed in HUVEC in the present study were small, and large interexperimental variation in cellular responsiveness to stimuli resulted in few statistically significant changes. Therefore, the significance of the present study is limited.

4.3.4 Superoxide production

Preliminary investigation of superoxide generation by HUVEC revealed that experimental hyperglycaemia had no effect on O_2^- levels compared to normoglycaemic control (Figure 4-15). In addition, O_2^- levels were higher when co-incubating cells with the eNOS inhibitor L-NAME, indicating that functional NO synthesis reduces O_2^- levels. This may suggest that inhibition of NO production may increase eNOS-mediated superoxide production, or that the superoxide produced during uninhibited eNOS activity rapidly reacts with NO to form peroxynitrite (Reiter *et al.*, 2000), thus becoming undetectable by means of the lucigenin-based superoxide assay employed here. Greater TNFa-stimulated superoxide production in hyperglycaemic HUVEC may suggest that experimental hyperglycaemia sensitizes HUVEC to TNFa; however, given that TNFa treatment was carried out in singlicate, this thought is highly speculative.

Several other studies have found that superoxide levels in vascular endothelial cells were altered by experimental hyperglycaemia, and were frequently linked to eNOS expression or activity levels: Culturing of HAEC with 22.2 mM glucose for 5 days increased eNOS mRNA and protein levels 2-fold and O_2^- levels 3-fold, while increasing NO levels by only 1.4-fold, leading to an imbalance between O_2^- and NO (Cosentino *et al.*, 1997). Similarly, HUVEC showed a 40% increase in NO production and a 300% rise in O_2^- generation, along with elevated eNOS expression, after 2 weeks of experimental hyperglycaemia (20 mM) (Quagliaro *et al.*, 2007).

High glucose concentrations (22 mM) abolished insulin-stimulated eNOS activity in BAEC, thus impairing the NO synthesis pathway, while simultaneously increasing oxidative stress as indirectly measured by 3-fold increased superoxide dismutase (SOD)-1 expression in hyperglycaemic cells (Noyman *et al.*, 2002). Du and co-workers reported decreased eNOS activity (as measured by L-arginine conversion) and O_2^- overproduction in hyperglycaemic BAEC, although this overproduction was attributed to mitochondrial activity (Du *et al.*, 2001), rather than uncoupled eNOS activity. Another group also showed that experimental hyperglycaemia induced mitochondrial superoxide production (Nishikawa *et al.*, 2000).

Experimental hyperglycaemia may also increase oxidative stress by modulating the levels of other reactive oxygen species, such as hydrogen peroxide, which was increased in HUVEC after 48h with 33 mM glucose (Ho *et al.*, 1999). A correlation between decreased eNOS expression, reduced nitrite levels and increased mitochondrial ROS production in

hyperglycaemic HAEC after 7 days was postulated by another group (Srinivasan *et al.*, 2004). Decreased eNOS promoter activity in HAEC was ameliorated by quenching of ROS. In addition, inhibition of mitochondrial ROS production normalised eNOS mRNA levels in diabetic mice (Srinivasan *et al.*, 2004). By contrast, it has also been suggested that ROS can increase eNOS mRNA expression via NF?B (Zhen *et al.*, 2008).

The reaction product of NO and O_2^-, peroxynitrite, has been suggested to suppress PKB activity and induce apoptosis during experimental hyperglycaemia by upregulation of PTEN (Song *et al.*, 2007). Although this and other findings described above stand in contrast to the present results of unchanged O_2^-, eNOS, PKB^{T308}, PKB^{S473} and PTEN levels, the experimental evidence from the single superoxide assay shown in the present study is not sufficient to draw definitive conclusions about superoxide generation under experimental hyperglycaemia in HUVEC. Therefore, further experiments are needed to elucidate the situation more fully.

Although insulin-stimulated NO synthesis has not been investigated in the present study, previous results in this laboratory demonstrated that 48h of experimental hyperglycaemia (25 mM) in HAEC decreased insulin-stimulated NO production by 60% (Salt *et al.*, 2003). Given the frequently postulated imbalance between NO and O_2^-/ROS production (Cosentino *et al.*, 1997, Ho *et al.*, 1999, Noyman *et al.*, 2002, Srinivasan *et al.*, 2004, Quagliaro *et al.*, 2007), and its potential involvement in causing endothelial dysfunction and atherogenesis, measurement of NO synthesis by HUVEC - and its relation to superoxide/ROS levels - under the experimental hyperglycaemic conditions employed here would be a valuable addition to the present study.

5 The Subcellular Localisation of eNOS in Human Vascular Endothelial Cells

5.1 Introduction

5.1.1 Background

The localisation of a molecule within the cell is important to its function. Initially, eNOS was found in the particulate subcellular fraction of bovine aortic endothelial cells (Forstermann *et al.*, 1991, Pollock *et al.*, 1991) and eNOS-transfecetd COS-7 cells (Busconi & Michel, 1993). Later studies showed that eNOS is targeted to the Golgi body of eNOS-transfected HEK cells (Sessa *et al.*, 1995). In the cell line ECV304, exogenous eNOS localised to the plasma membrane and the perinuclear/Golgi area (Sowa *et al.*, 1999), but the endothelial nature of ECV-304 cells is doubtful (Brown *et al.*, 2000). At the plasma membrane, eNOS is thought to localise to caveolae, plasma membrane microdomains coated with the protein caveolin (Garcia-Cardena *et al.*, 1996a, Garcia-Cardena *et al.*, 1996b, Shaul *et al.*, 1996). However, it is unclear whether eNOS also localises to other cellular compartments.

Targeting of eNOS to caveolae is determined by dual acylation with the fatty acids myristate and palmitate (Liu & Sessa, 1994, Garcia-Cardena *et al.*, 1996b, Shaul *et al.*, 1996). Its presence at the plasma membrane is thought to optimise eNOS activation and nitric oxide release to the extracellular environment (Garcia-Cardena *et al.*, 1996b, Shaul *et al.*, 1996). Based on data from eNOS-transfected COS-7 cells, the plasma membrane- and Golgi-associated pools of eNOS are thought to respond differently to activation by PKB and calcium-dependent mechanisms (Fulton *et al.*, 2004a). To date, little is known about the effect of agonists on the subcellular distribution of eNOS. Furthermore, much of the work so far has been carried out in non-endothelial cell lines or cells whose endothelial origin is debated. In addition, the subcellular localisation of phospho-eNOS species has not been fully investigated.

5.1.2 Aims of the chapter

So far, it is not known how stimulation with insulin affects the subcellular distribution of eNOS within human vascular endothelial cells. Therefore, the aim of this chapter was to investigate the effect of acute insulin stimulation on the subcellular localisation of eNOS and its distribution within different cellular compartments of human aortic endothelial cells.

5.2 Results

5.2.1 Selection of experimental conditions

Human aortic endothelial cells were used to investigate the subcellular distribution of eNOS, since the central macrovascular origin of HAEC makes them a more relevant model system than HUVEC for the study of responses to acute insulin stimulation. In addition, no previous reports addressing eNOS localisation in HAEC have been published to date.

HAEC were left untreated or stimulated acutely with 1 µM insulin for 10 minutes prior to fixation in 4% (w/v) formaldehyde. An ammonium chloride blocking step was used to prevent overfixation of cells. HAEC were permeabilised gently (0.5-1% (v/v) Triton X-100, 7 min) to avoid detachment of the plasma membrane. For co-labelling experiments, cells were co-incubated with anti-eNOS and anti-caveolin-1 antibodies. After washing, cells were co-incubated with both secondary antibodies. DAPI dye was used to stain nuclei (see section 2.2.13 for a detailed description).

For subcellular fractionation experiments, iodixanol was chosen because of its ability to form a continuous gradient upon centrifugation, which results in good yields of cellular organelles at high purity (Graham *et al.*, 1994).

5.2.2 Subcellular localisation of eNOS

In order to investigate the subcellular localisation of eNOS, HAEC were immunolabelled with anti-eNOS antibody and stained with DAPI. Subsets of cells were co-labelled with anti-caveolin-1 antibody. Confocal microscopy of immunolabelled HAEC showed that eNOS is present throughout the cell, including the nucleus (Figure 5-1, panels A, C-E). Frequently, prominent eNOS labelling was observed in the perinuclear area (Figure 5-1, panel F). eNOS was also found at the plasma membrane, and also colocalised with the membrane marker caveolin-1 (Figure 5-1, panels B and E).

It was investigated whether acute treatment with insulin affected the subcellular localisation of eNOS. Subsets of HAEC were stimulated with insulin for 10 minutes prior to fixation and immunolabelling. Confocal analysis and subsequent quantification of fluorescence intensity in nucleus, perinuclear area and cytoplasm demonstrated that there was no difference between insulin-treated and control HAEC (Figure 5-2). The majority of eNOS localised to the perinuclear region, where 1.8-fold greater quantities of eNOS were detected than in the nuclei of untreated and insulin-stimulated HAEC. The smallest proportion of eNOS was seen in the cytoplasm (34% and 32% compared to 100% nuclear eNOS content in untreated and insulin-stimulated cells, respectively). Insulin had no discernible effect on the subcellular localisation of eNOS in HAEC. Statistical analysis could not be performed on this singlicate experiment, but the ranges of eNOS fluorescence are indicated in the graph in Figure 5-2, panel C.

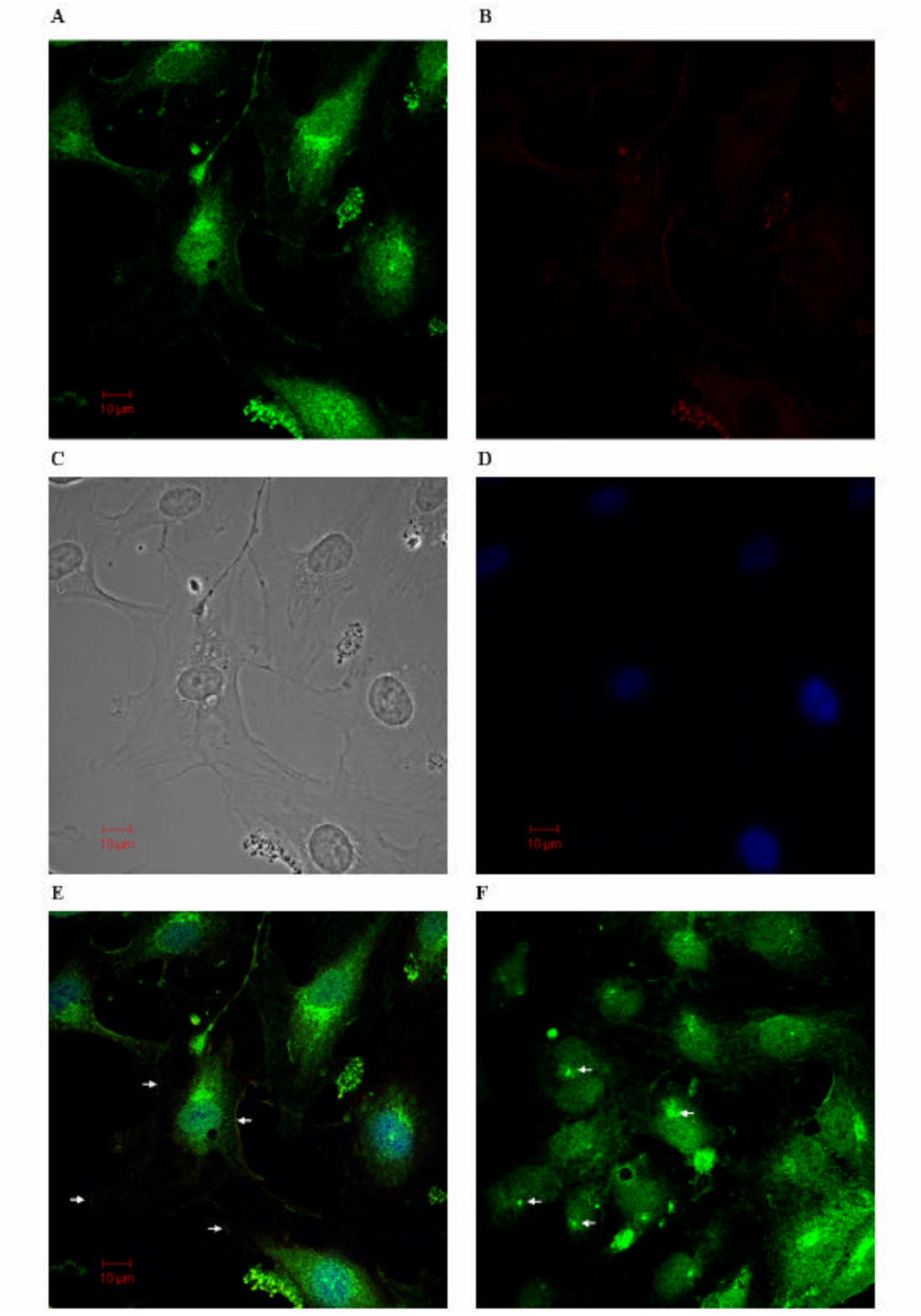

Figure 5-1 eNOS localises to the plasma membrane and the perinuclear region.

HAEC were immunolabelled with anti-eNOS (green, panel A) and anti-caveolin-1 (red, panel B) antibodies and stained with DAPI (blue, panel D). Confocal images of fluorescence and brightfield channels were taken (see sections 2.2.13 and 2.2.13.1). Representative images from two separate fields (Panels A-E, panel F) are shown. Membrane localisation of eNOS and co-localisation with the membrane-marker caveolin-1 (panel E) and perinuclear localisation of eNOS (panel F) are indicated by arrows. To normalise against background fluorescence, separate controls were performed in absence of primary antibody and in presence of irrelevant secondary antibody.

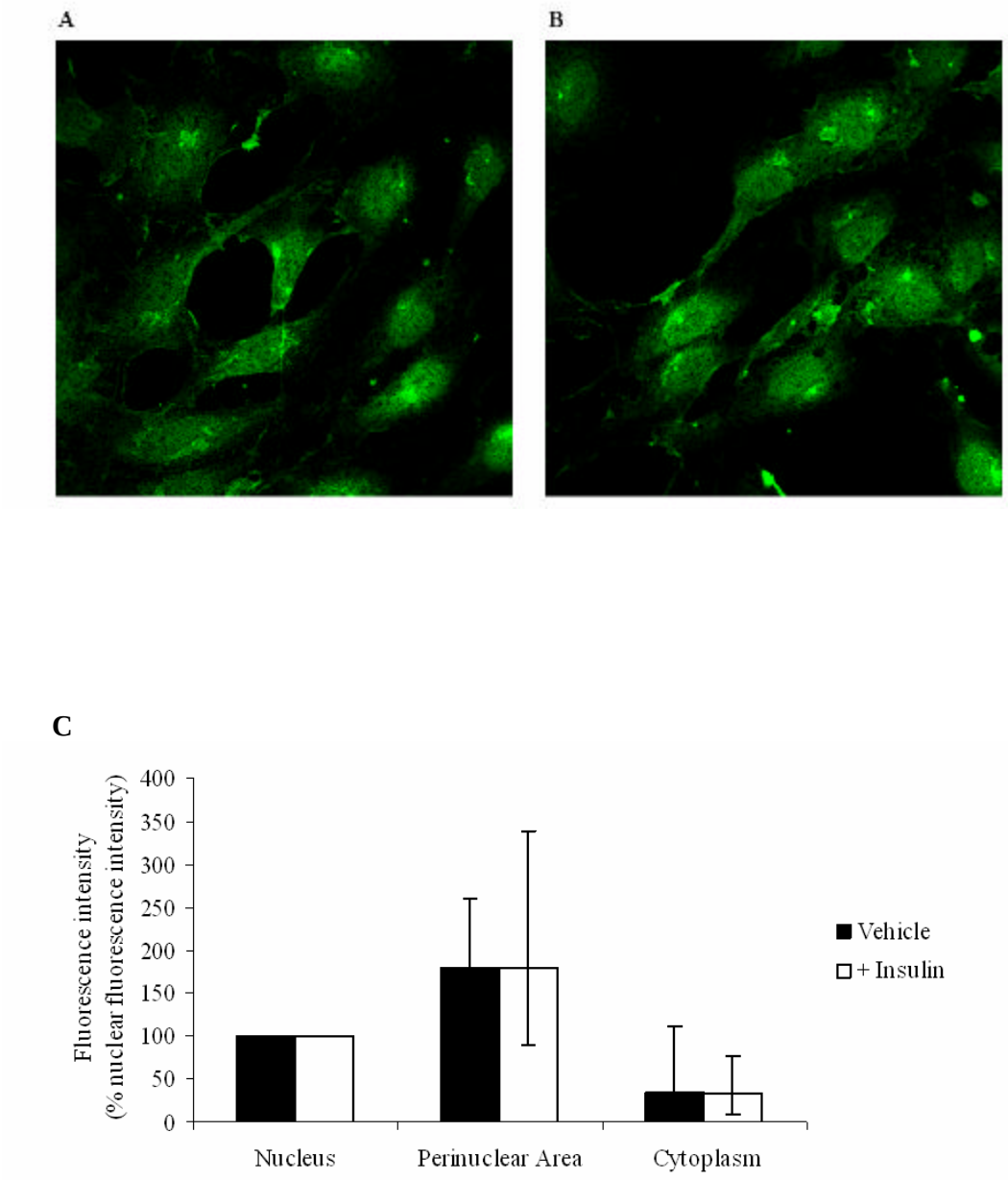

Figure 5-2 Insulin has no effect on eNOS localisation.

HAEC were stimulated with 1 µM insulin for 10 min or left untreated before fixation in 4% formaldehyde and immunolabelling with anti-eNOS antibody as described in section 2.2.13. Representative confocal images of untreated (panel A) and insulin-stimulated (panel B) HAEC are shown. To normalise against background fluorescence, separate controls were performed in absence of primary antibody and in presence of irrelevant secondary antibody. Panel C shows the quantification of fluorescence intensity in different cellular regions relative to nuclear fluorescence intensity as mean ± range. Per treatment group, 30 individual cells were analysed. For cytoplasmic measurements, three separate measurements were taken from the cytoplasm of each cell, covering areas of high, medium and low fluorescence intensity, and expressed as a ratio to nuclear fluorescence intensity before calculation of the mean.

5.2.3 Distribution of eNOS within different cellular compartments

To obtain a more detailed picture of the subcellular distribution of eNOS, iodixanol gradient centrifugation was performed to yield purified cellular organelles. Resulting fractions of the gradient were TCA-precipitated prior to Western blot analysis. Antibodies against marker proteins for different cellular organelles were used to determine which organelles were contained in individual fractions.

Fractions 1-3 contained the plasma membrane marker Na^+/K^+-ATPase and the caveolae marker caveolin-1. Fractions 4-7 contained markers for Golgi body and late endosomes, fractions 5-7 the markers for early endosomes and cytoplasm. As expected, eNOS was detected mainly in the plasma membrane fractions and in the denser fractions containing endosome, Golgi and cytoplasm markers. Probing of Western blots with phospho-specific antibodies against $eNOS^{T495}$, $eNOS^{S615}$ and $eNOS^{S1177}$ demonstrated that $eNOS^{T495}$ and $eNOS^{S615}$ localised almost exclusively to the plasma membrane, whereas $eNOS^{S1177}$ localised predominantly to plasma membrane and, to a lesser degree, early endosome-containing fractions. PKB localised to cytoplasmic and Golgi body-containing fractions, but was not found at the plasma membrane (Figure 5-3).

The distribution of marker proteins within fractions from insulin-treated cells differed slightly from that of untreated cells. However, in most cases, there was no marked difference in the subcellular distribution of eNOS species between insulin-treated and non-treated cells as judged by co-fractionation with marker proteins. Interestingly, a higher molecular weight species, recognised by the anti-$eNOS^{T495}$ and anti-eNOS antibodies, was detected in the endosomal/cytoplasmic fractions of unstimulated HAEC. Abundance of this species was lower in insulin-treated cells.

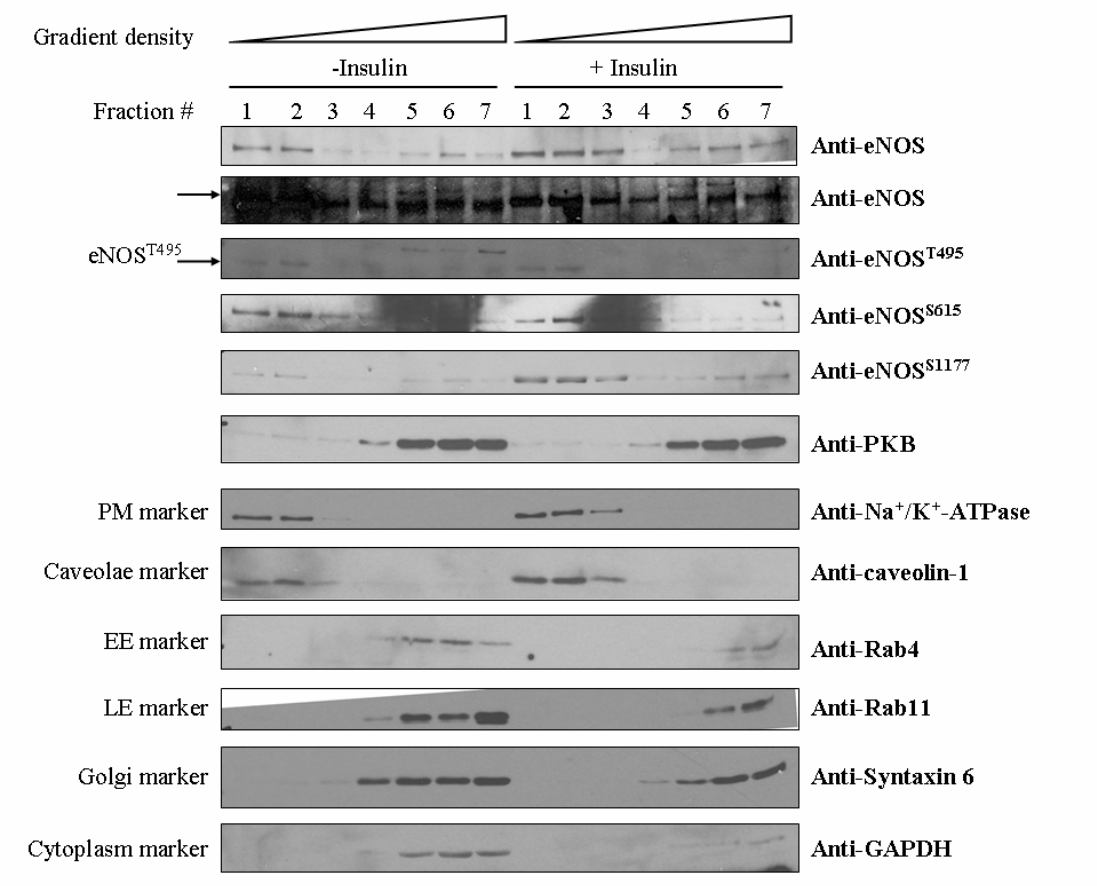

Figure 5-3 eNOS localises to different cellular compartments.

HAEC were stimulated acutely with 1 µM insulin or left untreated before preparation of cell homogenates and centrifugation on an iodixanol gradient (10-40%) (see section 2.2.4 for details). After centrifugation, 500 µl fractions were collected from the top of centrifuge tubes and TCA-precipitated prior to Western blot analysis with specific antibodies as indicated. Antibodies against markers of cellular organelles were used to determine the content of each fraction. Two different exposures of total eNOS are shown to illustrate the presence of a higher molecular weight eNOS species in fractions 4-7 of unstimulated HAEC lysates (see arrow). This species is also detectable by anti-eNOS^{T495}. Data are shown are representative blots from 2 separate experiments.
PM = plasma membrane, EE = early endosome, LE = late endosome

5.3 Discussion

In the present study, confocal microscopy analysis of eNOS-immunolabelled HAEC showed that eNOS is detectable at the plasma membrane and in the nuclei, perinuclear regions and the cytoplasm of HAEC. Proportionally, the greatest eNOS abundance was found in the perinuclear region, which most likely corresponds to the Golgi body. eNOS abundance in the cytoplasm was low (Figure 5-1). eNOS abundance at the plasma membrane was not quantified from confocal images, as the plasma membrane represents too small a proportion of the cell in a given plane of a confocal image.

Previous studies have shown that eNOS localises to the plasma membrane and perinuclear/Golgi area in foetal lamb pulmonary artery endothelial cells (Shaul *et al.*, 1996) and BAEC (Garcia-Cardena *et al.*, 1996a, Garcia-Cardena *et al.*, 1996b), but this is the first report to show that eNOS is also detectable in the nuclei of human aortic endothelial cells. In line with the present findings, cytosolic and nuclear localisation of eNOS was reported for bone marrow-derived mesenchymal stem cells (Klinz *et al.*, 2005).

A more detailed picture of the distribution of eNOS within the cell was obtained by iodixanol gradient fractionation of HAEC homogenates. As expected, eNOS was detected primarily in the plasma membrane fractions and in the denser fractions containing endosome, Golgi and cytoplasm markers, confirming microscopy data. In order to obtain improved resolution and purity of organelles and molecules, the gradient fraction size could be reduced, thus providing greater accuracy in determining localisation of different cellular components. The protocol employed for iodixanol gradient centrifugation involves pelleting of the nuclei prior to gradient centrifugation; hence, eNOS abundance in nuclei could not be quantified by this method.

To date, the distribution of different phospho-eNOS species within human vascular endothelial cells has not been fully investigated. The present study showed that eNOS^{T495} and eNOS^{S615} localised almost exclusively to the plasma membrane, whereas eNOS^{S1177} localised predominantly to the plasma membrane and, to a lesser degree, to early endosome-containing fractions (Figure 5-3). In BAEC, eNOS^{S1179} was shown to localise to caveolae and Golgi domains (Fulton *et al.*, 2002), supporting the present findings. In mesenchymal stem cells, eNOS^{S1177} was found in filamentous perinuclear structures (Klinz *et al.*, 2005). eNOS^{S1177} was also detected in the perinuclear region and, interestingly, the nucleoli of rat glioma cells (Klinz *et al.*, 2007). Together, these data suggest that eNOS^{S1177} localises to the plasma membrane and the Golgi body in several different cell types.

Furthermore, eNOS^{S114} was heavily enriched in the nucleus of mesenchymal stem cells (Klinz *et al.*, 2005).

As each eNOS phospho-species was detected only once in two separate experiments, it needs to be clarified whether these and other phospho-eNOS species are also present in other cellular compartments of human vascular endothelial cells. The above data indicate that the distribution of eNOS can vary according to its phosphorylation status. While it is thought that the phosphorylation status influences the activity and function of eNOS, the localisation of eNOS and its phospho-species may play an equally important role in regulating its activity. For example, previous experiments with eNOS-targeting mutants in BAEC have shown that eNOS-mediated NO production is more effective and more responsive to calcium-dependent agonists and the PKB activator angiopoietin when eNOS is located at the plasma membrane, rather than the Golgi body, whereas the response of both pools of eNOS to insulin was comparable (Zhang *et al.*, 2006). Therefore, it is speculative that agonists will promote the presence of active eNOS species (such as eNOS^{S1177}) at the plasma membrane.

Interestingly, a higher molecular weight species was detected with the anti-eNOS^{T495} and anti-eNOS antibodies in the endosomal/cytoplasmic fractions of unstimulated HAEC. Abundance of this species was lower in insulin-treated cells. If this higher molecular weight species is a modified form of eNOS^{T495}, this may indicate that i) acute stimulation with insulin likely reduces the amount of eNOS^{T495} and/or the higher molecular weight species in the cell and ii) eNOS^{T495} may be labelled for degradation, for example by ubiquitin-conjugation, and trafficked in endosomes. This lends support to the idea that trafficking and cellular localisation of eNOS and its phospho-species may influence its activity.

Other than eNOS^{T495}, acute treatment with insulin did not modify the distribution of eNOS or phospho-eNOS species, as determined by confocal microscopy and subcellular fractionation. In a previous study, stimulation of BAEC with the eNOS-agonist vascular endothelial growth factor (VEGF) was found not to affect eNOS^{S1179} localisation (Fulton *et al.*, 2002). As the present subcellular fractionation data were derived from a single experiment, these studies need to be repeated in order to clarify the distribution of eNOS and its phospho-species within different cellular compartments. It would be interesting to map the trafficking of eNOS and its phospho-species within endothelial cells, and to investigate their fate following stimulation with insulin and other agonists.

Co-localisation of eNOS with caveolin-1, a marker of caveolae in the plasma membrane, was demonstrated in the present study. Interaction between eNOS and caveolin-1 has previously been reported in bovine aortic endothelial cells (Feron *et al.*, 1996, Garcia-Cardena *et al.*, 1996a, Garcia-Cardena *et al.*, 1997, Feron *et al.*, 1998, Ghosh *et al.*, 1998). Tyrosine phosphorylation of eNOS has been suggested to influence its activity, trafficking and localisation, as well as its interaction with caveolin-1 in bovine aortic endothelial cells (Garcia-Cardena *et al.*, 1996a). Interaction with caveolin-1 is thought to inactivate eNOS, blocking NO synthesis (Garcia-Cardena *et al.*, 1997). Disruption of this association by binding of Ca^{2+}-calmodulin to eNOS is postulated to lead to eNOS activation (Michel *et al.*, 1997, Feron *et al.*, 1998, Ghosh *et al.*, 1998). Furthermore, Ca^{2+}-mobilising agonists regulate the cycle of dissociation and re-association between eNOS and caveolin, which is thought to influence NO-dependent signalling in the vascular wall (Feron *et al.*, 1998). Thus, the localisation of eNOS and its molecular interactions play important roles in regulating eNOS activity.

Other studies also support the idea that the localisation of a molecule within the cell has crucial implications for its activity and downstream effects. In pancreatic beta-cells, the effect of insulin signalling through its two receptor isoforms is thought to be determined by specific localisation of the receptor subtypes within the plasma membrane (Uhles *et al.*, 2003). Importantly, in 3T3L1 adipocytes, the insulin receptor colocalises and directly interacts with caveolin (Kimura *et al.*, 2002). If this association of the insulin receptor and caveolin also occurs in vascular endothelial cells, this would bring the receptor close to its downstream targets such as eNOS. Rapid recruitment of downstream signalling molecules and enzymes is vital for effective signal transduction and appropriate cellular response to a stimulus.

In the present study, the eNOS-activating kinase PKB localised to cytoplasmic and Golgi body-containing fractions, but was not found at the plasma membrane, suggesting that it was not associated with eNOS at the plasma membrane. Previous studies have shown that eNOS forms a complex with PKB and the molecular chaperone hsp90 (Garcia-Cardena *et al.*, 1998, Fontana *et al.*, 2002, Takahashi & Mendelsohn, 2003), enabling rapid activation of eNOS. However, the precise location of this complex has not been determined, and thus needs to be investigated further. It has also been suggested that association of eNOS with different polymerisation states of actin modulates eNOS activity in porcine pulmonary artery endothelial cells (Su *et al.*, 2003). To clarify interactions between eNOS and other

cellular molecules, including cytoskeletal components, co-immunoprecipitation experiments and co-labelling confocal microscopy could be used.

The cellular localisation and association of eNOS with its interaction partners represents a sophisticated mechanism for regulation of eNOS activity. More extensive investigations of the effect of insulin and other agonists on the localisation and association of eNOS and its interaction partners are necessary to clarify the precise nature of these regulatory mechanisms.

6 The Inhibitory Role of AMPK in Proinflammatory Activation of Human Vascular Endothelial Cells

6.1 Introduction

6.1.1 Background

It has been suggested that patients with diabetes are in a state of chronic low level inflammation (Fernandez-Real & Ricart, 2003, Wellen & Hotamisligil, 2005), which promotes atherogenesis. In this study, low-level inflammation was mimicked by treatment of HAEC with TNFa. During atherogenesis, monocytes attach to vascular endothelial cells and eventually migrate through the endothelium in a process called transendothelial migration (transmigration) or diapedesis. This process involves the expression of chemokines, which attract leukocytes/monocytes to the vascular endothelium.

The AMP-dependent protein kinase (AMPK) is an energy-sensor which regulates energy metabolism. It is a target for the hypoglycaemic drug metformin, which is thought to lower blood glucose levels by inhibiting gluconeogenesis (Zhou *et al.*, 2001, Shaw *et al.*, 2005). Importantly, in the context of the present study, AMPK can activate eNOS by phosphorylating Ser1177, thus increasing NO production in bovine and human aortic endothelial cells (Chen *et al.*, 1999, Morrow *et al.*, 2003). Given the potential antiatherogenic properties of NO (Li *et al.*, 2002, Dickhout *et al.*, 2005, Rask-Madsen & King, 2005, Tesauro *et al.*, 2005, Rask-Madsen & King, 2007), this evidence suggests that AMPK is involved not only in glucose homeostasis, but also promotes an antiatherogenic phenotype by increasing NO synthesis, which is likely to increase vasodilation and reduce the potential of leukocyte-endothelium interactions.

Previous work carried out by Dr Marie-Ann Ewart in the laboratory has demonstrated that AMPK attenuates the TNFa-induced expression of cell surface adhesion molecules in human aortic endothelial cells after 4h of stimulation with the AMPK agonist AICAR, but this effect was not observed after short-term (45 min) stimulation of AMPK (see Figure 6-1). Furthermore, monocyte adhesion to HAEC was downregulated by acute (45 min) stimulation of AMPK activity in a nitric oxide-dependent fashion. Prolonged (4h) stimulation of AMPK activity was more effective at decreasing monocyte adhesion, but this effect was not NO-dependent (see Figure 6-2) (unpublished observations).

Since these phenomena could not be explained by the effect of AMPK on adhesion molecule expression, it was decided to investigate endothelial chemokine production, which is a key event in attracting monocytes to the vascular endothelium. It was speculated

that acutely, AMPK activity negatively regulates chemokine production, while longer-term AMPK activity downregulates adhesion molecule expression in vascular endothelial cells.

In addition, the impact of AMPK activity and NO bioavailability on monocyte migration was investigated, since work by other groups has suggested that AMPK activity can reduce migration of monocytic and hepatic stellar cells (Kanellis *et al.*, 2006, Caligiuri *et al.*, 2008).

6.1.2 Aims of the chapter

The aim of this chapter was to look at the potential antiatherogenic properties of AMPK activity and NO bioavailability. Specifically, the effect of short-term and prolonged AMPK activity on NO-mediated regulation of chemokine production in human aortic endothelial cells was investigated. Furthermore, the effect of AMPK activity and NO bioavailability on monocyte migration was assessed.

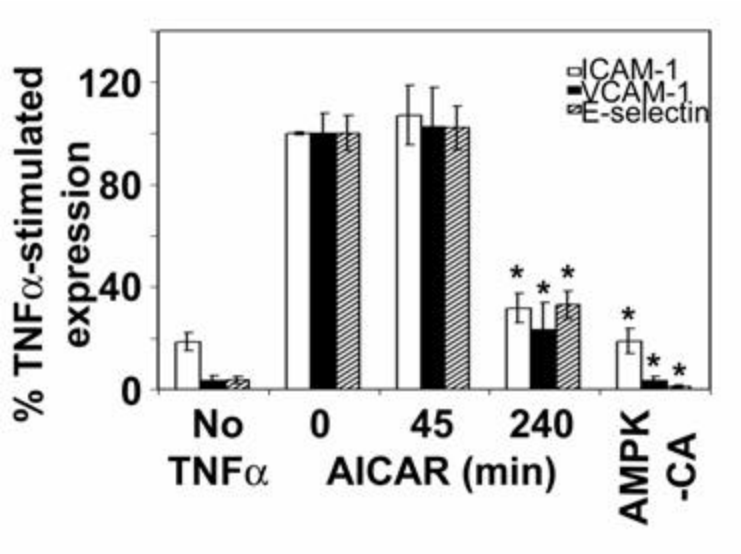

Figure 6-1 Prolonged but not rapid AMPK activation inhibits TNFa-stimulated cell surface expression of adhesion molecules.

HAEC were infected with adenovirus encoding constitutively active AMPK (AMPK-CA) for 24h prior to incubation in the presence or absence of TNFa (10 ng/ml, 6h) and in the presence or absence of 2 mM AICAR for the final 45 or 240 min. Cell surface expression of ICAM-1, VCAM-1 and E-selectin was assessed by flow cytometry. The results shown are from six independent experiments performed in triplicate. *p<0.01 relative to TNFa-stimulated value in absence of AICAR or AMPK-CA
This work was carried out by Dr Marie-Ann Ewart in the laboratory.

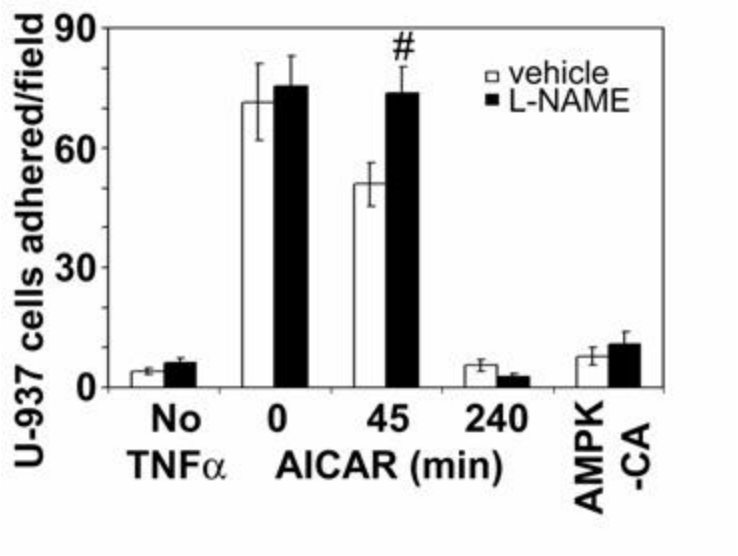

Figure 6-2 The effects of rapid, but not prolonged stimulation of AMPK on U937 cell adhesion are sensitive to L-NAME.

HAEC were infected with control adenoviruses or AMPK-CA-encoding virus 24h prior to incubation in the presence or absence of TNFa (10 ng/ml, 6h) after preincubation (30 min) in the presence or absence of 1 mM L-NAME. For the final 45 or 240 min subsets of cells were also incubated with 2 mM AICAR. The results of seven independent U-937 cell adhesion assays are shown. # p<0.05 relative to value in the absence of L-NAME
This work was carried out by Dr Marie-Ann Ewart in the laboratory.

6.2 Results

6.2.1 Experimental conditions

A literature search was performed to determine which chemokines were produced by vascular endothelial cells. The range of chemokines secreted by vascular endothelial cells included MCP-1, -2 and -3, MIP-1a and -1ß, MIG, Eotaxin, RANTES, GRO and IP-10. Therefore, secretion of each of these proteins from stimulated HAEC was assessed using an antibody-based chemokine assay.

HAEC were first stimulated with the AMPK activator, AICAR, for 45 min or 4h with or without co-incubation with 10 ng/ml TNFa for 4h and/or the eNOS inhibitor L-NAME. In a parallel set of experiments, HAEC were infected with adenovirus encoding for constitutively active AMPK (AMPK-CA), dominant-negative AMPK (AMPK-DN), or an empty expression cassette. HAEC were then treated with AICAR and/or TNFa and/or the eNOS inhibitor L-NAME (see section 2.2.11 for a detailed description). In each case, the cell culture medium was aspirated at the end of the treatment period, and replaced with fresh, serum-free RPMI (SF-RPMI) after thorough washing, to obtain conditioned medium containing secreted chemokines. It should be noted that under these conditions, both TNFa and AICAR had been washed away prior to collection of conditioned medium. This conditioned medium was used for chemokine analysis (section 6.2.2) and monocyte migration assays (section 0).

6.2.2 Chemokine production by HAEC

Previous work in the laboratory has shown that monocyte adhesion to HAEC is decreased by acute (45min) AMPK activation, but this was not dependent on cell surface adhesion molecule expression (see Figure 6-1and Figure 6-2). Therefore, it was speculated that AMPK acutely regulates the secretion of endothelial cell chemokines, thereby influencing the attraction of monocytes to endothelial cells. Hence, production of the chemokines MCP-1, -2 and -3, MIP-1a and -1ß, MIG, Eotaxin, RANTES, GRO and IP-10 by HAEC was assessed using a Human Chemokine Multiplex Bead Immunoassay and a Luminex 100^{TM}-based detection system (see section 2.2.12 for details).

Analysis of chemokine secretion showed that treated and untreated HAEC secrete measurable levels of MCP-1, MCP-2, Eotaxin, RANTES and IP-10; however, only MCP-1 secretion was stimulated by TNFa; hence, only MCP-1 data are illustrated in Figure 6-3. Secretion levels of MCP-3, MIP-1a and -1ß, MIG, and GRO were below the detection limits of the assay.

As expected, treatment of HAEC with TNFa for 4h strongly induced production of MCP-1 to 47.7±5.3-fold above basal ($p < 0.001$; Figure 6-3). Treatment with AICAR alone for 45 minutes or 4h had no effect on chemokine production. Prolonged stimulation of AMPK activity by AICAR (4h) significantly reduced TNFa-induced MCP-1 secretion, both in the absence (2.0±0.3-fold, $p<0.005$) and presence of L-NAME (1.8±0.2, $p<0.05$; paired t-tests).

Incubation of TNFa-treated cells with AICAR for 45 minutes also reduced TNFa-induced MCP-1 secretion in the absence of L-NAME (1.9±0.5-fold, $p = 0.0653$; paired t-test), but not in the presence of L-NAME. For all treatments, addition of L-NAME slightly increased the secretion of MCP-1, resulting in a 2.6±1.5-fold increase in chemokine production under control conditions ($p = 0.393$).

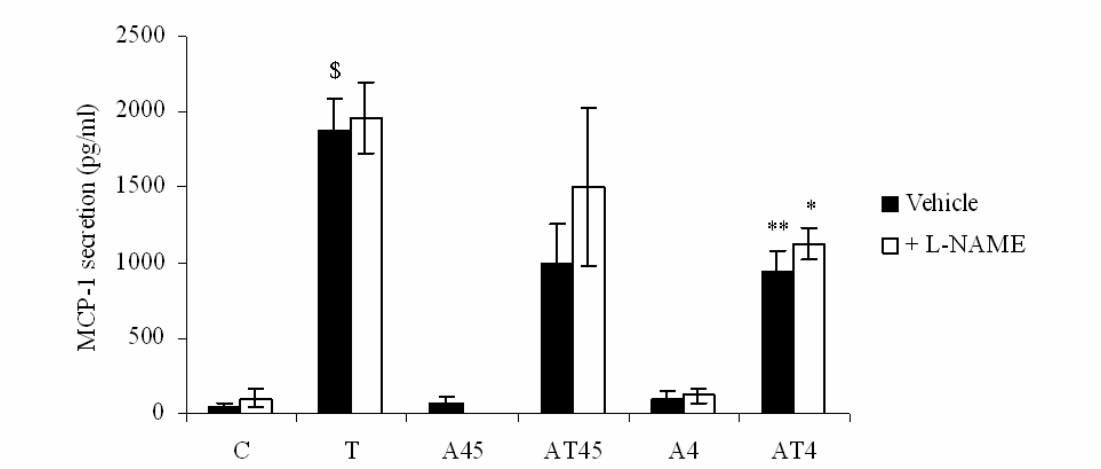

Figure 6-3 MCP-1 production in HAEC is downregulated by AMPK activity.

Chemokine production by HAEC was assessed using antibody-based technology. HAEC were treated with 2 mM AICAR for 45 min (A45) or 4h (A4) in the presence (AT45; AT4) and absence of 10 ng/ml TNFa (T, 4h) and/or 200 µM L-NAME (4h) as indicated. Thereafter, cells were washed thoroughly and incubated with fresh SF-RPMI for 1h at 37°C. This conditioned medium was collected and used for chemokine analysis using BioSource^{TM} technology. The graph shows MCP-1 secretion data from 5 (vehicle) or 4 (+ L-NAME) independent experiments as mean ± SEM. TNFa strongly induced MCP-1 secretion ($p<0.001, paired t-test). Treatment with AICAR for 4h significantly reduced TNFa-induced MCP-1 secretion (**p<0.005 for AT4 compared to T without L-NAME; *p<0.05 for AT4 compared to T with L-NAME; paired t-tests). C = untreated control

6.3 Discussion

In the present study, HAEC were found to secrete low levels of the chemokines MCP-1, MCP-2, Eotaxin, RANTES and IP-10. Basal MCP-1 secretion was about 5 times higher compared to all other chemokines measured. TNFa markedly stimulated the secretion of MCP-1 only; hence, only MCP-1 data are included in this thesis. In line with the hypothesis, treatment with AICAR for 4h or 45 minutes slightly reduced TNFa-induced secretion of MCP-1; this was statistically significant for 4h of AICAR treatment (see Figure 6-3).

As predicted by the hypothesis, inhibition of NO synthesis through L-NAME increased TNFa-stimulated secretion of MCP-1 under all conditions (Figure 6-3), indicating that negative regulation of MCP-1 production in HAEC is (partially) NO-dependent or at least enhanced by NO bioavailability. These data suggest that decreased NO bioavailability promotes a proatherogenic endothelial profile. The present findings are corroborated by clinical evidence which suggests that patients with hyperinsulinaemia and diabetes, which have decreased NO bioavailability, show an increased risk for atherosclerosis (Li *et al.*, 2002, Dickhout *et al.*, 2005, Rask-Madsen & King, 2005, Tesauro *et al.*, 2005, Rask-Madsen & King, 2007).

The present data suggest that the attenuating effect of AMPK activity on TNFa-stimulated MCP-1 production was NO-dependent in the short-term, but not during prolonged AMPK activation (Figure 6-3). Acute (45 min) stimulation of AMPK reduced TNFa-stimulated MCP-1 secretion in the absence, but not in the presence of L-NAME (results not statistically significant due to spread of data points). Prolonged AMPK stimulation (4h) significantly decreased TNFa-stimulated MCP-1 secretion in HAEC independently of NO synthesis. These findings suggest that acutely, AMPK stimulates eNOS-mediated NO production, whereas prolonged AMPK activity reduces chemokine secretion via (an) eNOS- and NO-independent pathway(s). The precise nature of this/these pathway(s) remains to be investigated.

Furthermore, the present data indicate that AMPK-mediated downregulation of MCP-1 secretion occurs before downregulation of cell surface adhesion molecule expression in HAEC (see Figure 6-1), but also persists over longer periods of time. These studies need to be extended to confirm the time course of events in the regulation of endothelial chemokine secretion and adhesion molecule expression. It would also be of interest to

study the effect of AMPK activity and NO bioavailability on the secretion of other chemokines which have not been measured in the present study.

Based on the higher levels of secreted MCP-1 and its monocyte chemotactic role, conditioned medium from HAEC treated with TNFa should be able to stimulate monocyte migration. This speculation will have to be validated by monocyte migration assays using conditioned medium from HAEC.

Previous studies have shown that AMPK activation through AICAR reduces chemokinesis and chemotaxis of U937 pre-monocytic cells by ~50% (Kanellis *et al.*, 2006). Work on hepatic stellar cells showed that activation of AMPK reduced proliferation, migration and MCP-1 secretion, thus reducing the activated phenotype of these cells (Caligiuri *et al.*, 2008). While these studies were carried out in different cell types, the findings correlate with the present study in that AMPK activation through AICAR reduced MCP-1 secretion, which would be expected to attenuate monocyte migration.

Overall, the present findings support an antiatherogenic role for AMPK, as AMPK activity can compensate for reduced NO bioavailability and decrease the atherogenic profile of HAEC cultured with proinflammatory stimuli. This has already been proposed by other groups who found that AMPK may have an anti-inflammatory role *in vitro* and *in vivo*. It was postulated that AMPK plays an important role in decreasing inflammation via inhibition of NF?B signalling in animal models of experimental autoimmune encephalitis (EAE) (Nath *et al.*, 2005, Prasad *et al.*, 2006). In addition, AICAR-stimulated AMPK activity prevented lipopolysaccharide-induced cytokine and iNOS expression in cultured rat astrocytes, microglia and macrophages, and in rats *in vivo*, by prevention of NF?B activation (Giri *et al.*, 2004). Further studies are required to define the molecular mechanism underlying the potential AMPK-mediated antiatherogenic effects in the present study.

7 Discussion

The vascular endothelium plays a crucial role in the maintenance of vascular health by regulating vascular tone, platelet aggregation, coagulation, fibrinolysis and monocyte adhesion, amongst others. Endothelial regulation of vascular tone occurs through the coordinated secretion of endothelial vasodilators and vasoconstrictors. The principal endothelial vasodilator is NO, which is produced by endothelial nitric oxide synthase. NO mediates vasodilation *in vivo* and *ex vivo*, and is thought to have vasoprotective properties (Gewaltig & Kojda, 2002, Hsueh & Quinones, 2003, Wheatcroft *et al.*, 2003). In several disorders, including insulin resistance, diabetes and atherosclerosis, endothelial function can be impaired, which promotes adverse cardiovascular effects such as hypertension, cardiac infarction and strokes, as well as microvascular disease. NO bioavailability has been shown to be reduced in patients with hyperinsulinaemia and diabetes (reviewed in (Rask-Madsen & King, 2007)). However, the causal relationship between impaired NO bioavailability, endothelial dysfunction and disease is still under debate.

Insulin is a vasoactive hormone that stimulates vasodilation by activating eNOS through the insulin signalling pathway (Scherrer *et al.*, 1993, Scherrer *et al.*, 1994, Zeng & Quon, 1996, Zeng *et al.*, 2000). Hyperinsulinaemia/insulin resistance is closely linked to endothelial dysfunction, which in turn is frequently associated with decreased NO bioavailability and proatherogenic processes in patients (Li *et al.*, 2002, Dickhout *et al.*, 2005, Rask-Madsen & King, 2005, Tesauro *et al.*, 2005). Current evidence suggests that hyperinsulinaemia impairs eNOS-mediated NO synthesis *in vitro* and *in vivo* (Steinberg *et al.*, 1996, Hogikyan *et al.*, 1998, O'Driscoll *et al.*, 1999, Balletshofer *et al.*, 2000, Cheetham *et al.*, 2000, Cleland *et al.*, 2000, Ding *et al.*, 2000, Arcaro *et al.*, 2002, Fulton *et al.*, 2004b, Katakam *et al.*, 2005, Pandolfi *et al.*, 2005, Potenza *et al.*, 2005). However, the contribution of hyperinsulinaemia *per se* to these disorders, and the molecular mechanisms responsible, are poorly characterised. To date, the effect of hyperinsulinaemia on insulin-stimulated endothelial NO production has not been investigated in endothelial cells or the vasculature.

In chapter 3, the present study therefore addressed how experimental hyperinsulinaemia affects eNOS-mediated NO production and the insulin signalling pathway in human aortic endothelial cells. Experimental hyperinsulinaemia (100 nM, 48h) in this study was designed to model high pathological hyperinsulinaemia in patients with insulin resistance. While insulin stimulated NO synthesis to a lesser degree than expected, this increase was statistically significant under control but not under experimental hyperinsulinaemic conditions, although overall NO production was comparable between the two treatment

groups. These findings can be explained by increased basal NO synthesis in hyperinsulinaemic cells and interexperimental variation in the insulin-sensitivity of HAEC. Ionomycin-responsive NO synthesis was blunted in hyperinsulinaemic HAEC, indicating that hyperinsulinaemia may have a negative effect on Ca^{2+}-dependent NO synthesis. At the molecular level, eNOS protein expression in hyperinsulinaemic HAEC remained unchanged. Basal and insulin-stimulated $eNOS^{S1177}$ phosphorylation compared to total eNOS tended to increase slightly over time, while $eNOS^{T495}$ phosphorylation in hyperinsulinaemic cells showed a tendency toward increased phosphorylation levels following acute stimulation with insulin.

The protein expression levels of insulin signalling pathway components and the eNOS-activating kinase AMPK were assessed. No changes were found in the expression of PKB, PI3K, PDK-1, PTEN or AMPK. PKB^{S473} phosphorylation remained insulin-sensitive under experimental hyperinsulinaemia, but the fold-stimulation elicited by insulin was decreased by 50% in hyperinsulinaemic cells after 48h (data not statistically significant). Stimulated $AMPK^{T172}$ phosphorylation was decreased and basal phosphorylation was increased after 48h of experimental hyperinsulinaemia (data not statistically significant).

Interestingly, acute treatment with insulin markedly increased the phosphorylation of $AMPK^{T172}$, which is a novel and somewhat unexpected finding, given AMPK's role in shutting down energy-consuming pathways. Under physiological conditions, insulin is released when glucose levels are high and therefore, energy is readily available. Activation of AMPK by phosphorylation would therefore make little sense in the context of energy conservation. However, in the context of vasodilation, the metabolic insulin signalling pathway and AMPK both act on eNOS to increase NO production, and it would therefore make perfect sense for these two components to act in synergy to promote increased vasodilation and blood flow in response to nutrient intake. Increased blood flow would result in glucose uptake into peripheral target tissues and thus, overall energy conservation. Insulin may therefore selectively upregulate the eNOS-activating kinase activity of AMPK, without affecting other AMPK-mediated events. Further investigation of this theory would be an interesting endeavour.

Since insulin-stimulated $eNOS^{S1177}$ and PKB^{S473} phosphorylation and NO production were not significantly impaired in hyperinsulinaemic HAEC, this suggests that the insulin signalling pathway is functional after 48h of experimental hyperinsulinaemia. In conjunction with the present AMPK data, this also indicates that insulin-stimulated NO

production is mediated via the PI3K-PKB pathway, rather than the AMPK pathway, which was slightly impaired after 48h of experimental hyperinsulinaemia , but did not show a negative effect on NO synthesis. Basal $eNOS^{S1177}$ phosphorylation may be increased by enhanced AMPK activity. These hypotheses need to be confirmed using kinase inhibitors and kinase activity assays to study the impact of individual pathway components (in particular, PI3K, PKB and AMPK) and their activity levels on eNOS-mediated NO production.

The present study also briefly investigated whether experimental hyperinsulinaemia differentially affected the metabolic and mitogenic branches of the insulin signalling pathway. Quantification of p44/42 MAPK levels indicated that MAPK levels were unchanged under experimental hyperinsulinaemia.

While these data require further confirmation, it is becoming clear that experimental hyperinsulinaemia in HAEC has distinct effects on different components of signalling pathways. Experimental hyperinsulinaemia for 48h had no marked effects on endothelial NO production in the present study. The present results stand in contrast to several studies using different types of tissues, which reported that NO production was impaired in hyperinsulinaemic states (Steinberg *et al.*, 1996, Balletshofer *et al.*, 2000, Cleland *et al.*, 2000). Therefore, the impact of the present results on endothelial function has to be clarified. In addition, extended periods of experimental hyperinsulinaemia along with investigation of other areas of endothelial function, such as angiogenesis, may yield valuable clues to the biological impact of hyperinsulinaemia. The small changes observed in HAEC under experimental hyperinsulinaemia are illustrated in Figure 7-1.

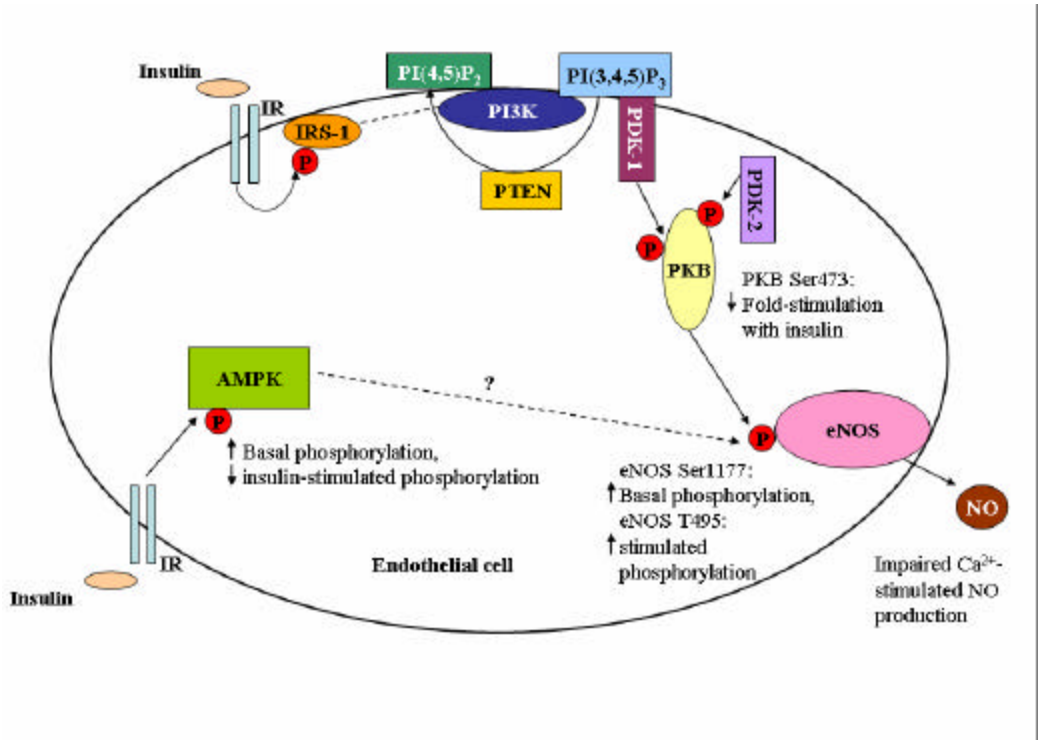

Figure 7-1 The effects of experimental hyperinsulinaemia in HAEC

Schematic diagram summarising the changes observed under experimental hyperinsulinaemia in HAEC. Note that none of the indicated changes were statistically significant.

Hyperinsulinaemia is a disease state that precedes hyperglycaemia and overt diabetes. Endothelial dysfunction and impairment of the underlying molecular mechanisms is likely to progress over time, and may therefore be exacerbated in hyperglycaemia. As with hyperinsulinaemia, endothelial function and NO bioavailability can be impaired by hyperglycaemia (Calver *et al.*, 1992, McVeigh *et al.*, 1992, Hogikyan *et al.*, 1998, De Vriese *et al.*, 2000, Rask-Madsen & King, 2007). *In vitro* and *in vivo* evidence suggests that hyperglycaemia dysregulates insulin signalling (Sobrevia *et al.*, 1998, Federici *et al.*, 2002, Salt *et al.*, 2003) and NO-mediated vasodilation (Tesfamariam *et al.*, 1990) and increases production of reactive oxygen species (Cosentino *et al.*, 1997, De Vriese *et al.*, 2000, Hink *et al.*, 2001, Srinivasan *et al.*, 2004). Previous studies on the effect of hyperglycaemia on eNOS phosphorylation have yieldedconflicting results, and the underlying mechanisms regulating eNOS phosphorylation are poorly characterised. In addition, the role of the individual eNOS phosphorylation sites is not clear.

Therefore, chapter 4 presents work on the effect of experimental hyperglycaemia on the regulation of eNOS phosphorylation and superoxide production in human umbilical vein endothelial cells. Furthermore, the effect of acute insulin treatment on eNOS phosphorylation at Ser114, Thr495, Ser615, Ser633 and Ser1177 was investigated in HUVEC. Acute insulin moderately stimulated the phosphorylation of $eNOS^{S615}$ and $eNOS^{S1177}$, and decreased the phosphorylation of $eNOS^{S114}$, $eNOS^{T495}$ and $eNOS^{S633}$ (data not statistically significant). Given insulin's role as an activator of eNOS-mediated NO synthesis, these results suggest that Ser114, Thr495 and Ser633 are inhibitory sites, while Ser615 and Ser1177 are activating sites of eNOS in insulin-stimulated HUVEC.

The nature of the stimulus and the tissue type studied may affect the interpretation of the roles of eNOS phosphorylation sites. The present findings are in agreement with previously published data on Thr495, Ser615 and Ser1177 (Chen *et al.*, 1999, Fleming *et al.*, 2001, Michell *et al.*, 2001, Montagnani *et al.*, 2001, Greif *et al.*, 2002, Michell *et al.*, 2002, Fleming & Busse, 2003, Matsubara *et al.*, 2003, Salt *et al.*, 2003, Ritchie *et al.*, 2007). The role of Ser114 is less clear, but it is dephosphorylated in response to the eNOS stimulator VEGF (Kou *et al.*, 2002). Ser633 has been shown to increase eNOS activity and was proposed to maintain prolonged activity of eNOS (Boo *et al.*, 2002, Michell *et al.*, 2002, Bauer *et al.*, 2003), which stands in contrast to the present findings. Further studies are needed to clarify the individual contributions of eNOS phosphorylation sites to eNOS activity and the effect of various stimuli on eNOS phosphorylation in a variety of vascular tissues.

To date the effect of hyperglycaemia on eNOS expression and phosphorylation is debated. In the present study, total eNOS expression was unaffected by experimental hyperglycaemia (25 mM, 48h). Basal phosphorylation of $eNOS^{S633}$ was reduced (non-significantly) and insulin-stimulated phosphorylation of $eNOS^{S114}$ was significantly reduced, whereas basal $eNOS^{S615}$ phosphorylation was increased (non-significantly) compared to control cells cultured with 4 mM glucose. Based on the roles of eNOS phosphorylation sites proposed above, these data indicate that experimental hyperglycaemia may promote eNOS activity. However, given the lack of effect on Ser 1177 and Thr495, it is unlikely that NO production would be enhanced under these conditions. More likely, these changes in phosphorylation modify the interaction of eNOS with other molecules such as PKB and hsp90 and the subcellular localisation of eNOS. Figure 7-2 summarises the present findings on eNOS phosphorylation.

The present study also addressed which regulatory pathways may be involved in mediating altered eNOS phosphorylation under experimental hyperglycaemia in HUVEC. Published evidence on eNOS regulatory pathways is controversial. The present findings showed that the metabolic insulin signalling pathway is not impaired by experimental hyperglycaemia in HUVEC. Preliminary experiments in the present study suggest that the stress-activated JNK pathway and the NF?B pathway were mildly (non-significantly) impaired by experimental hyperglycaemia, while the CAP-Cbl pathway was unaffected. The NF?B and JNK pathways have been implicated in promoting a proatherogenic profile through their involvement in adhesion molecule expression (Gilmore, 2006). Based on the limited effect on the NF?B and JNK pathways, the present study gives insufficient evidence to support a proatherogenic role for experimental hyperglycaemia in HUVEC. The molecular cause for altered eNOS phosphorylation will have to be further assessed, and the biological significance investigated.

Interestingly, the present data also demonstrated that high mannitol (20 mM + 5 mM glucose) in HUVEC affects the phosphorylation of $eNOS^{S633}$, $eNOS^{S1177}$, PKB^{S473} and $I?Ba^{S32}$ and the expression of IKKß when compared to cells cultured with 4 mM glucose alone. This effect has not been previously reported, and suggests that the use of equimolar mannitol as an osmotic control for hyperglycaemia is questionable. This should be kept in mind when interpreting data from studies using high mannitol as a control. Further investigations are needed to identify the mechanism(s) by which mannitol mediates its effects, and to determine whether such effects can also be seen in other cell types.

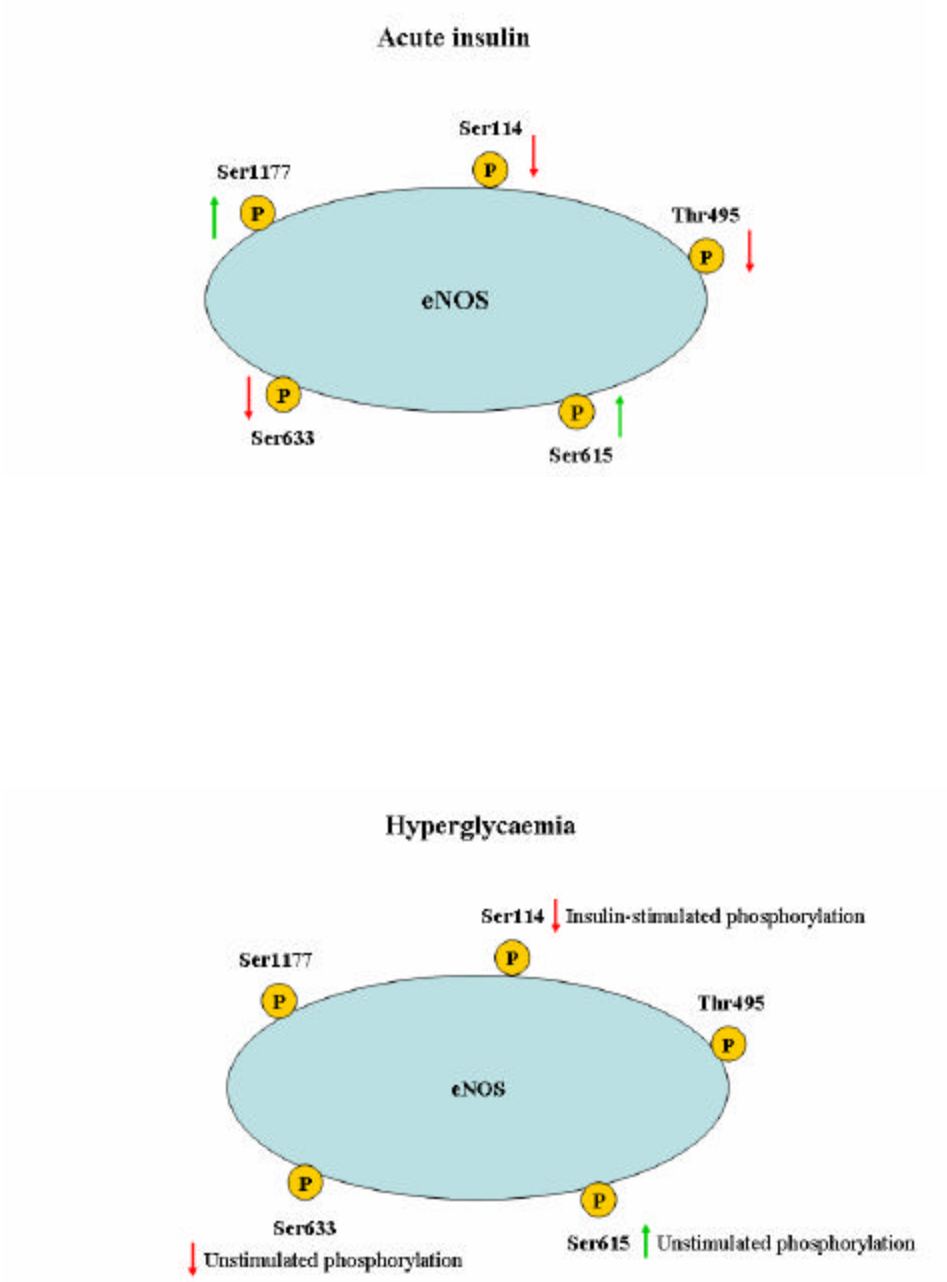

Figure 7-2 eNOS phosphorylation in HUVEC

The diagram summarises the changes in eNOS phosphorylation in HUVEC after acute treatment with insulin (top panel) and the changes compared to control after 48h of experimental hyperglycaemia (bottom panel). Note that only the effect on $eNOS^{S114}$ was statistically significant under experimental hyperglycaemia ($p<0.05$).

Previous results from our laboratory indicated that endothelial NO production was inhibited during experimental hyperglycaemia in HAEC (Salt *et al.*, 2003). Given the potential for eNOS-mediated ROS production, it was investigated whether experimental hyperglycaemia increased eNOS-mediated superoxide generation. In the present study, endothelial cell superoxide generation was unaffected by experimental hyperglycaemia, which contrasts previous findings (Cosentino *et al.*, 1997, De Vriese *et al.*, 2000, Hink *et al.*, 2001, Srinivasan *et al.*, 2004). As the present results are preliminary, these studies will have to be repeated. In the light of the above findings, the effect of hyperglycaemia on superoxide production in vascular endothelial cells ought to be compared to untreated control cells and osmotic controls to determine whether mannitol influences superoxide generation, perhaps through increased osmotic stress.

Chapter 5 addressed the question of how acute insulin stimulation affects the subcellular distribution of eNOS in HAEC. eNOS has been demonstrated to localise to the plasma membrane, caveolae, the Golgi body and nucleoli in various cell types (Garcia-Cardena *et al.*, 1996a, Garcia-Cardena *et al.*, 1996b, Shaul *et al.*, 1996, Klinz *et al.*, 2005), but the localisation of endogenous eNOS has not been characterised in human vascular endothelial cells. Since the localisation of eNOS within the cell is thought to have implications for its activity and function (Fulton *et al.*, 2004b), insulin may modify the subcellular distribution of eNOS. The subcellular distribution of $eNOS^{T495}$, $eNOS^{S615}$ and $eNOS^{S1177}$ was also investigated in the present study.

Confocal microscopy data shown in chapter 5 demonstrated that eNOS localised to the plasma membrane, the nucleus and perinuclear region and the cytoplasm. The greatest abundance of eNOS was found in the perinuclear region. At the plasma membrane, eNOS colocalised with caveolin-1, a marker of caveolae, confirming the previously reported interaction between eNOS and caveolin-1 (Feron *et al.*, 1996, Garcia-Cardena *et al.*, 1996a, Garcia-Cardena *et al.*, 1997, Feron *et al.*, 1998, Ghosh *et al.*, 1998). In agreement with these microscopy data, iodixanol gradient fractionation studies showed that eNOS was located principally in the plasma membrane fractions and in the denser fractions containing endosome, Golgi and cytoplasm markers. $eNOS^{T495}$ and $eNOS^{S615}$ localised almost exclusively to the plasma membrane, whereas $eNOS^{S1177}$ localised predominantly to the plasma membrane and, to a lesser degree, to early endosome-containing fractions of HAEC. These data are in agreement with previous findings by other groups (Fulton *et al.*, 2002, Klinz *et al.*, 2005, Klinz *et al.*, 2007).

Acute (10 min) insulin stimulation did not affect the distribution of eNOS, eNOS^{S615} or eNOS^{S1177}, but reduced the levels of a higher molecular weight species detected with anti-eNOS^{T495} and anti-eNOS antibodies. Given its detection in endosomal marker-containing fractions, this species may represent an ubiquitinated form of eNOS^{T495} destined for degradation. Its levels may be reduced by insulin-stimulated reduction of eNOS^{T495} phosphorylation. This lends support to the theory that extracellular agonists can modulate the distribution of molecules within the cell to coordinate their localisation with their effectors and targets, thus maximising their effectiveness. The relationship between eNOS subcellular localisation and function will have to be investigated further in human vascular endothelial cells.

The proposed antiatherogenic properties of NO bioavailability were investigated in chapter 6 by assessing the potential of AMPK- and NO mediated inhibition of chemokine production in HAEC. AMPK can directly phosphorylate eNOS^{S1177} and thus stimulate NO synthesis in HAEC (Morrow *et al.*, 2003). While AMPK is thought to be involved principally in the regulation of energy homeostasis, it may also promote an antiatherogenic phenotype by increasing NO synthesis, which is likely to increase vasodilation and reduce the potential of leukocyte-endothelium interactions. Previous work in our laboratory has indicated that prolonged, but not short-term activation of AMPK attenuates TNFα-induced expression of cell surface adhesion molecules in HAEC. However, short-term activation of AMPK reduced monocyte adhesion to HAEC in a NO-dependent fashion, whereas this same effect was enhanced by prolonged activation of AMPK in a NO-independent manner (unpublished observations). Therefore, it was speculated that early AMPK-mediated inhibition of monocyte adhesion was mediated through negative regulation of chemokine production.

In the present study, HAEC were found to secrete low concentrations of MCP-2, Eotaxin, RANTES and IP-10, and higher concentrations of MCP-1. In line with the hypothesis, treatment with AICAR for 4h or 45 minutes slightly reduced TNFα-induced secretion of MCP-1. As predicted, inhibition of NO synthesis through the eNOS inhibitor L-NAME increased TNFα-stimulated secretion of MCP-1. Decreased NO bioavailability therefore promotes a proatherogenic endothelial profile in HAEC. These data are in agreement with clinical data that decreased NO bioavailability in patients with hyperinsulinaemia and diabetes have an increased risk for atherosclerosis (Li *et al.*, 2002, Dickhout *et al.*, 2005, Rask-Madsen & King, 2005, Tesauro *et al.*, 2005, Rask-Madsen & King, 2007).

Furthermore, the present data suggest that the attenuating effect of AMPK activity on TNFa-stimulated MCP-1 production was at least partly NO-dependent in the short-term, but may be NO-independent during prolonged AMPK activation. It is therefore tentative to speculate that acutely, AMPK stimulates eNOS-mediated NO production, whereas prolonged AMPK activity reduces chemokine secretion in an eNOS- and NO-independent way. In addition, the present data indicate that negative regulation of HAEC chemokine production by AMPK occurs before downregulation of adhesion molecule expression, and this may contribute to the previously observed AMPK-mediated inhibition of monocyte adhesion. These findings, summarised in Figure 7-3, support an antiatherogenic role for AMPK, as AMPK activity can compensate for reduced NO bioavailability and decrease the atherogenic profile of HAEC cultured with proinflammatory stimuli. This is in agreement with results presented in chapter 3, which showed that insulin stimulates $AMPK^{T172}$ phosphorylation and may thus promote an antiatherogenic phenotype in HAEC. Further studies are required to define the antiatherogenic potential of AMPK activity and its impact on endothelial function *in vivo*.

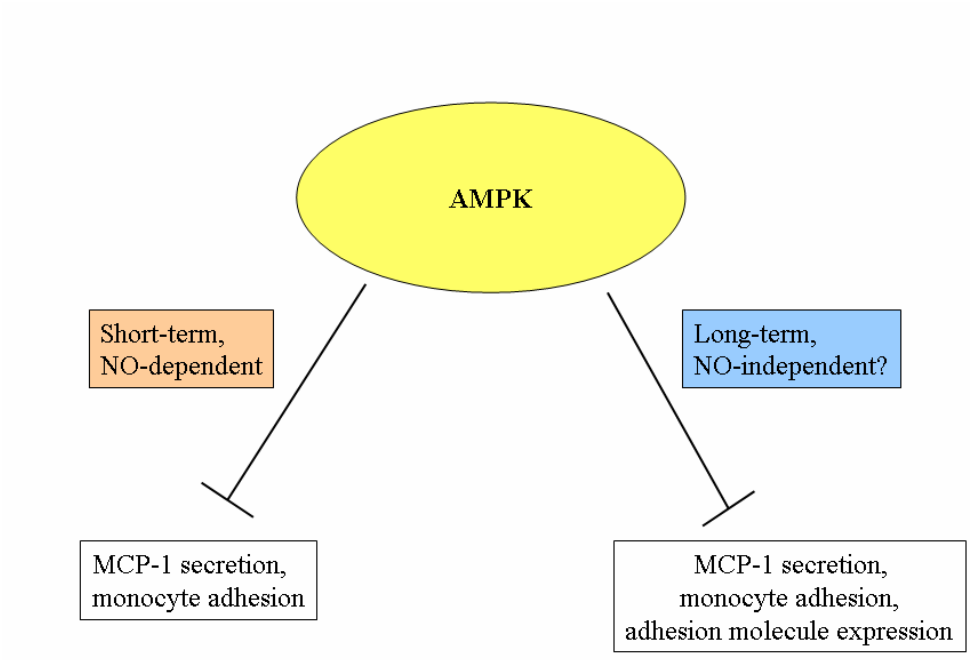

Figure 7-3 The antiatherogenic actions of AMPK

The diagram summarises present and previous findings from our laboratory regarding the antiatherogenic effects of AMPK activity and NO bioavailability.

7.1 Conclusions

The vascular endothelium is a key player in the maintenance of vascular tone and the prevention of atherosclerosis. Endothelial dysfunction is characteristic of disorders involving hyperinsulinaemia and/or hyperglycaemia. The present study demonstrated that neither experimental hyperinsulinaemia nor experimental hyperglycaemia significantly impaired the metabolic branch of the insulin signalling pathway in human vascular endothelial cells, although it provided evidence for mildly dysregulated eNOS phosphorylation under experimental hyperglycaemia in HUVEC. Other regulatory pathways were also predominantly unaltered. Superoxide production by HUVEC was not affected by experimental hyperglycaemia, but the significance of insulin-stimulated NO release by HAEC was lost during experimental hyperinsulinaemia.

eNOS was shown to localise to the plasma membrane, the nucleus, the perinuclear region and the cytoplasm of HAEC. Acute treatment with insulin did not change this distribution or that of $eNOS^{S615}$ and $eNOS^{S1177}$, but did alter the levels of a higher molecular weight species of $eNOS^{T495}$.

In HAEC, experimental hyperinsulinaemia had no effect on monocyte adhesion. AMPK and NO negatively regulated the secretion of MCP-1 in the present study, promoting an antiatherogenic profile.

In summary, this study has shown that 48h of experimental hyperinsulinaemia or experimental hyperglycaemia do not markedly alter cellular signalling pathways in human vascular endothelial cells and do not predispose to a proatherogenic cellular phenotype. By contrast, AMPK activity and NO bioavailability have been implicated in the regulation of endothelial chemokine production and mediation of an antiatherogenic profile. This study has therefore gone some way to elucidate potential molecular mechanisms underlying vascular endothelial dysfunction, but further investigations using more robustly insulin-sensitive cell models are required to gain a clearer understanding of the regulation of endothelial function in health and disease.

Bibliography

Alderton, W.K., Cooper, C.E. & Knowles, R.G. (2001). Nitric oxide synthases: structure, function and inhibition. *Biochem J* **357**, 593-615.

Alessi, D.R., Andjelkovic, M., Caudwell, B., Cron, P., Morrice, N., Cohen, P. & Hemmings, B.A. (1996). Mechanism of activation of protein kinase B by insulin and IGF-1. *Embo J* **15**, 6541-51.

Alioua, A., Tanaka, Y., Wallner, M., Hofmann, F., Ruth, P., Meera, P. & Toro, L. (1998). The large conductance, voltage-dependent, and calcium-sensitive K+ channel, Hslo, is a target of cGMP-dependent protein kinase phosphorylation in vivo. *J Biol Chem* **273**, 32950-6.

Aljada, A. & Dandona, P. (2000). Effect of insulin on human aortic endothelial nitric oxide synthase. *Metabolism: Clinical & Experimental. Vol. 49(2)(pp 147-150), 2000.*

Aljada, A., Ghanim, H., Saadeh, R. & Dandona, P. (2001). Insulin inhibits NFkappaB and MCP-1 expression in human aortic endothelial cells. *Journal of Clinical Endocrinology & Metabolism. Vol. 86(1)(pp 450-453), 2001.*

Aljada, A., Saadeh, R., Assian, E., Ghanim, H. & Dandona, P. (2000). Insulin inhibits the expression of intercellular adhesion molecule-1 by human aortic endothelial cells through stimulation of nitric oxide. *Journal of Clinical Endocrinology & Metabolism. Vol. 85(7)(pp 2572-2575), 2000.*

Ammendola, A., Geiselhoringer, A., Hofmann, F. & Schlossmann, J. (2001). Molecular determinants of the interaction between the inositol 1,4,5-trisphosphate receptor-associated cGMP kinase substrate (IRAG) and cGMP kinase Ibeta. *J Biol Chem* **276**, 24153-9.

Andrew, P.J. & Mayer, B. (1999). Enzymatic function of nitric oxide synthases. *Cardiovascular Research* **43**, 521-531.

Arcaro, G., Cretti, A., Balzano, S., Lechi, A., Muggeo, M., Bonora, E. & Bonadonna, R.C. (2002). Insulin causes endothelial dysfunction in humans: sites and mechanisms. *Circulation* **105**, 576-82.

Ardigo, D., Franzini, L., Valtuena, S., Monti, L.D., Reaven, G.M. & Zavaroni, I. (2006). Relation of Plasma Insulin Levels to Forearm Flow-Mediated Dilatation in Healthy Volunteers. *The American Journal of Cardiology* **97**, 1250.

Avruch, J., Zhang, X.F. & Kyriakis, J.M. (1994). Raf meets Ras: completing the framework of a signal transduction pathway. *Trends Biochem Sci* **19**, 279-83.

Azpiazu, I., Saltiel, A.R., Depaoli-Roach, A.A. & Lawrence, J.C. (1996). Regulation of both glycogen synthase and PHAS-I by insulin in rat skeletal muscle involves mitogen-activated protein kinase-independent and rapamycin-sensitive pathways. *J Biol Chem* **271**, 5033-9.

Baek, K.J., Thiel, B.A., Lucas, S. & Stuehr, D.J. (1993). Macrophage nitric oxide synthase subunits. Purification, characterization, and role of prosthetic groups and substrate in regulating their association into a dimeric enzyme. *J. Biol. Chem.* **268**, 21120-21129.

Bálint, Z., Krizbai, I., Wilhelm, I., Farkas, A., Párducz, Á., Szegletes, Z. & Váró, G. (2007). Changes induced by hyperosmotic mannitol in cerebral endothelial cells: an atomic force microscopic study. *European Biophysics Journal* **36**, 113.

Balletshofer, B.M., Rittig, K., Enderle, M.D., Volk, A., Maerker, E., Jacob, S., Matthaei, S., Rett, K. & Haring, H.U. (2000). Endothelial dysfunction is detectable in young normotensive first-degree relatives of subjects with type 2 diabetes in association with insulin resistance. *Circulation* **101**, 1780-4.

Barzilai, N. & Rossetti, L. (1993). Role of glucokinase and glucose-6-phosphatase in the acute and chronic regulation of hepatic glucose fluxes by insulin. *J Biol Chem* **268**, 25019-25.

Bastard, J.P., Maachi, M., Van Nhieu, J.T., Jardel, C., Bruckert, E., Grimaldi, A., Robert, J.J., Capeau, J. & Hainque, B. (2002). Adipose tissue IL-6 content correlates with resistance to insulin activation of glucose uptake both in vivo and in vitro. *J Clin Endocrinol Metab* **87**, 2084-9.

Basu, R., Schwenk, W.F. & Rizza, R.A. (2004). Both fasting glucose production and disappearance are abnormal in people with "mild" and "severe" type 2 diabetes. *Am J Physiol Endocrinol Metab* **287**, E55-62.

Bauer, P.M., Fulton, D., Boo, Y.C., Sorescu, G.P., Kemp, B.E., Jo, H. & Sessa, W.C. (2003). Compensatory Phosphorylation and Protein-Protein Interactions Revealed by Loss of Function and Gain of Function Mutants of Multiple Serine Phosphorylation Sites in Endothelial Nitric-oxide Synthase. *J. Biol. Chem.* **278**, 14841-14849.

Baumann, C.A., Ribon, V., Kanzaki, M., Thurmond, D.C., Mora, S., Shigematsu, S., Bickel, P.E., Pessin, J.E. & Saltiel, A.R. (2000). CAP defines a second signalling pathway required for insulin-stimulated glucose transport. *Nature* **407**, 202-7.

Baumann, C.A. & Saltiel, A.R. (2001). Spatial compartmentalization of signal transduction in insulin action. *Bioessays* **23**, 215-22.

Beg, Z.H., Allmann, D.W. & Gibson, D.M. (1973). Modulation of 3-hydroxy-3-methylgluta ryl coenzyme A reductase activity with cAMP and wth protein fractions of rat liver cytosol. *Biochem Biophys Res Commun* **54**, 1362-9.

Berti, L., Mosthaf, L., Kroder, G., Kellerer, M., Tippmer, S., Mushack, J., Seffer, E., Seedorf, K. & Haring, H. (1994). Glucose-induced translocation of protein kinase C isoforms in rat-1 fibroblasts is paralleled by inhibition of the insulin receptor tyrosine kinase. *J Biol Chem* **269**, 3381-6.

Bjornholm, M., He, A.R., Attersand, A., Lake, S., Liu, S.C., Lienhard, G.E., Taylor, S., Arner, P. & Zierath, J.R. (2002). Absence of functional insulin receptor substrate-3 (IRS-3) gene in humans. *Diabetologia* **45**, 1697-702.

Boger, R.H., Bode-Boger, S.M. & Frolich, J.C. (1996). The L-arginine-nitric oxide pathway: Role in atherosclerosis and therapeutic implications. *Atherosclerosis. Vol. 127(1)(pp 1-11), 1996.*

Bokemark, L., Wikstrand, J., Attvall, S., Hulthe, J., Wedel, H. & Fagerberg, B. (2001). Insulin resistance and intima-media thickness in the carotid and femoral arteries of clinically healthy 58-year-old men. The Atherosclerosis and Insulin Resistance Study (AIR). *J Intern Med* **249**, 59-67.

Bollag, G.E., Roth, R.A., Beaudoin, J., Mochly-Rosen, D. & Koshland, D.E., Jr. (1986). Protein kinase C directly phosphorylates the insulin receptor in vitro and reduces its protein-tyrosine kinase activity. *Proc Natl Acad Sci U S A* **83**, 5822-4.

Bolotina, V.M., Najibi, S., Palacino, J.J., Pagano, P.J. & Cohen, R.A. (1994). Nitric oxide directly activates calcium-dependent potassium channels in vascular smooth muscle. *Nature* **368**, 850-3.

Bondy, C.A., Zhou, J., Chin, E., Reinhardt, R.R., Ding, L. & Roth, R.A. (1994). Cellular distribution of insulin-degrading enzyme gene expression. Comparison with insulin and insulin-like growth factor receptors. *J Clin Invest* **93**, 966-73.

Boo, Y.C., Hwang, J., Sykes, M., Michell, B.J., Kemp, B.E., Lum, H. & Jo, H. (2002). Shear stress stimulates phosphorylation of eNOS at Ser(635) by a protein kinase A-dependent mechanism. *Am J Physiol Heart Circ Physiol* **283**, H1819-28.

Boo, Y.C., Sorescu, G.P., Bauer, P.M., Fulton, D., Kemp, B.E., Harrison, D.G., Sessa, W.C. & Jo, H. (2003). Endothelial NO synthase phosphorylated at SER635 produces NO without requiring intracellular calcium increase. *Free Radical Biology and Medicine* **35**, 729.

Bossenmaier, B., Mosthaf, L., Mischak, H., Ullrich, A. & Haring, H.U. (1997). Protein kinase C isoforms beta 1 and beta 2 inhibit the tyrosine kinase activity of the insulin receptor. *Diabetologia* **40**, 863-6.

Bradford, M.M. (1976). A rapid and sensitive method for the quantitation of microgram quantities of protein utilizing the principle of protein-dye binding. *Anal Biochem* **72**, 248-54.

Broillet, M.-C., Randin, O. & Chatton, J.-Y. (2001). Photoactivation and calcium sensitivity of the fluorescent NO indicator 4,5-diaminofluorescein (DAF-2): implications for cellular NO imaging. *FEBS Letters* **491**, 227.

Brown, D.A. & London, E. (1998). FUNCTIONS OF LIPID RAFTS IN BIOLOGICAL MEMBRANES. *Annual Review of Cell and Developmental Biology* **14**, 111-136.

Brown, J., Reading, S.J., Jones, S., Fitchett, C.J., Howl, J., Martin, A., Longland, C.L., Michelangeli, F., Dubrova, Y.E. & Brown, C.A. (2000). Critical evaluation of ECV304 as a human endothelial cell model defined by genetic analysis and functional responses: a comparison with the human bladder cancer derived epithelial cell line T24/83. *Lab Invest* **80**, 37-45.

Bruning, J.C., Winnay, J., Cheatham, B. & Kahn, C.R. (1997). Differential signaling by insulin receptor substrate 1 (IRS-1) and IRS-2 in IRS-1-deficient cells. *Mol Cell Biol* **17**, 1513-21.

Burgering, B.M. & Coffer, P.J. (1995). Protein kinase B (c-Akt) in phosphatidylinositol-3-OH kinase signal transduction. *Nature* **376**, 599-602.

Busconi, L. & Michel, T. (1993). Endothelial nitric oxide synthase. N-terminal myristoylation determines subcellular localization. *J. Biol. Chem.* **268**, 8410-8413.

Caligiuri, A., Bertolani, C., Guerra, C.T., Aleffi, S., Galastri, S., Trappoliere, M., Vizzutti, F., Gelmini, S., Laffi, G., Pinzani, M. & Marra, F. (2008). Adenosine monophosphate-activated protein kinase modulates the activated phenotype of hepatic stellate cells. *Hepatology* **47**, 668-676.

Calver, A., Collier, J. & Vallance, P. (1992). Inhibition and stimulation of nitric oxide synthesis in the human forearm arterial bed of patients with insulin-dependent diabetes. *J Clin Invest* **90**, 2548-54.

Cameron, N.E. & Cotter, M.A. (1992). Impaired contraction and relaxation in aorta from streptozotocin-diabetic rats: role of polyol pathway. *Diabetologia* **35**, 1011-9.

Cann, A.D. & Kohanski, R.A. (1997). Cis-autophosphorylation of juxtamembrane tyrosines in the insulin receptor kinase domain. *Biochemistry* **36**, 7681-9.

Carling, D., Zammit, V.A. & Hardie, D.G. (1987). A common bicyclic protein kinase cascade inactivates the regulatory enzymes of fatty acid and cholesterol biosynthesis. *FEBS Letters* **223**, 217.

Carlson, C.A. & Kim, K.-H. (1973). Regulation of Hepatic Acetyl Coenzyme A Carboxylase by Phosphorylation and Dephosphorylation. *J. Biol. Chem.* **248**, 378-380.

Carpentier, J.L. (1994). Insulin receptor internalization: molecular mechanisms and physiopathological implications. *Diabetologia* **37 Suppl 2**, S117-24.

Carr, M.E. (2001). Diabetes mellitus: A hypercoagulable state. *Journal of Diabetes and its Complications* **15**, 44.

Centers for Disease Control and Prevention (2003). National Diabetes Fact Sheet: National Estimates and General Information on Diabetes in the United States, 2000. Atlanta.

Charo, I.F. & Taubman, M.B. (2004). Chemokines in the Pathogenesis of Vascular Disease. *Circ Res* **95**, 858-866.

Cheetham, C., Collis, J., O'driscoll, G., Stanton, K., Taylor, R. & Green, D. (2000). Losartan, an angiotensin type 1 receptor antagonist, improves endothelial function in non-insulin-dependent diabetes. *J Am Coll Cardiol* **36**, 1461-6.

Chen, H., Montagnani, M., Funahashi, T., Shimomura, I. & Quon, M.J. (2003). Adiponectin Stimulates Production of Nitric Oxide in Vascular Endothelial Cells. *J. Biol. Chem.* **278**, 45021-45026.

Chen, Z.-P., Mitchelhill, K.I., Michell, B.J., Stapleton, D., Rodriguez-Crespo, I., Witters, L.A., Power, D.A., Ortiz De Montellano, P.R. & Kemp, B.E. (1999). AMP-

activated protein kinase phosphorylation of endothelial NO synthase. *FEBS Letters* **443**, 285.

Chiang, S.H., Baumann, C.A., Kanzaki, M., Thurmond, D.C., Watson, R.T., Neudauer, C.L., Macara, I.G., Pessin, J.E. & Saltiel, A.R. (2001). Insulin-stimulated GLUT4 translocation requires the CAP-dependent activation of TC10. *Nature* **410**, 944-8.

Chisholm, D.J., Campbell, L.V. & Kraegen, E.W. (1997). Pathogenesis of the insulin resistance syndrome (syndrome X). *Clin Exp Pharmacol Physiol* **24**, 782-4.

Chua, S.C., White, D.W., Wu-Peng, X.S., Liu, S.M., Okada, N., Kershaw, E.E., Chung, W.K., Power-Kehoe, L., Chua, M., Tartaglia, L.A. & Leibel, R.L. (1996). Phenotype of fatty due to Gln269Pro mutation in the leptin receptor (Lepr). *Diabetes* **45**, 1141-1143.

Clancy, R.M., Leszczynska-Piziak, J. & Abramson, S.B. (1992). Nitric oxide, an endothelial cell relaxation factor, inhibits neutrophil superoxide anion production via a direct action on the NADPH oxidase. *J Clin Invest* **90**, 1116-21.

Cleland, S.J., Petrie, J.R., Small, M., Elliott, H.L. & Connell, J.M.C. (2000). Insulin Action Is Associated With Endothelial Function in Hypertension and Type 2 Diabetes. *Hypertension* **35**, 507-511.

Corson, M.A., James, N.L., Latta, S.E., Nerem, R.M., Berk, B.C. & Harrison, D.G. (1996). Phosphorylation of Endothelial Nitric Oxide Synthase in Response to Fluid Shear Stress. *Circ Res* **79**, 984-991.

Cosentino, F., Hishikawa, K., Katusic, Z.S. & Luscher, T.F. (1997). High Glucose Increases Nitric Oxide Synthase Expression and Superoxide Anion Generation in Human Aortic Endothelial Cells. *Circulation* **96**, 25-28.

Cusi, K., Maezono, K., Osman, A., Pendergrass, M., Patti, M.E., Pratipanawatr, T., Defronzo, R.A., Kahn, C.R. & Mandarino, L.J. (2000). Insulin resistance differentially affects the PI 3-kinase- and MAP kinase-mediated signaling in human muscle. *J. Clin. Invest.* **105**, 311-320.

Czech, M.P. & Massague, J. (1982). Subunit structure and dynamics of the insulin receptor. *Fed Proc* **41**, 2719-23.

Da Silva Xavier, G., Leclerc, I., Salt, I.P., Doiron, B., Hardie, D.G., Kahn, A. & Rutter, G.A. (2000). Role of AMP-activated protein kinase in the regulation by glucose of islet beta cell gene expression. *Proceedings of the National Academy of Sciences* **97**, 4023-4028.

Dandona, P., Aljada, A., Chaudhuri, A. & Mohanty, P. (2004). Endothelial dysfunction, inflammation and diabetes. *Reviews in Endocrine & Metabolic Disorders. Vol. 5(3)(pp 189-197), 2004.*

Dandona, P., Aljada, A. & Mohanty, P. (2002). The anti-inflammatory and potential anti-atherogenic effect of insulin: a new paradigm. *Diabetologia* **45**, 924-30.

Dandona, P., Aljada, A., Mohanty, P., Ghanim, H., Hamouda, W., Assian, E. & Ahmad, S. (2001). Insulin inhibits intranuclear nuclear factor kappaB and stimulates IkappaB in mononuclear cells in obese subjects: Evidence for an anti-inflammatory effect? *Journal of Clinical Endocrinology & Metabolism. Vol. 86(7)(pp 3257-3265), 2001.*

De Mattia, G., Bravi, M.C., Costanzo, A., Laurenti, O., Cassone Faldetta, M., Armiento, A., De Luca, O. & Ferri, C. (1999). Effects of insulin on in vitro vascular cell adhesion molecule-1 expression and in vivo soluble VCAM-1 release. *Diabetologia* **42**, 1235-9.

De Meyts, P. & Whittaker, J. (2002). Structural biology of insulin and IGF1receptors: implications for drug design. *Nat Rev Drug Discov* **1**, 769-83.

De Vriese, A.S., Verbeuren, T.J., Van De Voorde, J., Lameire, N.H. & Vanhoutte, P.M. (2000). Endothelial dysfunction in diabetes. *Br J Pharmacol* **130**, 963-74.

Dedio, J., Konig, P., Wohlfart, P., Schroeder, C., Kummer, W. & Muller-Esterl, W. (2001). NOSIP, a novel modulator of endothelial nitric oxide synthase activity. *FASEB J.* **15**, 79-89.

Deller, M.C. & Yvonne Jones, E. (2000). Cell surface receptors. *Curr Opin Struct Biol* **10**, 213-9.

Denton, R.M. & Tavare, J.M. (1995). Does mitogen-activated-protein kinase have a role in insulin action? The cases for and against. *Eur J Biochem* **227**, 597-611.

Despres, J.P., Lamarche, B., Mauriege, P., Cantin, B., Lupien, P.J. & Dagenais, G.R. (1996). Risk factors for ischaemic heart disease: is it time to measure insulin? *Eur Heart J* **17**, 1453-4.

Di Guglielmo, G.M., Drake, P.G., Baass, P.C., Authier, F., Posner, B.I. & Bergeron, J.J. (1998). Insulin receptor internalization and signalling. *Mol Cell Biochem* **182**, 59-63.

Diabetes UK (2001). http://www.diabetes.org.uk/.

Dickhout, J.G., Hossain, G.S., Pozza, L.M., Zhou, J., Lhotak, S. & Austin, R.C. (2005). Peroxynitrite Causes Endoplasmic Reticulum Stress and Apoptosis in Human Vascular Endothelium: Implications in Atherogenesis. *Arterioscler Thromb Vasc Biol* **25**, 2623-2629.

Dimmeler, S., Fleming, I., Fisslthaler, B., Hermann, C., Busse, R. & Zeiher, A.M. (1999). Activation of nitric oxide synthase in endothelial cells by Akt-dependent phosphorylation. *Nature* **399**, 601-605.

Ding, Y., Vaziri, N.D., Coulson, R., Kamanna, V.S. & Roh, D.D. (2000). Effects of simulated hyperglycemia, insulin, and glucagon on endothelial nitric oxide synthase expression. *Am J Physiol Endocrinol Metab* **279**, E11-17.

Drew, B.G., Fidge, N.H., Gallon-Beaumier, G., Kemp, B.E. & Kingwell, B.A. (2004). High-density lipoprotein and apolipoprotein AI increase endothelial NO synthase activity by protein association and multisite phosphorylation. *Proc Natl Acad Sci U S A* **101**, 6999-7004.

Du, X.L., Edelstein, D., Dimmeler, S., Ju, Q., Sui, C. & Brownlee, M. (2001). Hyperglycemia inhibits endothelial nitric oxide synthase activity by posttranslational modification at the Akt site. *J Clin Invest* **108**, 1341-8.

Duncan, E.R., Walker, S.J., Ezzat, V.A., Wheatcroft, S.B., Li, J.-M., Shah, A.M. & Kearney, M.T. (2007). Accelerated endothelial dysfunction in mild prediabetic insulin resistance: the early role of reactive oxygen species. *Am J Physiol Endocrinol Metab* **293**, E1311-1319.

Ebina, Y., Ellis, L., Jarnagin, K. & Et Al. (1985). The human insulin receptor cDNA: The structural basis for hormone-activated transmembrane signalling. *Cell* **40**, 747-758.

Elchebly, M., Payette, P., Michaliszyn, E., Cromlish, W., Collins, S., Loy, A.L., Normandin, D., Cheng, A., Himms-Hagen, J., Chan, C.C., Ramachandran, C., Gresser, M.J., Tremblay, M.L. & Kennedy, B.P. (1999). Increased insulin sensitivity and obesity resistance in mice lacking the protein tyrosine phosphatase-1B gene. *Science* **283**, 1544-8.

Ellis, L., Clauser, E., Morgan, D.O., Edery, M., Roth, R.A. & Rutter, W.J. (1986). Replacement of insulin receptor tyrosine residues 1162 and 1163 compromises insulin-stimulated kinase activity and uptake of 2-deoxyglucose. *Cell* **45**, 721-32.

Fantl, W.J., Johnson, D.E. & Williams, L.T. (1993). Signalling by receptor tyrosine kinases. *Annu Rev Biochem* **62**, 453-81.

Federici, M., Menghini, R., Mauriello, A., Hribal, M.L., Ferrelli, F., Lauro, D., Sbraccia, P., Spagnoli, L.G., Sesti, G. & Lauro, R. (2002). Insulin-dependent activation of endothelial nitric oxide synthase is impaired by O-linked glycosylation modification of signaling proteins in human coronary endothelial cells. *Circulation* **106**, 466-72.

Federici, M., Pandolfi, A., De Filippis, E.A., Pellegrini, G., Menghini, R., Lauro, D., Cardellini, M., Romano, M., Sesti, G., Lauro, R. & Consoli, A. (2004). G972R IRS-1 variant impairs insulin regulation of endothelial nitric oxide synthase in cultured human endothelial cells. *Circulation* **109**, 399-405.

Feinstein, R., Kanety, H., Papa, M.Z., Lunenfeld, B. & Karasik, A. (1993). Tumor necrosis factor-alpha suppresses insulin-induced tyrosine phosphorylation of insulin receptor and its substrates. *J Biol Chem* **268**, 26055-8.

Fernandez-Real, J.M. & Ricart, W. (2003). Insulin Resistance and Chronic Cardiovascular Inflammatory Syndrome. *Endocr Rev* **24**, 278-301.

Feron, O., Belhassen, L., Kobzik, L., Smith, T.W., Kelly, R.A. & Michel, T. (1996). Endothelial nitric oxide synthase targeting to caveolae. Specific interactions with caveolin isoforms in cardiac myocytes and endothelial cells. *J Biol Chem* **271**, 22810-4.

Feron, O., Saldana, F., Michel, J.B. & Michel, T. (1998). The Endothelial Nitric-oxide Synthase-Caveolin Regulatory Cycle. *J. Biol. Chem.* **273**, 3125-3128.

Fisslthaler, B., Dimmeler, S., Hermann, C., Busse, R. & Fleming, I. (2000). Phosphorylation and activation of the endothelial nitric oxide synthase by fluid shear stress. *Acta Physiol Scand* **168**, 81-8.

Fleming, I., Bauersachs, J., Fisslthaler, B. & Busse, R. (1998). Ca2+-Independent Activation of the Endothelial Nitric Oxide Synthase in Response to Tyrosine Phosphatase Inhibitors and Fluid Shear Stress. *Circ Res* **82**, 686-695.

Fleming, I. & Busse, R. (2003). Molecular mechanisms involved in the regulation of the endothelial nitric oxide synthase. *Am J Physiol Regul Integr Comp Physiol* **284**, R1-12.

Fleming, I., Fisslthaler, B., Dimmeler, S., Kemp, B.E. & Busse, R. (2001). Phosphorylation of Thr495 Regulates Ca2+/Calmodulin-Dependent Endothelial Nitric Oxide Synthase Activity. *Circ Res* **88**, 68e-75.

Fontana, J., Fulton, D., Chen, Y., Fairchild, T.A., Mccabe, T.J., Fujita, N., Tsuruo, T. & Sessa, W.C. (2002). Domain Mapping Studies Reveal That the M Domain of hsp90 Serves as a Molecular Scaffold to Regulate Akt-Dependent Phosphorylation of Endothelial Nitric Oxide Synthase and NO Release. *Circ Res* **90**, 866-873.

Forstermann, U., Pollock, J.S., Schmidt, H.H.H., Heller, M. & Murad, F. (1991). Calmodulin-Dependent Endothelium-Derived Relaxing Factor/Nitric Oxide Synthase Activity is Present in the Particulate and Cytosolic Fractions of Bovine Aortic Endothelial Cells. *Proceedings of the National Academy of Sciences* **88**, 1788-1792.

Franke, T.F., Yang, S.I., Chan, T.O., Datta, K., Kazlauskas, A., Morrison, D.K., Kaplan, D.R. & Tsichlis, P.N. (1995). The protein kinase encoded by the Akt proto-oncogene is a target of the PDGF-activated phosphatidylinositol 3-kinase. *Cell* **81**, 727-36.

Frattali, A.L., Treadway, J.L. & Pessin, J.E. (1992). Transmembrane signaling by the human insulin receptor kinase. Relationship between intramolecular beta subunit trans- and cis-autophosphorylation and substrate kinase activation. *J Biol Chem* **267**, 19521-8.

Friday, R.P., Trucco, M. & Pietropaolo, M. (1999). Genetics of type 1 diabetes mellitus. *Diabetes, Nutrition & Metabolism - Clinical & Experimental. Vol. 12(1)(pp 3-26), 1999.*

Fujiwara, T. & Horikoshi, H. (2000). Troglitazone and related compounds: Therapeutic potential beyond diabetes. *Life Sciences* **67**, 2405.

Fukuda, K., Tesch, G.H. & Nikolic-Paterson, D.J. (2008). c-Jun amino terminal kinase 1 deficient mice are protected from streptozotocin-induced islet injury. *Biochemical and Biophysical Research Communications* **366**, 710.

Fulton, D., Babbitt, R., Zoellner, S., Fontana, J., Acevedo, L., Mccabe, T.J., Iwakiri, Y. & Sessa, W.C. (2004a). Targeting of Endothelial Nitric-oxide Synthase to the Cytoplasmic Face of the Golgi Complex or Plasma Membrane Regulates Akt- Versus Calcium-dependent Mechanisms for Nitric Oxide Release. *J. Biol. Chem.* **279**, 30349-30357.

Fulton, D., Fontana, J., Sowa, G., Gratton, J.-P., Lin, M., Li, K.-X., Michell, B., Kemp, B.E., Rodman, D. & Sessa, W.C. (2002). Localization of Endothelial Nitric-oxide Synthase Phosphorylated on Serine 1179 and Nitric Oxide in Golgi and Plasma Membrane Defines the Existence of Two Pools of Active Enzyme. *J. Biol. Chem.* **277**, 4277-4284.

Fulton, D., Gratton, J.-P., Mccabe, T.J., Fontana, J., Fujio, Y., Walsh, K., Franke, T.F., Papapetropoulos, A. & Sessa, W.C. (1999). Regulation of endothelium-derived nitric oxide production by the protein kinase Akt. *Nature* **399**, 597-601.

Fulton, D., Harris, M.B., Kemp, B.E., Venema, R.C., Marrero, M.B. & Stepp, D.W. (2004b). Insulin resistance does not diminish eNOS expression, phosphorylation, or binding to HSP-90. *Am J Physiol Heart Circ Physiol* **287**, H2384-2393.

Furchgott, R.F. & Zawadzki, J.V. (1980). The obligatory role of endothelial cells in the relaxation of arterial smooth muscle by acetylcholine. *Nature* **288**, 373-6.

Gallis, B., Corthals, G.L., Goodlett, D.R., Ueba, H., Kim, F., Presnell, S.R., Figeys, D., Harrison, D.G., Berk, B.C., Aebersold, R. & Corson, M.A. (1999). Identification of flow-dependent endothelial nitric-oxide synthase phosphorylation sites by mass spectrometry and regulation of phosphorylation and nitric oxide production by the phosphatidylinositol 3-kinase inhibitor LY294002. *J Biol Chem* **274**, 30101-8.

Garcia-Cardena, G., Fan, R., Shah, V., Sorrentino, R., Cirino, G., Papapetropoulos, A. & Sessa, W.C. (1998). Dynamic activation of endothelial nitric oxide synthase by Hsp90. *Nature* **392**, 821.

Garcia-Cardena, G., Fan, R., Stern, D.F., Liu, J. & Sessa, W.C. (1996a). Endothelial Nitric Oxide Synthase Is Regulated by Tyrosine Phosphorylation and Interacts with Caveolin-1. *J. Biol. Chem.* **271**, 27237-27240.

Garcia-Cardena, G., Martasek, P., Masters, B.S.S., Skidd, P.M., Couet, J., Li, S., Lisanti, M.P. & Sessa, W.C. (1997). Dissecting the Interaction between Nitric Oxide Synthase (NOS) and Caveolin. FUNCTIONAL SIGNIFICANCE OF THE NOS CAVEOLIN BINDING DOMAIN IN VIVO. *J. Biol. Chem.* **272**, 25437-25440.

Garcia-Cardena, G., Oh, P., Liu, J., Schnitzer, J.E. & Sessa, W.C. (1996b). Targeting of nitric oxide synthase to endothelial cell caveolae via palmitoylation: Implications for nitric oxide signaling. *PNAS* **93**, 6448-6453.

Garg, U.C. & Hassid, A. (1989). Nitric oxide-generating vasodilators and 8-bromo-cyclic guanosine monophosphate inhibit mitogenesis and proliferation of cultured rat vascular smooth muscle cells. *J Clin Invest* **83**, 1774-7.

Gewaltig, M.T. & Kojda, G. (2002). Vasoprotection by nitric oxide: mechanisms and therapeutic potential. *Cardiovasc Res* **55**, 250-60.

Ghosh, S., Gachhui, R., Crooks, C., Wu, C., Lisanti, M.P. & Stuehr, D.J. (1998). Interaction between caveolin-1 and the reductase domain of endothelial nitric-oxide synthase. Consequences for catalysis. *Journal of Biological Chemistry. Vol. 273(35)(pp 22267-22271), 1998. Date of Publication: 28 AUG 1998.*

Gilmore, T.D. (2006). Introduction to NF-[kappa]B: players, pathways, perspectives. *Oncogene* **25**, 6680.

Ginsberg, H.N. (2000). Insulin resistance and cardiovascular disease. *J Clin Invest* **106**, 453-8.

Giri, S., Nath, N., Smith, B., Viollet, B., Singh, A.K. & Singh, I. (2004). 5-aminoimidazole-4-carboxamide-1-beta-4-ribofuranoside inhibits proinflammatory response in glial cells: a possible role of AMP-activated protein kinase. *J Neurosci* **24**, 479-87.

Graham, J., Ford, T. & Rickwood, D. (1994). The preparation of subcellular organelles from mouse liver in self-generated gradients of iodixanol. *Anal Biochem* **220**, 367-73.

Greif, D.M., Kou, R. & Michel, T. (2002). Site-Specific Dephosphorylation of Endothelial Nitric Oxide Synthase by Protein Phosphatase 2A: Evidence for Crosstalk between Phosphorylation Sites. *Biochemistry* **41**, 15845-15853.

Griffith, T.M., Edwards, D.H., Lewis, M.J., Newby, A.C. & Henderson, A.H. (1984). The nature of endothelium-derived vascular relaxant factor. *Nature* **308**, 645-7.

Gual, P., Baron, V., Lequoy, V. & Van Obberghen, E. (1998). Interaction of Janus kinases JAK-1 and JAK-2 with the insulin receptor and the insulin-like growth factor-1 receptor. *Endocrinology* **139**, 884-93.

Gustafson, T.A., He, W., Craparo, A., Schaub, C.D. & O'neill, T.J. (1995). Phosphotyrosine-dependent interaction of SHC and insulin receptor substrate 1 with the NPEY motif of the insulin receptor via a novel non-SH2 domain. *Mol Cell Biol* **15**, 2500-8.

Haffner, S.M., Valdez, R.A., Hazuda, H.P., Mitchell, B.D., Morales, P.A. & Stern, M.P. (1992). Prospective analysis of the insulin-resistance syndrome (syndrome X). *Diabetes* **41**, 715-22.

Hall, S.K. & Armstrong, D.L. (2000). Conditional and unconditional inhibition of calcium-activated potassium channels by reversible protein phosphorylation. *J Biol Chem* **275**, 3749-54.

Halse, R., Pearson, S.L., Mccormack, J.G., Yeaman, S.J. & Taylor, R. (2001). Effects of tumor necrosis factor-alpha on insulin action in cultured human muscle cells. *Diabetes* **50**, 1102-9.

Hartell, N.A., Archer, H.E. & Bailey, C.J. (2005). Insulin-stimulated endothelial nitric oxide release is calcium independent and mediate d via protein kinase B. *Biochemical Pharmacology* **69**, 781.

Hawley, S.A., Boudeau, J., Reid, J.L., Mustard, K.J., Udd, L., Makela, T.P., Alessi, D.R. & Hardie, D.G. (2003). Complexes between the LKB1 tumor suppressor, STRAD alpha/beta and MO25 alpha/beta are upstream kinases in the AMP-activated protein kinase cascade. *J Biol* **2**, 28.

Hawley, S.A., Pan, D.A., Mustard, K.J., Ross, L., Bain, J., Edelman, A.M., Frenguelli, B.G. & Hardie, D.G. (2005). Calmodulin-dependent protein kinase kinase-[beta] is an alternative upstream kinase for AMP-activated protein kinase. *Cell Metabolism* **2**, 9.

He, Z., Opland, D.M., Way, K.J., Ueki, K., Bodyak, N., Kang, P.M., Izumo, S., Kulkarni, R.N., Wang, B., Liao, R., Kahn, C.R. & King, G.L. (2006). Regulation of vascular endothelial growth factor expression and vascularization in the myocardium by insulin receptor and PI3K/Akt pathways in insulin resistance and ischemia. *Arterioscler Thromb Vasc Biol* **26**, 787-93.

Hedner, T., Kjeldsen, S.E. & Narkiewicz, K. (2005). Health economy of the metabolic syndrome pandemic. *Blood Press* **14**, 131-2.

Heinzel, B., John, M., Klatt, P., Bohme, E. & Mayer, B. (1992). Ca2+/calmodulin-dependent formation of hydrogen peroxide by brain nitric oxide synthase. *Biochemical Journal. Vol. 281(3)(pp 627-630)*.

Heyne, B., Maurel, V. & Scaiano, J.C. (2006). Mechanism of ac tion of sensors for reactive oxygen species based on fluorescein-phenol coupling: the case of 2-[6-(4'-hydroxy)phenoxy-3H-xanthen-3-on-9-yl]benzoic acid. *Org Biomol Chem* **4**, 802-7.

Hink, U., Li, H., Mollnau, H., Oelze, M., Matheis, E., Hartmann, M., Skatchkov, M., Thaiss, F., Stahl, R.A., Warnholtz, A., Meinertz, T., Griendling, K., Harrison, D.G., Forstermann, U. & Munzel, T. (2001). Mechanisms underlying endothelial dysfunction in diabetes mellitus. *Circ Res* **88**, E14-22.

Hirasaka, K., Kohno, S., Goto, J., Furochi, H., Mawatari, K., Harada, N., Hosaka, T., Nakaya, Y., Ishidoh, K., Obata, T., Ebina, Y., Gu, H., Takeda, S.I., Kishi, K. & Nikawa, T. (2007). Deficiency of Cbl-b Gene Enhances Infiltration and Activation

of Macrophages in Adipose Tissue and Causes Peripheral Insulin Resistance in Mice. *Diabetes* **56**, 2511-2522.

Ho, E., Quan, N., Tsai, Y.-H., Lai, W. & Bray, T.M. (2001). Dietary Zinc Supplementation Inhibits NF {{kappa}}B Activation and Protects Against Chemically Induced Diabetes in CD1 Mice. *Experimental Biology and Medicine* **226**, 103-111.

Ho, F.M., Liu, S.H., Liau, C.S., Huang, P.J., Shiah, S.G. & Lin-Shiau, S.Y. (1999). Nitric oxide prevents apoptosis of human endothelial cells from high glucose exposure during early stage. *J Cell Biochem* **75**, 258-63.

Hofmann, C., Lorenz, K., Williams, D., Palazuk, B.J. & Colca, J.R. (1995). Insulin sensitization in diabetic rat liver by an antihyperglycemic agent. *Metabolism* **44**, 384.

Hogikyan, R.V., Galecki, A.T., Pitt, B., Halter, J.B., Greene, D.A. & Supiano, M.A. (1998). Specific Impairment of Endothelium-Dependent Vasodilation in Subjects with Type 2 Diabetes Independent of Obesity. *J Clin Endocrinol Metab* **83**, 1946-1952.

Hotamisligil, G.S., Budavari, A., Murray, D. & Spiegelman, B.M. (1994a). Reduced tyrosine kinase activity of the insulin receptor in obesity-diabetes. Central role of tumor necrosis factor-alpha. *J Clin Invest* **94**, 1543-9.

Hotamisligil, G.S., Murray, D.L., Choy, L.N. & Spiegelman, B.M. (1994b). Tumor necrosis factor alpha inhibits signaling from the insulin receptor. *Proc Natl Acad Sci U S A* **91**, 4854-8.

Hotamisligil, G.S., Peraldi, P., Budavari, A., Ellis, R., White, M.F. & Spiegelman, B.M. (1996). IRS-1-mediated inhibition of insulin receptor tyrosine kinase activity in TNF-alpha- and obesity-induced insulin resistance. *Science* **271**, 665-8.

House, P.D. & Weidemann, M.J. (1970). Characterization of an [125 I]-insulin binding plasma membrane fraction from rat liver. *Biochem Biophys Res Commun* **41**, 541-8.

Howard, G., O'leary, D.H., Zaccaro, D., Haffner, S., Rewers, M., Hamman, R., Selby, J.V., Saad, M.F., Savage, P. & Bergman, R. (1996). Insulin sensitivity and atherosclerosis. The Insulin Resistance Atherosclerosis Study (IRAS) Investigators. *Circulation* **93**, 1809-17.

Hsueh, W.A. & Law, R. (2003). The central role of fat and effect of peroxisome proliferator-activated receptor-gamma on progression of insulin resistance and cardiovascular disease. *Am J Cardiol* **92**, 3J-9J.

Hsueh, W.A. & Quinones, M.J. (2003). Role of endothelial dysfunction in insulin resistance. *The American Journal of Cardiology* **92**, 10.

Hu, J., Liu, J., Ghirlando, R., Saltiel, A.R. & Hubbard, S.R. (2003). Structural basis for recruitment of the adaptor protein APS to the activated insulin receptor. *Mol Cell* **12**, 1379-89.

Huang, P.L., Huang, Z., Mashimo, H., Bloch, K.D., Moskowitz, M.A., Bevan, J.A. & Fishman, M.C. (1995). Hypertension in mice lacking the gene for endothelial nitric oxide synthase. *Nature* **377**, 239-42.

Huang, X.L., El Kebir, D., De Buys Roessingh, A.S., Schneider, J.C., Jacob, L., Mercier, J.C., Dall'ava-Santucci, J. & Dinh-Xuan, A.T. (2002). Role of tyrosine phosphatase in the modulation of pulmonary vascular tone. *Eur Respir J* **19**, 525-529.

Hubbard, S.R. & Till, J.H. (2000). Protein tyrosine kinase structure and function. *Annu Rev Biochem* **69**, 373-98.

Hundal, R.S., Petersen, K.F., Mayerson, A.B., Randhawa, P.S., Inzucchi, S., Shoelson, S.E. & Shulman, G.I. (2002). Mechanism by which high-dose aspirin improves glucose metabolism in type 2 diabetes. *J Clin Invest* **109**, 1321-6.

Ignarro, L.J., Buga, G.M., Wood, K.S., Byrns, R.E. & Chaudhuri, G. (1987). Endothelium-derived relaxing factor produced and released from artery and vein is nitric oxide. *Proc Natl Acad Sci U S A* **84**, 9265-9.

Jiang, Z.Y., Lin, Y.W., Clemont, A., Feener, E.P., Hein, K.D., Igarashi, M., Yamauchi, T., White, M.F. & King, G.L. (1999a). Characterization of selective resistance to insulin signaling in the vasculature of obese Zucker (fa/fa) rats. *J Clin Invest* **104**, 447-57.

Jiang, Z.Y., Zhou, Q.L., Chatterjee, A., Feener, E.P., Myers, M.G., Jr., White, M.F. & King, G.L. (1999b). Endothelin-1 modulates insulin signaling through phosphatidylinositol 3-kinase pathway in vascular smooth muscle cells. *Diabetes* **48**, 1120-30.

Jilma, B., Dallinger, S., Hergovich, N., Eichler, H.G., Richter, V. & Wagner, O.F. (2000). Effects of hyperinsulinemia on plasma levels of circulating adhesion molecules. *J Clin Endocrinol Metab* **85**, 1748-51.

Juan, C.C., Fang, V.S., Kwok, C.F., Perng, J.C., Chou, Y.C. & Ho, L.T. (1999). Exogenous hyperinsulinemia causes insulin resistance, hyperendothelinemia, and subsequent hypertension in rats. *Metabolism* **48**, 465-71.

Kanellis, J., Kandane, R.K., Etemadmoghadam, D., Fraser, S.A., Mount, P.F., Levidiotis, V., Kemp, B.E. & Power, D.A. (2006). Activators of the energy sensing kinase AMPK inhibit random cell movement and chemotaxis in U937 cells. *Immunol Cell Biol* **84**, 6-12.

Kaneto, H., Matsuoka, T.A., Katakami, N., Kawamori, D., Miyatsuka, T., Yoshiuchi, K., Yasuda, T., Sakamoto, K., Yamasaki, Y. & Matsuhisa, M. (2007). Oxidative stress and the JNK pathway are involved in the development of type 1 and type 2 diabetes. *Curr Mol Med* **7**, 674-86.

Karantzoulis-Fegaras, F., Antoniou, H., Lai, S.L., Kulkarni, G., D'abreo, C., Wong, G.K., Miller, T.L., Chan, Y., Atkins, J., Wang, Y. & Marsden, P.A. (1999). Characterization of the human endothelial nitric-oxide synthase promoter. *J Biol Chem* **274**, 3076-93.

Kasiske, B.L., O'donnell, M.P. & Keane, W.F. (1992). The Zucker rat model of obesity, insulin resistance, hyperlipidemia, and renal injury. *Hypertension* **19**, I110-5.

Kasuga, M., Zick, Y., Blithe, D.L., Crettaz, M. & Kahn, C.R. (1982). Insulin stimulates tyrosine phosphorylation of the insulin receptor in a cell-free system. *Nature* **298**, 667-9.

Katakam, P.G.V., Pollock, J.S., Pollock, D.M., Ujhelyi, M.R. & Miller, A.W. (2001). Enhanced endothelin-1 response and receptor expression in small mesenteric arteries of insulin-resistant rats. *Am J Physiol Heart Circ Physiol* **280**, H522-527.

Katakam, P.V., Tulbert, C.D., Snipes, J.A., Erdos, B., Miller, A.W. & Busija, D.W. (2005). Impaired insulin-induced vasodilation in small coronary arteries of Zucker obese rats is mediated by reactive oxygen species. *Am J Physiol Heart Circ Physiol* **288**, H854-60.

Ki, S.H., Choi, M.J., Lee, C.H. & Kim, S.G. (2007). G{alpha}12 Specifically Regulates COX-2 Induction by Sphingosine 1-Phosphate: ROLE FOR JNK-DEPENDENT UBIQUITINATION AND DEGRADATION OF I{kappa}B{alpha}. *J. Biol. Chem.* **282**, 1938-1947.

Kido, Y., Burks, D.J., Withers, D., Bruning, J.C., Kahn, C.R., White, M.F. & Accili, D. (2000). Tissue-specific insulin resistance in mice with mutations in the insulin receptor, IRS-1, and IRS-2. *J Clin Invest* **105**, 199-205.

Kim, F., Gallis, B. & Corson, M.A. (2001). TNF-{alpha} inhibits flow and insulin signaling leading to NO production in aortic endothelial cells. *Am J Physiol Cell Physiol* **280**, C1057-1065.

Kimura, A., Mora, S., Shigematsu, S., Pessin, J.E. & Saltiel, A.R. (2002). The Insulin Receptor Catalyzes the Tyrosine Phosphorylation of Caveolin-1. *J. Biol. Chem.* **277**, 30153-30158.

Kishi, K., Yuasa, T., Minami, A., Yamada, M., Hagi, A., Hayashi, H., Kemp, B.E., Witters, L.A. & Ebina, Y. (2000). AMP-Activated Protein Kinase Is Activated by

the Stimulations of Gq-Coupled Receptors. *Biochemical and Biophysical Research Communications* **276**, 16.

Klaman, L.D., Boss, O., Peroni, O.D., Kim, J.K., Martino, J.L., Zabolotny, J.M., Moghal, N., Lubkin, M., Kim, Y.B., Sharpe, A.H., Stricker-Krongrad, A., Shulman, G.I., Neel, B.G. & Kahn, B.B. (2000). Increased energy expenditure, decreased adiposity, and tissue-specific insulin sensitivity in protein-tyrosine phosphatase 1B-deficient mice. *Mol Cell Biol* **20**, 5479-89.

Klatt, P., Pfeiffer, S., List, B.M., Lehner, D., Glatter, O., Bächinger, H.P., Werner, E.R., Schmidt, K. & Mayer, B. (1996). Characterization of Heme-deficient Neuronal Nitric-oxide Synthase Reveals a Role for Heme in Subunit Dimerization and Binding of the Amino Acid Substrate and Tetrahydrobiopterin. *J. Biol. Chem.* **271**, 7336-7342.

Klinz, F.-J., Herberg, N., Arnhold, S., Addicks, K. & Bloch, W. (2007). Phospho-eNOS Ser-1176 is associated with the nucleoli and the Golgi complex in C6 rat glioma cells. *Neuroscience Letters* **421**, 224.

Klinz, F.J., Schmidt, A., Schinkothe, T., Arnhold, S., Desai, B., Popken, F., Brixius, K., Schwinger, R., Mehlhorn, U., Staib, P., Addicks, K. & Bloch, W. (2005). Phospho-eNOS Ser-114 in human mesenchymal stem cells: constitutive phosphorylation, nuclear localization and upregulation during mitosis. *Eur J Cell Biol* **84**, 809-18.

Knowles, R.G. & Moncada, S. (1994). Nitric oxide synthases in mammals. *Biochem J* **298 (Pt 2)**, 249-58.

Kobayashi, K., Forte, T.M., Taniguchi, S., Ishida, B.Y., Oka, K. & Chan, L. (2000). The db/db mouse, a model for diabetic dyslipidemia: molecular characterization and effects of Western diet feeding. *Metabolism* **49**, 22-31.

Kou, R., Greif, D. & Michel, T. (2002). Dephosphorylation of Endothelial Nitric-oxide Synthase by Vascular Endothelial Growth Factor. IMPLICATIONS FOR THE VASCULAR RESPONSES TO CYCLOSPORIN A. *J. Biol. Chem.* **277**, 29669-29673.

Kovacina, K.S. & Roth, R.A. (1993). Identification of SHC as a substrate of the insulin receptor kinase distinct from the GAP-associated 62 kDa tyrosine phosphoprotein. *Biochem Biophys Res Commun* **192**, 1303-11.

Kroner, C., Eybrechts, K. & Akkerman, J.-W.N. (2000). Dual Regulation of Platelet Protein Kinase B. *J. Biol. Chem.* **275**, 27790-27798.

Kubes, P., Suzuki, M. & Granger, D.N. (1991). Nitric oxide: an endogenous modulator of leukocyte adhesion. *Proc Natl Acad Sci U S A* **88**, 4651-5.

Kurlawalla-Martinez, C., Stiles, B., Wang, Y., Devaskar, S.U., Kahn, B.B. & Wu, H. (2005). Insulin Hypersensitivity and Resistance to Streptozotocin-Induced Diabetes in Mice Lacking PTEN in Adipose Tissue. *Mol. Cell. Biol.* **25**, 2498-2510.

Laakso, M. (1995). Epidemiology of diabetic dyslipidemia. *Diabetes Review* **3**, 408-422.

Laemmli, U.K. (1970). Cleavage of structural proteins during the assembly of the head of bacteriophage T4. *Nature* **227**, 680-5.

Laine, H., Yki-Jarvinen, H., Kirvela, O., Tolvanen, T., Raitakari, M., Solin, O., Haaparanta, M., Knuuti, J. & Nuutila, P. (1998). Insulin resistance of glucose uptake in skeletal muscle cannot be ameliorated by enhancing endothelium-dependent blood flow in obesity. *J Clin Invest* **101**, 1156-62.

Lamas, S., Marsden, P.A., Li, G.K., Tempst, P. & Michel, T. (1992). Endothelial nitric oxide synthase: molecular cloning and characterization of a distinct constitutive enzyme isoform. *Proc Natl Acad Sci U S A* **89**, 6348-52.

Lane, P. & Gross, S.S. (2002). Disabling a C-terminal Autoinhibitory Control Element in Endothelial Nitric-oxide Synthase by Phosphorylation Provides a Molecular Explanation for Activation of Vascular NO Synthesis by Diverse Physiological Stimuli. *J. Biol. Chem.* **277**, 19087-19094.

Laumonnier, Y., Nadaud, S., Agrapart, M. & Soubrier, F. (2000). Characterization of an upstream enhancer region in the promoter of the human endothelial nitric-oxide synthase gene. *J Biol Chem* **275**, 40732-41.

Lavan, B.E., Fantin, V.R., Chang, E.T., Lane, W.S., Keller, S.R. & Lienhard, G.E. (1997a). A novel 160-kDa phosphotyrosine protein in insulin-treated embryonic kidney cells is a new member of the insulin receptor substrate family. *J Biol Chem* **272**, 21403-7.

Lavan, B.E., Lane, W.S. & Lienhard, G.E. (1997b). The 60-kDa phosphotyrosine protein in insulin-treated adipocytes is a new member of the insulin receptor substrate family. *J Biol Chem* **272**, 11439-43.

Lawlor, M.A. & Alessi, D.R. (2001). PKB/Akt: a key mediator of cell proliferation, survival and insulin responses? *J Cell Sci* **114**, 2903-10.

Lazar, D.F., Wiese, R.J., Brady, M.J., Mastick, C.C., Waters, S.B., Yamauchi, K., Pessin, J.E., Cuatrecasas, P. & Saltiel, A.R. (1995). Mitogen-activated protein kinase kinase inhibition does not block the stimulation of glucose utilization by insulin. *J Biol Chem* **270**, 20801-7.

Le, M.N., Kohanski, R.A., Wang, L.H. & Sadowski, H.B. (2002). Dual mechanism of signal transducer and activator of transcription 5 activation by the insulin receptor. *Mol Endocrinol* **16**, 2764-79.

Leonetti, F., Iozzo, P., Giaccari, A., Sbraccia, P., Buongiorno, A., Tamburrano, G. & Andreani, D. (1993). Absence of clinically overt atherosclerotic vascular disease and adverse changes in cardiovascular risk factors in 70 patients with insulinoma. *J Endocrinol Invest* **16**, 875-80.

Li, H., Junk, P., Huwiler, A., Burkhardt, C., Wallerath, T., Pfeilschifter, J. & Forstermann, U. (2002). Dual Effect of Ceramide on Human Endothelial Cells: Induction of Oxidative Stress and Transcriptional Upregulation of Endothelial Nitric Oxide Synthase. *Circulation* **106**, 2250-2256.

Lin, L.Y., Lin, C.Y., Ho, F.M. & Liau, C.S. (2005). Up-regulation of the association between heat shock protein 90 and endothelial nitric oxide synthase prevents high glucose-induced apoptosis in human endothelial cells. *J Cell Biochem* **94**, 194-201.

Liochev, S.I. & Fridovich, I. (1997). Lucigenin luminescence as a measure of intracellular superoxide dismutase activity in Escherichia coli. *Proceedings of the National Academy of Sciences* **94**, 2891-2896.

List, B.M., Klosch, B., Volker, C., Gorren, A.C.F., Sessa, W.C., Werner, E.R., Kukovietz, W.R., Schmidt, K. & Mayer, B. (1997). Characterization of bovine endothelial nitric oxide synthase as a homodimer with down-regulated uncoupled NADPH oxidase activity: Tetrahydrobiopterin binding kinetics and role of haem in dimerization. *Biochemical Journal. Vol. 323(1)(pp 159-165).*

Liu, C. & Hermann, T.E. (1978). Characterization of ionomycin as a calcium ionophore. *J. Biol. Chem.* **253**, 5892-5894.

Liu, F. & Roth, R.A. (1994). Identification of serines-1035/1037 in the kinase domain of the insulin receptor as protein kinase C alpha mediated phosphorylation sites. *FEBS Lett* **352**, 389-92.

Liu, J., Garcia-Cardena, G. & Sessa, W.C. (1996). Palmitoylation of Endothelial Nitric Oxide Synthase Is Necessary for Optimal Stimulated Release of Nitric Oxide: Implications for Caveolae Localization. *Biochemistry* **35**, 13277-13281.

Liu, J. & Sessa, W.C. (1994). Identification of covalently bound amino-terminal myristic acid in endothelial nitric oxide synthase. *J. Biol. Chem.* **269**, 11691-11694.

Liu, W., Schoenkerman, A. & Lowe, W.L., Jr. (2000). Activation of members of the mitogen-activated protein kinase family by glucose in endothelial cells. *Am J Physiol Endocrinol Metab* **279**, E782-790.

Lo, Y.T., Tsao, C.J., Liu, I.M., Liou, S.S. & Cheng, J.T. (2004). Increase of PTEN Gene Expression in Insulin Resistance. *Hormone and Metabolic Research*, 662.

Macmicking, J., Xie, Q.W. & Nathan, C. (1997). Nitric oxide and macrophage function. *Annu Rev Immunol* **15**, 323-50.

Madonna, R., Pandolfi, A., Massaro, M., Consoli, A. & De Caterina, R. (2004). Insulin enhances vascular cell adhesion molecule-1 expression in human cultured endothelial cells through a pro-atherogenic pathway mediated by p38 mitogen-activated protein-kinase. *Diabetologia* **47**, 532-6.

Malek, A.M., Goss, G.G., Jiang, L., Izumo, S., Alper, S.L. & Hsu, C.Y. (1998). Mannitol at Clinical Concentrations Activates Multiple Signaling Pathways and Induces Apoptosis in Endothelial Cells • Editorial Comment. *Stroke* **29**, 2631-2640.

Marban, S.L., Deloia, J.A. & Gearhart, J.D. (1989). Hyperinsulinemia in transgenic mice carrying multiple copies of the human insulin gene. *Dev Genet* **10**, 356-64.

Mather, K., Anderson, T.J. & Verma, S. (2001). Insulin action in the vasculature: physiology and pathophysiology. *J Vasc Res* **38**, 415-22.

Matsubara, M., Hayashi, N., Jing, T. & Titani, K. (2003). Regulation of Endothelial Nitric Oxide Synthase by Protein Kinase C. *J Biochem (Tokyo)* **133**, 773-781.

Matsuda, H. & Iyanagi, T. (1999). Calmodulin activates intramolecular electron transfer between the two flavins of neuronal nitric oxide synthase flavin domain. *Biochim Biophys Acta* **1473**, 345-55.

Mayer, B. & Hemmens, B. (1997). Biosynthesis and action of nitric oxide in mammalian cells. *Trends in Biochemical Sciences* **22**, 477-481.

Mayer, B., John, M., Heinzel, B., Werner, E.R., Wachter, H., Schultz, G. & Bohme, E. (1991). Brain nitric oxide synthase is a biopterin- and flavin-containing multi-functional oxido-reductase. *FEBS Letters. Vol. 288(1-2)(pp 187-191), 1991.*

Mcveigh, G.E., Brennan, G.M., Johnston, G.D., Mcdermott, B.J., Mcgrath, L.T., Henry, W.R., Andrews, J.W. & Hayes, J.R. (1992). Impaired endothelium-dependent and independent vasodilation in patients with type 2 (non-insulin-dependent) diabetes mellitus. *Diabetologia* **35**, 771-6.

Michel, J.B., Feron, O., Sacks, D. & Michel, T. (1997). Reciprocal Regulation of Endothelial Nitric-oxide Synthase by Ca2+-Calmodulin and Caveolin. *J. Biol. Chem.* **272**, 15583-15586.

Michell, B.J., Chen, Z.-P., Tiganis, T., Stapleton, D., Katsis, F., Power, D.A., Sim, A.T. & Kemp, B.E. (2001). Coordinated Control of Endothelial Nitric-oxide Synthase Phosphorylation by Protein Kinase C and the cAMP-dependent Protein Kinase. *J. Biol. Chem.* **276**, 17625-17628.

Michell, B.J., Harris, M.B., Chen, Z.P., Ju, H., Venema, V.J., Blackstone, M.A., Huang, W., Venema, R.C. & Kemp, B.E. (2002). Identification of regulatory sites of phosphorylation of the bovine endothelial nitric-oxide synthase at serine 617 and serine 635. *J Biol Chem* **277**, 42344-51.

Minokoshi, Y., Alquier, T., Furukawa, N., Kim, Y.-B., Lee, A., Xue, B., Mu, J., Foufelle, F., Ferre, P., Birnbaum, M.J., Stuck, B.J. & Kahn, B.B. (2004). AMP-kinase regulates food intake by responding to hormonal and nutrient signals in the hypothalamus. *Nature* **428**, 569.

Minokoshi, Y., Kim, Y.-B., Peroni, O.D., Fryer, L.G.D., Muller, C., Carling, D. & Kahn, B.B. (2002). Leptin stimulates fatty-acid oxidation by activating AMP-activated protein kinase. *Nature* **415**, 339.

Moncada, S. & Higgs, E.A. (1991). Endogenous nitric oxide: physiology, pathology and clinical relevance. *Eur J Clin Invest* **21**, 361-74.

Montagnani, M., Chen, H., Barr, V.A. & Quon, M.J. (2001). Insulin-stimulated Activation of eNOS Is Independent of Ca2+ but Requires Phosphorylation by Akt at Ser1179. *J. Biol. Chem.* **276**, 30392-30398.

Montagnani, M., Golovchenko, I., Kim, I., Koh, G.Y., Goalstone, M.L., Mundhekar, A.N., Johansen, M., Kucik, D.F., Quon, M.J. & Draznin, B. (2002). Inhibition of

Phosphatidylinositol 3-Kinase Enhances Mitogenic Actions of Insulin in Endothelial Cells. *J. Biol. Chem.* **277**, 1794-1799.

Morrow, V.A., Foufelle, F., Connell, J.M.C., Petrie, J.R., Gould, G.W. & Salt, I.P. (2003). Direct Activation of AMP-activated Protein Kinase Stimulates Nitric-oxide Synthesis in Human Aortic Endothelial Cells. *J. Biol. Chem.* **278**, 31629-31639.

Mosthaf, L., Berti, L., Kellerer, M., Mushack, J., Seffer, E., Bossenmaier, B., Coghlan, M., Siddle, K., Ullrich, A. & Haring, H.U. (1995). C-terminus or juxtamembrane deletions in the insulin receptor do not affect the glucose-dependent inhibition of the tyrosine kinase activity. *Eur J Biochem* **227**, 787-91.

Mount, P.F., Kemp, B.E. & Power, D.A. (2007). Regulation of endothelial and myocardial NO synthesis by multi-site eNOS phosphorylation. *Journal of Molecular and Cellular Cardiology* **42**, 271.

Moxham, C.P., Duronio, V. & Jacobs, S. (1989). Insulin-like growth factor I receptor beta-subunit heterogeneity. Evidence for hybrid tetramers composed of insulin-like growth factor I and insulin receptor heterodimers. *J Biol Chem* **264**, 13238-44.

Murphy, M.E. & Sies, H. (1991). Reversible conversion of nitroxyl anion to nitric oxide by superoxide dismutase. *Proc Natl Acad Sci U S A* **88**, 10860-4.

Musicki, B., Kramer, M.F., Becker, R.E. & Burnett, A.L. (2005). Inactivation of phosphorylated endothelial nitric oxide synthase (Ser-1177) by O-GlcNAc in diabetes-associated erectile dysfunction. *Proc Natl Acad Sci U S A* **102**, 11870-5.

Naruse, K., Rask-Madsen, C., Takahara, N., Ha, S.-W., Suzuma, K., Way, K.J., Jacobs, J.R.C., Clermont, A.C., Ueki, K., Ohshiro, Y., Zhang, J., Goldfine, A.B. & King, G.L. (2006). Activation of Vascular Protein Kinase C-{beta} Inhibits Akt-Dependent Endothelial Nitric Oxide Synthase Function in Obesity-Associated Insulin Resistance. *Diabetes* **55**, 691-698.

Nath, N., Giri, S., Prasad, R., Salem, M.L., Singh, A.K. & Singh, I. (2005). 5-aminoimidazole-4-carboxamide ribonucleoside: a novel immunomodulator with therapeutic efficacy in experimental autoimmune encephalomyelitis. *J Immunol* **175**, 566-74.

Nathan, C. & Xie, Q.W. (1994). Regulation of biosynthesis of nitric oxide. *J. Biol. Chem.* **269**, 13725-13728.

Nishikawa, T., Edelstein, D., Du, X.L., Yamagishi, S.-I., Matsumura, T., Kaneda, Y., Yorek, M.A., Beebe, D., Oates, P.J., Hammes, H.-P., Giardino, I. & Brownlee, M. (2000). Normalizing mitochondrial superoxide production blocks three pathways of hyperglycaemic damage. *Nature* **404**, 787.

Noyman, I., Marikovsky, M., Sasson, S., Stark, A.H., Bernath, K., Seger, R. & Madar, Z. (2002). Hyperglycemia reduces nitric oxide synthase and glycogen synthase activity in endothelial cells. *Nitric Oxide* **7**, 187.

O'brien, R.M. & Granner, D.K. (1996). Regulation of gene expression by insulin. *Physiol Rev* **76**, 1109-61.

O'brien, R.M., Streeper, R.S., Ayala, J.E., Stadelmaier, B.T. & Hornbuckle, L.A. (2001). Insulin-regulated gene expression. *Biochem Soc Trans* **29**, 552-8.

O'driscoll, G., Green, D., Maiorana, A., Stanton, K., Colreavy, F. & Taylor, R. (1999). Improvement in endothelial function by angiotensin-converting enzyme inhibition in non-insulin-dependent diabetes mellitus. *J Am Coll Cardiol* **33**, 1506-11.

Ohmura, C., Watada, H., Hirose, T., Tanaka, Y. & Kawamori, R. (2005). Acute onset and worsening of diabetes concurrent with administration of statins. *Endocr J* **52**, 369-72.

Okada, S., Matsuda, M., Anafi, M., Pawson, T. & Pessin, J.E. (1998). Insulin regulates the dynamic balance between Ras and Rap1 signaling by coordinating the assembly states of the Grb2-SOS and CrkII-C3G complexes. *Embo J* **17**, 2554-65.

Okouchi, M., Okayama, N., Imai, S., Omi, H., Shimizu, M., Fukutomi, T. & Itoh, M. (2002a). High insulin enhances neutrophil transendothelial migration through

increasing surface expression of platelet endothelial cell adhesion molecule-1 via activation of mitogen activated protein kinase. *Diabetologia* **45**, 1449-56.

Okouchi, M., Okayama, N., Omi, H., Imaeda, K., Shimizu, M., Fukutomi, T. & Itoh, M. (2003). Cerivastatin ameliorates high insulin-enhanced neutrophil-endothelial cell adhesion and endothelial intercellular adhesion molecule-1 expression by inhibiting mitogen-activated protein kinase activation. *J Diabetes Complications* **17**, 380-6.

Okouchi, M., Okayama, N., Shimizu, M., Omi, H., Fukutomi, T. & Itoh, M. (2002b). High insulin exacerbates neutrophil-endothelial cell adhesion through endothelial surface expression of intercellular adhesion molecule-1 via activation of protein kinase C and mitogen-activated protein kinase. *Diabetologia* **45**, 556-9.

Ottensmeyer, F.P., Beniac, D.R., Luo, R.Z. & Yip, C.C. (2000). Mechanism of transmembrane signaling: insulin binding and the insulin receptor. *Biochemistry* **39**, 12103-12.

Oudit, G.Y., Sun, H., Kerfant, B.G., Crackower, M.A., Penninger, J.M. & Backx, P.H. (2004). The role of phosphoinositide-3 kinase and PTEN in cardiovascular physiology and disease. *J Mol Cell Cardiol* **37**, 449-71.

Palmer, R.M., Ferrige, A.G. & Moncada, S. (1987). Nitric oxide release accounts for the biological activity of endothelium-derived relaxing factor. *Nature* **327**, 524-6.

Pandey, S.K., He, H.-J., Chesley, A., Juhaszova, M., Crow, M.T. & Bernier, M. (2002). Wortmannin-Sensitive Pathway Is Required for Insulin-Stimulated Phosphorylation of Inhibitor {kappa}B{alpha}. *Endocrinology* **143**, 375-385.

Pandolfi, A., Solini, A., Pellegrini, G., Mincione, G., Di Silvestre, S., Chiozzi, P., Giardinelli, A., Di Marcantonio, M.C., Piccirelli, A., Capani, F. & Consoli, A. (2005). Selective Insulin Resistance Affecting Nitric Oxide Release But Not Plasminogen Activator Inhibitor-1 Synthesis in Fibroblasts From Insulin-Resistant Individuals. *Arterioscler Thromb Vasc Biol* **25**, 2392-2397.

Patel, S., Lipina, C. & Sutherland, C. (2003). Different mechanisms are used by insulin to repress three genes that contain a homologous thymine-rich insulin response element. *FEBS Letters* **549**, 72.

Pellegrino, A., Ria, R., Pietro, G.D., Cirulli, T., Surico, G., Pennisi, A., Morabito, F., Ribatti, D. & Vacca, A. (2005). Bone marrow endothelial cells in multiple myeloma secrete CXC-chemokines that mediate interactions with plasma cells. *British Journal of Haematology* **129**, 248-256.

Peraldi, P., Xu, M. & Spiegelman, B.M. (1997). Thiazolidinediones block tumor necrosis factor-alpha-induced inhibition of insulin signaling. *J Clin Invest* **100**, 1863-9.

Perticone, F., Sciacqua, A., Scozzafava, A., Ventura, G., Laratta, E., Pujia, A., Federici, M., Lauro, R. & Sesti, G. (2004). Impaired endothelial function in never-treated hypertensive subjects carrying the Arg972 polymorphism in the insulin receptor substrate-1 gene. *J Clin Endocrinol Metab* **89**, 3606-9.

Petrie, J.R., Ueda, S., Webb, D.J., Elliott, H.L. & Connell, J.M.C. (1996). Endothelial Nitric Oxide Production and Insulin Sensitivity: A Physiological Link With Implications for Pathogenesis of Cardiovascular Disease. *Circulation* **93**, 1331-1333.

Pfeifer, A., Klatt, P., Massberg, S., Ny, L., Sausbier, M., Hirneiss, C., Wang, G.X., Korth, M., Aszodi, A., Andersson, K.E., Krombach, F., Mayerhofer, A., Ruth, P., Fassler, R. & Hofmann, F. (1998). Defective smooth muscle regulation in cGMP kinase I-deficient mice. *Embo J* **17**, 3045-51.

Pickup, J.C., Mattock, M.B., Chusney, G.D. & Burt, D. (1997). NIDDM as a disease of the innate immune system: association of acute-phase reactants and interleukin-6 with metabolic syndrome X. *Diabetologia* **40**, 1286-92.

Pieper, G.M. & Riaz Ul, H. (1997). Activation of nuclear factor-kappaB in cultured endothelial cells by increased glucose concentration: prevention by calphostin C. *J Cardiovasc Pharmacol* **30**, 528-32.

Pillay, T.S., Xiao, S. & Olefsky, J.M. (1996). Glucose-induced phosphorylation of the insulin receptor. Functional effects and characterization of phosphorylation sites. *J Clin Invest* **97**, 613-20.

Pinkney, J.H., Stehouwer, C.D., Coppack, S.W. & Yudkin, J.S. (1997). Endothelial dysfunction: cause of the insulin resistance syndrome. *Diabetes* **46 Suppl 2**, S9-13.

Pollock, J.S., Forstermann, U., Mitchell, J.A., Warner, T.D., Schmidt, H., Nakane, M. & Murad, F. (1991). Purification and Characterization of Particulate Endothelium-Derived Relaxing Factor Synthase from Cultured and Native Bovine Aortic Endothelial Cells. *Proceedings of the National Academy of Sciences* **88**, 10480-10484.

Potenza, M.A., Marasciulo, F.L., Chieppa, D.M., Brigiani, G.S., Formoso, G., Quon, M.J. & Montagnani, M. (2005). Insulin resistance in spontaneously hypertensive rats is associated with endothelial dysfunction characterized by imbalance between NO and ET-1 production. *Am J Physiol Heart Circ Physiol* **289**, H813-822.

Prasad, R., Giri, S., Nath, N., Singh, I. & Singh, A.K. (2006). 5-aminoimidazole-4-carboxamide-1-beta-4-ribofuranoside attenuates experimental autoimmune encephalomyelitis via modulation of endothelial-monocyte interaction. *Journal of Neuroscience Research* **84**, 614-625.

Pronk, G.J., Mcglade, J., Pelicci, G., Pawson, T. & Bos, J.L. (1993). Insulin-induced phosphorylation of the 46- and 52-kDa Shc proteins. *J Biol Chem* **268**, 5748-53.

Quagliaro, L., Piconi, L., Assaloni, R., Da Ros, R., Szabo, C. & Ceriello, A. (2007). Primary role of superoxide anion generation in the cascade of events leading to endothelial dysfunction and damage in high glucose treated HUVEC. *Nutr Metab Cardiovasc Dis* **17**, 257-67.

Rahman, S., Rahman, T., Ismail, A.A.-S. & Rashid, A.R.A. (2007). Diabetes-associated macrovasculopathy: pathophysiology and pathogenesis. *Diabetes, Obesity and Metabolism* **9**, 767-780.

Rask-Madsen, C. & King, G.L. (2005). Proatherosclerotic Mechanisms Involving Protein Kinase C in Diabetes and Insulin Resistance. *Arterioscler Thromb Vasc Biol* **25**, 487-496.

Rask-Madsen, C. & King, G.L. (2007). Mechanisms of Disease: endothelial dysfunction in insulin resistance and diabetes. *Nat Clin Pract Endocrinol Metab* **3**, 46-56.

Reaven, G.M. (1988). Banting lecture 1988. Role of insulin resistance in human disease. *Diabetes* **37**, 1595-1607.

Reaven, G.M. (2005). THE INSULIN RESISTANCE SYNDROME: Definition and Dietary Approaches to Treatment. *Annual Review of Nutrition* **25**, 391-406.

Reihill, J.A., Ewart, M.A., Hardie, D.G. & Salt, I.P. (2007). AMP-activated protein kinase mediates VEGF-stimulated endothelial NO production. *Biochem Biophys Res Commun* **354**, 1084-8.

Reiter, C.D., Teng, R.J. & Beckman, J.S. (2000). Superoxide reacts with nitric oxide to nitrate tyrosine at physiological pH via peroxynitrite. *J Biol Chem* **275**, 32460-6.

Resta, T.C., Gonzales, R.J., Dail, W.G., Sanders, T.C. & Walker, B.R. (1997). Selective upregulation of arterial endothelial nitric oxide synthase in pulmonary hypertension. *Am J Physiol Heart Circ Physiol* **272**, H806-813.

Ritchie, S.A., Connell, J.M.C. & Salt, I.P. (2007). Identification of a novel insulin-stimulated phosphorylation site on Endothelial Nitric Oxide Synthase (eNOS). *Diabetic Medicine* **24**, 39-39.

Ritchie, S.A., Ewart, M.A., Perry, C.G., Connell, J.M. & Salt, I.P. (2004). The role of insulin and the adipocytokines in regulation of vascular endothelial function. *Clin Sci (Lond)* **107**, 519-32.

Rivero-Vilches, F.J., De Frutos, S., Saura, M., Rodriguez-Puyol, D. & Rodriguez-Puyol, M. (2003). Differential relaxing responses to particulate or soluble guanylyl cyclase

activation on endothelial cells: a mechanism dependent on PKG-I alpha activation by NO/cGMP. *Am J Physiol Cell Physiol* **285**, C891-8.

Rojas, S., Rojas, R., Lamperti, L., Casanello, P. & Sobrevia, L. (2003). Hyperglycaemia inhibits thymidine incorporation and cell growth via protein kinase C, mitogen-activated protein kinases and nitric oxide in human umbilical vein endothelium. *Exp Physiol* **88**, 209-219.

Rosenberg, R.B., Broner, C.W. & O'dorisio, M.S. (1994). Modulation of cyclic guanosine monophosphate production during Escherichia coli septic shock. *Biochem Med Metab Biol* **51**, 149-55.

Salt, I.P., Johnson, G., Ashcroft, S.J. & Hardie, D.G. (1998). AMP-activated protein kinase is activated by low glucose in cell lines derived from pancreatic beta cells, and may regulate insulin release. *Biochem J* **335 (Pt 3)**, 533-9.

Salt, I.P., Morrow, V.A., Brandie, F.M., Connell, J.M. & Petrie, J.R. (2003). High glucose inhibits insulin-stimulated nitric oxide production without reducing endothelial nitric-oxide synthase Ser1177 phosphorylation in human aortic endothelial cells. *J Biol Chem* **278**, 18791-7.

Saltiel, A.R. & Pessin, J.E. (2003). Insulin signaling in microdomains of the plasma membrane. *Traffic* **4**, 711-6.

Sausbier, M., Schubert, R., Voigt, V., Hirneiss, C., Pfeifer, A., Korth, M., Kleppisch, T., Ruth, P. & Hofmann, F. (2000). Mechanisms of NO/cGMP-dependent vasorelaxation. *Circ Res* **87**, 825-30.

Sawka-Verhelle, D., Tartare-Deckert, S., Decaux, J.F., Girard, J. & Van Obberghen, E. (2000). Stat 5B, activated by insulin in a Jak-independent fashion, plays a role in glucokinase gene transcription. *Endocrinology* **141**, 1977-88.

Scherrer, U., Randin, D., Vollenweider, P., Vollenweider, L. & Nicod, P. (1994). Nitric oxide release accounts for insulin's vascular effects in humans. *J Clin Invest* **94**, 2511-5.

Scherrer, U., Vollenweider, P., Randin, D., Jequier, E., Nicod, P. & Tappy, L. (1993). Suppression of insulin-induced sympathetic activation and vasodilation by dexamethasone in humans. *Circulation* **88**, 388-94.

Schulze, M.B. & Hu, F.B. (2005). PRIMARY PREVENTION OF DIABETES: What Can Be Done and How Much Can Be Prevented? *Annual Review of Public Health* **26**, 445-467.

Searles, C.D. (2006). Transcriptional and posttranscriptional regulation of endothelial nitric oxide synthase expression. *Am J Physiol Cell Physiol* **291**, C803-816.

Sessa, W.C., Garca-Cardea, G., Liu, J., Keh, A., Pollock, J.S., Bradley, J., Thiru, S., Braverman, I.M. & Desai, K.M. (1995). The Golgi Association of Endothelial Nitric Oxide Synthase Is Necessary for the Efficient Synthesis of Nitric Oxide. *J. Biol. Chem.* **270**, 17641-17644.

Shankar, R.R., Wu, Y., Shen, H.Q., Zhu, J.S. & Baron, A.D. (2000). Mice with gene disruption of both endothelial and neuronal nitric oxide synthase exhibit insulin resistance. *Diabetes* **49**, 684-7.

Shaul, P.W., Smart, E.J., Robinson, L.J., German, Z., Yuhanna, I.S., Ying, Y., Anderson, R.G.W. & Michel, T. (1996). Acylation Targets Endothelial Nitric-oxide Synthase to Plasmalemmal Caveolae. *J. Biol. Chem.* **271**, 6518-6522.

Shaw, G. (1993). Identification of Novel Pleckstrin Homology (PH) Domains Provides a Hypothesis for PH Domain Function. *Biochemical and Biophysical Research Communications* **195**, 1145-1151.

Shaw, R.J., Lamia, K.A., Vasquez, D., Koo, S.-H., Bardeesy, N., Depinho, R.A., Montminy, M. & Cantley, L.C. (2005). The Kinase LKB1 Mediates Glucose Homeostasis in Liver and Therapeutic Effects of Metformin. *Science* **310**, 1642-1646.

Shears, L.L., Ii, Kawaharada, N., Tzeng, E., Billiar, T.R., Watkins, S.C., Kovesdi, I., Lizonova, A. & Pham, S.M. (1997). Inducible Nitric Oxide Synthase Suppresses the Development of Allograft Arteriosclerosis. *J. Clin. Invest.* **100**, 2035-2042.

Shen, Y.H., Zhang, L., Gan, Y., Wang, X., Wang, J., Lemaire, S.A., Coselli, J.S. & Wang, X.L. (2006a). Up-regulation of PTEN (Phosphatase and Tensin Homolog Deleted on Chromosome Ten) Mediates p38 MAPK Stress Signal-induced Inhibition of Insulin Signaling: A CROSS-TALK BETWEEN STRESS SIGNALING AND INSULIN SIGNALING IN RESISTIN-TREATED HUMAN ENDOTHELIAL CELLS. *J. Biol. Chem.* **281**, 7727-7736.

Shen, Y.H., Zhang, L., Utama, B., Wang, J., Gan, Y., Wang, X., Wang, J., Chen, L., Vercellotti, G.M., Coselli, J.S., Mehta, J.L. & Wang, X.L. (2006b). Human cytomegalovirus inhibits Akt-mediated eNOS activation through upregulating PTEN (phosphatase and tensin homolog deleted on chromosome 10). *Cardiovascular Research* **69**, 502.

Shepherd, P.R., Withers, D.J. & Siddle, K. (1998). Phosphoinositide 3-kinase: the key switch mechanism in insulin signalling. *Biochem J* **333 (Pt 3)**, 471-90.

Shesely, E.G., Maeda, N., Kim, H.S., Desai, K.M., Krege, J.H., Laubach, V.E., Sherman, P.A., Sessa, W.C. & Smithies, O. (1996). Elevated blood pressures in mice lacking endothelial nitric oxide synthase. *Proc Natl Acad Sci U S A* **93**, 13176-81.

Shinozaki, K., Kashiwagi, A., Nishio, Y., Okamura, T., Yoshida, Y., Masada, M., Toda, N. & Kikkawa, R. (1999). Abnormal biopterin metabolism is a major cause of impaired endothelium-dependent relaxation through nitric oxide/O2- imbalance in insulin-resistant rat aorta. *Diabetes* **48**, 2437-45.

Siddhanta, U., Wu, C., Abu-Soud, H.M., Zhang, J., Ghosh, D.K. & Stuehr, D.J. (1996). Heme iron reduction and catalysis by a nitric oxide synthase heterodimer containing one reductase and two oxygenase domains. *J Biol Chem* **271**, 7309-12.

Siddle, K. (2005). The Insulin Receptor and Downstream Signalling. In *Insulin Resistance - Insulin action and its disturbances in disease*, 1st edn, pp. 1-62. Edited by O'rahilly. Chichester: John Wiley & Sons Ltd.

Sim, A.T.R. & Hardie, D.G. (1988). The low activity of acetyl-CoA car☐ylase in basal and glucagon-stimulated hepatocytes is due to phosphorylation by the AMP-activated protein kinase and not cyclic AMP-dependent protein kinase. *FEBS Letters* **233**, 294.

Simionescu, M. (2007). Implications of early structural-functional changes in the endothelium for vascular disease. *Arterioscler Thromb Vasc Biol* **27**, 266-74.

Skolnik, E.Y., Lee, C.H., Batzer, A., Vicentini, L.M., Zhou, M., Daly, R., Myers, M.J., Jr., Backer, J.M., Ullrich, A., White, M.F. & Et Al. (1993). The SH2/SH3 domain-containing protein GRB2 interacts with tyrosine-phosphorylated IRS1 and Shc: implications for insulin control of ras signalling. *Embo J* **12**, 1929-36.

Smits, P., Kapma, J.A., Jacobs, M.C., Lutterman, J. & Thien, T. (1993). Endothelium-dependent vascular relaxation in patients with type I diabetes. *Diabetes* **42**, 148-53.

Sobrevia, L., Nadal, A., Yudilevich, D.L. & Mann, G.E. (1996). Activation of L-arginine transport (system y+) and nitric oxide synthase by elevated glucose and insulin in human endothelial cells. *J Physiol* **490 (Pt 3)**, 775-81.

Sobrevia, L., Yudilevich, D.L. & Mann, G.E. (1998). Elevated D-glucose induces insulin insensitivity in human umbilical endothelial cells isolated from gestational diabetic pregnancies. *J Physiol* **506 (Pt 1)**, 219-30.

Son, H., Hawkins, R.D., Martin, K., Kiebler, M., Huang, P.L., Fishman, M.C. & Kandel, E.R. (1996). Long-term potentiation is reduced in mice that are doubly mutant in endothelial and neuronal nitric oxide synthase. *Cell* **87**, 1015-23.

Song, P., Wu, Y., Xu, J., Xie, Z., Dong, Y., Zhang, M. & Zou, M.H. (2007). Reactive nitrogen species induced by hyperglycemia suppresses Akt signaling and triggers apoptosis by upregulating phosphatase PTEN (phosphatase and tensin homologue

deleted on chromosome 10) in an LKB1-dependent manner. *Circulation* **116**, 1585-95.

Soos, M.A. & Siddle, K. (1989). Immunological relationships between receptors for insulin and insulin-like growth factor I. Evidence for structural heterogeneity of insulin-like growth factor I receptors involving hybrids with insulin receptors. *Biochem J* **263**, 553-63.

Sowa, G., Liu, J., Papapetropoulos, A., Rex-Haffner, M., Hughes, T.E. & Sessa, W.C. (1999). Trafficking of Endothelial Nitric-oxide Synthase in Living Cells. QUANTITATIVE EVIDENCE SUPPORTING THE ROLE OF PALMITOYLATION AS A KINETIC TRAPPING MECHANISM LIMITING MEMBRANE DIFFUSION. *J. Biol. Chem.* **274**, 22524-22531.

Srinivasan, S., Hatley, M.E., Bolick, D.T., Palmer, L.A., Edelstein, D., Brownlee, M. & Hedrick, C.C. (2004). Hyperglycaemia-induced superoxide production decreases eNOS expression via AP-1 activation in aortic endothelial cells. *Diabetologia* **47**, 1727-34.

Stahmann, N., Woods, A., Carling, D. & Heller, R. (2006). Thrombin Activates AMP-Activated Protein Kinase in Endothelial Cells via a Pathway Involving Ca2+/Calmodulin-Dependent Protein Kinase Kinase {beta}. *Mol. Cell. Biol.* **26**, 5933-5945.

Stalker, T.J., Skvarka, C.B. & Scalia, R. (2003). A novel role for calpains in the endothelial dysfunction of hyperglycemia. *FASEB J.*, 02-1213fje.

Stamler, J.S., Loh, E., Roddy, M.A., Currie, K.E. & Creager, M.A. (1994). Nitric oxide regulates basal systemic and pulmonary vascular resistance in healthy humans. *Circulation* **89**, 2035-40.

Stein, E.G., Ghirlando, R. & Hubbard, S.R. (2003). Structural basis for dimerization of the Grb10 Src homology 2 domain. Implications for ligand specificity. *J Biol Chem* **278**, 13257-64.

Steinberg, H.O., Chaker, H., Leaming, R., Johnson, A., Brechtel, G. & Baron, A.D. (1996). Obesity/Insulin Resistance Is Associated with Endothelial Dysfunction. Implications for the Syndrome of Insulin Resistance. *J. Clin. Invest.* **97**, 2601-2610.

Stolar, M.W. & Chilton, R.J. (2003). Type 2 diabetes, cardiovascular risk, and the link to insulin resistance. *Clin Ther* **25 Suppl B**, B4-31.

Strack, V., Hennige, A.M., Krutzfeldt, J., Bossenmaier, B., Klein, H.H., Kellerer, M., Lammers, R. & Haring, H.U. (2000). Serine residues 994 and 1023/25 are important for insulin receptor kinase inhibition by protein kinase C isoforms beta2 and theta. *Diabetologia* **43**, 443-9.

Stratton, I.M., Adler, A.I., Neil, H.A., Matthews, D.R., Manley, S.E., Cull, C.A., Hadden, D., Turner, R.C. & Holman, R.R. (2000). Association of glycaemia with macrovascular and microvascular complications of type 2 diabetes (UKPDS 35): prospective observational study. *Bmj* **321**, 405-12.

Stuehr, D.J. (1999). Mammalian nitric oxide synthases. *Biochimica et Biophysica Acta (BBA) - Bioenergetics* **1411**, 217.

Su, Y., Edwards-Bennett, S., Bubb, M.R. & Block, E.R. (2003). Regulation of endothelial nitric oxide synthase by the actin cytoskeleton. *Am J Physiol Cell Physiol* **284**, C1542-1549.

Sun, X.J., Rothenberg, P., Kahn, C.R., Backer, J.M., Araki, E., Wilden, P.A., Cahill, D.A., Goldstein, B.J. & White, M.F. (1991). Structure of the insulin receptor substrate IRS-1 defines a unique signal transduction protein. *Nature* **352**, 73-7.

Sun, X.J., Wang, L.-M., Zhang, Y., Yenush, L., Myers Jr, M.G., Glasheen, E., Lane, W.S., Pierce, J.H. & White, M.F. (1995). Role of IRS-2 in insulin and cytokine signalling. **377**, 173-177.

Sundell, J., Laine, H., Nuutila, P., Ronnemaa, T., Luotolahti, M., Raitakari, O. & Knuuti, J. (2002). The effects of insulin and short-term hyperglycaemia on myocardial blood flow in young men with uncomplicated Type I diabetes. *Diabetologia* **45**, 775-82.

Surinya, K.H., Molina, L., Soos, M.A., Brandt, J., Kristensen, C. & Siddle, K. (2002). Role of Insulin Receptor Dimerization Domains in Ligand Binding, Cooperativity, and Modulation by Anti-receptor Antibodies. *J. Biol. Chem.* **277**, 16718-16725.

Surks, H.K., Mochizuki, N., Kasai, Y., Georgescu, S.P., Tang, K.M., Ito, M., Lincoln, T.M. & Mendelsohn, M.E. (1999). Regulation of myosin phosphatase by a specific interaction with cGMP- dependent protein kinase Ialpha. *Science* **286**, 1583-7.

Takahashi, S. & Mendelsohn, M.E. (2003). Synergistic Activation of Endothelial Nitric-oxide Synthase (eNOS) by HSP90 and Akt: CALCIUM-INDEPENDENT eNOS ACTIVATION INVOLVES FORMATION OF AN HSP90-Akt-CaM-BOUND eNOS COMPLEX. *J. Biol. Chem.* **278**, 30821-30827.

Taniguchi, C.M., Tran, T.T., Kondo, T., Luo, J., Ueki, K., Cantley, L.C. & Kahn, C.R. (2006). Phosphoinositide 3-kinase regulatory subunit p85alpha suppresses insulin action via positive regulation of PTEN. *Proc Natl Acad Sci U S A* **103**, 12093-7.

Tesauro, M., Schinzari, F., Iantorno, M., Rizza, S., Melina, D., Lauro, D. & Cardillo, C. (2005). Ghrelin Improves Endothelial Function in Patients With Metabolic Syndrome. *Circulation* **112**, 2986-2992.

Tesfamariam, B., Brown, M.L., Deykin, D. & Cohen, R.A. (1990). Elevated glucose promotes generation of endothelium-derived vasoconstrictor prostanoids in rabbit aorta. *J Clin Invest* **85**, 929-32.

Thiemermann, C. & Vane, J. (1990). Inhibition of nitric oxide synthesis reduces the hypotension induced by bacterial lipopolysaccharides in the rat in vivo. *Eur J Pharmacol* **182**, 591-5.

Toba, H., Gomyo, E., Miki, S., Shimizu, T., Yoshimura, A., Inoue, R., Sawai, N., Tsukamoto, R., Asayama, J., Kobara, M. & Nakata, T. (2006). HYPERINSULINAEMIA INCREASES THE GENE EXPRESSION OF ENDOTHELIAL NITRIC OXIDE SYNTHASE AND THE PHOSPHATIDYLINOSITOL 3-KINASE/AKT PATHWAY IN RAT AORTA. *Clinical and Experimental Pharmacology and Physiology* **33**, 440-447.

Tomas, E., Tsao, T.-S., Saha, A.K., Murrey, H.E., Zhang, C.C., Itani, S.I., Lodish, H.F. & Ruderman, N.B. (2002). Enhanced muscle fat oxidation and glucose transport by ACRP30 globular domain: Acetyl-CoA carboxylase inhibition and AMP-activated protein kinase activation. *Proceedings of the National Academy of Sciences* **99**, 16309-16313.

Towler, M.C. & Hardie, D.G. (2007). AMP-Activated Protein Kinase in Metabolic Control and Insulin Signaling. *Circ Res* **100**, 328-341.

Treadway, J., Morrison, B., Goldfine, I. & Pessin, J. (1989). Assembly of insulin/insulin-like growth factor-1 hybrid receptors in vitro. *J. Biol. Chem.* **264**, 21450-21453.

Trinh, K.Y., O'doherty, R.M., Anderson, P., Lange, A.J. & Newgard, C.B. (1998). Perturbation of fuel homeostasis caused by overexpression of the glucose-6-phosphatase catalytic subunit in liver of normal rats. *Journal of Biological Chemistry* **273**, 31615.

Tschöp, M. & Heiman, M. (2001). Rodent obesity models: An overview. *Exp Clin Endocrinol Diabetes*, 307.

Uhles, S., Moede, T., Leibiger, B., Berggren, P.O. & Leibiger, I.B. (2003). Isoform-specific insulin receptor signaling involves different plasma membrane domains. *J Cell Biol* **163**, 1327-37.

Ullrich, A., Gray, A., Tam, A.W., Yang-Feng, T., Tsubokawa, M., Collins, C., Henzel, W., Le Bon, T., Kathuria, S., Chen, E. & Et Al. (1986). Insulin-like growth factor I receptor primary structure: comparison with insulin receptor suggests structural determinants that define functional specificity. *Embo J* **5**, 2503-12.

Upchurch, G.R., Welch, G.N., Fabian, A.J., Pigazzi, A., Keaney, J.F. & Loscalzo, J. (1997). Stimulation of endothelial nitric oxide production by homocyst(e)ine. *Atherosclerosis* **132**, 177.

Valera, A., Pujol, A., Pelegrin, M. & Bosch, F. (1994). Transgenic mice overexpressing phosphoenolpyruvate carboxykinase develop non-insulin-dependent diabetes mellitus. *Proceedings of the National Academy of Sciences of the United States of America* **91**, 9151.

Valverde, A.M., Teruel, T., Navarro, P., Benito, M. & Lorenzo, M. (1998). Tumor necrosis factor-alpha causes insulin receptor substrate-2-mediated insulin resistance and inhibits insulin-induced adipogenesis in fetal brown adipocytes. *Endocrinology* **139**, 1229-38.

Van Der Wal, A.C., Becker, A.E., Van Der Loos, C.M. & Das, P.K. (1994). Site of intimal rupture or erosion of thrombosed coronary atherosclerotic plaques is characterized by an inflammatory process irrespective of the dominant plaque morphology. *Circulation* **89**, 36-44.

Vanhaesebroeck, B. & Alessi, D.R. (2000). The PI3K-PDK1 connection: more than just a road to PKB. *Biochem J* **346 Pt 3**, 561-76.

Varma, S., Lal, B.K., Zheng, R., Breslin, J.W., Saito, S., Pappas, P.J., Hobson, R.W., Ii & Duran, W.N. (2005). Hyperglycemia alters PI3k and Akt signaling and leads to endothelial cell proliferative dysfunction. *Am J Physiol Heart Circ Physiol* **289**, H1744-1751.

Vasquez-Vivar, J., Kalyanaraman, B., Martasek, P., Hogg, N., Masters, B.S.S., Karoui, H., Tordo, P. & Pritchard, K.A., Jr. (1998). Superoxide generation by endothelial nitric oxide synthase: The influence of cofactors. *Proceedings of the National Academy of Sciences* **95**, 9220-9225.

Venema, V.J., Ju, H., Zou, R. & Venema, R.C. (1997). Interaction of Neuronal Nitric-oxide Synthase with Caveolin-3 in Skeletal Muscle. IDENTIFICATION OF A NOVEL CAVEOLIN SCAFFOLDING/INHIBITORY DOMAIN. *J. Biol. Chem.* **272**, 28187-28190.

Vicent, D., Ilany, J., Kondo, T., Naruse, K., Fisher, S.J., Kisanuki, Y.Y., Bursell, S., Yanagisawa, M., King, G.L. & Kahn, C.R. (2003). The role of endothelial insulin signaling in the regulation of vascular tone and insulin resistance. *J Clin Invest* **111**, 1373-80.

Vivanco, I. & Sawyers, C.L. (2002). The phosphatidylinositol 3-Kinase AKT pathway in human cancer. *Nat Rev Cancer* **2**, 489-501.

Wang, Q., Somwar, R., Bilan, P.J., Liu, Z., Jin, J., Woodgett, J.R. & Klip, A. (1999). Protein Kinase B/Akt Participates in GLUT4 Translocation by Insulin in L6 Myoblasts. *Mol. Cell. Biol.* **19**, 4008-4018.

Wang, X.L., Zhang, L., Youker, K., Zhang, M.-X., Wang, J., Lemaire, S.A., Coselli, J.S. & Shen, Y.H. (2006). Free Fatty Acids Inhibit Insulin Signaling-Stimulated Endothelial Nitric Oxide Synthase Activation Through Upregulating PTEN or Inhibiting Akt Kinase. *Diabetes* **55**, 2301-2310.

Welborn, T.A., Breckenridge, A., Rubinstein, A.H., Dollery, C.T. & Fraser, T.R. (1966). Serum-insulin in essential hypertension and in peripheral vascular disease. *Lancet* **1**, 1336-7.

Wellen, K.E. & Hotamisligil, G.S. (2005). Inflammation, stress, and diabetes. *J Clin Invest* **115**, 1111-9.

Wheatcroft, S.B., Shah, A.M., Li, J.-M., Duncan, E., Noronha, B.T., Crossey, P.A. & Kearney, M.T. (2004). Preserved Glucoregulation but Attenuation of the Vascular Actions of Insulin in Mice Heterozygous for Knockout of the Insulin Receptor. *Diabetes* **53**, 2645-2652.

Wheatcroft, S.B., Williams, I.L., Shah, A.M. & Kearney, M.T. (2003). Pathophysiological implications of insulin resistance on vascular endothelial function. *Diabet Med* **20**, 255-68.

White, M.F. (1998). The IRS-signaling system: a network of docking proteins that mediate insulin and cytokine action. *Recent Prog Horm Res* **53**, 119-38.

White, M.F. (2002). IRS proteins and the common path to diabetes. *Am J Physiol Endocrinol Metab* **283**, E413-22.

White, M.F., Maron, R. & Kahn, C.R. (1985). Insulin rapidly stimulates tyrosine phosphorylation of a Mr-185,000 protein in intact cells. *Nature* **318**, 183-6.

Whiteman, E.L., Cho, H. & Birnbaum, M.J. (2002). Role of Akt/protein kinase B in metabolism. *Trends Endocrinol Metab* **13**, 444-51.

Wick, M.J., Dong, L.Q., Riojas, R.A., Ramos, F.J. & Liu, F. (2000). Mechanism of Phosphorylation of Protein Kinase B/Akt by a Constitutively Active 3-Phosphoinositide-dependent Protein Kinase-1. *J. Biol. Chem.* **275**, 40400-40406.

Wijesekara, N., Konrad, D., Eweida, M., Jefferies, C., Liadis, N., Giacca, A., Crackower, M., Suzuki, A., Mak, T.W., Kahn, C.R., Klip, A. & Woo, M. (2005). Muscle-Specific Pten Deletion Protects against Insulin Resistance and Diabetes. *Mol. Cell. Biol.* **25**, 1135-1145.

Wild, S., Roglic, G., Green, A., Sicree, R. & King, H. (2004). Global Prevalence of Diabetes: Estimates for the year 2000 and projections for 2030. *Diabetes Care* **27**, 1047-1053.

Wilson, R.I., Yanovsky, J., Godecke, A., Stevens, D.R., Schrader, J. & Haas, H.L. (1997). Endothelial nitric oxide synthase and LTP. *Nature* **386**, 338.

Winkler, G., Lakatos, P., Salamon, F., Nagy, Z., Speer, G., Kovacs, M., Harmos, G., Dworak, O. & Cseh, K. (1999). Elevated serum TNF-alpha level as a link between endothelial dysfunction and insulin resistance in normotensive obese patients. *Diabet Med* **16**, 207-11.

Wolf, G., Trub, T., Ottinger, E., Groninga, L., Lynch, A., White, M.F., Miyazaki, M., Lee, J. & Shoelson, S.E. (1995). PTB domains of IRS-1 and Shc have distinct but overlapping binding specificities. *J Biol Chem* **270**, 27407-10.

Woods, A., Dickerson, K., Heath, R., Hong, S.-P., Momcilovic, M., Johnstone, S.R., Carlson, M. & Carling, D. (2005). Ca2+/calmodulin-dependent protein kinase kinase-[beta] acts upstream of AMP-activated protein kinase in mammalian cells. *Cell Metabolism* **2**, 21.

Woods, A., Salt, I., Scott, J., Hardie, D.G. & Carling, D. (1996). The [alpha]1 and [alpha]2 isoforms of the AMP-activated protein kinase have similar activities in rat liver but exhibit differences in substrate specificity in vitro. *FEBS Letters* **397**, 347.

World Health Organisation (2002). The World Health Report 2002 - Reducing Risks, Promoting Healthy Life. Statistical Annex 7.

Xia, Y., Tsai, A.-L., Berka, V. & Zweier, J.L. (1998). Superoxide Generation from Endothelial Nitric-oxide Synthase. A Ca2+/CALMODULIN-DEPENDENT AND TETRAHYDROBIOPTERIN REGULATORY PROCESS. *J. Biol. Chem.* **273**, 25804-25808.

Yamauchi, T., Kamon, J., Minokoshi, Y., Ito, Y., Waki, H., Uchida, S., Yamashita, S., Noda, M., Kita, S., Ueki, K., Eto, K., Akanuma, Y., Froguel, P., Foufelle, F., Ferre, P., Carling, D., Kimura, S., Nagai, R., Kahn, B.B. & Kadowaki, T. (2002). Adiponectin stimulates glucose utilization and fatty-acid oxidation by activating AMP-activated protein kinase. *Nat Med* **8**, 1288-95.

Yanagisawa, M., Kurihara, H., Kimura, S., Tomobe, Y., Kobayashi, M., Mitsui, Y., Yazaki, Y., Goto, K. & Masaki, T. (1988). A novel potent vasoconstrictor peptide produced by vascular endothelial cells. *Nature* **332**, 411.

Yang, Y. & Santamaria, P. (2006). Lessons on autoimmune diabetes from animal models. *Clin Sci (Lond)* **110**, 627-39.

Yip, C.C., Yeung, C.W. & Moule, M.L. (1978). Photoaffinity labeling of insulin receptor of rat adiopocyte plasma membrane. *J Biol Chem* **253**, 1743-5.

Yudkin, J.S., Stehouwer, C.D., Emeis, J.J. & Coppack, S.W. (1999). C-reactive protein in healthy subjects: associations with obesity, insulin resistance, and endothelial dysfunction: a potential role for cytokines originating from adipose tissue? *Arterioscler Thromb Vasc Biol* **19**, 972-8.

Zeiher, A.M., Fisslthaler, B., Schray-Utz, B. & Busse, R. (1995). Nitric oxide modulates the expression of monocyte chemoattractant protein 1 in cultured human endothelial cells. *Circ Res* **76**, 980-6.

Zeng, G., Nystrom, F.H., Ravichandran, L.V., Cong, L.-N., Kirby, M., Mostowski, H. & Quon, M.J. (2000). Roles for Insulin Receptor, PI3-Kinase, and Akt in Insulin-Signaling Pathways Related to Production of Nitric Oxide in Human Vascular Endothelial Cells. *Circulation* **101**, 1539-1545.

Zeng, G. & Quon, M.J. (1996). Insulin-stimulated Production of Nitric Oxide Is Inhibited by Wortmannin. Direct Measurement in Vascular Endothelial Cells. *J. Clin. Invest.* **98**, 894-898.

Zhang, B. Insulin Signaling and Action- glucose, lipids, and protein. In *DIABETES AND CARBOHYDRATE METABOLISM*, pp. Web-textbook. E dited by Goldfine.

Zhang, B. & Roth, R.A. (1992). The insulin receptor-related receptor. Tissue expression, ligand binding specificity, and signaling capabilities. *J Biol Chem* **267**, 18320-8.

Zhang, Q., Church, J.E., Jagnandan, D., Catravas, J.D., Sessa, W.C. & Fulton, D. (2006). Functional Relevance of Golgi- and Plasma Membrane-Localized Endothelial NO Synthase in Reconstituted Endothelial Cells. *Arterioscler Thromb Vasc Biol* **26**, 1015-1021.

Zhen, J., Lu, H., Wang, X.Q., Vaziri, N.D. & Zhou, X.J. (2008). Upregulation of endothelial and inducible nitric oxide synthase expression by reactive oxygen species. *Am J Hypertens* **21**, 28-34.

Zhou, G., Myers, R., Li, Y., Chen, Y., Shen, X., Fenyk-Melody, J., Wu, M., Ventre, J., Doebber, T., Fujii, N., Musi, N., Hirshman, M.F., Goodyear, L.J. & Moller, D.E. (2001). Role of AMP-activated protein kinase in mechanism of metformin action. *J Clin Invest* **108**, 1167-74.

Zhou, Q., Dolan, P.L. & Dohm, G.L. (1999). Dephosphorylation increases insulin-stimulated receptor kinase activity in skeletal muscle of obese Zucker rats. *Mol Cell Biochem* **194**, 209-16.

Ziccardi, P., Nappo, F., Giugliano, G., Esposito, K., Marfella, R., Cioffi, M., D'andrea, F., Molinari, A.M. & Giugliano, D. (2002). Reduction of inflammatory cytokine concentrations and improvement of endothelial functions in obese women after weight loss over one year. *Circulation* **105**, 804-9.

Zimmermann, K., Opitz, N., Dedio, J., Renne, C., Muller-Esterl, W. & Oess, S. (2002). From the Cover: NOSTRIN: A protein modulating nitric oxide release and subcellular distribution of endothelial nitric oxide synthase. *PNAS* **99**, 17167-17172.

Zou, M.H., Shi, C. & Cohen, R.A. (2002). Oxidation of the zinc-thiolate complex and uncoupling of endothelial nitric oxide synthase by peroxynitrite. *J Clin Invest* **109**, 817-26.